

2007

# Effects of hyperbaric oxygen on oxidative stress, angiogenesis factors and endothelial cell injury

Yuan, Jianfeng

<http://hdl.handle.net/10026.1/2451>

---

<http://dx.doi.org/10.24382/1581>

University of Plymouth

---

*All content in PEARL is protected by copyright law. Author manuscripts are made available in accordance with publisher policies. Please cite only the published version using the details provided on the item record or document. In the absence of an open licence (e.g. Creative Commons), permissions for further reuse of content should be sought from the publisher or author.*

**EFFECTS OF HYPERBARIC OXYGEN  
ON OXIDATIVE STRESS,  
ANGIOGENESIS FACTORS  
AND ENDOTHELIAL CELL INJURY**

**JIANFENG YUAN**

**PhD 2007**

This copy of the thesis has been supplied on condition that anyone who consults it is understood to recognise that its copyright rests with its author and that no quotation from the thesis and no information derived from it may be published without the author's prior consent.

Copyright © December 2007 by Jianfeng Yuan

**EFFECTS OF HYPERBARIC OXYGEN ON  
OXIDATIVE STRESS, ANGIOGENESIS FACTORS  
AND ENDOTHELIAL CELL INJURY**

by

**JIANFENG YUAN**

B.Med., Shandong Medical University, 1996

M.Med., China National Research Institute of Sports Sciences, 2002

A thesis submitted to the University of Plymouth

in partial fulfilment for the degree of

**DOCTOR OF PHILOSOPHY**

School of Biological Sciences

Faculty of Sciences

**December 2007**

University of Plymouth  
Library

9007951429  
THESIS 6:17.114 YU/A

# EFFECTS OF HYPERBARIC OXYGEN ON OXIDATIVE STRESS, ANGIOGENESIS FACTORS, AND ENDOTHELIAL CELL INJURY

Jianfeng Yuan

## Abstract

Hyperbaric oxygen (HBO) therapy is the administration of 100% oxygen at more than one atmosphere. It greatly improves tissue oxygenation and facilitates mechanisms of wound healing, which in turn benefits some patients with chronic wounds. A prominent fact in therapeutic HBO is the acceleration of neoangiogenesis during granulation tissue formation. Angiogenesis is a highly orchestrated event, a diverse range of cells and angiogenesis factors are involved in the process. The formation of reactive oxidative species (ROS) during HBO has been controversially considered as signalling regulator for angiogenic factors, as well as harmful originator for oxidative stress-induced cyto- and geno-toxicity in cells. This thesis contributes to this interesting while challenging topic.

The project starts with investigation the direct HBO effects on blood vessel *in vitro* under physiological conditions and pathological conditions. The data clearly show that a single HBO treatment does not induce oxidative stress and cell damage under physiological conditions. Nevertheless, under pathological conditions, HBO induces oxidative stress with more ROS formation and cell damage. Interestingly, no evidence has been shown that HBO alone or synergically promotes nitric oxide and vascular endothelial growth factor production in either condition. The response of blood vessel to HBO treatment is not explained by autocrine release of angiogenesis factors locally in the blood vessel.

Next, HBO-induced intracellular calcium ( $\text{Ca}^{2+}$ ) changes and DNA damage were investigated using cultured human umbilical vein endothelial cells. A single HBO treatment significantly elevates intracellular  $\text{Ca}^{2+}$  level without inducing cell damage. Furthermore, HBO treatment has small but significant effect on DNA migration when evaluated by comet assay (e.g.  $6.8 \pm 0.8$  % comparing to  $4.6 \pm 0.2$  % DNA in tail of air treatment). However, this effect is totally reversible after 24h recovery. Importantly, HBO treatment protects endothelial cells against subsequent oxidative stress attack, and an increased antioxidant capacity was found as reflected in higher ratio of GSH to GSSG. The findings suggest that the beneficial effect of HBO is possibly via HBO-induced adaptation in cellular redox status. However, the details of  $\text{Ca}^{2+}$  signalling and roles of antioxidants in HBO treatment are areas for further research.

**Keywords:** Hyperbaric Oxygen, Oxidative Stress, Vascular Endothelial Growth Factor, Nitric Oxide, Endothelial Cells, Calcium, DNA Damage

To  
my parents, Shengtang Yuan and Yuqin Zhao,  
my husband, Dr. Qi Wang,  
and my brother, Jizhou Yuan.

# Table of Contents

Abstract .....	i
Table of Contents .....	iii
List of Figures .....	vii
List of Tables .....	ix
List of Abbreviations.....	x
Acknowledgements .....	xvi
Author's Declaration.....	xvii
<b>Chapter 1.....</b>	<b>1</b>
<b>Background Review: Effects of Hyperbaric Oxygen Therapy on Angiogenesis in Chronic Wound Healing.....</b>	<b>1</b>
1.1 Introduction .....	1
1.2 Wound Healing Process.....	2
1.2.1. The Inflammatory Phase .....	2
1.2.2. The Proliferative Phase .....	3
1.2.3. The Remodelling Phase.....	5
1.3 Angiogenesis in Wound Healing.....	6
1.4 Chronic Wound and Hypoxia.....	11
1.5 Hyperbaric Oxygen Therapy.....	12
1.5.1. Introduction .....	12
1.5.2. Application of Hyperbaric Oxygen Therapy to Chronic Wound .....	13
1.5.3. Role of Oxygen and HBOT in Chronic Wound Healing .....	16
1.5.4. Hyperbaric Oxygen Therapy and Oxidative Stress .....	20
1.6 Regulation of Wound Angiogenesis during HBO Treatment.....	26
1.6.1. Mechanisms of HBO-induced Angiogenesis .....	26
1.6.2. HBO Treatment and VEGF Regulation in Wound Healing.....	27
1.6.3. HBO Treatment and Nitric Oxide.....	38
1.7 Summary .....	49
<b>Chapter 2.....</b>	<b>51</b>
<b>Methods Development.....</b>	<b>51</b>
2.1 Rat Aorta Segment in Vitro Model.....	51
2.1.1. Animals and Aorta Preparations .....	52
2.1.2. Histology Examination.....	53
2.1.3. Tissue Damage.....	55
2.1.4. Conclusion.....	57
2.2 Detection of Reactive Metabolites of Oxygen and Nitrogen.....	57
2.2.1. Hydrogen Peroxide Detection .....	58
2.2.2. Nitric Oxide Measurement .....	64
2.3 Glutathione Measurement.....	68
2.3.1. Glutathione Pool: Indicator of Oxidative Stress <i>in Vivo</i> .....	68
2.3.2. Analysis of Glutathione.....	70
2.3.3. Defined Glutathione Assay for Total Glutathione Measurement .....	71
2.4 Lactate Measurement.....	72
2.5 VEGF ELISA Application.....	74

2.5.1.	Enzyme Linked ImmunoSorbent Assay.....	74
2.5.2.	VEGF ELISA Measurement of Rat Aorta Segment Samples.....	75
2.5.3.	Protein Content Measurement.....	76
2.6	Summary.....	77
<b>Chapter 3.....</b>		<b>79</b>
<b>Effect of Hyperbaric Oxygen on Blood Vessel <i>in Vitro</i>.....</b>		<b>79</b>
3.1	Introduction.....	79
3.2	Material and Methods.....	80
3.2.1.	Animals and Tissue Preparations.....	80
3.2.2.	Experimental Design.....	80
3.2.3.	Biochemical Analysis.....	81
3.2.4.	Histological Examination.....	81
3.2.5.	Statistics.....	82
3.3	Results.....	82
3.3.1.	Histological Examination of Aorta.....	82
3.3.2.	LDH Release.....	84
3.3.3.	Lactate Release.....	85
3.3.4.	Hydrogen Peroxide in Medium.....	86
3.3.5.	Total Glutathione Levels in Medium.....	87
3.3.6.	Nitric Oxide Production of Aorta Segment.....	88
3.3.7.	VEGF Production.....	90
3.3.8.	Correlation Test.....	91
3.4	Discussion.....	92
3.4.1.	The Viability of Aorta Segments during HBO Treatment.....	93
3.4.2.	Oxidative Stress and HBO Treatment.....	93
3.4.3.	Response of Lactate in Aorta Metabolism of HBO Treatment.....	95
3.4.4.	Nitric Oxide, VEGF and HBO Treatment.....	97
3.5	Summary.....	100
<b>Chapter 4.....</b>		<b>101</b>
<b>Effects of HBO on Blood Vessel under Pathological Condition or with Arginine Supplement <i>in Vitro</i>.....</b>		<b>101</b>
4.1	Introduction.....	101
4.2	Material and Methods.....	102
4.2.1.	Experimental Protocol.....	102
4.2.2.	Biochemical Analysis.....	103
4.2.3.	Statistic Analysis.....	104
4.3	Results.....	105
4.3.1.	LDH Release.....	105
4.3.2.	H <sub>2</sub> O <sub>2</sub> Production and Total Glutathione Level in the Media.....	108
4.3.3.	Nitric Oxide Production.....	114
4.3.4.	Angiogenic Factor: VEGF Changes in Tissue Homogenates.....	118
4.3.5.	Lactate Level in the Media.....	121
4.4	Discussion.....	123
4.4.1.	L-arginine Supplement and HBO Treatment.....	123
4.4.2.	Sodium L-lactate Supplement and HBO Treatment.....	127
4.4.3.	L-Arginine, Sodium L-lactate Supplement and HBO Treatment.....	128

<b>Chapter 5</b> .....	<b>131</b>
<b>Oxygen Regulates <math>[Ca^{2+}]_i</math> in Human Umbilical Vein Endothelial Cells</b> .....	<b>131</b>
5.1 Abstract.....	131
5.2 Introduction.....	131
5.3 Material and Methods.....	138
5.3.1 Chemicals and Reagents.....	138
5.3.2 HUVECs Culture Protocol.....	139
5.3.3 <i>In Situ</i> Recording of $Ca^{2+}$ Changes in Single HUVEC.....	139
5.3.4 $[Ca^{2+}]_i$ Measurement Using Fluorescence Plate Reader.....	142
5.4 Results.....	144
5.4.1 Intracellular Calcium Changes of Single HUVEC.....	144
5.4.2 Oxygen Effects on $[Ca^{2+}]_i$ in Population of HUVECs.....	152
5.5 Discussion.....	157
<b>Chapter 6</b> .....	<b>162</b>
<b>Hyperbaric Oxygen Treatment Protects Endothelial Cells against <math>H_2O_2</math> - induced DNA Damage</b> .....	<b>162</b>
6.1 Abstract.....	162
6.2 Introduction.....	163
6.3 Material and Methods.....	167
6.3.1 Cell Culture.....	167
6.3.2 Response of HUVECs to $H_2O_2$ Treatment.....	168
6.3.3 HBO Treatment and Subsequent $H_2O_2$ Incubation.....	168
6.3.4 Glutathione Pool Measurement.....	169
6.3.5 Detecting HUVECs DNA Damage Using Alkaline Comet Assay.....	170
6.3.6 Statistical Analysis.....	172
6.4 Results.....	173
6.4.1 HUVECs' Comet Images.....	173
6.4.2 Response of HUVECs to Different Dose of $H_2O_2$ .....	174
6.4.3 DNA Migrations of HUVECs to HBO and Subsequent $H_2O_2$ Incubation.....	176
6.4.4 Glutathione Pool Changes of HUVECs.....	181
6.4.5 Correlations of DNA Migration Levels and Glutathione Pool.....	185
6.5 Discussions.....	185
6.5.1 HBO-induced Repairable DNA Migration Changes in HUVECs.....	185
6.5.2 Protective Effect of HBO on $H_2O_2$ -induced DNA Damage.....	186
6.5.3 Glutathione: Possible Mechanism for HBO Protective Effect.....	189
6.6 Conclusion.....	192
<b>Chapter 7</b> .....	<b>193</b>
<b>General Discussions and Future Work</b> .....	<b>193</b>
7.1 Summary of the Project.....	193
7.1.1 Main Findings of the Project.....	195
7.1.2 Technical Contributions.....	196
7.1.3 General Discussion.....	197
7.2 Limitations of the Current Work.....	203
7.2.1 Limited Considerations on Pathological Conditions.....	203
7.2.2 Limited Validation of ROS Functions.....	203
7.2.3 Limited Work of <i>in vivo</i> Investigation.....	203

7.3	Future Work .....	204
7.3.1.	Effects of HBO Treatment on Hypoxia Condition .....	204
7.3.2.	Antioxidants Implication to Validate ROS Function .....	204
7.3.3.	Calcium Changes in HBO Treatment .....	204
7.3.4.	<i>In vivo</i> Experiment of HBO Treatment .....	205
7.4	Conclusion.....	205
	<b>Bibliography.....</b>	<b>207</b>

# List of Figures

Fig 1. 1 VEGF signaling pathway in endothelial cell. ....	29
Fig 1. 2 Role of ROS in induction of VEGF production under hypoxia/hyperoxia. ....	38
Fig 1. 3 Reciprocal relationship between VEGF and NO. ....	44
Fig 1. 4 Possible mechanisms of HBO on wound healing process. ....	50
Fig 2. 1 Rat aorta after exposure to normobaric air for 0.5h or 8h, respectively. ....	55
Fig 2. 2 Measurable LDH level of aorta segment and tissue homogenate after Triton X-100 lysis. ....	57
Fig 2. 3 Fluorescence intensity changes upon 0 – 20 nmol of H <sub>2</sub> O <sub>2</sub> ....	59
Fig 2. 4 Influence of HRP concentration and HBO treatment on fluorescence intensity changes. ....	61
Fig 2. 5 HBO treatment affects the standard curve of H <sub>2</sub> O <sub>2</sub> relative fluorescence changes upon the addition of H <sub>2</sub> O <sub>2</sub> . ....	62
Fig 2. 6 Standard curve for detection of nitrite and NO <sub>x</sub> using method described by Schmidt and Kelm (1996). ....	67
Fig 2. 7 Standard curves for the detection of nitrite and nitrate using our modified NO <sub>x</sub> assay. ....	68
Fig 2. 8 Diagram illustrating the use of GSH. ....	70
Fig 2. 9 Standard curve of modified total glutathione assay. ....	72
Fig 2. 10 Standard curve of modified lactate assay. ....	73
Fig 2. 11 Standard Curve of VEGF ELISA assay. ....	76
Fig 2. 12 Standard curve of modified protein assay. ....	77
Fig 3. 1 Histological images of aorta segment during experiments (×400). ....	83
Fig 3. 2 LDH release in the medium. ....	84
Fig 3. 3 Lactate concentration in the medium. ....	85
Fig 3. 4 Hydrogen peroxide concentration in the medium. ....	86
Fig 3. 5 Total glutathione concentration in the medium. ....	87
Fig 3. 6 NO <sub>x</sub> changes in the medium. ....	89
Fig 3. 7 VEGF content in aorta tissue homogenates. ....	91
Fig 4. 1 Cumulative LDH release from segments of aorta into specific media. ....	107
Fig 4. 2 H <sub>2</sub> O <sub>2</sub> generation of aorta segments in specific media. ....	110
Fig 4. 3 Total Glutathione concentration released from aorta segments into specific media ....	113
Fig 4. 4 Concentration of NO <sub>x</sub> and Nitrite, and their ratio in specific media. ....	117

Fig 4. 5 VEGF content of aorta segment homogenate in specific media.....	120
Fig 4. 6 Lactate concentration in specific media .....	122
Fig 5. 1 Photomicrographes of Fura-2 loaded HUVECs during perfusion (×400).....	145
Fig 5. 2 Fluorescence intensity ratio at 340nm to 380nm of HUVEC perfusion with control solution.. .....	146
Fig 5. 3 Ratio of fluorescence intensity of HUVEC perfusion with control solution and then switched to hypoxia solution.....	147
Fig 5. 4 Ratio of fluorescence intensity of HUVEC perfusion with control solution and then switched to hyperoxia solution.....	148
Fig 5. 5 Fluorescence intensity ratio of HBO-treated HUVEC perfusion with control solution.. .....	150
Fig 5. 6 Ratio of fluorescence intensity of HBO-treated HUVEC perfusion with hypoxia solution (HBSS gassed with 95% N <sub>2</sub> + 5% CO <sub>2</sub> ). .....	151
Fig 5. 7 Ratio of fluorescence intensity at 340nm to 380nm of HBO-treated HUVEC perfusion with hyperoxia solution.....	151
Fig 5. 8 Fluorescence intensity ratio of population of HUVECs prior to treatments.. .....	152
Fig 5. 9 Changes of fluorescence intensity ratio of HUVECs post treatment.....	154
Fig 5. 10 Relative absorbance intensity of treated HUVECs to blank healthy control cells in neutral red intake ability .....	155
Fig 5. 11 [Ca <sup>2+</sup> ] <sub>i</sub> calibrations from fluorescence intensity ratio of 340 to 380 nm with Fura-2 AM loading.....	156
Fig 6. 1 General schematic flow of the alkaline comet assay protocol for HUVECs.....	171
Fig 6. 2 H <sub>2</sub> O <sub>2</sub> -induced DNA migration patterns of HUVECs.....	173
Fig 6. 3 Comet images of HUVECs response to different dose of H <sub>2</sub> O <sub>2</sub> .....	175
Fig 6. 4 H <sub>2</sub> O <sub>2</sub> -dependent response in DNA of HUVECs.....	175
Fig 6. 5 HUVECs' comet images with HBO or Air treatment only.. .....	177
Fig 6. 6 Extent of DNA migration (% DNA in tail) in HUVECs after HBO or Air exposure.....	177
Fig 6. 7 Comet images with HBO or Air-treated cells after further incubation with 0.1 mM (A2-D2) and 0.2 mM of H <sub>2</sub> O <sub>2</sub> (A3-D3). .....	179
Fig 6. 8 Effects on DNA migration after subsequent incubation with 0.1 mM and 0.2 mM of H <sub>2</sub> O <sub>2</sub> of HBO- or Air-treated HUVECs.....	180
Fig 6. 9 Glutathione pool changes of HUVECs after HBO or Air treatment only.....	182
Fig 6. 10 Glutathione pool responses to subsequent incubation with 0.1 and 0.2 mM of H <sub>2</sub> O <sub>2</sub> of Air or HBO treated HUVECs.....	184

# List of Tables

Table 1. 1 Normal wound healing process.....	6
Table 1. 2 Main regulators in angiogenesis and wound healing and process.....	10
Table 1. 3 $pO_2$ or $tcpO_2$ at different oxygen and pressure conditions.....	14
Table 3. 1 The endothelium index of aorta segment.....	84
Table 3. 2 The correlation test results.....	92
Table 5. 1 Free calcium concentration calculation of Ca-EGTA buffers.....	144
Table 6. 1 The cell viability.....	176
Table 6. 2 The correlation test results.....	185

# List of Abbreviations

7-NI	7-nitroindazole
ACh	acetylcholine
ADP	adenosine diphosphate
ADPR/pADPR	mono/poly ADP-ribosylation
ADRP	adenosine diphosphoribose
AH <sub>2</sub>	hydrogen donors
Air	expose to room air at ambient pressure
Ang-1,2	Angiopoietin-1,2
ArSH	2-nitro-5-thiobenzoic acid
ATA	atmosphere absolute
BAECs	bovine aortic endothelial cells
bFGF	basic fibroblast growth factor
Ca <sup>2+</sup>	calcium
[Ca <sup>2+</sup> ] <sub>i</sub>	intracellular calcium concentration
cADPR	cyclic ADP ribose
CAT	catalase
CBF	cerebral blood flow
CO <sub>2</sub>	carbon dioxide
DMSO	Dimethyl Sulfoxide

D-PBS	Dulbecco's phosphate buffered saline
DTNB	5,5-dithiobis-2-nitrobenzoic acid
ECGS	endothelial cell growth supplement
ECs	endothelial cells
ECM	extracellular matrix
EDTA	ethylenediaminetetraacetic acid
EGF	epidermal growth factor
EGTA	ethylene glycol bis ( $\beta$ -aminoethyl ether)- $N,N'$ -tetraacetate
ELISA	Enzyme Linked ImmunoSorbent Assay
eNOS	Endothelial nitric oxide synthase
EPC	endothelial progenitor cells
EPR	electron paramagnetic resonance
ER	endoplasmic reticulum
ET-1	endothelin-1
FPG	formamidopyrimidine DNA glycosylase
Fura-2	Fura-2 acetoxymethyl ester
GAGs	glycosaminoglycans
GM1899A	human lymphoblastoid
GPCRs	G-protein-coupled receptors
GPx	glutathione peroxidase

GSH	reduced glutathione
GSSG	oxidized glutathione
GR	glutathione reductase
GST	glutathione S-transferases
Hela	human transformed epithelial cells
HBO	hyperbaric oxygen
HBOT	hyperbaric oxygen therapy
HBSS	Hanks' balanced salt solution
HIF-1	hypoxia inducible factor-1
HO <sub>2</sub> <sup>·</sup>	hydroperoxyl radicals
H <sub>2</sub> O <sub>2</sub>	hydrogen peroxide
HRE	hypoxia-response element
HRP	horseradish peroxidase
HVA	homovanillic acid (3-methoxy-4-hydroxyphenylacetic acid)
HUVECs	human umbilical vein endothelial cells
ICAM-1	intercellular adhesion molecule-1
IGF-1,-2	insulin growth factor-1, -2
IL	interleukin
InsP <sub>3</sub>	inositol-1,4,5-trisphosphate
iNOS	inducible nitric oxide synthase

KGF	keratinocyte growth factor
LDL	low density lipoprotein
LDH	lactate dehydrogenase
L-NAME	NG-nitro-L-arginine methyl ester
L-NMMA	NG-monomethyl-L-arginine
LPS	lipopolysaccharide
MDA	malondialdehyde
MMPs	extracellular matrix proteins
NAADP	nicotinic acid-adenine dinucleotide phosphate
NADH	nicotinamide adenine dinucleotide
NADPH	nicotinamide adenine dinucleotide phosphate-oxidase
NAT	2,3-naphthotriazole
NBO	100% oxygen at 1 ATA
NEDA	N-(1-naphthyl) ethylenediamine
nNOS	neuronal nitric oxide synthase
NO	nitric oxide
NO <sub>2</sub> <sup>-</sup>	nitrite
NO <sub>3</sub> <sup>-</sup>	nitrate
NO <sub>x</sub>	NO <sub>2</sub> <sup>-</sup> + NO <sub>3</sub> <sup>-</sup>
NR	nitrate reductase

·OH	hydroxyl radicals
O <sub>2</sub>	molecular oxygen
O <sub>2</sub> <sup>-</sup>	superoxide
PAEC	pulmonary artery endothelial cells
PAI-1	plasminogen activator inhibitor type 1
PAF	platelet-activating factor
PDGF	platelet-derived growth factor
PI3K	phosphatidylinositol 3-kinase
PlGF	Placenta growth factor
PKC	protein kinase C
PMCA	plasma membrane Ca <sup>2+</sup> ATPase
PMN	polymorphonuclear leukocytes
pO <sub>2</sub>	Partial oxygen pressure
Ras-PI3-K-Akt	Ras/phosphatidylinositol 3-kinase/Akt
ROM	reactive oxygen metabolites
ROOH	hydroperoxides
ROS	reactive oxidative species
RTKs	receptor tyrosine kinases
RyR	ryanodine receptor
S1P	sphingosine 1-phosphate

scopoletin	7-hydroxy-6-methoxy-coumarin
SERCA	sarco-endoplasmic reticulum:Ca <sup>2+</sup> ATPase
SMC	smooth muscle cells
SOD	superoxide dismutase
SR	sarcoplasmic reticulum
TBARS	thiobarbituric acid reactive substances
tcpO <sub>2</sub>	transcutaneous oxygen pressure
TGF- $\alpha$ , $\beta$	transforming growth factor alpha, beta
TNB	trinitrobenzenesulphonic acid
TNF	tumour necrosis factor
tp	tissue protein
tPA	tissue plasminogen activator
tw	tissue weight
uPA	urokinse-type plasminogen activator
VCAM-1	vascular cell adhesion molecule-1
VEGF	vascular endothelial growth factor
VEGFR1,2	VEGF receptor-1,-2
vWF	von Willebrand factor

# Acknowledgments

First of all, I would like to thank Diving Diseases Research Centre, Plymouth and the University of Plymouth for giving me the opportunity to start this interesting project.

I own many people a sincere thank you for their unforgettable aids to have helped me through this long, difficult yet rewarding process of my Ph.D. research. I would like to thank Dr. Richard Handy, my director of studies, for his consistent encouragement, enormous patience and professional supervision throughout the whole course; and to Dr. John Moody, my secondary supervisor, who is always there to help me to overcome those difficulties; and to Dr. Phil Bryson and Dr. Gary Smerdon, for their support and valuable advice on the project from the clinical view.

I am very grateful to Dr. Stephen Thompson for his detailed review of my preliminary work and constructive suggestions on the project; and technicians, Lynne Cooper, Nicholas Crocker, Michael Whiffen, Andrew Atfield, Paul Waines, Trevor Worsey, Chris Coleman and Angela Watson, for their excellent and skilful technical support. Dr. Jackie Whatmore, Selina McHary (Peninsular Medical School), and Dr. Teresa Neuparth have generously helped me with this project, and deserve my sincere appreciation. I have also enjoyed the company of research group members, and value the useful discussions with them and other colleagues in our school.

Finally, my family deserve a particular recognition for their tremendous love and unconditional support during the past years. Surely, my most special love goes to my dear husband, who always loves me and supports me without any reservation, and shares my laughs and tears with greatest understanding in my everyday life throughout all these years.

I love you all!

# Author's Declaration

At no time during the registration for the degree of Doctor of Philosophy has the author been registered for any other University award.

This study was financed with the aid of a studentship from the Diving Diseases Research Centre, Plymouth and the University of Plymouth; and carried out in Laboratory of School of Biological Sciences, University of Plymouth.

A programme of advanced study was undertaken, which included a summer school course in Bioinformatics, the General Teaching Associate's (GTA) course, Home Office approved Rodent Licensee Course – Modules 1-3, and courses on safety and hazard assessment of liquid nitrogen, cylinder gases and etc.

Relevant scientific seminars and conferences were regularly attended at which work was often presented; external institutions were visited for consultation purposes.

## Publications:

1. Yuan, J., Moody, A.J., Smerdon, G. & Handy, R.D. (2006) Hyperbaric oxygen protects endothelial cells against H<sub>2</sub>O<sub>2</sub>-induced DNA damage, Proc. BioScience for the 21<sup>st</sup> century, 23-27<sup>th</sup> July, 2006, Glasgow. P147
2. J Yuan, R Handy, J Moody and P Bryson (2006) "Hyperbaric oxygen therapy does not stimulate production of detectable nitric oxide, vascular endothelial growth factor, or damage blood vessels *in vitro*." *Comparative Biochemistry and Physiology, Part A*, Vol 143, S107 (originally presented at Society Annual Meeting, 2-3 April, 2006, University of Kent, UK).
3. J Yuan, R Handy, P Bryson and J Moody. "Hyperbaric oxygen therapy does not stimulate detectable nitric oxide production, vascular endothelial growth factor, or

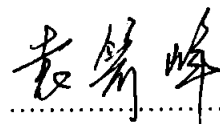
damage blood vessels *in vitro*." Proc. The Physiological Society Meeting, 17-20<sup>th</sup> Dec 2004, London, UK. P166-167

4. J Yuan, Y Chang, R Handy and J Moody. (2003) "The effects of endurance training on cardiomyocyte apoptosis and its related genes expression." *British Journal of Sports Medicine*, 37(5): 465 (originally presented at TheCuttingEdge, Joint conference of The British Association of Sport and Exercise Sciences and The British Association of Sport and Exercise Medicine, 3-6 Sep, 2003. Sheffield, UK).

#### Papers in Preparation

5. J. Yuan; R. Handy; J. Moody; and P. Bryson. "Effects of Therapeutic Hyperbaric Oxygen Treatment on Oxidative Stress and Angiogenesis Factors of Blood Vessel *In Vitro*", to be submitted to *American Journal of Physiology - Heart and Circulatory Physiology*.
6. J. Yuan; R. Handy; J. Moody; and P. Bryson. "Hyperbaric Oxygen Treatment Protects Human Umbilical Vein Endothelial Cells from Hydrogen Peroxide-induced DNA Damage", to be submitted to *Mutation Research*.

Word count of main body of thesis: 54,130

Signed  .....

Date 12/12/2007 .....

# **Chapter 1**

## **Background Review: Effects of Hyperbaric Oxygen Therapy on Angiogenesis in Chronic Wound Healing**

### **1.1 Introduction**

This chapter reviews the existing scientific and clinical evidence on the effects and proposed mechanisms on angiogenesis regulation in chronic wound healing during hyperbaric oxygen therapy. It starts with an introduction to the scientific background of wound healing, angiogenesis, followed by an overview on the clinical application of HBO therapy that stresses on chronic wound healing. Secondly, the role of oxygen in the wound healing process and in the regulation of angiogenesis is described in detail. Thirdly, the proposed mechanisms of HBO treatment facilitating angiogenesis are addressed and attention is focused on the angiogenesis factors such as vascular endothelial growth factor, nitric oxide and their interactions with reactive oxygen species. Finally, the summary is given in 1.7. The study described in Chapter 3 and 4 is mainly inspired by this review, and additional relevant research background emerging during the progress of the project is surveyed in the subsequent chapters wherever appropriate, mainly in the Introductions.

## 1.2 Wound Healing Process

Wound healing is a dynamic and highly structured process, which has been artificially divided into three phases: the inflammatory, proliferative, and remodelling phases. This coordinated process involves the appearance of specific cell types in the wound environment in a specific order: platelets, neutrophils, macrophages, lymphocytes and then fibroblasts and new blood vessels (Bates et al., 2003).

### 1.2.1. The Inflammatory Phase

The inflammation phase includes hemostasis and inflammation, and is a period of preparation of the wound environment for healing. Hemostasis starts immediately after the insult and may continue for a few days. The bleeding after blood vessel disruption initiates vasoconstriction via physical action and potent vasoconstrictors secretion (e.g. thromboxane A<sub>2</sub> and prostaglandin 2 $\alpha$ ). During constriction, platelets are activated. They adhere to damaged endothelium and discharge adenosine diphosphate (ADP), which promotes thrombocyte clumping to dam the wound. In addition, to initiate blood clotting, platelets also secrete several mediators such as platelet-derived growth factor (PDGF), transforming growth factor beta (TGF- $\beta$ ), epidermal growth factor (EGF), insulin growth factor-1 (IGF-1), fibronectin, von Willebrand factor (vWF) etc (see Jurk and Kehrel, 2005 for review). These factors help stabilise the wound through clot formation and many of them are chemotactic for inflammatory cells, keratinocytes, fibroblasts, and endothelial cells (ECs). For example, platelet degranulation activates the complement cascade, specifically C<sub>5a</sub>, which is a potent chemoattractant for neutrophils. In addition, the fibronectin/fibrin-rich clot provides a provisional matrix for cell migration.

After a brief period of constriction (5-10 min), these same vessels dilate and the permeability of capillaries increases local histamine release, allowing plasma, blood components, and inflammatory cells into the injured area. The early inflammatory phase happens within the first 6-8 hours and is characterized by the influx of neutrophils. Neutrophils are responsible for debris scavenging, complement-mediated opsonization of bacteria, and bacteria destruction via the oxidative burst mechanisms (i.e. superoxide and hydrogen peroxide formation). The timeline for inflammatory cell migration in a normal wound healing process is predictable. When the polymorphonuclear leukocytes (PMNs) engorge the wound, the inflammation process is underway. The PMNs attain their maximal numbers in 24-48 hours and commence their departure by hour 72.

About 24 hours after arrival of the PMNs, a larger and less specific type of phagocytic cell, called the macrophage, enters the wound area and remains for an extended period. This type of cell is vital for the initiation of granulation tissue formation. A wound may heal in the absence of PMNs, but it can not heal in the absence of macrophages. During days 3-4, the macrophages phagocytose microorganisms and wound debris, and meanwhile manufacture many biological factors such as collagenases, interleukins, tumour necrosis factor (TNF), TGF- $\beta$ , VEGF and PDGF that stimulate epithelial cell growth, angiogenesis, and attraction of fibroblasts.

### **1.2.2. The Proliferative Phase**

The proliferative phase constitutes fibroplasia, matrix deposition, angiogenesis, and epithelialization (Cho, 1998). As early as 24 to 48 hours after injury, fibroblasts and vascular ECs begin proliferating to form a specialised soft, pink granular tissue known as granulation tissue. This is a fragile tissue that bleeds easily due to its numerous newly developed capillary buds, and it forms the foundation for scar tissue development.

Collagen synthesis by fibroblasts and capillary proliferation occur simultaneously: the growth of new blood vessels is required to provide oxygen for collagen production; and collagen secreted from fibroblasts is required to form a supportive matrix for new capillary growth.

Fibroblasts are connective tissue cells that actively synthesize and secrete extracellular matrix proteins (MMPs) such as glycosaminoglycans (GAGs), fibronectin and new collagen of subtypes I and III. Collagen synthesis reaches a peak within 5-7 days and continues for several weeks, depending on wound size. Fibroblasts also produce a family of growth factors that are already present within the wound bed to enforce the induction of angiogenesis and endothelial cell proliferation and migration. Keratinocyte growth factor (KGF), which is unique to fibroblasts, acts specifically to stimulate keratinocyte migration and proliferation (Wener, 1998). The fibroblast is a source of proteinases and protease inhibitors, which aid in the process of endothelial cell migration and matrix reorganisation.

Angiogenesis is the product of parent vessel offshoots. The formation of new vasculature requires extracellular matrix (ECM) and basement membrane degradation followed by migration, mitosis and maturation of ECs. The new capillaries deliver nutrients to the wound and help maintain the granulation tissue bed. The migration of capillaries into the wound bed is critical for proper wound healing (Folkman, 1997). Wounds that heal by secondary intention have more necrotic debris and exudate to remove, so they involve larger amounts of granulation tissue (King, 2001). The newly formed blood vessels in granulation tissue are leaky, which allows plasma proteins and white blood cells to infiltrate into the surrounding tissue (Mercandetti, 2002). The angiogenesis is regulated by various angiogenesis factors, which is a hot topic in wound management field as well as in cancer research.

Re-epithelization begins with the cell migration during the inflammatory phase and is completed during the proliferative phase. If the basement membrane remains intact, the epithelial cells migrate upward in the normal pattern and are restored in 2-3 days. This is equivalent to a first-degree skin burn. If the basement membrane has been destroyed, similar to a second- or third-degree burn, the wound is re-epithelialized from the normal cells in the periphery and from the skin appendages between the scab and the underlying viable tissue. When a significant portion of the wound has been covered with epithelial tissue, the scab lifts off, which is important for the restoration of the normal skin barrier function and prevention of wound infection.

### **1.2.3. The Remodelling Phase**

The final phase of wound healing is remodelling phase, or maturational phase. It begins about 3 weeks after injury and can continue for 6 months to 2 years, depending on extent of the wound. Collagen is degraded and deposited in an equilibrium-producing fashion, and the wound undergoes contraction, ultimately resulting in a smaller amount of apparent scar tissue. Apoptosis removes differentiated myofibroblasts from the wound bed, and blood vessels regress (Gabbiani, 1996; Savill, 1997). The extracellular matrix changes from a provisional wound matrix composed predominantly of fibronectin and nonsulfated glycosaminoglycans to that of a dermal matrix composed of thickened collagen bundles and sulfated proteoglycans. During this phase, the epidermis becomes thinner and the normal pattern of differentiation is restored, but most wounds do not gain the full tensile strength as undamaged skin even after healing is completed. The best ultimate resultant scar has only 80% of the tensile strength of the original skin (Mutsaers et al., 1997).

The main tissue events and cellular responses in the three phases of normal wound healing process are summarised in Table 1.1.

Table 1. 1 Normal wound healing process.

Phases	Duration	Stage Description	Cells Involved	Factor Released
<b>Inflammatory</b>	From immediately after the injury to a few days	Influx of neutrophils; Clot formation; Secret soluble mediators; Phagocytization of micro-organisms and wound debris; Initiation of granulation tissue formation; Re-epithelialization begins;	Platelet; PMNs; Macrophage; Lymphocyte;	PDGF; VEGF; TGF- $\alpha$ ; TGF- $\beta$ ; bFGF; IGF-1; EGF; C <sub>3a</sub> ; C <sub>5a</sub> ; IL-1; TNF; etc
<b>Proliferative</b>	From days 3-7 to 4 weeks or longer	Influx of and interaction among fibroblasts, endothelial cell, and keratinocytes; Wound contraction; ECM production; Angiogenesis; Re-epithelialization complete; Wound closed and healed;	Fibroblasts; Endothelial cell; Epithelial cell	KGF; proteinases; proteinase inhibitors; GAGs; plasminogen activator; collagenase; etc
<b>Remodelling</b>	From the third week to years	Normal pattern of differentiation restored; Apoptosis happen; ECM changes from provisional wound matrix to a dermal matrix	Myofibroblasts	Growth factors Proteinase.

Summarized from Bennett and Schultz, 1993a, 1993b; Mutsaers, 1997; Singer, 1999; Staiano-Coico, 2000.

### 1.3 Angiogenesis in Wound Healing

Angiogenesis consists of local disruption of blood vessel basement membrane, migration into the local interstitial stroma, cell proliferation, new vessel formation, stabilization, and eventually involution of the newly formed vascular bed (Madri and Marx, 1992). Although angiogenesis is an important phenomenon that occurs during the proliferative phase, many signals and regulatory mediators for angiogenesis occur or are secreted in the inflammatory phase.

Microvascular endothelial cells are the principal parenchymal cells involved in wound angiogenesis (Madri et al., 1996). Upon injury, angiogenic growth factors (proteins) produced or released from injured tissues bind to their specific receptors located on the ECs to activate the ECs. Sprout formation during the initial steps of the angiogenic process,

is commonly preceded by strong and persistent vasodilation and increased vascular permeability (Morbidelli et al., 2003). Vascular endothelial growth factor (VEGF) is a major player in angiogenesis initiation based on its ability to induce vascular relaxation via endothelial NO production and increase ECs' permeability, which is a prerequisite for ECs to enter the angiogenic cascade, and morphologic changes in ECs decrease the confluence status to make them susceptible to mitogens (Ziche et al., 1997; Folkman, 1997).

The activated ECs of existing blood vessels must degrade the underlying basement membrane and invade into the stroma of the neighbouring tissue. Invasion and migration of ECs requires the cooperative activity of proteolytic enzymes such as serine proteases and matrix metalloproteinases (MMPs), which are produced by surrounding cells as well as ECs themselves. The urokinase-type plasminogen activator (uPA) and tissue plasminogen activator (tPA) are serine proteases that catalyse the conversion of plasminogen into plasmin. The fibrinolytic activity in blood is mainly regulated by tPA, whereas the activation of plasminogen in tissues is regulated by uPA (Mignatti and Rifkin, 1996). Plasmin has broad substrate specificity and degrades several extracellular matrix (ECM) components, including fibrin, fibronectin, laminin, and the protein core of proteoglycans (Mignatti and Rifkin, 1996). In addition, plasmin may activate several MMPs such as MMP-1, MMP-3, and MMP-9. Matrix metalloproteinases (MMPs) are a large family of enzymes that degrade the extracellular matrix. MMPs have been classified according to their domain structure or substrate specificity. For example, MMP-2 and MMP-9, also called type IV collagenases or gelatinases, are related enzymes that break down type IV collagen which is the main structure protein of basement membrane (Hostikka and Tryggvason, 1988; Liotta, et al., 1980). The expression of uPA, uPAR and MMPs of ECs and fibroblast is upregulated by angiogenic growth factors such as bFGF (Giuliani, et al. 1999), VEGF (Mandriota and Pepper, 1997), TGF- $\beta$ 1 (Uria, et al. 1998) and cytokines

(van Hinsbergh, et al. 1990). It should be noted that PAs and MMPs are secreted together with and regulated by their inhibitors PAIs and TIMPs, ensuring a stringent control of local proteolytic activity, and the activity of plasmin is also regulated by  $\alpha$ 2-antiplasimin. A tight control of proteolysis is necessary for normal angiogenesis in order to preserve normal tissue structure (see Liekens, et al., 2001 for review).

Following proteolytic degradation of the ECM, 'leader' ECs start to penetrate the basement membrane. These are followed by proliferating ECs, whose growth has been stimulated in part by soluble factors released by hypoxic tissue and partly by growth factors released from the degraded ECM. Specific cell adhesion molecules serve as "grappling hooks" to pull the sprouting new blood vessels forward towards the hypoxia site. Cell adhesion molecules can be classified into four families depending on their biochemical and structural characteristics. These families include the selectins, the immunoglobulin supergene family, the cadherins, and the integrins. ECs express several distinct integrins, which allows the attachment to a wide variety of ECM proteins and also mediates the EC-ECM interaction (Eliceiri and Cheresh, 1999). Integrin  $\alpha_v\beta_3$ , is a receptor for a number of proteins with an exposed Arg-Gly-Asp sequence (e.g. fibronectin, vitronectin, laminin, vWF, fibrinogen, and denatured collagen), has been found to be particularly important during angiogenesis. It is nearly undetectable on quiescent endothelium, but is highly up-regulated during cytokine-induced angiogenesis. Other cell adhesion molecules such as intercellular adhesion molecule-1 (ICAM-1), and vascular cell adhesion molecule-1 (VCAM-1), members of the immunoglobulin supergene family are all expressed on the ECs' surface and involved into endothelial cell-cell adhesion to partly modulate ECs' migration and signalling (Albelda and Buck, 1990).

Sprouting ECs roll up to form a blood vessel tube and then individual blood vessel tubes connect to form vascular loops. Finally, newly formed blood vessel tubes are

stabilised by specialised muscle cells (smooth muscle cells and pericytes) that provide structural support. ECs' interaction with ECM and mesenchymal cells is a prerequisite to form a stable vasculature and angiopoietins and cytokines mediate this interaction (Griffioen and Molema., 2000). Angiopoietins receptor tyrosine kinase Tie1 and Tie2 play critical roles in these stages of angiogenesis by establishing stable cellular and biochemical interactions with the surrounding mesenchyme (Maisonpierre et al., 1997). Tie1 function is related to endothelial cell differentiation and the establishment of blood vessel integrity (Puri et al., 1995) and Tie2 is particularly important for vascular network formation (Sato et al., 1995). Both angiopoietin-1 and angiopoietin-2 are Tie2-specific ligands, but only the binding of angiopoietin-1 results in signal transduction and regulation of blood vessel maturation (Suri, et al. 1996). Angiopoietin-2 antagonizes angiopoietin-1 in the vasculature in vivo and may act as a check on angiopoietin-1/Tie2-mediated angiogenesis to prevent excessive branching and sprouting of blood vessels (Maisonpierre, et al., 1997). In addition, angiopoietin-2 renders endothelium sensitive to angiogenic factors such as VEGF via induction of smooth muscle cell/pericyte loss and hence destabilizes the neovasculature (Maisonpierre et al., 1997; Asahara et al., 1998).

Every stage of angiogenesis is highly regulated by signals from both the serum and the surrounding specialized extracellular matrix (Risau, 1997). The healthy body normally maintains a perfect balance of angiogenesis modulators. The 'angiogenic switch' is 'off' when the effect of pro-angiogenic molecules is balanced by that of anti-angiogenic molecules, and is 'on' when the net balance is tipped in favour of angiogenesis. In normal wound healing process, the 'switch on' of angiogenesis is successfully regulation by growth factors. The main molecules in wound healing and how they affect ECs in angiogenesis are summarised in Table 1.2.

**Table 1. 2 Main regulators in angiogenesis and wound healing and process.**

Stimulators	Major source in wound healing	Target cells and major effects in wound healing	Effects on endothelial cells and angiogenesis			
			Prolifera- tion	Migration	Differentia- tion	Others
VEGF (Vascular endothelial growth factor)	epidermal cells, macrophages, endothelial cells, platelets	angiogenesis, increased vascular permeability	yes	yes	yes	(+) permeability (+) uPA/PAI-1 production (-) apoptosis
bFGF (Fibroblast growth factor)	macrophages, endothelial cells	angiogenesis, fibroblast proliferation	yes	yes	yes	(+) uPA/protease production (+) tube formation
PDGF (Platelet-derived growth factor)	platelets, macrophages, epidermal cells	fibroblast proliferation and chemoattraction; macrophage chemoattraction and activation	yes	yes	yes	(+) chords formation in vitro (+) recruitment of smooth muscle cells and pericytes
TGF- $\alpha$ (Transforming growth factor $\alpha$ )	macrophages, keratinocytes	mitogenesis for keratinocytes and fibroblasts; keratinocyte migration	yes	yes	yes	(+) angiogenesis in vivo
TGF- $\beta$ (Transforming growth factor $\beta$ )	platelets, macrophages	keratinocytes mobility; chemotaxias of macrophages and fibroblasts; ECM synthesis and remodelling	Inhibition	no	yes	(+) in vivo angiogenesis in presence of inflammatory response Produce net antiproteolytic activity ( $\uparrow$ ) vessel wall stability
Ang-1 (angiopoictin-1)	endothelial cells, mesenchymal cells	Angiogenesis	no	yes	yes	(+) in vitro sprout formation ( $\uparrow$ ) girth and stability of endothelium

Summarised from Mutsaers, et al., 1997; Staiano-coico, et al., 2000; Reenstra-Buras, 2003; Papetti and Herman, 2001; Liekens, et al., 2001; Griffioen and Molema., 2000.

## 1.4 Chronic Wound and Hypoxia

Normal wound healing is a highly orchestrated process of events and the biologically phases are coordinated to allow a wound to heal without delay. However, wound healing process may be disrupted and delayed by many factors such as malnutrition; impaired blood flow and oxygen delivery; impaired inflammatory and immune responses; wound contamination and infection; age effects etc (Stevens, 2000). A wound that does not heal within three months is considered chronic, and impaired wound healing mostly affects people over the age of 60 with an incidence of 0.78% (Mustoe, 2004). As the population ages, the number of chronic wounds is expected to rise. The vast majority of chronic wounds can be classified into three categories: venous ulcers, diabetic ulcers, and pressure ulcers. A small number of wounds that do not fall into these categories may be due to causes such as radiation poisoning or ischemia (Mustoe, 2004).

The predominant pathophysiological manifestation of chronic wound includes ischemia/hypoxia, infection and impaired production of growth factors and proteolytic enzymes. Although a transient ischemia and hypoxia in vasoconstriction during the inflammatory phase is essential to initiate the wound healing cascades, persistent hypoxia and blood flow deficiency will cause defective leukocyte killing, impaired neoangiogenesis, and defective macrophage and fibroblast function (for details, see 1.5). A wound partial pressure of oxygen less than 30 to 40 mm Hg is associated with decreased or deficient cellular activity and clinically has been shown to result in poor wound healing (Wu, 1995). Neutrophils and other leukocytes consume oxygen to produce reactive oxidative species (ROS) and inflammatory cytokines to fight pathogens, which when overwhelmed also jeopardise cells and prevent cell proliferation and wound closure by damaging DNA, lipids, proteins, the ECM, and cytokines that speed healing at the same time (Mustoe, 2004,

Snyder et al., 2005; Alleva et al., 2005). The repetitive infections in chronic wounds keep neutrophils stay longer and attract more neutrophils, which contribute to further hypoxia and higher levels of inflammatory cytokines and ROS (Taylor et al., 2005). In addition, chronic wounds seem to have a higher concentration of proteolytic enzymes such as elastase and MMPs in their fluids (Schönfelder et al., 2005), and the oxygen-related growth factors such as PDGF, VEGF, KGF etc are lower in chronic wound sites (Edwards et al., 2004). Growth factors are imperative for timely wound healing, especially in promoting new vascular formation to resume oxygen supply. However, in chronic wounds, the formation and release of growth factors may be prevented or degraded in excess by cellular or bacterial proteases (Crovetti et al., 2004). Together, the three syndromes in chronic wound tie up and interact to aggravate the status of wound. The injured tissue has an increased metabolic demand for oxygen utilisation to initiate and support wound healing, while the disrupted capillary network fails to reconstruct on time due to impaired factors in the chronic wound site; therefore, hyperbaric oxygen therapy that convert the persistent hypoxia condition will make a principal contribution for facilitating chronic wound healing.

## **1.5 Hyperbaric Oxygen Therapy**

### **1.5.1. Introduction**

Compressed air has been used as a therapeutic tool since medieval times with variable success and without any knowledge of what may cause of its beneficial effect on disease. Hyperbaric oxygen therapy (HBOT) has been used clinically as early as mid 1800s. It is not until 1930s that HBOT has been used safely to help deep-sea divers with decompression sickness. Clinical trials in the 1950s uncovered a number of beneficial outcomes from exposure to hyperbaric oxygen (HBO). These experiments were the

forerunners of contemporary applications of HBOT in the clinical setting. HBOT was first used to assist wound healing when it was noted in 1965 that burns of the victims of a coal mine explosion, treated with HBO for their carbon monoxide poisoning, healed faster. Today, the Undersea & Hyperbaric Medical Society through its Committee on Hyperbaric Oxygen Therapy continually reviews and evaluates current and potential indications for hyperbaric oxygen therapy. Recommendations are made in its "Hyperbaric Oxygen Therapy Committee Report" (UHMS, 2002).

(A) HBOT is currently indicated as the primary mode of therapy for: air or gas embolism, decompression sickness and carbon monoxide poisoning.

(B) HBOT is currently indicated as an important adjunctive therapy for: radiation tissue damage, clostridial myonecrosis, compromised skin grafts and flaps, crush injury, compartment syndrome, acute traumatic ischemias, necrotizing soft tissue infections, and problem non-healing wounds.

### **1.5.2. Application of Hyperbaric Oxygen Therapy to Chronic Wound**

The Earth's atmosphere normally exerts 14.7 pounds per square inch of pressure (760 mmHg) at sea level. That is equivalent to one atmosphere absolute (abbreviated as 1 ATA). Hyperbaric Oxygen Therapy (HBOT) is defined as a treatment mode in which the patient is entirely enclosed in a pressure chamber breathing 100% pure oxygen at a pressure greater than 1 ATA. However, breathing 100% oxygen at 1 ATA or applying oxygen outside a pressurised chamber is not considered hyperbaric oxygenation.

As a comparison, an average person breathes in about 6 pounds of oxygen a day, while by giving high concentrations of oxygen under increased pressure (2.0– 2.4 ATA), a person will take in about 2.4 pounds of oxygen in a single hour of HBOT. The partial oxygen pressure in normobaric air is about 160 mm Hg, which decreases to 1-3 mm Hg in

mitochondria as the oxygen is delivered to cell and tissue by blood through cardiovascular system. Normally, most of the oxygen in blood is carried by haemoglobin, with minimal additional oxygen dissolved in the plasma. During HBOT, the dissolved oxygen in the blood can make a more than 30% significantly increase in oxygen-carrying capacity. This increase saturates the tissues with oxygen, and reverses any areas in hypoxia. By comparing partial oxygen pressure ( $pO_2$ ) or transcutaneous oxygen pressure ( $tcpO_2$ ) values under different oxygen and pressure conditions, we can see the powerful effects of HBOT on oxygen delivery and tissue oxygenation (see Table 1.3).

**Table 1.3  $pO_2$  or  $tcpO_2$  at different oxygen and pressure conditions (adapted from Sheffield, 1998).**

Oxygen	21% Oxygen (Air)	100% Oxygen	100% Oxygen
Atmosphere Pressure (ATA)	1.0	1.0	2.4
Air $pO_2$ (mm Hg)	159	760	1824
Alveolar $pO_2$ (mm Hg)	104	673	1737
Arterial $pO_2$ (mm Hg)	100	660	1700
Venous $pO_2$ (mm Hg)	36	60	1650
Muscle $pO_2$ (mm Hg)	29	59	250
Subcutaneous $pO_2$ (mm Hg)	40	200-300	250-500
Chest $tcpO_2$ (mm Hg)	67	450	1312
Foot $tcpO_2$ (mm Hg)	63	280	919
Chronic Wound $pO_2$ (mm Hg)	15	200-400	660

The clinical HBOT regimen for chronic wounds is dependent on the severity of the situation. In the absence of infection, HBO once per day at 2.0–2.4 ATA for 90–120 minutes is sufficient to stimulate wound healing. In the presence of infection or a high risk of limb loss, treatment twice per day is recommended (Stone and Cianci, 1997). Even though treatment sessions are relatively brief, oxygen tensions may remain elevated in subcutaneous tissue for several hours after exposure (Thom, 1989). HBOT is considered unnecessary for simple, well-perfused wounds, but has helped many hypoxic or ischemic wounds to recovery successfully (Zamboni, et al. 2003; Stone and Cianci., 2003). The beneficial effect of HBOT for chronic wound includes vasoconstriction to reduce oedema

and promote oxygen diffusion rate; hyperoxygenation of tissue to provide oxygen needed to stimulate and support wound healing; and favourably influence important cytokines and growth factors (Wright, 2001).

Although there have been decades of reported beneficial clinical trails of HBOT on chronic wound healing, there are still failed cases reported (Davis, 1987; Ciaravino et al., 1996). It seems that not all patients with chronic wound respond to HBOT and an index is needed to predict HBOT outcome and response. Transcutaneous oxygen tension (TcPO<sub>2</sub>) has been proved suitable to evaluate tissue hypoxia, wound healing potential, patient selection for HBOT, and to monitor progress during therapy. As early as 1988, Wyss et al reported that in postoperative patients, at sea-level air TcPO<sub>2</sub> readings < 20 mm Hg with poor healing, 20 – 40 mm Hg with intermediate healing, and > 40 mm Hg with good healing. This was supported by the finding that wound partial pressure of oxygen less than 30 to 40 mm Hg is associated with decreased or deficient cellular activity and clinically has been shown to result in poor wound healing (Wu, 1995). In 2002, Fife et al retrospectively analysed TcPO<sub>2</sub> values of 1144 lower extremity wound patients to determine the reliability of TcPO<sub>2</sub> in predicting outcomes of HBO therapy. TcPO<sub>2</sub> data were provided under breathing air, breathing oxygen at sea level, and breathing oxygen in the pressure chamber. Patients with baseline air TcPO<sub>2</sub> greater than 40 mm Hg were generally excluded from HBOT. The failure rate was only 35% for the 629 hyperbaric patients, and 48% of them had a baseline TcPO<sub>2</sub> below 20mm Hg. This may suggest the TcPO<sub>2</sub> of baseline sea-level air only identified the degree of tissue hypoxia and whether the wound is likely to heal spontaneously, but had little statistical relationship with outcome prediction because some patients healed after HBOT despite very low pre-hyperbaric TcPO<sub>2</sub> values. TcPO<sub>2</sub> value of breathing oxygen at sea level was 68% reliable for predicting success but unreliable for predicting failure after HBOT. The patients with 35

mm Hg or greater sea-level oxygen TcPO<sub>2</sub> were likely to benefit from HBOT. This result was consistent with the finding of Sheffield (2001) that a minimum 50% increase or a minimum floor (35 mm Hg) of sea-level oxygen TcPO<sub>2</sub> for predicting successful HBOT. The in-chamber TcPO<sub>2</sub> was originally described by Wattel et al (1991) to use as a predicative tool, and Fife et al (2002) agreed that in-chamber TcPO<sub>2</sub> provided the best single discriminator between success and failure of HBOT, and set forward a cutoff score of 200 mmHg. When a sea-level air TcPO<sub>2</sub> < 15 mmHg is combined with an in-chamber TcPO<sub>2</sub> < 400 mmHg, a better predictive result is achieved with reliability of 75.8% on predicting failure HBOT and 73.3% on predicting positive HBOT, respectively. Therefore, oxygen level is the key factor for wound healing and a good response to oxygen is needed for a successful HBO treatment in chronic wound.

### **1.5.3. Role of Oxygen and HBOT in Chronic Wound Healing**

Oxygen is a critical nutritional substrate for healing tissue and the oxygen tension is a major controlling factor in bacterial killing, resistance to infection, collagen synthesis, angiogenesis, and epithelization. The clinical evidence and scientific research on HBO treatment of chronic wound have all shown promising benefits.

Wound healing commences with blood coagulation followed by infiltration of neutrophils and macrophages, which release reactive oxygen species (ROS) by an oxygen-consuming respiratory burst (Sen et al., 2002). The oxidants in this early stage serve mainly to kill bacteria and prevent wound infection (Babior et al., 1973). A local PO<sub>2</sub> of 30 mm Hg or higher is needed for phagocytes to kill bacteria effectively (Knighton et al., 1984) and Allen et al (1997) demonstrated that the ability of neutrophils to produce oxygen radicals and to kill bacteria via oxidative mechanisms is directly proportional to local oxygen tension; the half-maximal oxidant production of neutrophils occurred in the range

of 45 to 80 mm Hg  $PO_2$ , and maximal at  $PO_2$  higher than 300 mm Hg. The oxygen tension of non-healing wounds ranges from 5 to 20 mm Hg, which limits the leukocyte's function. Thus, polymicrobial infection and impaired immune cell function are one of the predominant characters of chronic wound (Sapico, et al., 1984; Millington and Norris, 2000). HBOT not only increases the host antimicrobial defenses via provision of more oxygen for leukocytes, and also has a direct bacteriostatic effect on anaerobic microorganisms although this is rather limited – only seen in restricted media at high ATA (Knighton et al., 1984, 1986; Mader et al., 1987, 1989).

Fibroblasts require oxygen for collagen synthesis and deposition, which is a fundamental step in wound healing to provide the matrix for angiogenesis and tissue remodelling. All the key enzymes in collagen synthesis such as prolyl hydroxylase, lysyl hydroxylase and lysyl oxidase require molecular oxygen as a cofactor to perform their functions.) A  $PO_2$  of 20 mmHg was the critical level for new collagen formation and accumulation, and maximal collagen synthesis occurred at levels approaching 250 mmHg (Myllyla, et al. 1977; Niinikoski, 1980), and the hypoxia in chronic wound compromises collagen synthesis by fibroblasts (Niinikoski, 1972; Hunt et al, 1972, 1974; Siddiqui et al., 1996;). Lerman et al (2003) reported that adult diabetic mouse fibroblasts exhibited a 75% reduction in migration compared to normal fibroblasts and were not significantly stimulated by hypoxia (1%  $O_2$ ), whereas wild-type fibroblast migration was up-regulated nearly two fold in hypoxic conditions; this might suggest why diabetics have a high incidence of chronic wounds. Oxygen supplement increases wound oxygenation and improves collagen deposition and tensile strength (Niinikoski, 1970; Stephens and Hunt, 1971; Hunt and Pai, 1972; Gordillo et al., 2003). Tompach et al (1997) reported increased fibroblast proliferation after 120 min exposure to HBO and this stimulation lasted 72 h after exposure. The HBO effect varies according to treatment pressure and time; prolonged

expose to high concentration of oxygen and expose to high pressure may cause damage. Dimitrijevič et al. (1999) demonstrated increased human fibroblast proliferation from 2 to 5 days at 1, 2, 2.5 and 3 ATA HBO treatments; the most stimulatory effect appeared at 1 ATA after 2 days of treatment. They also confirmed that prolonged hyperoxia (12 h of HBO at 2 ATA to 3 ATA) caused adverse effects ranging from morphological changes to cytotoxicity and suppression of collagen synthesis was seen after day 5 at 3 ATA. Similar findings were reported by Conconi et al (2003), at 1 ATA, all HBO exposure (15, 30, 60 or 120 min) increased the proliferation rate of cultured fibroblasts; whereas at 2.5 ATA, only 30 and 60 min exposures raised the proliferation rate; 120 min exposure exerted a marked pro-apoptotic effect.

The beneficial effects of HBO treatment on endothelial cell proliferation and function are confirmed mostly by in vitro studies. Endothelial cells mediate the local inflammatory response through modulation of vascular tone and local blood flow, change in vascular permeability, induction of a prothrombotic surface as well as stimulation and direction of extravasation in granulation tissue formation (Ranby, 1982). As little as 15 min HBO exposure at 2.4 ATA significantly increased the <sup>3</sup>H-labeled thymidine incorporation level of endothelial cells, and a maximal level was reached after 60 min exposure. However, longer HBO treatment (up to 120 min) or a second exposure on the same day resulted in little or no additional proliferation increase (Tompach et al., 1997). Endothelial cells produce tissue plasminogen activator (t-PA) and plasminogen activator inhibitor type 1 (PAI-1), which plays essential antagonising roles in the fibrinolytic system (van Hinsbergh, 1988). HBO affects endothelial cell function and their fibrinolytic response. Tjamstrom et al (1999 and 2001) suggested that HBO treatment (2.5 ATA) increased gene expression for both t-PA and PAI-1 in endothelium and has a swift influence on the release of t-PA and PAI-1 from endothelium. They found that both t-PA and PAI-1 levels in medium showed significant

higher than control group immediate post HBO treatment, but at 6 h post treatment only PAI-1 kept at high level while the t-PA level did not. There might be a synergistic effect on the secretion of PAI-1 of HBO by raising ambient pressure and partial pressure of O<sub>2</sub>. They furthered their study to investigate the effect of HBO treatment on fibrinolytic factors of cultured endothelial cells in a simulated ischaemia-reperfusion model in 2001. Endothelial cells were subjected to anoxia for 8 h, followed by reperfusion with either HBO or normobaric air for 1.5 h. Anoxia appeared to stimulate the endothelial cells to produce and secrete t-PA, PAI-1 and uPA, and this effect was then augmented after reoxygenation with HBO, but was not seen after reoxygenation with normobaric air. Immediately after 8 h anoxia and reoxygenation with HBO for 1.5 h, the concentrations of t-PA, PAI-1 and uPA were significantly increased in the medium. The increase persisted throughout the experiment at 1.5 h, 6 h and 24 h post anoxia. This indicated that HBO did not decrease the secretion by endothelial cells and on the contrary that HBO reoxygenation sustained the increased secretion of fibrolytic proteins of hypoxic endothelial cells. Buras et al (2000) reported that hypoxia/hypoglycaemia increased ICAM-1 expression and adhesion of polymorphonuclear leukocytes (PMN) to endothelial cells; HBO treatment reduced these increases to control levels through induction of the synthesis of endothelial cell nitric oxide synthase (eNOS). Lin et al (2002) also reported that nitric oxide signalling pathway was required for HBO induced Ang2 expression in endothelial cells.

The evidence that HBO treatment promotes angiogenesis in chronic wound is provided mostly via in vivo studies. Sheffield (1988) has demonstrated improvement in capillaries and in blood flow over the first 3 weeks of HBO by measuring transcutaneous oxygen over healing tissue in the diabetic foot. Similar positive vascularity was observed in ischemic irradiated tissue (Marx, 1990) and muscle flaps (Bayati et al., 1998). Mechine et al (1999) presents significant higher vascular density and height of the granulation tissue

bud after 7 days HBO treatment. In recent years, Muhonen et al (2004) reported that HBO induced a markedly increase of angiogenic response histomorphometrically in radiotherapy-disturbed mandibular distraction bone formation of rabbits, and Sheikh et al (2005) used laser Doppler imaging to measure wound bed perfusion of mice full-thickness dorsal dermal wounds as an indication for wound angiogenesis and demonstrated a significant increase of blood flow from day 7 of HBO treatment (90 min at 2.1 ATA for 7 days); and a significant 20% higher wound blood flow on day 10 in the HBO group.

Although clinical experience and scientific studies have provided abundant evidence for the beneficial effects of HBO treatment on angiogenesis in chronic wound healing, and studies on its pathophysiological mechanisms have been carried out throughout the history of HBOT, because of the complexity of human body and the limitation of technology, the mechanism of how HBOT facilitates wound angiogenesis is still far from understood. On the other hand, the application of 100% pure oxygen under pressure leads to hyperoxic reoxygenation as shown in Table 1.3. Studies on the HBO therapy suggested that HBO strategies should be purposely selected to minimize possible adverse effects and guarantee clinical benefits.

### **1.5.4. Hyperbaric Oxygen Therapy and Oxidative Stress**

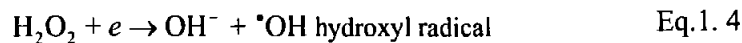
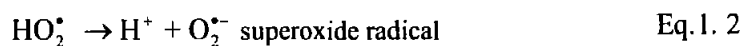
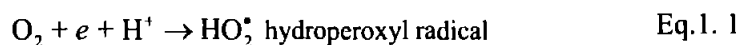
Hyperoxia or hyperoxic environment implies one in which the partial pressure of oxygen is above the normally seen by the particular animal organ or organelle. Exposing to hyperoxia may cause hyperoxic toxicity (Jamieson et al., 1986). Animals exposed to HBO over 2 ATA experience abnormal motor activity such as shivering, jerks, and "wet-dog" shakes, which may progress to tonic-clonic seizures and death if the HBO exposure is prolonged (Balentine, 1973). Further investigation suggested that the animal death may due to the hyperoxia-induced pulmonary damage characterized by such macroscopic

changes as pulmonary edema and alveolar hemorrhage (Jamieson et al., 1986). HBO toxic effects in human have been described such as visual changes, nausea, muscle twitching, irritability, dizziness, and/or convulsions (Gabb and Robin, 1987). The toxic effects of HBO normally happened at high pressure and prolonged duration, which are believed to due to the production of reactive oxygen species at a rate in excess of the capacity of the cellular antioxidant defence mechanisms (Fridovich, 1978).

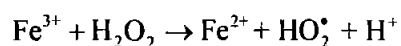
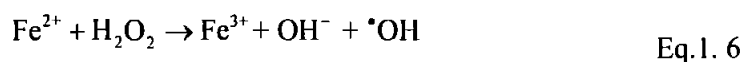
#### 1.5.4.1. Reactive Oxidative Species and Antioxidants

ROS are characterised by their high chemical reactivity, and which include both free radicals (that is, species with one or more unpaired electrons, such as superoxide ( $O_2^{\cdot-}$ ) and hydroxyl radicals ( $\cdot OH$ )), and non-radical species such as hydrogen peroxide ( $H_2O_2$ ) (Shah and Channon, 2004).

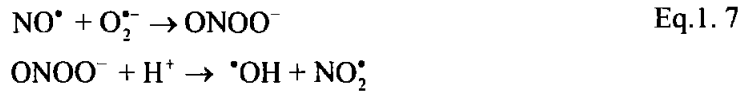
Under normal condition, molecular oxygen ( $O_2$ ) is stable, but when it is reduced by the stepwise addition of electrons, for example during electron transfer in mitochondria, two free radicals ( $HO_2^{\cdot}$ ,  $\cdot OH$ ) are formed (Eq.1.1 and Eq.1.4), together with  $H_2O_2$  (Eq.1.3). At a physiological pH value of 7.4 the hydroperoxyl radicals ( $HO_2^{\cdot}$ ) dissociate to give the superoxide anion radical ( $O_2^{\cdot-}$ ) (Eq.1.2) (Gutteridge, 1994).



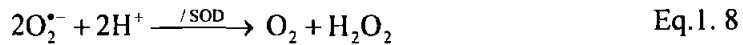
Besides the mitochondrial electron transfer reaction, iron salts and hydrogen peroxide react to produce hydroxyl radical and hydroperoxyl radical, which is known as 'Fenton reaction'(Eq.1.6).



In addition, nitric oxide (NO) can react with another endogenous free radical, superoxide, to produce a reactive intermediate peroxynitrite (ONOO<sup>-</sup>)(Eq.1.7)(Saran and Bors, 1990).



At pH 7.4, little HO<sub>2</sub><sup>·</sup> can be presented by quickly reduced to superoxide. Superoxide is a relatively weak oxidant that is able to oxidise ascorbic acid, and thiols. In mammal cells, superoxide rapidly dismutates to hydrogen peroxide and oxygen by superoxide dismutase (SOD)(Eq.1.8).



Hydrogen peroxide is a relatively stable weak oxidant in the absence of transition metal ions. The molecule H<sub>2</sub>O<sub>2</sub> has an uncharged covalent structure and readily mixes with water, and is treated as a water molecule by the body, rapidly diffusing across cell membranes (Gutteridge, 1994). Hydrogen peroxide is detoxified by the action of enzymes mainly catalase (CAT), glutathione peroxidase (GPx, selenium containing).

The hydroxyl radical (<sup>·</sup>OH) is an extremely aggressive oxidant that attacks most biological molecules at an almost diffusion-controlled rate. Peroxynitrite is a powerful oxidant too, which is able to oxidise many biological molecules and can also decompose to release hydroxyl radicals independent of metal catalysis (Eq.1.7).

The generation of ROS is an inevitable consequence of life in an aerobic environment. During the generation of ATP in mitochondria, although most of the transferred electrons go into the formation of water, about 1-4% of the passing electrons leak onto the oxygen molecules and are converted to superoxide. Other potential ROS sources include xanthine oxidase, cytochrome P450 based enzymes, NADPH oxidases, and infiltrating inflammatory cells (Muller et al., 2005). Consequently, life has necessitated the evolution of specialised

antioxidants to protect against the toxic properties of oxygen. The antioxidants are defined by Gutteridge (1994) as 'any substance that when present at low concentrations, compared to those of oxidizable substrate, significantly delays, or inhibits oxidation of that substrate'. Enzymes such as SOD, catalase, glutathione peroxidase and molecular scavengers such as reduced glutathione (GSH), vitamin E ( $\alpha$ -tocopherol), vitamin C (ascorbic acid), and metal chelators are all considered to be biological antioxidants. GSH plays important roles in antioxidant defense as an antioxidant substrate for enzymes such as glutathione peroxidases, and it is also involved in the regulation of the cell cycle and gene expression (Ziegler, 1985; Arrigo, 1999). Ascorbic acid is well known for its ability to scavenge superoxide, hydroxyl radical and singlet oxygen (Narkowicz et al., 1993). And the fat-soluble  $\alpha$ -tocopherol is extremely effective when incorporated into cell membranes and acts as a chain-breaking antioxidant to protect them from lipid peroxidation (Kagan et al., 1990). Antioxidants act at several different levels to protect cells from oxidative damage. They can prevent the formation of radicals; intercept radicals; repair oxidative damage and increase elimination of damaged molecules; and they also recognize excessively non-repaired damaged molecules in order to prevent mutations occur (Gutteridge, 1994).

### 1.5.4.2. HBO Therapy and Oxidative Stress

Oxidative stress is the redox imbalance caused by increased reactive oxygen species (ROS) production and/or reduced antioxidant reserve, which enhances susceptibility of lipid, protein and DNA oxidation by ROS, and subsequently damages cells.

The damaging effects of hyperoxia on lung tissue with increased rate of superoxide, hydrogen peroxide and lipid peroxide formation has been well described (see Jamieson et al., 1986) and increased oxidative damage and lipid peroxides was also found in rodents brain and erythrocytes (Harabin et al., 1990; Etlik et al., 1997). Narkowicz and his colleagues (1993) using electron spin resonance (ESR) spectroscopy, which allows the

direct measurement of free radical levels, detected a free radical signal in blood samples from persons undergoing HBO exposure (95% oxygen at 2.7 ATA for a total  $3 \times 20$  minute period as used therapeutically), but this signal diminished within 10 minutes of cessation of HBO exposure. Due to the transient nature of oxygen radicals, it is difficult to obtain direct measurement of sample ROS levels, and as the antioxidant system act to reduce ROS, the redox balance (the balance of oxidant to antioxidant) has been widely used to reflect and explain the status of oxidative stress and the antioxidant defence efficiency. The effects of HBO treatment on antioxidants are controversial amongst studies. Benedetti et al (2004) reported that when twelve patients with chronic wounds were exposed to 15 consecutive HBO treatments at 2.5 ATA for  $2 \times 30$  min periods, the repeated exposures to HBO led to a significant accumulation of plasma reactive oxygen metabolites (ROM) and malondialdehyde (MDA). After 15 HBO sessions, no differences were detected for GSH and  $\alpha$ -tocopherol plasma levels; however, a significant decrease in erythrocyte SOD and CAT activity was observed when compared to the 1st HBO exposure; glutathione peroxidase (GPx) activity remained almost unchanged. The results implied that prolonged HBO treatment leads to a condition of oxidative stress that seems to affect in particular the response of the enzymatic antioxidant defence system. However, Ozden et al (2004) found that HBO treatment improved liver regeneration in rats by benefiting redox state after exposure to HBO (at 2.5 ATA for 80 min, 4 times on 1<sup>st</sup> day, 3 times on 2<sup>nd</sup> – 4<sup>th</sup> day and 2 times 5<sup>th</sup> – 7<sup>th</sup> day) and decreased MDA production and increased SOD activity, GSH and Zn levels were also reported. Kudchodkar et al (2006) reported daily HBO treatment (at 2.4 ATA for 90 min, and once a day) for 10 weeks had an atheroprotective effect and elicited an antioxidant response in apoE KO mice. They found significant reductions of oxidative modified LDL (low density lipoprotein) in plasma, and TBARS (thiobarbituric acid reactive substances) and oxidized glutathione (GSSG) in liver; and

significant increase of the levels of GSH, glutathione reductase (GR), transferase, Se-dependent GPx and CAT in liver and aorta tissues. Muth et al (2004) investigated the effects of oral SOD supplement on HBO-induced DNA damage and antioxidant changes of twenty healthy volunteers (exposing to 100% oxygen at 2.5 ATA for a total of 60 min). Neither SOD and CAT, nor GSH and GSSG were significantly affected by the SOD intake or HBO exposure. In contrast, blood GPx activity was significantly lower in the SOD-group before and after HBO exposure. Another study (Eken et al., 2005) investigated blood samples from fifteen patients with various hypoxia pathologies after exposure to HBO treatment (at 2.5 ATA for 3 × 20 min period at the end of the 1st, 10th and 20th HBO sessions), and no changes in erythrocyte antioxidant capacity and lipid peroxidation were observed as erythrocyte SOD, selenium-dependent GPx and MDA levels showed no differences at the end of the 1st HBO therapy and the prolonged HBO exposure compared to before HBO treatment. In this study, although Vitamin E and Vitamin C were given daily to the patients, the antioxidant supplement effects were not considered.

From the research outlined above, it seems that although HBO treatment increases ROS generation, due to the reaction of antioxidant systems, it may paradoxically be a trigger that leads to protection from oxidative stress. Clinical applications have proved that controlled HBO therapy can be used successfully for a variety of pathological conditions. Recent discoveries have shown that at high concentrations reactive oxygen species (ROS) overwhelm the antioxidant defence system and trigger indiscriminate tissue damage thereby delaying healing (Watanabe et al., 1998; Steiling et al., 1999). However, in moderate concentrations, ROS may act as a signalling mediator that modulates a wide variety of cellular responses which are involved in protecting the cells from oxidative damage and facilitating production of growth factors involved in angiogenesis regulation (Sen, 2002a and 2002b).

## **1.6 Regulation of Wound Angiogenesis during HBO Treatment**

### **1.6.1. Mechanisms of HBO-induced Angiogenesis**

The mechanism by which HBO therapy facilitates wound angiogenesis is under investigation and so far two hypotheses have been proposed. The oxygen gradient theory was put forth by Remensnyder in 1968, and supported by Knighton et al (1981). It states that an oxygen gradient exists between the central and the peripheral of the wound; the hypoxia in wound centre stimulates the initiation of angiogenesis, and peripheral wound hyperoxia drives the process to completion, which obliterates the oxygen gradient. HBO therapy increases the oxygen gradient, thereby promoting wound angiogenesis (Gimbel and Hunt, 2003). Another consonant theory advocated by Mustoe et al (1997) reasons that molecular oxygen, when delivered at high pressure, can function both as a respiratory metabolite and as a signal transducer. This was supported by the increased production of ROS during HBO and the fact that ROS regulates production of vascular endothelial growth factor (VEGF) and other growth factors. In addition, Hunt and his colleagues furthered this idea with the finding that high concentration of lactate in wound sites is involved in oxygen-related regulation of angiogenesis (Ghani et al. 2003; Jensen and Hunt, 1986; Hussain et al., 1989).

## **1.6.2. HBO Treatment and VEGF Regulation in Wound Healing**

### **1.6.2.1. Origination and Biological Activity of VEGF**

Vascular endothelial growth factor (VEGF) gene family plays a fundamental role in the growth and differentiation of vascular as well as lymphatic endothelial cells (Ferrara, 2001). The broad term 'VEGF' includes several members including VEGF-A, placenta growth factor (PlGF), VEGF-B, VEGF-C and VEGF-D. All members of the VEGF family stimulate cellular responses by binding to a family of receptor tyrosine kinase (the VEGFRs) on the cell surface, causing them to dimerize and become activated through transphosphorylation. The VEGF receptors have an extracellular portion consisting of 7 immunoglobulin-like domains, a single transmembrane spanning region and an intracellular portion containing a split tyrosine-kinase domain.

In this thesis, VEGF-A is simply referred to as VEGF throughout, which is a major regulator of normal and abnormal angiogenesis (Ferrara, 2001). By alternative exon splicing of a single gene consisting of eight exons, five human VEGF isoforms were described by their amino acid number: VEGF<sub>121</sub>, VEGF<sub>145</sub>, VEGF<sub>165</sub>, VEGF<sub>189</sub>, and VEGF<sub>206</sub>. Mouse and rat VEGF isoforms are shorter by one amino acid per variant (Ferrara and Davis-Smyth, 1997). The cellular effects of VEGF-A (VEGF) are mediated via binding to VEGFR-1 (Flt-1) and VEGFR-2 (KDR/Flk-1). Most functional VEGF-A signalling described today is mediated via VEGFR-2 or strongly suspected to involve VEGFR-2 (Kliche and Waltenberger, 2001). After binding to the receptor, VEGF activates several signalling cascades in endothelial cells (Fig 1.1): activation of phospholipase C- $\gamma$  leads to increased activity of protein kinase C (PKC) and the mobilization of intracellular calcium via the production of Ins(1,4,5)P<sub>3</sub> (IP<sub>3</sub>); activation of phosphoinositide 3-kinase (PI<sub>3</sub>K)-dependent Akt/protein kinase B (PKB) pathway; and inducing activation of the

MAPK cascade via Ras/Raf stimulation. Through these signaling pathways, VEGF regulates several endothelial cell functions, including proliferation, differentiation, permeability, vascular tone, the production of vasoactive molecules and modulates gene expression (Waltenberger et al., 1994; Kroll and Waltenberger, 1999; Zachary and Glick, 2001; Kroll and Waltenberger, 1998). VEGF is a potent mitogen for micro- and macrovascular endothelial cells derived from arteries, veins, and lymphatics (Ferrara and Davis-Smyth, 1997). VEGF has been shown to induce confluent microvascular endothelial cells to invade collagen gels and form capillary-like structures in a tridimensional in vitro model (Pepper et al., 1992). Also VEGF induced sprouting from rat aortic rings embedded in a collagen gel (Nicosia et al., 1994). In vivo, VEGF produced strong angiogenic responses in chick chorioallantoic membrane (Leung et al., 1989), rabbit cornea (Phillips et al., 1995), and the primate iris (Tolentino et al., 1996). VEGF stimulates extracellular matrix (ECM) degradation by increasing the expression of uPA and tPA, PAI-1, and the metalloproteinase interstitial collagenase (e.g. MMPs) (Pepper et al., 1991; Unemori et al., 1992). The co-induction of PAs and collagenase by VEGF is consistent with a prodegradative environment that facilitates migration and sprouting of endothelial cells; and PAI-1 provides a negative regulatory step that serves to balance the proteolytic process (Pepper and Montesano., 1990). In vivo, VEGF has been shown to regulate vascular permeability, which is a crucial step for the initiation of angiogenesis in wounds (Senger et al., 1983; Dvorak et al., 1986).

VEGFR-1 has been reported to mediate monocyte migration (Barleon et al., 1996; Clauss et al., 1996) and function as a negative regulator of VEGFR-2 (Hiratsuka et al., 1998). VEGF-C and VEGF-D, but not VEGF-A, are ligands for a third receptor (VEGFR-3), which mediates lymphoangiogenesis.

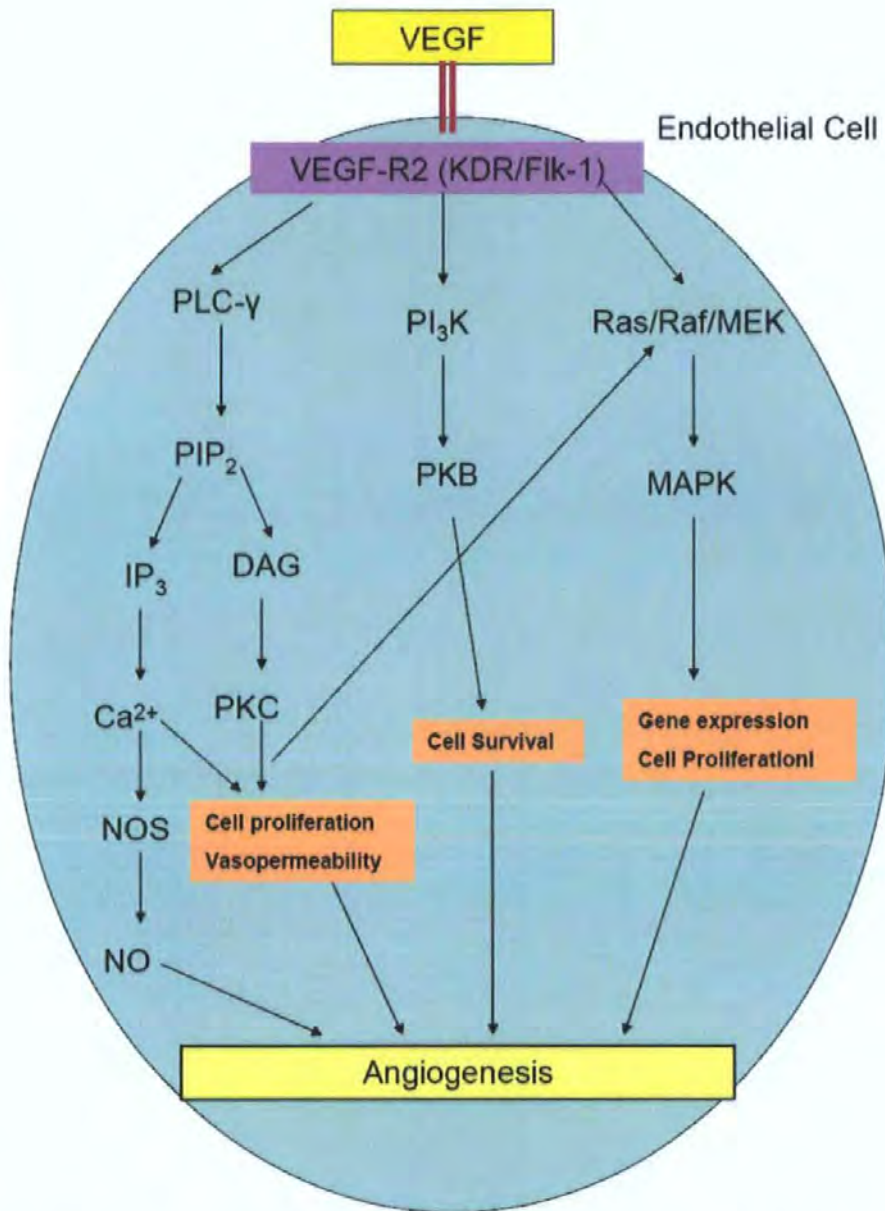


Fig 1. 1 VEGF signaling pathway in endothelial cell. Ligation of VEGF to its receptor (VEGF-R2) leads to phosphorylation of the receptor tyrosines, which allows the receptor to associate with and activate a range of signaling molecules. VEGF receptor activation can induce activation of the MAPK cascade via Ras/Raf/MEK leading to gene expression and cell proliferation, activation of PI3K leading to PKB activation and cell survival, activation of PLC- $\gamma$  leading to cell proliferation, vasopermeability. All these activation are related with angiogenesis (revised from

[http://www.sigmaaldrich.com/Area\\_of\\_Interest/Life\\_Science/Cell\\_Signaling/Key\\_Resources/Pathway\\_Slides\\_Charts/Signaling\\_Pathways\\_.html](http://www.sigmaaldrich.com/Area_of_Interest/Life_Science/Cell_Signaling/Key_Resources/Pathway_Slides_Charts/Signaling_Pathways_.html))

#### 1.6.2.2. Role of VEGF in Neoangiogenesis of Wound Healing Process

In wound sites, platelets, fibroblasts, endothelial cells, vascular smooth muscle cells and keratinocytes, have all documented to be able to produce VEGF (Berse et al., 1992).

VEGF may be crucial for angiogenesis during the proliferation phase of granular tissue formation during wound repair (Nissen et al., 1998). After mechanical denudation injury of the vascular wall, VEGF was infused into rat carotid arteries within 3 minutes immediately after injury and increased endothelial cell proliferation for up to 30 hours (Burke et al. 1995). Another examples are that adding the neutralizing anti-VEGF antibody to a healing wound strongly inhibited wound granulation tissue formation (Howdieshell et al., 2001) and that a single local injection of plasmid cDNA encoding recombinant human VEGF to an esophageal ulcer significantly enhanced angiogenesis and accelerated oesophageal ulcer healing (Baatar et al., 2002).

Importantly, VEGF is shown to play a consistent and prolonged angiogenic function during wound healing in several experimental *in vivo* wounds. In a full-thickness incision on dorsal skin of mice, expression of bFGF was detected in the nuclei of epidermal cells and fibroblasts in the early 0.5 h to 1 h phases and the late 24 h to 144 h phases. Expression of VEGF was detected in the cytoplasm of epidermal cells in the 24 h to 144 h phases (Takamiya, 2002). In maxillofacial blast injury rabbit model, the content of VEGF in wound fluid increased steadily from the 1st day post-injury and reached a peak value at the 7th day; whilst bFGF reached peak value at 6 h after injury, declined close to the serum level 3-5 days after injury, and then increased slightly on 7th day (Zhang et al., 2001). Surgical wound fluid samples (n = 70) were collected daily for up to 7 postoperative days from 14 patients undergoing mastectomy or neck dissection. VEGF levels in surgical wound fluid were lowest on postoperative day 0, approximating to serum values, but increased steadily through postoperative day 7. An opposite pattern was noted for bFGF, which exhibited highest levels at postoperative day 0, declining to near serum levels by postoperative day 3. Surgical wound fluid from all time points stimulated marked endothelial cell chemotaxis and induced a brisk neovascular response in the rat corneal

micropocket angiogenesis assay. In addition, antibody neutralization of VEGF did not affect the chemotactic or angiogenic activity of early wound samples from postoperative day 0. In contrast, VEGF neutralization significantly attenuated both chemotactic activity and angiogenic of later wound samples of postoperative day 3 and 6 (Nissen et al., 1998). These results suggest that for wound angiogenesis, the initial angiogenic stimulus seem to be supplied by bFGF, followed by a subsequent and more prolonged angiogenic stimulus mediated by VEGF; bFGF may be an endogenous inducer for VEGF. Furthermore, Corral et al (1999) reported the outcomes of applying VEGF<sub>121</sub> and bFGF on dermal ulcers in normal and ischemic rabbits' ears. They found that VEGF improved granulation tissue formation especially in ischemic wounds while bFGF had no significant effect on either the normal or the ischemic wound.

As VEGF plays an important role in stimulating and sustaining the angiogenesis in normal wound healing process, it is not surprised to find that a defect in VEGF regulation delays the healing process and is related to chronic wound healing. Frank et al (1995) compared the time course of VEGF mRNA expression during wound healing between healthy mice and genetically diabetic db/db mice that are characterized by impaired wound healing. In normal mice, elevated VEGF mRNA levels occur during the period of granulation tissue formation. In db/db mice, VEGF mRNA levels even declined during this period. Altavilla et al (2001) confirmed these findings in their study on diabetic mice. VEGF mRNA levels, after a slight initial increase (day 3), were significantly lower in diabetic mice than in normal littermates; the latter had a strong induction between day 3 and day 6 after injury. The exudates from non-healing venous ulcers patient have also been shown to have lower levels of VEGF, and these exudates inhibited experimental angiogenesis (Drinkwater et al., 2002).

Clinical application of VEGF for therapeutic angiogenesis has been used successfully. A replication-deficient recombinant adenovirus vector carrying the human VEGF<sub>165</sub> gene was topically applied on excision wounds of streptozotocin-induced diabetic mice; this significantly accelerated wound closure (Romano Di Peppe, et al. 2002). In another study naked plasmid DNA encoding human phVEGF<sub>165</sub> was directly administered (im.) into the ischemic limb area for patients with critical limb ischemia or thromboangiitis obliterans. Newly formed collateral blood vessels were visualised by angiography and ischemic ulcers markedly improved or healed, resulting in successful limb salvage (Baumgartner et al., 1998; Isner et al., 1998). Therefore, these preliminary studies show that VEGF levels in wound is important in mediating wound angiogenesis and deficient VEGF production may be one reason for non-healing wounds. Hence, more knowledge about VEGF regulation will be very helpful in promoting therapeutic angiogenesis.

### **1.6.2.3. Regulation of VEGF Production in Wound Healing Process**

Intracellular oxygen concentration is controlled within a narrow range to meet the requirements of oxidative phosphorylation, in order to generate sufficient ATP. It is known that either decreased oxygen supply (hypoxia) or excess oxygen supply (hyperoxia) is a risk factor for metabolic damage. For this reason, considerable efforts have been undertaken to understand how cells sense and respond to changes in oxygen partial pressure. Hypoxia has been shown to induce VEGF production by a wide variety of cells involved in tissue repair, such as fibroblasts, endothelial cells, vascular smooth muscle cells and macrophages (Minchenko et al., 1994; Shweiki et al., 1992; Brogi et al., 1994; Detmar et al., 1997; Steinbrech et al., 1999). Hypoxia also increases VEGF gene transcription, its mRNA stability and up-regulates its translation (Forsythe et al., 1996; Levy et al., 1996; Stein et al., 1995 and 1998).

Forsythe et al (1996) presented direct evidence that hypoxia inducible factor-1 (HIF-1) is implicated in the activation of the VEGF gene transcription during hypoxia. HIF-1 is a heterodimer composed of one of three alpha subunits (HIF-1 $\alpha$ , HIF-2 $\alpha$  and HIF-3 $\alpha$ ), and the 91-94kDa HIF-1 $\beta$  subunits (Wang et al., 1995). HIF-1 $\beta$  is constitutively expressed. HIF-1 $\alpha$  expression is low, often undetectable under normoxia but is induced, accumulated and translocated into nucleus where it binds to HIF-1 $\beta$  forming HIF-1 in a hypoxic environment. HIF-1 binds to co-activators CBP/p300 and is then activated. The HIF-1 heterodimer recognizes and binds to specific *cis*-elements in the promoters of specific genes that promote glycolysis, angiogenesis and cell proliferation. HIF-1 is the first ubiquitously expressed transcription factor known to be activated within the physiological range of O<sub>2</sub> concentrations, and mediates gene transcription in response to reduced cellular O<sub>2</sub> tension in order to maintain oxygen homeostasis. HIF-1 $\alpha$  protein levels and HIF-1 DNA binding activity increased exponentially upon exposure to decreased O<sub>2</sub> concentrations. Half-maximal induction was found between 1.5% and 2% O<sub>2</sub>, and maximal response was at 0.5% O<sub>2</sub>. Below 0.5% O<sub>2</sub>, HIF-1 protein levels decreased again (the normoxia O<sub>2</sub> concentration in kidney and liver tissue is approximately 3 to 5%)(Jiang et al., 1996). HIF-1 acts as a master transcription switch for the regulation of over 40 genes that are specifically involved in oxygen homeostasis such as VEGF, iNOS, lactate dehydrogenase (LDH), IGF-2, etc (Wenger and Gassmann, 1997). Several studies have indicated that HIF-1 expression is up-regulated during the wound healing process. Albina et al (2001) found that HIF-1 $\alpha$  mRNA was maximally expressed in wound cells 6 h after injury and HIF-1 protein was detectable in wound cells 1 and 5 days after injury. Data from transgenic mice expressing constitutively active HIF-1 $\alpha$  in epidermis displayed a 66% increase in dermal capillaries and 13-fold elevation of total VEGF expression (Elson et al., 2000). Mazure et al (1997, 2003) showed involvement of a Ras/phosphatidylinositol

3-kinase/Akt (Ras-PI3-K-Akt) signalling pathway in hypoxia-dependent induction of VEGF in Ha-ras-transformed cells and identified a hypoxia-response element (HRE) as a specific site for HIF-1 binding.

Besides hypoxia-induced VEGF expression, further examination of VEGF in wounds has suggested that there seem to alternative pathways of in VEGF production. Using punch biopsy wounds in rats, Haroon et al (2000) found that hypoxia was absent on day 1 in the provisional fibrin matrix, a time when angiogenesis and maximal expression of VEGF, TGF-2 were observed in wounds. Hypoxia peaked in the granulation tissue stage at day 4 and correlated with peak cellular proliferation. From day 4, hypoxia started to decrease, a time when wound cellularity decreased and wound contraction occurred. These results suggest that hypoxia probably does not play a role in the initial onset of cytokine expression that occurs at 1 day after wounding; alternate pathways may exist that mimic hypoxia conditions to initiate tissue repair and angiogenesis during the early stage of wound healing. Howdieshell et al (1998) demonstrated that wound VEGF levels remain notably high despite the fact that PO<sub>2</sub> in the wounds continuously approached the level of arterial blood. Clinical and experimental evidence demonstrate that increasing the oxygen concentration in severely ischemic and/or hypoxic wounds results in accelerated healing in the form of increased blood vessel growth. Sheikh et al (2000) administered HBO therapy for 90 minutes, twice daily at 2.1 ATA for 7 days after injury of rats. Wound oxygen rose from nearly 0 mm Hg to as high as 600 mm Hg. The peak level occurred at the end of the 90-minute treatment, and hyperoxia persisted for approximately 1 hour. The VEGF levels significantly increased with HBO by approximately 40% 5 days following wounding and decreased to control levels 3 days after exposures are stopped. Gimbel and Hunt (1999) also showed that cultured macrophages increased production of VEGF when exposed to oxygen at high tensions of about 300 mm Hg. Kang et al (2004) found the VEGF level in

propagated human dermal fibroblasts slightly increased on day one of HBO treatment, while Lin (2002) reported exposing HUVECs to HBO showed no effects on VEGF expression.

The question of how hyperoxia influence VEGF level and angiogenesis is not resolved yet. Current literature shows that some chemicals (e.g. ROS, lactate) could mimic hypoxia and hence stimulate VEGF secretion. In 1967, Hunt and his colleagues first reported that healing wounds produce and accumulate large concentrations (10–15 mM) of lactate. Ongoing research found that disruption of microcirculation, inflammation and rapid cell growth, and subsequently increased oxygen consumption led to the production of lactate (Ghani et al., 2003). Furthermore, high concentrations of lactate (15 mM) show the same effect as hypoxia in eliciting collagen synthesis by cultured fibroblasts (Green and Goldberg, 1964), and stimulate VEGF production by macrophages (Knighton et al., 1983; Jensen et al., 1986). These actions of lactate were hypothesized to be mediated by the ADPR/pADPR system (Hunt and Hussain, 1992). ADPR/pADPR (mono/poly ADP-ribosylation) is a post-translational modification of proteins in which molecules of ADP-ribose are added successively on to acceptor proteins to form branched polymers, thereby altering the acceptor proteins' structure and function (D'Amours et al., 1999). ADP-ribosylation is not only involved with DNA repair, but also represents a link between cell energy status and cell phenotype because of the requirement of  $\text{NAD}^+$  as its precursor or immediate substrate (Loetscher et al., 1987). Accumulation of high concentrations of lactate forces lactic dehydrogenase-catalyzed conversion of  $\text{NAD}^+$  to NADH. The decline in the  $\text{NAD}^+$  pool subsequently reduces the ADPR/pADPR level, which in turn alters the function of some transcription factors involved in collagen synthetic enzymes and VEGF regulation. Zebel et al (1996) reported that cultured macrophages in 15 mM lactate showed 40% lower  $\text{NAD}^+$  and 40% less pADPR synthesis than that in 0 mM lactate solution.

## 1.6 Regulation of Wound Angiogenesis during HBO Treatment

---

Subsequently, Constant et al (1996) measured VEGF levels in media conditioned by macrophages grown in normoxia, hypoxia, 15 mM lactate, or hypoxia and lactate together. Both hypoxia and lactate alone stimulated increased VEGF levels and the highest concentration occurred with the combination of lactate and hypoxia. Later Constant et al (2000) reported that hypoxia, lactate, and nicotinamide elicited significantly increased levels of VEGF mRNA and VEGF protein in the conditioned media, and these levels were paralleled by their angiogenic activity. They also proposed that redox changes ( $\text{NAD}^+/\text{NADH}$ ) associated with the alteration of cellular ADPR/pADPR level could be involved in lactate-mediated VEGF expression. Lactate levels remain elevated in healing wounds even when oxygen tensions in the wounds were increased (Hunt et al., 1978). With HBO treatment, the VEGF levels were elevated while the lactate level remained unchanged in wound exudates (Sheikh et al., 2000).

Recent discoveries have illuminated that in moderate concentrations, ROS may act as a signalling mediator that modulates a wide variety of cellular responses involved in angiogenesis regulation (Sen, 2002a,b). This seems, in part, to explain the different effects of HBO on wound healing and cell function. The wound site is rich in both oxygen- and nitrogen-centred reactive species along with their derivatives, mostly contributed by the respiratory burst of neutrophils and macrophages. The concentration of  $\text{O}_2$  necessary to achieve half maximal ROS production (the  $K_m$ ) is in the range of 45 to 80 mm Hg, with maximal ROS production seen when  $p\text{O}_2 > 300$  mm Hg (Allen et al., 1997). Hyperbaric oxygen has been shown to stimulate respiratory burst activity to produce more ROS (Conconi et al., 2003; Mader et al., 1980). Among the various forms of ROS,  $\text{H}_2\text{O}_2$  is relatively stable, membrane-permeable, and therefore a good candidate to serve as a cellular messenger (Bauerle et al., 1996). Cho et al (2001) discovered that  $\text{H}_2\text{O}_2$  increased macrophage VEGF production through an oxidant induction of the VEGF promoter, and

this oxidant stimulation could be mediated by activated neutrophils. ROS eliciting VEGF release has also been seen in vascular smooth muscle cells (Ruef et al., 1997). Sen et al (2002) demonstrated that at  $\mu\text{M}$  concentrations oxidant induces VEGF expression and that oxidant-induced VEGF expression is independent of HIF-1 and dependent on Sp1 activation. Richard et al (2000) found that ROS played an essential role in activate HIF-1 gene of vascular smooth muscle cells during induction of VEGF mRNA expression by thrombin, PDGF and angiotensin II, and they suggest that while hypoxia remains the undisputed ubiquitous inducer of HIF-1, other factors could also modulate increases in HIF-1 $\alpha$  protein levels in a cell-specific manner. As demonstrated by Richard, the non-hypoxia induction of the HIF-1 transcription factor via vasoactive hormones is triggered by a dual mechanism. One is a diacylglycerol-sensitive protein kinase C (PKC) -mediated increase in HIF-1 $\alpha$  transcription and the other is ROS -dependent activation of PI3-kinase (PI3K) that increases the translation of HIF-1 $\alpha$  by acting on the 5'-untranslated region. HIF-1 then binds a specific hypoxia-response element sequence and increases the expression of VEGF. The role of ROS in induction of VEGF gene is described in Fig 1.2.

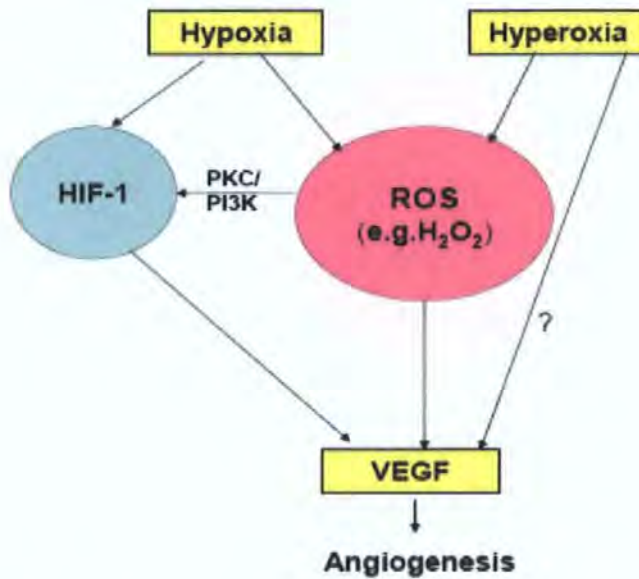
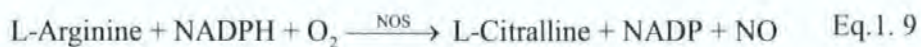


Fig 1. 2 Role of ROS in induction of VEGF production under hypoxia/hyperoxia. Hypoxia stabilizes HIF-1 gene and then permits transcription of VEGF gene. The ROS generated from either hypoxic or hyperoxic condition may increase the transcription of HIF-1 gene by stimulate PKC. The HIF-1 mRNA is then translated by increased activation of the PI3K pathway, which results in the increased HIF-1. Exogenous ROS and hyperoxia can also stimulate VEGF production via HIF-1 independent ways.

### 1.6.3. HBO treatment and Nitric Oxide

#### 1.6.3.1. Nitric Oxide in Wound Healing

Nitric oxide (NO) has an unpaired electron and is thus a free radical capable of rapid reaction with other molecules. NO, continuously produced at nanomolar (nM) concentration, is responsible for a wide range of physiological functions such as vasodilatation, promoting smooth muscle relaxation and preventing platelet adhesion and aggregation. NO is produced by nitric oxide synthase (NOS) which catalyses a five-electron oxidation of the guanidine nitrogen of arginine into citrulline with consumption of NADPH and oxygen (Eq.1.9) (Marletta, 1993; and Knowles, 1994).



There are three subtypes of NOS: neuronal NOS (nNOS), inducible NOS (iNOS), and endothelial NOS (eNOS). nNOS is mainly expressed in neuronal cells which exist in large

numbers in brain, spinal cord, sympathetic ganglia, and kidney (Murakami et al., 1998); here the NO produced functions as a neurotransmitter. eNOS is mainly found in endothelial cells and plays an important role in vasodilation (Pollock et al., 1993). eNOS is constitutively produced and may be up-regulated by the shear force of flow and hyperoxia, which requires the presence of intracellular calcium and calmodulin (Nishida et al., 1992; North et al., 1996; Malek et al., 1999). nNOS and eNOS bind calmodulin in a reversible and calcium-dependent fashion. iNOS is usually induced during inflammation by certain inflammatory cytokines and/or bacterial products. iNOS function is calcium- and calmodulin-independent because calmodulin is tightly bound to this isoform in a noncovalent manner and trace levels of intracellular calcium are able to maintain its activity. iNOS protein levels are either very low or undetectable in most cells, while stimulation leads to increased transcription of the iNOS gene, with subsequent production of high concentrations of NO. As a result, the production of NO by iNOS lasts longer and is much higher than from the other isoforms (Lirk et al., 2002).

Elevated levels of nitrite and citrulline, end products of NOS-mediated reaction, appear in wound fluid during the first 3 days of wound healing until the second week, confirming that NO is produced during wound repair (Albina et al., 1990; Schaffer et al., 1996). A number of cells involved in wound repair are capable of producing NO using either eNOS or iNOS. These include macrophages (iNOS) (Reichner et al., 1999), keratinocytes (eNOS and iNOS) (Heck et al., 1992; Arany et al., 1996), endothelial cells (eNOS and iNOS) (Hood et al., 1998; van der Zee et al., 1997), and fibroblasts (eNOS and iNOS) (van der Zee et al., 1997; Wang et al., 1997).

In wound healing, NO plays important roles throughout the inflammatory phase right through scar remodelling. Diabetic rats had decreased nitrite/nitrate (the metabolite oxides of nitrogen used as indicators of NO production) in wound fluid as well as impaired

breaking strength and decreased collagen content of healing wounds (Schaffer et al. 1997a). In a three week wound healing experiment, Amadeu and Costa (2006) investigated the effects of NO synthesis on rat cutaneous wound healing by blocking the NO synthesis with N(G)-nitro-L-arginine methyl ester (L-NAME), a non-selective inhibitor of NO synthases. L-NAME-treated animals presented delayed wound contraction, alterations in collagen organization and neoepidermis thickness with decreased volume density and smaller surface density of vessels.

### 1.6.3.2. Roles of iNOS and eNOS in Wound Healing Process

The investigations on the changes of NO production and NOS suggested that iNOS and eNOS are highly co-ordinated to provide NO for normal wound repair. Schaffer et al (1997b) found increased nitrite/nitrate level until the second week postwounding and demonstrated that iNOS expression in macrophages was the major source of wound nitric oxide. Consistent with this study, using a five-week healing wound model, Lee et al (2001) showed that nitrite/nitrate levels in wound fluid increased steadily from day 1 to day 14 after wounding indicated a sustained production of NO and NOS activity up to 10 days in the wound with the iNOS gene expression paralleled NOS biochemical activity. And the peak NOS activity was at 24 h after wounding, macrophages appeared to be a source of nitric oxide production in this early phase of wound healing.

NO has been shown to increase angiogenesis in ischemic limb (Murohara et al., 1998), and eNOS inhibitors impair angiogenesis in granulation tissue (Konturek et al., 1993). Ma and Wallace (2000) investigated the relative effects of eNOS and iNOS on gastric ulcer healing in rats, and they found that iNOS mRNA was expressed in inflammatory cells in the ulcer bed and only detected in ulcerated tissue (maximal at day 3), whereas eNOS mRNA was found in endothelium and in some mucosal cells in both normal and ulcerated tissue and increased during the ulcer healing process; moreover, angiogenesis change was

in parallel with eNOS expression. They suggested that eNOS plays a significant role in endothelial cell-induced angiogenesis and that iNOS made a great contribution in the early stage of gastric ulcer healing process. Lee and his colleagues (1999) confirmed the requirement of eNOS for wound angiogenesis by using eNOS gene knockout mice (KO mice). Capillary ingrowth into subcutaneously implanted Matrigel plugs was significantly reduced in eNOS-deficient mice and in vitro endothelial cell sprouting assays demonstrated that eNOS is required for proper endothelial cell migration, proliferation, and differentiation.

NO production by NOS was also shown the ability to facilitating wound angiogenesis by regulating angiogenic growth factors. Akimoto et al (2000) measured the concentration of VEGF, NO and endothelin-1 (ET-1) of biopsy samples from 61 gastric ulcer patients in active stage (15 cases), 23 were healing stage (23 cases), or scarring stage (23 cases). Nitrite/nitrate showed highest concentration in early mucosal repair stage (active stage), all three factors showed high levels in healing stage, and significant lower concentration were found in scarring stage. Interestingly, the distribution of ET- and iNOS-positive cells differed according to the ulcer stage. In particular, ET- and iNOS-positive cells were primarily endothelial cells during active and healing stages and during scarring stage were mainly vascular smooth muscle cells in the vascular wall. Howdieshell et al (2003) presented that iNOS inhibition resulted in reductions of wound VEGF expression and granulation tissue formation. Therefore, NO produced via iNOS of macrophages and endothelial cells at the early stage might be the original signal to active endothelial cells and to stimulate secretion of other growth factors such as VEGF to initiate and sustain wound repair and angiogenesis; and at the late stage the effects of NO produced via eNOS and iNOS might involve in regulating the proliferation of smooth muscles and other cells related to vascular remodelling.

### 1.6.3.3. Evidence of NO as An Mediator in Angiogenesis

Nitric oxide has been implied to be regulated by a variety of growth factors as well as cytokines such as VEGF, including platelet-activating factor (PAF), bFGF, IL-2, TNF- $\alpha$ , IL-1 $\alpha$  (Dulak and Jozkowicz., 2003). Based on the accumulated evidences that NO could induce or be induced by VEGF, nitric oxide is expected to serve as both an upstream and downstream modulator of VEGF-mediated angiogenesis.

Van der Zee et al (1997) found that VEGF produced a dose-dependent rise in NO concentration from vascular segments of rabbit thoracic aorta, pulmonary artery, and inferior vena cava. Comparison to stimulation with acetylcholine, the onset of increased (NO) after administration of VEGF was slower, reaching a maximum value after 8 min. Preincubation of the aortic segments with L-arginine raised by twofold both baseline (NO) and (NO) stimulated by addition of 2.5  $\mu\text{g}/\text{mL}$  VEGF. Removal of calcium from the Krebs solution, disruption of the endothelium, and administration of NG-monomethyl-L-arginine (L-NMMA, inhibits eNOS) abrogated the stimulatory effect of VEGF (10  $\mu\text{g}/\text{mL}$ ). The authors also documented a similar finding with an NO-specific polarographic electrode to measure NO released from cultured HUVECs.

When HUVECs were incubated with VEGF, NO was produced in both acute (1 h) and chronic (>24 h) ways, and the NO generation was confirmed to be VEGF-elicited and dose-dependent. The lone-term exposure to VEGF increased eNOS protein level, and short-term stimulation with VEGF promoted NO release through mechanisms involving tyrosine and PI-3K (Papapetropoulos et al., 1997). VEGF-stimulated NO production required activation of tyrosine kinases and increases in intracellular calcium, since tyrosine kinase inhibitor and calcium chelator attenuated VEGF-induced NO release (Hood et al., 1998; Papapetropoulos et al., 1997). A consistent effect was demonstrated by Bouloumie et al (1999) that VEGF<sub>165</sub> enhances the expression of eNOS in cultured (HUVECs) and

native (rat aorta ring) endothelial cells, and that this can be abolished by tyrosine kinase inhibitors. Kroll and Waltenberger (1998) found that stimulating HUVEC with VEGF for 24 hours induces both iNOS and eNOS expression and protein levels. They also used porcine aortic endothelial cells over-expressing either VEGF receptor-2 (PAE/KDR cells) or VEGF receptor-1 (PAE/Flt-1 cells) to study the regulation of iNOS and eNOS expression in response to VEGF stimulation. The activation of VEGF receptor-2 led to an upregulation of both eNOS and iNOS protein, while stimulation of VEGF receptor-1 did not generate such a signal. Therefore, VEGF augmented NO release mediated by binding to VEGF receptor-2 of endothelial cells to stimulate expression and production of eNOS and iNOS protein.

Other evidence has shown that NO could alternatively regulate VEGF production. During cutaneous wound repairs, VEGF expression increased concomitantly with iNOS expression in keratinocytes (Frank et al., 1999), and in macrophages (Xiong et al., 1998). In vascular smooth muscle cells, the expression of VEGF mRNA and protein synthesis can be enhanced both by low doses of NO (such as those generated by eNOS) and by high amounts of NO derived from iNOS or NO donors. Dulak et al (2000) found VEGF expression and protein synthesis was upregulated after either IL-1 $\beta$  induced iNOS expression or NOS transfected to increase NO generation of rat vascular smooth muscle cells, and inhibition of NO generation by L-NAME decreased VEGF synthesis in both the models. Jozkowica et al (2001) showed a similar increase in VEGF protein production by exposing rat and human vascular smooth muscle cells to exogenous NO donors (2-fold), or to genetic augmentation of eNOS or iNOS by transfection (3-fold), which was reversed after treatment with the NOS antagonist L-NAME. In addition, the VEGF protein produced by NOS-transfected VSMC was biologically active and capable of increasing endothelial cell proliferation. Although the mechanism of NO activating VEGF production is unknown,

studies have indicated that hypoxia and NO may use similar components, pathways and/or modifications to evoke HIF-1 $\alpha$  accumulation as exposure of various cells to NO under normoxic conditions induced HIF-1 $\alpha$  accumulation and HIF-1-DNA binding (Kimura et al. 2000; 2001), which may then activate the downstream target gene expression (e.g. VEGF) (Brune and Zhou, 2003). The reciprocal regulation between NO and VEGF is summarized in Fig 1.3.

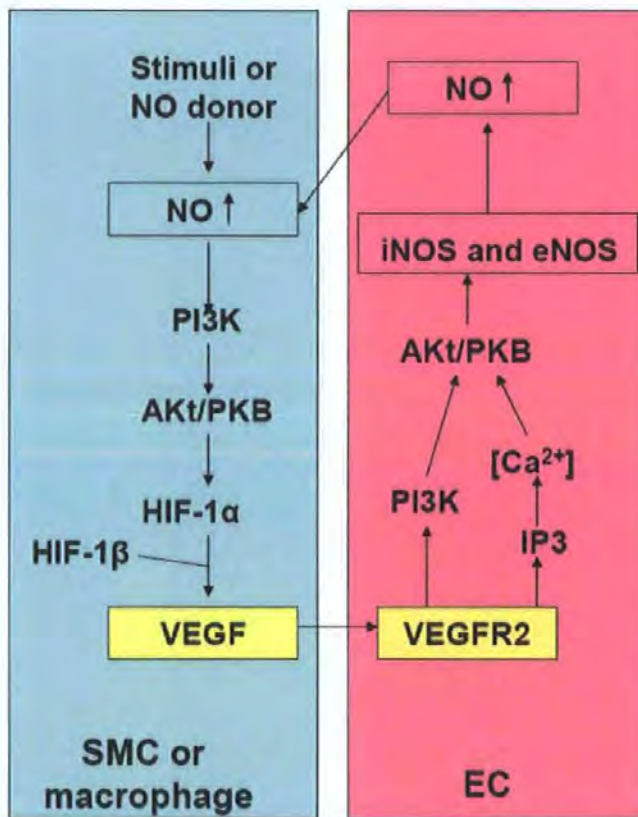


Fig 1. 3 Reciprocal relationship between VEGF and NO. In smooth muscle cells or macrophages, VEGF is enhanced by NO generated by eNOS, iNOS or NO donors, which may be mediated by HIF-1 pathway. In endothelial cells, VEGF binds to VEGF receptor-2 and induces NO synthesis through the CaM-Akt or the PI3K-Akt pathways.

#### 1.6.3.4. HBO Treatment Regulates NO Production

Oxygen and hyperbaric oxygen therapy are known to affect the NO production and the expression of both eNOS and iNOS. The first evidence of HBO influencing NO generation came from a report that NO might be an important mediator in oxygen toxicity (6 ATA) in central nervous system (Oury et al., 1992). The study of Wang et al (1998)

suggested that the increased NO production as well as neuronal intracellular  $\text{Ca}^{2+}$  overload during HBO (5 ATA) exposure was responsible for HBO-induced seizures, and Chavko et al (2001) reported significantly higher activity of calcium-dependent NOS and protein expression of nNOS at 1 and 2 days after HBO-induced seizures (5 ATA), while calcium-independent NOS activity and protein expression of eNOS and iNOS were not changed. A protective effect against HBO-induced seizures was achieved by the nNOS-specific inhibitor 7-nitroindazole (7-NI). Using NOS-deficient mice, Demchenko et al (2003) demonstrated the same effect of nNOS-catalysed NO mediated HBO (5 ATA) toxic effects by reaction with superoxide to generate peroxynitrite; and they also found an eNOS-dependent NO production to induce cerebral vasoconstriction and related with the development of hyperoxic hyperaemia. The close relationship of increased cerebral blood flow (CBF) and upregulated NO concentration during HBO treatment was supposed to be the reason for hyperaemia under HBO (5 ATA) exposure (Sato et al., 2001; Hagioka et al., 2005). However the regulation of NO production in HBO treatment is not that simple, Zhiliaev et al (2002) reported a reduced cerebral blood flow under hyperbaric oxygen (4 ATA) due to inactivation of NO by superoxide anions, and another study from the same research team reported that oxygen at a pressure of 4 ATA induced cerebral vasoconstriction and decreased blood flow by 11-18% during 60 min exposure to hyperbaric oxygenation. Paroxysmal electroencephalography (EEG) activity and oxygen convulsions did not occur in rats at 4 ATA of  $\text{O}_2$ , while at 5 ATA, convulsive activity appeared on the EEG at  $41 \pm 1.9$  min, and blood flow decreased significantly during the first 20 min; and then blood flow increased by  $23 \pm 9\%$  before the appearance of convulsions on the EEG. Prior inhibition of nNOS and eNOS with L-NAME or inhibition only of NOS I with 7-nitroindazole (7-NI) prevented the development of hyperoxic hyperaemia and paroxysmal spikes on the EEG during hyperbaric oxygenation at 5 ATA.

These results show that hyperbaric oxygen induces changes in cerebral blood flow which modulate its neurotoxic action via nitric oxide synthesized both in neurons and in cerebral vessels (Moskvin et al., 2003). Zhang et al (1995) exposed rats to HBO at 3 ATA for 15 min and found that although HBO significantly increased the brain O<sub>2</sub> tension but not CBF, and inhibition of NOS with L-NAME did not change either brain O<sub>2</sub> tension or CBF.

HBO-induced nNOS-mediated NO production contributes to oxygen toxicity of the central nervous system at above 5 ATA, and inhibition of NOS significantly protects animals from hyperbaric oxygen (HBO)-mediated convulsions. At lower pressure such as 4 ATA and 3 ATA, the oxygen toxicity was limited, possibly by reduced NO production. In addition, NOS isoforms might react differently to HBO stimulation and that could be the basis of an explanation of the HBO beneficial effects at treatment pressure.

Exposure of mice to HBO or hyperbaric air treatment significantly reduced the cytostatic activity, peroxynitrite synthesis and transcription of iNOS mRNA of their macrophages stimulated with lipopolysaccharide (LPS) and interferon-gamma (Kurata et al., 1995). LPS is an endotoxin and is able to induce a strong response from normal animal immune systems. Intravenous administration of LPS to rats significantly increased nitrite/nitrate concentration in plasma was after 5-6 h after injection; and HBO treatment at 3 ATA for 90 min significantly depressed nitrite/nitrate production 1 h after LPS injection (Sunakawa and Yusa, 1997). Recently, HBO treatment also reported to attenuate LPS-induced and sepsis-induced acute lung injury by decreasing NO production and iNOS protein expression in rats (Huang et al., 2005; Chu et al., 2006; Chang et al., 2006).

Zymosan, a cell wall component of the yeast *Saccharomyces cerevisiae*, induces inflammation by causing the production of various cytokines and pro-inflammatory mediators. The administration of zymosan to rats represents a new experimental shock model by inducing acute peritonitis, severe hypotension, and signs of systemic illness

characterized by ruffled fur, lethargy, conjunctivitis, diarrhoea, and a significant loss of body weight. Zymosan led a time-dependent increase of nitrite/nitrate in peritoneal and plasma. HBO treatment (at 2 ATA) significantly attenuated morbidity of zymosan-shocked rats with a great reduction of either peritoneal leukocytes and exudates, or plasma and peritoneal nitrite/nitrate concentrations (Luongo et al., 1998). Imperatore and colleagues (2004) observed that HBO therapy (at 2 ATA) attenuated zymosan-induced vasoplegic response and improved vascular alteration by increased contraction (induced by norepinephrine and endothelin-1) as well as acetylcholine (ACh)-induced dilation in rat aorta rings. At the same time, HBO therapy also attenuated the increase of MDA levels in the aorta and protein level of nitrotyrosine and iNOS in tissue sections obtained from zymosan-treated rats.

Exposing rats with colitis to HBO (100% oxygen at 2.4 ATA for one hour twice on the day of colitis induction and once daily thereafter) for seven days effectively decreases colitis induced by acetic acid and trinitrobenzenesulphonic acid (TNB) and the markedly decreased activity of NOS and myeloperoxidase and prostaglandin E<sub>2</sub> generation (Rachmilewitz et al., 1998). Yuan et al (2004) demonstrated that HBO treatment suppressed the iNOS expression and apoptosis of chondrocytes, and hence protected cartilage from injury. Applying HBOT twice a day during early wound healing significantly ameliorated the negative effects of psychological stress on wound healing (iNOS expression increased 205% in stressed mice day 1 post-wounding) by reducing iNOS expression (62.6%). Interestingly, no significant effect on wound healing and iNOS expression was shown in control animals without stress (Gajendrareddy et al., 2005).

The beneficial effects of therapeutic HBO treatment on variable pathophysiological conditions have been widely studied, and the reduction of NO generation via iNOS may be among the mechanisms responsible for the anti-inflammatory effect of HBO therapy. On

## 1.6 Regulation of Wound Angiogenesis during HBO Treatment

---

the other hand, it is known that HBO increases nitric oxide levels in perivascular tissues via stimulation of nitric oxide synthase (NOS). North et al. (1996) reported that increased oxygen tension at normobaric pressure (exposing to PO<sub>2</sub> 150 mmHg for 48 h) led to an induction of 2.7-fold greater eNOS mRNA and protein expression up to 24 hours in early passage ovine fetal pulmonary artery endothelial cells (PAEC). Buras et al (2000) demonstrated that hyperbaric oxygen induced the synthesis of eNOS in human umbilical vein endothelial cells (HUVECs) and bovine aortic endothelial cells (BAECs) and reduced the expression of ICAM-1 to control levels. Adhesion of PMNs to BAECs was increased following hypoxia/hypoglycemia exposure (3.4-fold) and was reduced to control levels with exposure to HBO. The NOS inhibitor L-NAME attenuated HBO-mediated inhibition of ICAM-1 expression. Hink et al (2006) found that exposure rat aorta rings to HBO at 2.8 ATA in vitro decreased ACh relaxation. This effect remained unchanged, despite treatment with SOD-polyethylene glycol and catalase-polyethylene glycol, suggesting that the reduction in endothelium-derived NO bioavailability was independent of superoxide production. In vitro HBO induced contraction of resting aortic rings with and without endothelium, and these contractions were reduced by the NOS inhibitor N(omega)-nitro-l-arginine. In addition, in vitro HBO attenuated the vascular contraction produced by norepinephrine, and this effect was reversed by N(omega)-nitro-l-arginine, but not by endothelial denudation. These indicated stimulation of extraendothelial NO production during HBO exposure. Catalytic activity of eNOS in cell homogenates of rat aortic endothelial cells was not decreased by HBO, and in vivo HBO exposure to 2.8 ATA was without effect on eNOS activity and/or vascular NO bioavailability in vitro. HBO reduced endothelium-derived NO bioavailability and increased the resting tone of rat aortic rings and attenuated the contractile response to norepinephrine by endothelium-independent mechanisms that involve extraendothelial NO production. Another study showed HBO

increases bone marrow NO as a physiological trigger for mobilisation in vivo thereby increasing release of endothelial progenitor cells (EPC) into circulation; mobilization of EPC is associated with increased lower limb spontaneous circulatory recovery after femoral ligation and enhanced closure of ischemic wounds. Both the effects were inhibited by NOS inhibitor L-NAME (Goldstein et al., 2006).

Given the fact that VEGF is actively involved in regulating endothelial function and vascular tone in chronic wounds and ROS such as NO and hydrogen peroxide have been affected by HBO treatment, it is more likely that the interaction and regulatory mechanism of these factors are greatly responsible for better understanding of HBO effects.

## **1.7 Summary**

The world-wide rapidly ageing society with multiple concomitant pathological conditions such as diabetes and cancer presents an increasing population of patients with nonhealing and problem wounds. Application of hyperbaric oxygen therapy to problem wound healing has been recommended by the UHMS and approved to accelerate wound closure and improve cell function in multiple ways. Angiogenesis in wounds plays a critical role in granulation tissue formation during the wound healing process. A number of studies have demonstrated that hyperbaric oxygen therapy promotes new vessel formation as well as enhancing endothelial cells migration, proliferation and tube formation. However, the cellular and molecular effects of hyperbaric oxygen therapy on angiogenesis in chronic wound are still not clearly defined. Wound angiogenesis is a physical process, which is highly regulated by growth factors, cytokines and other factors. Vascular endothelial growth factor (VEGF) is believed to be the most powerful angiogenesis growth factor identified so far, and its expression is highly regulated by oxygen tension. Defective VEGF regulation is associated with chronic wound healing. VEGF expression is up-

regulated in both hypoxia (e.g. in a normal wound site) and hyperoxia (e.g. during hyperbaric oxygen treatment). On the other hand, HBO treatment is capable of regulating ROS and NO production which may depend on HBO strategies and pathological condition. In addition, recent studies have suggested that ROS such as hydrogen peroxide, and nitric oxide; or high level of lactate are involved in VEGF regulation in chronic wound. The effects of hyperbaric oxygen therapy on VEGF, nitric oxide and hydrogen peroxide levels are controversial but promising; the changes of these factors are tightly related to oxygen supply (Fig 1.4). However, there have not been studies to investigate the response and interaction of these factors to hyperbaric oxygen treatment. We believe that studies on this aspect will contribute to our knowledge of the role of hyperbaric medicine and help to clarify the mechanisms underlying the magical effect of oxygen, and ultimately provide a better basis for the application of hyperbaric oxygen therapy.



Fig 1. 4 Possible mechanisms of HBO on wound healing process.

## Chapter 2

### Methods Development

In the work described in this chapter, we successfully established an *in vitro* blood vessel model of HBO treatment, which was verified using tests of tissue viability and histological examination, and set up the appropriate biochemical methods to quantify the level of hydrogen peroxide, nitric oxide, glutathione, lactate and vascular endothelial growth factor (VEGF) for our specific model. These assay protocols and *in vitro* model are mainly used in Chapter 3 and Chapter 4. All the chemicals and reagents used except mentioned were obtained from Sigma (Poole, UK).

#### 2.1 Rat Aorta Segment *in Vitro* Model

Isolated blood vessels, especially rat aorta provide an ideal *in vitro* model to investigate the vascular responsiveness as well as behaviour of endothelial cells or smooth muscle cells to all sorts of mechanical, physical or chemical stimuli and treatments. The aorta layers from innermost to outermost are endothelial cell layer, vascular smooth muscle cell layer and adventitia consists of fibroblasts, extracellular connective tissue, small blood vessels and others. The endothelial and smooth muscle cells interact, making isolated blood vessels a more realistic *in vitro* model than either cell type on their own. The structural advantages and convenient availability have the *in vitro* rat aorta model extensively used in research into the mechanisms and influencing factors in hypertension, atherosclerosis, diabetes and other vascular-related diseases (Lorok et al., 2006; Loomis et al., 2005; Jen et al., 2000; Agren and Arnquist, 1981; Kulchai et al., 1978). Moreover, it

also has been used as a quantitative assay for the study of angiogenesis and for the identification of potential angiogenic agents and screening for pharmacological inhibitors by embedding rat aorta rings in gels of fibrin or collagen and optimized culture medium to generate branching microvessels (Nicosia and Ottinetti., 1990; Blacher et al., 2001). Angiogenesis in wound healing involves the generation and interaction of angiogenesis factors such as ROS, nitric oxide, VEGF and lactate in wound sites. The effects of HBO treatment on the generation of those factors from blood cells, macrophages, fibroblasts have been investigated and are considered significantly important in regulating wound angiogenesis and the wound healing process (See 1.6 for review). Neovascular formation in granulation tissue is initiated from the existing blood vessels, but to our knowledge there are no studies that investigate the direct effect of HBO treatment on those angiogenesis factors of blood vessel. For this purpose, the rat aorta provides an ideal model to investigate the effects of HBO treatment on production of reactive oxygen species, nitric oxide, lactate and VEGF in physiological and pathological conditions *in vitro*.

### **2.1.1. Animals and Aorta Preparations**

Male Sprague Dawley rats (350 - 400 g) were purchased from Harlan UK Ltd (Shaw's Farm Blackthorn, Bicester, UK). They were kept in a 12 h dark: 12 h light cycle and had free to access food and water before collection the tissue. Experiments were conducted in accordance with ethical approval.

Rats were euthanized with intraperitoneal injection of Sagatal (90 mg kg<sup>-1</sup> body wt, Rhône Mérieux Limited, Harlow, Essex, UK). The abdominal cavity was dissected, then visceral organs and abdominal fat were removed, the aorta was firstly located in the retroperitoneum distal to the kidneys by spreading the retroperitoneal fat. Once the aorta was found, the abdominal aorta was dissected distally until the branching site of the iliac

arteries. To dissect the thoracic aorta, the diaphragm was cut and dissection continued through where the aorta passed the diaphragm and reached the aorta arch. The aorta arch derives from the heart and is fixed by surrounding connective tissues and arteries, so the surrounding fat and connective tissue was cleaned and the intercostal, left subclavian and left carotid arteries were dissected to free the aorta from the retroperitoneum. The aorta was then dissected from the arch down to the iliac bifurcation. The vessel was bathed with ice cold phosphate buffered saline (PBS at pH 7.4) throughout dissection.

Once the aorta (8 -10 cm) was removed, it was washed in 250 ml of ice-cold PBS and then spread in a culture dish with 10 ml of modified Krebs-Ringer solution (composition in mM: NaCl 118.6, KCl 4.7, CaCl<sub>2</sub> 2.5, MgSO<sub>4</sub> 1.2, KH<sub>2</sub>PO<sub>4</sub> 1.2, NaHCO<sub>3</sub> 25.1, Hepes 10, glucose 10, pH 7.4) to carefully remove any remaining fat from the exterior of the blood vessel. The aorta was sectioned into 1 cm segments, and then placed in wells of Nunclon Delta SI 6-well tissue culture plates (Nunc, InterMed, Denmark) containing 6 ml of Krebs-Ringer solution. The plate was transferred to a 37 °C incubator with air supply for up to 8 hours, and tissue and medium samples (10 aorta segments from 2 rats) were collected at 0.5 h and 8 h post incubation for histological and tissue toxic examination.

### **2.1.2. Histology Examination**

#### **2.1.2.1. Rat Aorta Segment Routine Histological Protocol**

Aorta segments were first fixed with 15 ml of Bouin's solution for 24 hours. Bouin's solution is an alternative to formaldehyde-based fixative and contains 75 ml of 1% saturated aqueous picric acid, 25 ml of 10% Formalin and 5 ml of glacial acetic acid. Fixation preserves the tissue structure and chemical composition in a state as close as possible to the living condition and the right fixative and proper fixation time are important for a good histological section. Secondly, fixed aorta segments were diffused in graded

alcohol to remove excess water (70% × 2, 90% × 1 and 100% × 2 for 2 h each). Since alcohol and paraffin are immiscible, an intermediate step, clearing through solution that is freely miscible with both is needed. The aorta segments were placed in three changes of xylene for 1 h, 0.5 h and 0.5 h, respectively, to displace alcohol and also leave tissue transparent ready for paraffin infiltration. Subsequently, the aorta segments were infiltrated with liquid paraffin in the paraffin oven (58 - 60°C) for 2 × 2 h to ensure the tissue was free of xylene and fully permeated with the paraffin. And then, aorta segment was carefully placed to the proper section angle in a molten paraffin-filled embedding mould. The paraffin blocks were then cooled and hardened overnight. The solidified paraffin was within and around aorta segment, and aorta segment was enclosed in a solid mass. These tissue paraffin blocks were cut in transverse sections of 8 µm and mounted on slides. All slides were stained with Mellory's trichrome, and mounted with clear coverslips for the following histological examination.

### **2.1.2.2. Light Microscopy**

Slides were stained with Mellory's trichrome, and sections were examined and photographed using a Nikon E990 digital camera at magnifications with a Leica DM1RB light microscope. Histology of the aortic preparations showed a thin intima and a thick media in all specimens, some adventitial tissue in most specimens, but minimal amounts of fat. The aorta wall transverse sections showed intact structure and normal histology at either 0.5 h (control) or after 8 h incubation in air (Fig 2.1).

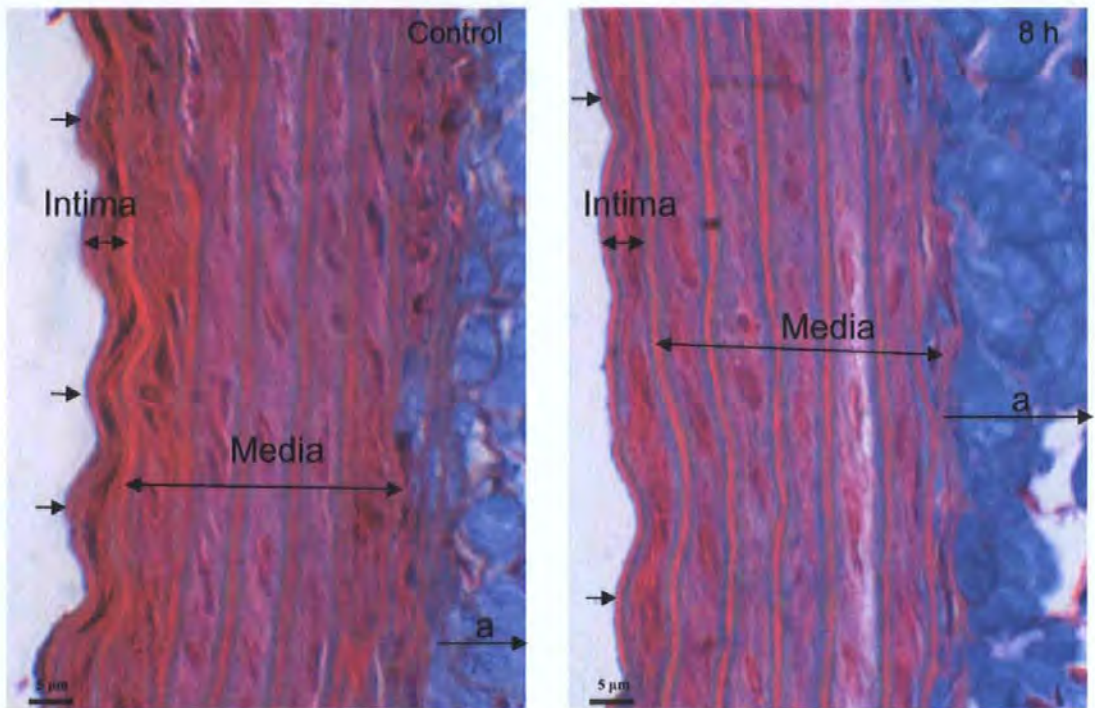


Fig 2. 1 Rat aorta after exposure to normobaric air for 0.5h (control) or 8h, respectively. Tunica intima (Intima) composed of endothelial cells (arrows), tunica media (Media), tunica adventitia (a). Mallory's trichrome stain  $\times 400$ .

### 2.1.3. Tissue Damage

#### 2.1.3.1. Measurement of LDH Activity

Lactate dehydrogenase (LDH) is released from the cells when tissue damage occurs. So by monitoring LDH release in the medium, tissue damage was evaluated. LDH activity was tested using method described by Plummer (1987). Briefly, 0.1 ml of 21 mM sodium pyruvate solution was rapidly added into a 4 ml cuvette which already contained a mixture of 0.3 ml medium sample, 2.5 ml phosphate buffer (0.1 M, pH 7.4) and 0.1 ml of 3.5 mM nicotinamide adenine dinucleotide (NADH). The latter mixture had been equilibrated in a 37°C thermostatically heated cell housing in the ultraviolet spectrophotometer (PERKIN ELMER, UV/VIS, Bio 20). The changes in absorbance at 340 nm were recorded for 3 min. Enzyme activities are calculated dividing by the molar extinction coefficient of NADH at 340 nm ( $6.3 \text{ mM}^{-1} \text{ cm}^{-1}$ ) and converting to enzyme units (unit definition: one unit will reduce 1.0  $\mu\text{mol}$  of pyruvate to L-lactate per min at pH 7.5 at 37 °C).

The cumulative LDH activity in 6 ml medium at 0.5 h and 8 h post incubation was  $0.01 \pm 0.01$  U  $\text{mg}^{-1}$  tissue weight (tw) and  $0.02 \pm 0.02$  U  $\text{mg}^{-1}$  tissue weight (tw) (means  $\pm$  SD of three replicates) respectively.

### 2.1.3.2. Total LDH Content in Aorta Segments

In theory, the maximal LDH release is the sum of LDH left in the tissue and the LDH released in the medium. By calculating the percentage of the LDH in medium relative to maximal LDH release, cell damage can be estimated and expressed quantitatively.

In our experiment, the maximal LDH release from the aorta segment was estimated by measuring the total LDH content in aorta segment tissue. At first, we tried to lyse the fresh dissected aorta segment with different concentrations of Triton X-100, but low and variable results implied insufficient solubilisation of membranes with Triton X-100 lysis only (Fig 2.2). The insufficient membrane breakdown may due to the tight connection of smooth muscle cells in the aorta segments; therefore instead we mechanically homogenized the aorta segment using a TD20 rotor of CAT-X5 20 D homogenizer at 16,000 rpm for  $3 \times 10$  seconds. The LDH content in rat aorta homogenate was more than three-fold of the value obtained with only Triton X-100 treatment. Further treatment of the tissue homogenate with Triton X-100 slightly improved the LDH value, and best results were shown in homogenate treated with 0.3% of Triton X-100 solution ( $0.38 \pm 0.05$ ,  $n = 3$ ), which was only 2.7% higher than only tissue homogenate LDH measurement ( $0.37 \pm 0.05$ ,  $n = 3$ ) (Fig 2.3). Since further Triton X-100 treatment had no significant effect on LDH release from the samples, it seems that high speed homogenization was sufficient to release nearly all the LDH content from aorta segments. Therefore, the maximal LDH content in our rat aorta tissue homogenate was  $0.19 \pm 0.02$  U  $\text{mg}^{-1}$  tw (means  $\pm$  SEM of six replicates). Comparing with the maximum LDH level, although LDH release in the

medium increased over incubation, the LDH released was still less than 10% of the total LDH content up to 8 h incubation.

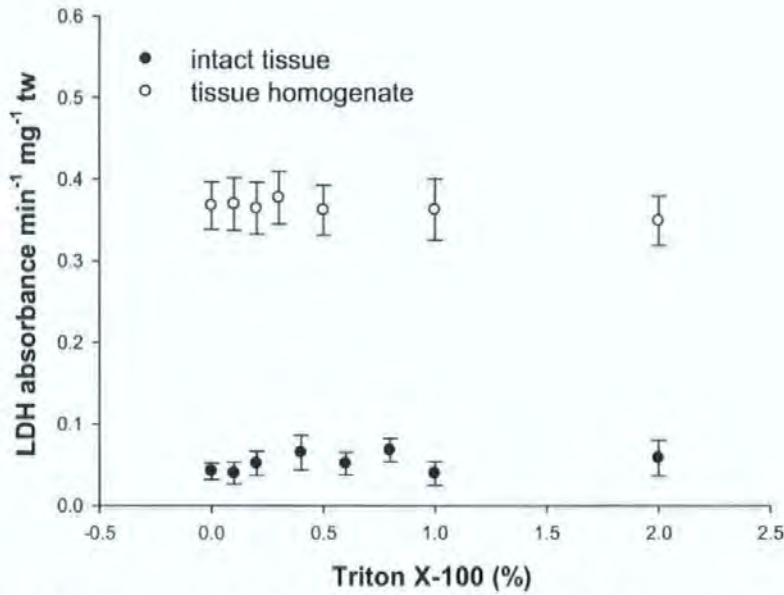


Fig 2. 2 Measurable LDH level of aorta segment and tissue homogenate after Triton X-100 lysis. Data are represented of means  $\pm$  SD of three replicates, respectively.

#### 2.1.4. Conclusion

Histological examination confirmed that the aorta wall kept intact and all the cells showed normal histological structure, which means that aorta segment preparation and culture did not damage the tissues. And further evidence of less than 10% LDH release supported this conclusion biochemically. Therefore, rat aorta segment can be healthy cultured in modified Krebs-Ringers solution in air at 37 °C for up to 8 hours.

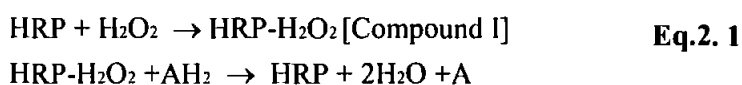
## 2.2 Detection of Reactive Metabolites of Oxygen and Nitrogen

Elevated concentrations or production rates of reactive oxygen and nitrogen species are known to mediate cytotoxicity through alterations in protein, lipid, and nucleic acid

structure and function, with resultant disruption of cellular homeostatic mechanisms. However, small molecular weight ROS such as nitric oxide and hydrogen peroxide may also critically impact cellular homeostasis to play physiological roles in initiating signalling cascades. Thus, sensitive, specific, and reliable methods for detecting changes in these substances are essential to understand their roles in both physiological and pathological states.

### 2.2.1. Hydrogen Peroxide Detection

Horseradish peroxidase (HRP)-linked assays have been reported to detect H<sub>2</sub>O<sub>2</sub> generation in several experimental conditions (Eq.2. 1). The principle of this assay is that in the presence of H<sub>2</sub>O<sub>2</sub>, hydrogen donors (AH<sub>2</sub>) are oxidized by HRP, and the amount of H<sub>2</sub>O<sub>2</sub> is estimated by following the fluorescence changes of initial fluoregenic probes such as scopoletin (7-hydroxy-6-methoxy-coumarin), homovanillic acid (3-methoxy-4-hydroxyphenylacetic acid), and other types of hydrogen donors (Tarpey et al., 2004).



The oxidation of homovanillic acid (HVA) to give a highly fluorescent dimer is quite efficient. One unit of HRP per ml and 100  $\mu\text{M}$  HVA were found to give completion of the reaction with H<sub>2</sub>O<sub>2</sub> in less than 5 min and produced a linear relationship over the test range of 0.1 – 10 nanomoles H<sub>2</sub>O<sub>2</sub> ( $r = 0.999$ ) without affecting cell viability; in addition the fluorescence of the product remained constant for at least 2 h at room temperature (Ruch et al., 1983). These properties made HVA the most suitable fluoregenic hydrogen donor for our specific samples. The analytical conditions, the concentrations of HVA and standard calculation curve were optimized and validated for the determination of the H<sub>2</sub>O<sub>2</sub> release by aorta segments.

### 2.2.1.1. Conditions for the H<sub>2</sub>O<sub>2</sub> Assay

When measuring cellular or subcellular H<sub>2</sub>O<sub>2</sub> accumulation, accuracy of the assay can be improved by separation of the incubation media from cellular components before addition of the detection system, thus limiting confounding interactions of the detection system with cellular elements (Staniek and Nohl, 2002). Therefore, at first, we set up the standard reaction by adding different amounts of H<sub>2</sub>O<sub>2</sub> to a reaction mixture consisting of 2 ml modified Krebs-Ringers solution, 100  $\mu$ M HVA and 5 U ml<sup>-1</sup> of HRP. Fluorescence measurements were performed using a Perkin Elmer luminescence spectrometer (LS50B) at 700V PMT voltages. Excitation and emission wavelengths were 312 and 420 nm, respectively, with 2.5 nm slit widths for both excitation and emission. Over the test range of 2 – 20 nmol H<sub>2</sub>O<sub>2</sub> (1 - 10  $\mu$ M), and the correlation coefficient of the quadratic analysis was calculated at 0.999 (Fig 2.3).

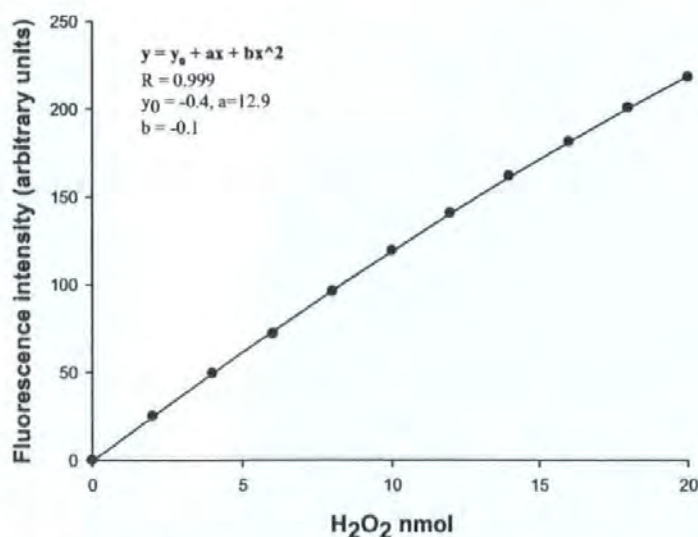


Fig 2. 3 Fluorescence intensity changes upon 0 – 20 nmol of H<sub>2</sub>O<sub>2</sub> (1 - 10  $\mu$ M). Graded amounts of H<sub>2</sub>O<sub>2</sub> were added to a reaction mixture of 2 ml modified Krebs-Ringers solution containing 100  $\mu$ M HVA and 5 U ml<sup>-1</sup> of HRP. The fluorescence intensity values were corrected by subtracting the background fluorescence intensity value (5.75). The curve was obtained by quadratic fitting analysis using Sigmaplot 10.0 software.

### 2.2.1.2. Conditions for Aorta Segment H<sub>2</sub>O<sub>2</sub> Accumulation Measurement

When medium samples were added to the reaction system, unfortunately, there was no signal that showed the presence of H<sub>2</sub>O<sub>2</sub>. It is always difficult to measure in situ H<sub>2</sub>O<sub>2</sub> accumulation in live cells and tissue because of its relatively short half-life (seconds) and the efficient antioxidant scavenging systems, so any detection assay must be sensitive enough to effectively compete with these antioxidant scavengers. It was therefore necessary to add the reaction reagents directly to the culture medium for detection of H<sub>2</sub>O<sub>2</sub> accumulation. In our experiments, due to the possible interactions of the detection system with cellular elements and oxygen exposure, investigations on the detection sensitivity of different concentration of HRP and the influences of hyperbaric oxygen (HBO) on the standard curve were performed in the absence or presence of aorta segments.

Thoracic aorta segments (1 cm) were placed in culture wells containing 6 ml Krebs-Ringer solution with different concentration of HRP (1U, 5U, 10U and 20U ml<sup>-1</sup>) and 100 μM HVA. Another matching culture well of the same plate containing the same buffer was used as a blank control. Samples were exposed to 100% oxygen at 2.2 ATA for 90 min, 1.5 ml medium was collected from both the sample well and corresponding control well at prior to treatment (Pre), immediately after 90 min treatment (Post), and 4 h after treatment (4h). Initial H<sub>2</sub>O<sub>2</sub> levels were measured immediately after collection of each time point, and followed by adding different concentration of H<sub>2</sub>O<sub>2</sub> to the reaction system to measure the H<sub>2</sub>O<sub>2</sub>-dependent response. Fluorescent density was measured using a Perkin Elmer luminescence spectrometer (LS50B) at 700 V PMT voltages, and 2.5 nm slit widths both for excitation and emission. Excitation and emission wavelengths were 312 and 420 nm, respectively. There were clearly measurable H<sub>2</sub>O<sub>2</sub> accumulations in medium containing aorta segments (Fig 2.4B), which were much higher than the corresponding control values (see Fig 2.4A). The oxygen treatment and prolonged incubation time also increased the

baseline fluorescence level (Fig 2.4A). Although 1 U ml<sup>-1</sup> of HRP gave lower levels of fluorescence, increasing the HRP concentration from 5 U ml<sup>-1</sup> to 20 U ml<sup>-1</sup>, did not show a HRP concentration dependent increase in assay sensitivity (Fig 2.4). It looks like that 5U ml<sup>-1</sup> HRP would be sufficient to measure the level of H<sub>2</sub>O<sub>2</sub> in our specific medium.

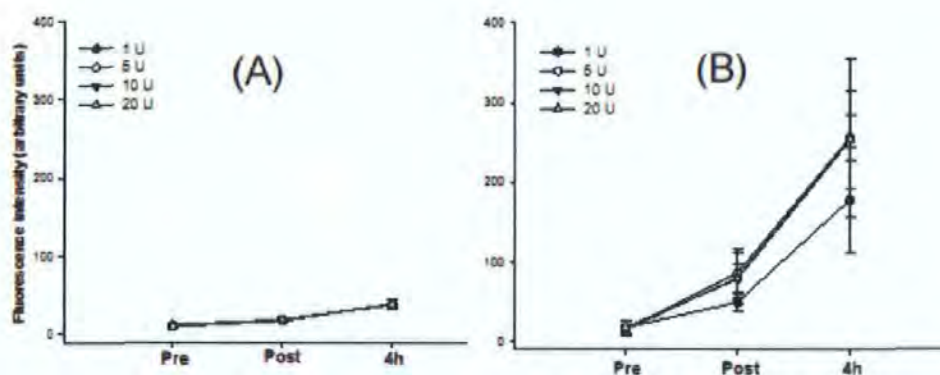


**Fig 2. 4** Influence of HRP concentration and HBO treatment on fluorescence intensity changes. 6 ml of Krebs-Ringer solution containing HVA (100  $\mu$ M) and HRP of 1, 5, 10 and 20 U per ml, respectively, were exposed to HBO at 2.2 ATA for 90 min. Three replicates were used and the results were expressed as means  $\pm$  SD for each case. Fluorescence intensity was measured with 1.5 ml of reaction reagent-containing culture medium at pre, immediate post and 4h post HBO. (A) the corresponding blank values in the absence of aorta tissue; and (B) the accumulated fluorescent intensity value with aorta tissue in culture medium.

For further detecting the effects of HBO treatment on standard curve in experimental reaction system, H<sub>2</sub>O<sub>2</sub> (1 nmol and 2 nmol, respectively) were added to reaction system containing 100  $\mu$ M of HVA and 5U ml<sup>-1</sup> of HRP. A nearly linear fluorescence changes were found in the blank control medium at all three time points (Fig 2.5A). In tissue-containing medium, a linear fluorescence changes was only found at pre-treatment, but neither at immediately post treatment nor at 4h post treatment (Fig 2.5B). In addition, the samples of tissue-containing medium showed much less fluorescence change than that of blank medium when H<sub>2</sub>O<sub>2</sub> was added, and significant differences were shown at 4h after exposure ( $P < 0.05$ , unpaired t-test). These may because that the increase of H<sub>2</sub>O<sub>2</sub> level with HBO treatment consumed the reaction reagents, and that limited the sensitivity of reaction system to H<sub>2</sub>O<sub>2</sub>. Therefore, when calculating H<sub>2</sub>O<sub>2</sub> concentration in sample medium, it

should be converted from the calibration curve generated from corresponding blank medium but not from the sample medium itself.

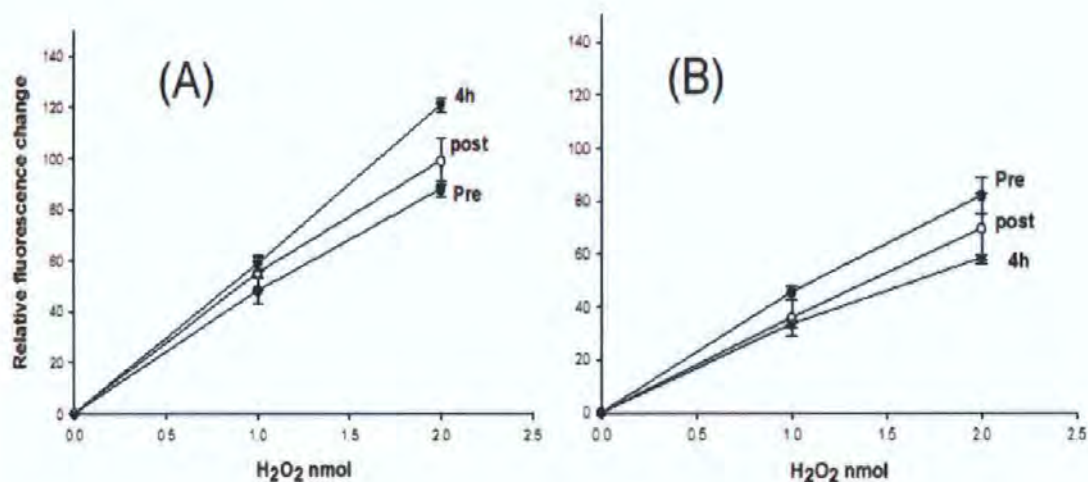


Fig 2. 5 HBO treatment affects the standard curve of H<sub>2</sub>O<sub>2</sub> relative fluorescence changes upon the addition of H<sub>2</sub>O<sub>2</sub>. 6 ml of Krebs-Ringer solution containing HVA (100  $\mu$ M) and HRP (5 U ml<sup>-1</sup>) were exposed to HBO at 2.2 ATA for 90 min and fluorescence values were collected at pre, immediate post and 4h post HBO. At each time-point, fluorescence changes were measured from 1.5 ml of blank control medium, and tissue-containing medium, respectively. Then, H<sub>2</sub>O<sub>2</sub> was added to medium and H<sub>2</sub>O<sub>2</sub>-dependent relative fluorescence changes were obtained by subtracting the corresponding initial fluorescence value. (A) is the corresponding values in blank control medium in the absence of aorta tissue after 1 or 2 nmol of H<sub>2</sub>O<sub>2</sub> were added, respectively; (B) is the accumulated fluorescent value with aorta tissue after 1 or 2 nmol of H<sub>2</sub>O<sub>2</sub> were added, respectively. The results are expressed as means  $\pm$  SD of three replicates.

### 2.2.1.3. Protocol Summary

As H<sub>2</sub>O<sub>2</sub> production by cultured aorta segments could only be achieved when the reaction reagents were added to the culture medium, we compared the effects of HRP concentration on assay sensitivity and HBO exposure to H<sub>2</sub>O<sub>2</sub>-dependent standard curves in our specific model. The sensitivity of H<sub>2</sub>O<sub>2</sub> measurement was not totally dependent on the concentration of HRP, and that 5 U ml<sup>-1</sup> of HRP and 100  $\mu$ M of HVA were sufficient for determination of relatively large amounts of H<sub>2</sub>O<sub>2</sub>; in addition, HBO treatment affect the H<sub>2</sub>O<sub>2</sub>-dependent fluorescent response in tissue containing medium, so it was necessary to set up a corresponding control blank well containing the same volume of Krebs-Ringer solution and the same concentrations of reagents but without aorta tissue, and the calculation of H<sub>2</sub>O<sub>2</sub> concentration in sample medium should be calculated from the

calibration curve generated from corresponding blank control medium to avoid overestimate  $\text{H}_2\text{O}_2$  concentrations..

To be cautious about those reaction reagents (HRP and HVA) that may cause aorta tissue damage during incubation, LDH level was measured from the sample medium. And the LDH level at 4h after exposure from these preparations ( $0.028 \pm 0.008 \text{ U mg}^{-1} \text{ tw}$ ) were not higher than a control group without these reagents ( $0.026 \pm 0.009 \text{ U mg}^{-1} \text{ tw}$ ) ( $P = 0.57$ , means  $\pm$  SEM,  $n = 3$ , unpaired t-test).

For the first time, we presented here a protocol to measure in situ  $\text{H}_2\text{O}_2$  accumulation in blood vessels by optimizing and validating HRP-linked  $\text{H}_2\text{O}_2$  assay by using homovanillic acid as a hydrogen donor in our studies. In studies of Chapter 3 and 4, a separate series of experiments was done by adding the reagents directly to the culture wells which allowed us to focus only on  $\text{H}_2\text{O}_2$  production. Briefly, a thoracic aorta was sectioned into  $3 \times 1 \text{ cm}$  segments, and then placed in culture wells containing 6 ml respective culture medium with  $5 \text{ U ml}^{-1}$  of HRP and  $100 \mu\text{M}$  of HVA. Matching culture wells of the same plate containing the same buffer was used as a blank. The plates were exposed to required treatments, prior to exposure, immediately after treatment, and 4 h after treatment, 1.7 ml of medium was collected from each sample well and control blank well, and kept on ice until analysed for  $\text{H}_2\text{O}_2$ . The  $\text{H}_2\text{O}_2$  level was measured immediately after collection of each time point by transferring 1.5 ml of medium to a fluorescence cuvette. Fluorescence intensity was measured using a Perkin Elmer luminescence spectrometer (LS50B) at 700 V PMT voltages, and 2.5 nm slit widths both for excitation and emission. Excitation and emission wavelengths were 312 and 420 nm respectively. The fluorescence of sample medium (F1) and blank control medium (F2) were measured. Actual fluorescence intensity was obtained by subtracting the blank fluorescence from the tissue sample data (F1-F2). Cumulative  $\text{H}_2\text{O}_2$  concentration in sample medium was obtained by converting from the

calibration curve, which was generated by adding known levels of  $\text{H}_2\text{O}_2$  into the blank medium.

### 2.2.2. Nitric Oxide Measurement

#### 2.2.2.1. Nitric Oxide Detection Methods

The measurement of nitric oxide (NO) is rather difficult since NO reacts rapidly with free oxygen, oxygen radicals, redox metals, sulphhydryls, disulfides and oxygenated haemoglobin (Stamler et al., 1992). Direct NO measurements have been reported using electron paramagnetic resonance (EPR) spectroscopy with nitroso- or haemoglobin spin traps (Arroyo and Kohno, 1991) or a NO-selective microelectrode to measure NO concentration through amperometric signals (Malinski et al., 1996a. b). However, the requirement for expensive instruments and specific training restricts the popularization of these techniques for most labs. Therefore, several commonly used methods for NO detection have been developed such as the oxyhemoglobin reaction assay, Griess reaction assay and fluorescence assays.

*In vivo*, most of the endogenously formed NO reacts with oxyhaemoglobin ( $\text{HbFe(II)O}_2$ ) to produce methaemoglobin (MetHb,  $\text{HbFe(III)}$ ) and nitrate in red blood cells (Wennmalm et al., 1993). The rates of NO binding and release for Fe(II)-haemoglobin are 5–6 fold greater than that of  $\text{O}_2$ , and NO metabolism has been shown to depend upon the oxygenation of red cell haemoglobin (Wennmalm et al., 1992). In contrast to nitrite, nitrate is biologically completely inactive, therefore oxidation of NO in erythrocytes to nitrate by oxyhaemoglobin *in vivo* is the most effective and definite inactivating metabolic fate for NO (Tsikas, 2006). The oxyhemoglobin reaction assay uses this principle to measure the shift of the optical absorption spectra when oxyhemoglobin Fe (II) reacts with NO to form methemoglobin Fe (III) (Feelisch and Noack., 1987). However, in this reaction, oxidation

products can lead to overestimated results particularly in the presence of cells, so in order to obtain coherent calibration results, one must work under very strict conditions of time, pH, and temperature because even small changes in these parameters can greatly influence the haemoglobin reaction. Besides, L-arginine and L-NMMA were also found to induce variations in the absorbance ratio (Privat et al., 1997).

In the aqueous phase, free of biological material, NO exclusively autoxidizes to nitrite, in which incorporation of O from H<sub>2</sub>O into NO seems to take place during hydrolysis of an intermediate, such as N<sub>2</sub>O<sub>3</sub> (Pogrebnyaya et al., 1975; Pires et al., 1994; Goldstein and Czapski., 1995). The half-life of NO in aqueous phosphate-buffered solution of pH 7.4 was estimated to be 130 s (Ford et al., 1993). The most frequently used method of detecting nitrite is based on a purple azo dye found more than 100 years ago by Griess (1897), which can be easily applied in the lab without a large and expensive experimental set up. Griess reaction is a two-step diazotization reaction in which an NO-derived N-nitrosating agent (e.g. N<sub>2</sub>O<sub>3</sub>), generated from the acid-catalyzed formation of nitrous acid from nitrite (or the interaction of NO with oxygen), reacts with sulphanilamide to produce a diazonium ion that is then coupled to N-(1-naphthyl) ethylenediamine (NEDA) to form a chromophoric azo product that absorbs strongly at 543 nm (Grisham et al., 1996). The Griess reaction itself is a simple, rapid, and inexpensive assay and has a practical sensitivity in the micromolar range. Van der Zee et al (1997) demonstrated that the nitrite level as measured by the Griess reaction method may give a clear indication of NO production by vessel segments (in this specific condition as no haemoglobin is present in the experimental system). However, this method has limitations regarding both sensitivity and its inability to detect nitrate. Consequently, total NO<sub>x</sub> (nitrate+nitrite, NO<sub>3</sub><sup>-</sup>+NO<sub>2</sub><sup>-</sup>) measurement has been developed, which first requires reduction of nitrate to nitrite, and then nitrite is determined by Griess reaction. The reduction of nitrate to nitrite can be achieved by bacterial nitrate

reductase or reducing metals such as cadmium (Green et al., 1982; Granger et al., 1995). Nowadays, a variety of methods have been developed to measure total NO<sub>x</sub> as an indirect indication of NO generation in physiological fluid such as blood serum, urine and cell or tissue culture media. Privat et al (1997) investigated NO<sub>x</sub> accumulation in the cultured medium of human umbilical vein endothelial cells (HUVECs) with NO<sub>x</sub> method and found a cumulative basal production of nitrite plus nitrate even over a relatively short incubation time (5 min), and the basal production was 10 times higher when NO<sub>x</sub> instead of nitrites were measured.

Fluorescence assays like the diaminonaphthalene (DAN) assay offer the additional sensitivity compared to the Griess reaction assay, and is capable of detecting NO production at the nanomolar level. In the DAN assay the nonfluorescent DAN reacts rapidly with the NO-derived N-nitrosating agent (N<sub>2</sub>O<sub>3</sub>) generated from the interaction of NO with oxygen or from the acid-catalyzed formation of nitrous acid from nitrite to yield the highly fluorescent product 2,3-naphthotriazole (NAT) (Miles et al., 1996).

### 2.2.2.2. Nitrate Measurement Using Nitrate Reductase and Griess Reaction

Initially, we applied the NO<sub>x</sub> method described by Schmidt and Kelm (1996). Nitrite measurement produced a stable linear standard curve ranging from 0.5 to 2.5 μM; however, this method failed to produce a linear calculation curve of nitrate in our hands as an absorbance drop was obtained above 1.5 μM of nitrate (Fig 2.6). In the Schmidt's method, 0.1U ml<sup>-1</sup> purified *Aspergillus niger* nitrate reductase (NR) and 0.03 mM of NADPH (nicotinamide adenine dinucleotide phosphate-oxidase) were used to reduce nitrate to nitrite, which may not be sufficient to complete the reduction of nitrate to nitrite. Another drawback of Schmidt's method is that it involves sample transfer and incubations at different temperature, which is inconvenient when handling large number of samples.

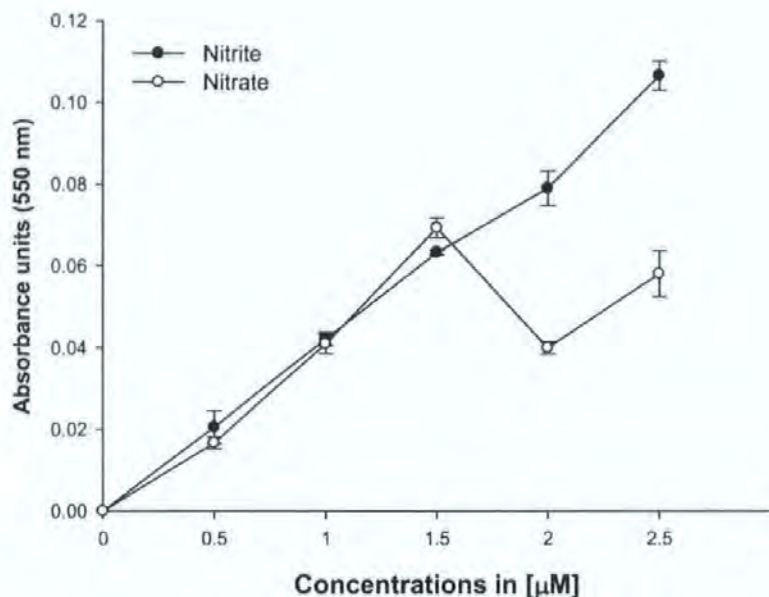


**Fig 2. 6** Standard curve for detection of nitrite (●) and NOx (○) using method described by Schmidt and Kelm (1996). Nitrite ( $\text{NaNO}_2$ ) and nitrate ( $\text{NaNO}_3$ ) standards (0.5 to 2.5  $\mu\text{M}$ ) were prepared in  $\text{H}_2\text{O}$ . Values are means  $\pm$  range of two observations, respectively.

Therefore, a modified NOx method has been developed, and the assay protocol is described as below. Assay mixture was prepared by mixing (per ml) 0.72 ml of 50 mM sodium phosphate buffer (pH 7.4), 0.08 ml (1.6 U/ml NR from *Aspergillus niger* in buffer), and 0.2 ml of 1 mM NADPH. 50  $\mu\text{l}$  of nitrate standard (up to 20  $\mu\text{M}$ ) or samples were mixed with 50  $\mu\text{l}$  assay mixture to give a final concentration of 0.1 U/ml NR and 0.2 mM NADPH in wells of a 96-well plate. And then the plate was incubated for 30 min at 20 °C to allow completely reduction of nitrate to nitrite. The diazotization reaction was started by adding 100  $\mu\text{l}$  of sulphanilamide (1% [w/v] in 1 M HCl), followed by 100  $\mu\text{l}$  of 0.1% NED 30–90 s later. Absorbance at 550 nm was measured a few minutes later in a Dynatech Laboratories MRX plate reader (Billingshurst, UK).

This modified assay is not only robust with perfectly reproducible calibration curves for both nitrite and nitrate measurements, but also save a lot of handling time as all the reactions are accomplished at room temperature within a well of 96-well plate. The detection range is between 2.5 to 50  $\mu\text{M}$ , and the standard curves derived from nitrite and

nitrate were similar which means that nitrate has been reduced to nitrite completely (Fig 2.7). The nitrate concentrations of our experimental samples were measured at 3 - 20  $\mu\text{M}$ , which fitted into the testing range of our modified assay. The nitrite concentrations of our sample ranged 0.1 - 1.5  $\mu\text{M}$ , which was much less than that of nitrate.

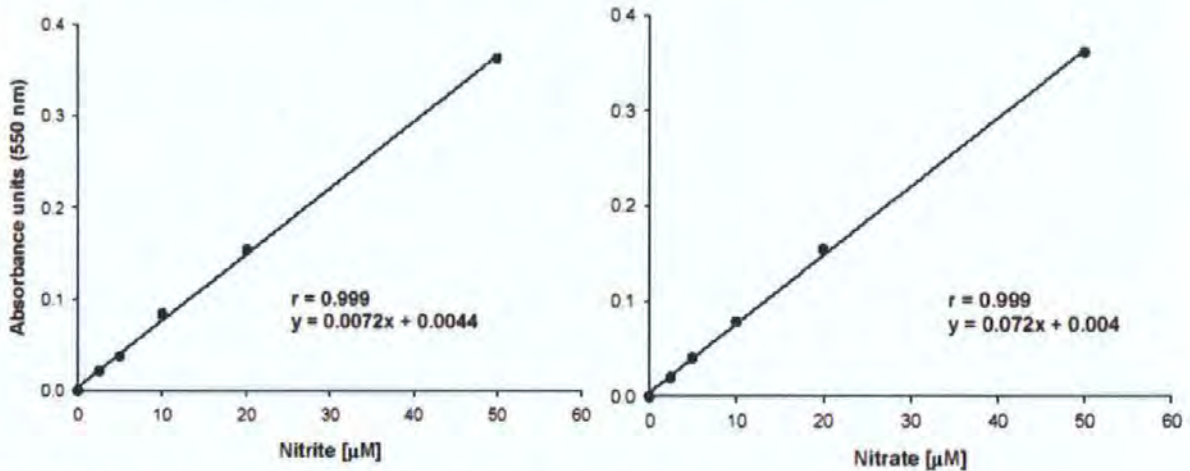


Fig 2. 7 Standard curves for the detection of nitrite and nitrate using our modified NOx assay. Nitrite ( $\text{NaNO}_2$ ) and nitrate ( $\text{NaNO}_3$ ) standards (0.5 to 50  $\mu\text{M}$ ) were prepared in  $\text{H}_2\text{O}$ . Curves were obtained by linear regression.

## 2.3 Glutathione Measurement

### 2.3.1. Glutathione Pool: Indicator of Oxidative Stress *in Vivo*

Glutathione (GSH) is a tripeptide characterized by a  $\gamma$ -glutamyl peptide linkage a reactive thiol group (Kosower, 1978). As the predominant non-protein thiol (-SH) in cells, GSH plays important roles ranging from antioxidant defence to modulation cell proliferation. As shown in Fig 2.8, GSH is among the most important antioxidants in cells, being used in enzymatic reactions to eliminate peroxides and in nonenzymatic reactions to maintain ascorbate and  $\alpha$ -tocopherol in their reduced and functional forms, in which GSH is converted to its disulfide form, GSSG (Jones, 2002). Glutathione disulfide, often referred to as oxidized glutathione, can be reduced to GSH by NADPH through the glutathione reductase (GR) reaction while NADPH levels are maintained by the pentose

phosphate shunt. The activity of the reductase increases in response to an increase in concentration of GSSG, so the increases in GSSG during oxidative stress are generally transient as reduction by GR is relatively rapid. Furthermore, an ATP-dependent transport mechanism can also decrease the intracellular content of GSSG through active export (Sharma et al., 1990). In addition, products of lipid peroxidation such as cyclopentanones or aldehydes and other xenobiotic products can react with GSH to form conjugates nonenzymatically or through the action of glutathione S-transferases (GST). Formation of conjugates can also result in depletion of GSH, thus once formed they are transported outside the cell through membrane transporters (Eaton and Bammler, 1999). The steady-state ratio of GSH to GSSG is important for maintaining cell function and membrane integrity, for example, GSSG is normally maintained at a range of 1% - 10% of total glutathione (Reeve et al., 2001). In cases of oxidative stress, oxidative free radicals and other deleterious compounds consume GSH, so changes in GSH content are typical of a cell's response to stress. In the process of GSH reactions to protect the cell by removing or altering the stress factors, more GSSG or mixed disulfides (GSX) are produced, which are transported outside the cell to maintain the redox balances inside the cell. This temporary depletion must be reversed through either enzymatic reduction of a disulfide or by *de novo* synthesis to restore baseline levels of GSH or cell damage even cell death will occur. Therefore, measurement of the kinetic changes in glutathione can be used as an indicator of oxidative stress.

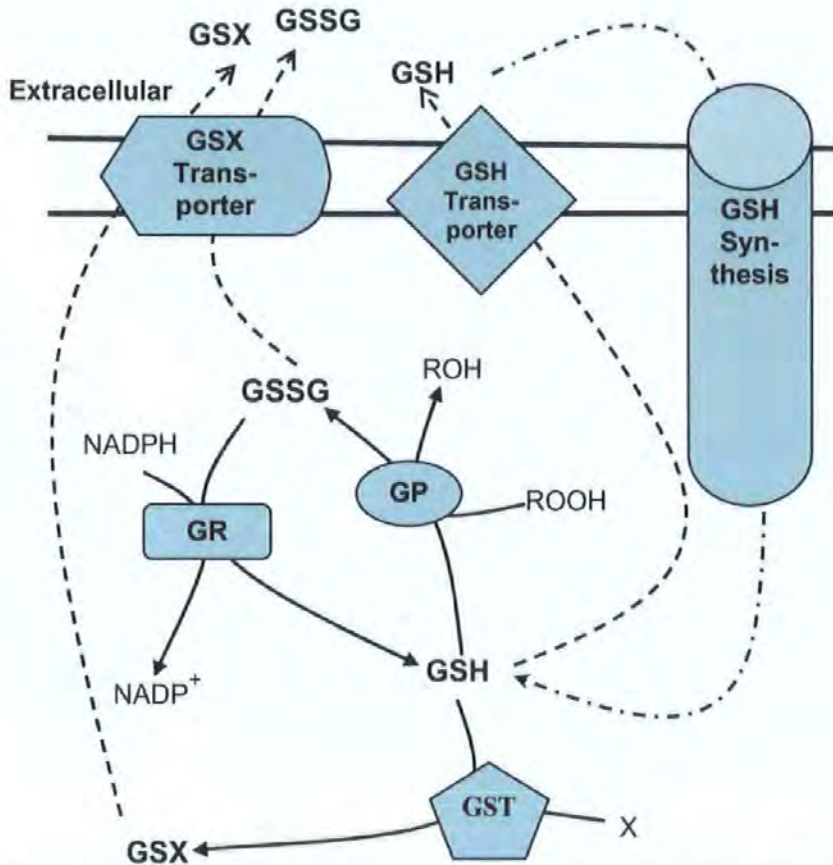
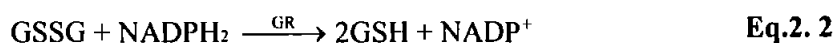


Fig 2. 8 Diagram illustrating the use of GSH (modified from Dickinson et al., 2003). Glutathione peroxidases (GPx) use GSH as a reductant in peroxidase reactions with various hydroperoxides (ROOH), and lipid peroxides (not shown) to form the corresponding alcohol (ROH) and glutathione disulfide (GSSG). GSSG can then either be reduced by glutathione reductase (GR) at the expense of NADPH to regenerate GSH, or can be exported from the cell via the transmembrane multi-drug resistance protein GSX transporter. Glutathione S-transferases (GST) use GSH in conjugation reactions with various xenobiotic compounds (X) to yield mixed disulfides (GSX), which are exported from the cell through the GSX transport protein. GSH can also be exported out of the cell through the transmembrane GSH transporter. Once outside the cell, GSH, GSSG and GSX are partially degraded to join the GSH synthesis pathway. Pathways showing transport are dashed; metabolic pathways are depicted by solid lines.

### 2.3.2. Analysis of Glutathione

The usual procedure for GSH analysis in a biological sample involves homogenization (when necessary), deproteinization, and non-specific or specific measurement of thiol content, the latter being used for cases in which precise knowledge of the GSH content is required (Kosovor., 1978). The thiol group analysis is based on the use of 5,5-dithiobis-2-nitrobenzoic acid (DTNB) (Ellman, 1959). The Glutathione assay is an enzymatic

recycling procedure in which GSSG is reduced to GSH by NADPH in the presence of GR (Eq.2. 2); and the total GSH is sequentially oxidized by DTNB (Eq.2. 3, where DTNB is written as ArSSAr). The rate of 2-nitro-5-thiobenzoic acid (ArSH) formation is monitored at 412 nm. The product GSSAr is cleaved either nonenzymically with GSH or enzymically to yield ArSH and GSSG or ArSH and GSH according to one of the following equations (Eq.2. 4 and Eq.2. 5). It is probable that GSH completes the reduction of ArSSG (Eq.2. 4) and relatively unlikely that ArSSG acts as a substrate for enzymic reduction (Eq.2. 5). Thus the GSH is regenerated and, with excess of NADPH and constant amount of enzyme, the rate of colour production is proportional to the total glutathione, including GSH, GSSG, and possibly, glutathione in disulfide linkage with other soluble thiols (Owens and Belcher., 1965; Griffith., 1980). Finally, the glutathione present is evaluated by comparison with a standard curve generated using known concentrations of GSH.



### 2.3.3. Defined Glutathione Assay for Total Glutathione Measurement

In our experiments, culture medium was exposed to oxygen for a couple of hours to investigate the time and treatment effects, so it was impossible and unnecessary to specify the glutathione measurements in terms of GSH or GSSG. Therefore, the total level of glutathione in culture medium was determined by the glutathione reductase enzyme recycling method as described by Adams et al (1983). The reagents volumes and concentrations have been optimised to conduct this assay on a 96-well plate, which saves time and effort when processing large number of samples.

The reaction buffer was prepared by mixing 16 U of glutathione reductase (GR) to 26 ml of assay buffer (100 mM potassium phosphate and 5 mM potassium EDTA, pH 7.5). 20  $\mu$ l of sample or GSH standard solution (up to 10  $\mu$ M) was mixed with 20  $\mu$ l of buffered DTNB (10 mM DTNB in Assay buffer). After equilibration for 1 min start the reaction by adding 20  $\mu$ l of 3.63 mM NADPH, and absorbance at 412 nm (A412) was measured for 5 min. The rate of A412 changes were calculated using OPTImax tunable kinetic microplate reader (Molecular Device, Sunnyvale, CA, USA). A linear standard curve was obtained over a range of 0.5 – 10  $\mu$ M of glutathione and the correlation efficient is 0.999 (Fig 2.9).

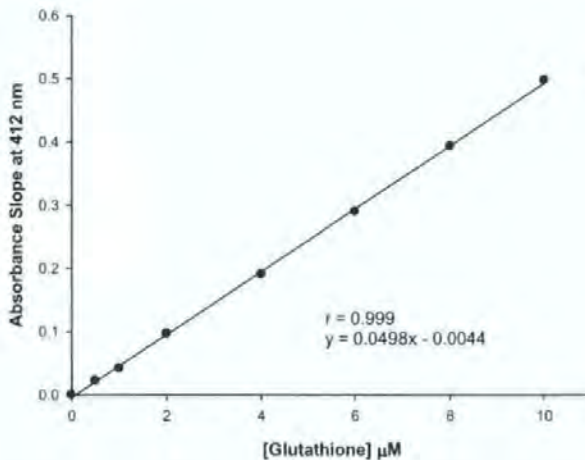
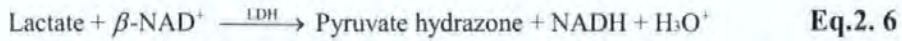


Fig 2. 9 Standard curve of modified total glutathione assay. GSH standards (0 to 10  $\mu$ M) were prepared in H<sub>2</sub>O. The curve was obtained by linear regression.

## 2.4 Lactate Measurement

The cell energy supply mostly depends on the oxidation of glucose. Under aerobic conditions, glucose is oxidized to pyruvate that is further metabolized to CO<sub>2</sub> and H<sub>2</sub>O. When oxygen is depleted, for example reduction of blood supply in tissue injury, pyruvate is converted to lactate by the enzyme lactate dehydrogenase (LDH). Lactate is an intermediate product of anaerobic glycolysis, and reflects the balance between level of hypoxia and energy metabolism in tissues and cells.

The Lactate measurement is based on the formation of NADH from the oxidation of lactate in alkaline conditions in the presence of LDH (Eq.2. 6). NADH absorbs light with a wavelength of 340 nm whereas  $\text{NAD}^+$  does not. Hence, the reaction is quantified by measuring the NADH formed from the increase in absorbance at 340 nm; this gives an indirect measurement of the lactate in the sample.



The reagent volumes and concentrations have been optimised to conduct this assay on a 96-well plate. Briefly, assay mixture contains 0.43 M of glycine, 0.34 M of hydrazine, 3.1 mM  $\beta\text{-NAD}^+$  and 19 U/ml of LDH. 30  $\mu\text{l}$  of sample or lactate standard solution (up to 2 mM) was mixed with 300  $\mu\text{l}$  of assay mixture, and then incubate at 37 °C for 30 min to complete reaction. Absorbance at 340 nm was measured in a Dynatech Laboratories MRX plate reader (Billingshurst, UK). Lactate standard curve in a range of 0 - 2 mM was generated (Fig 2.10).

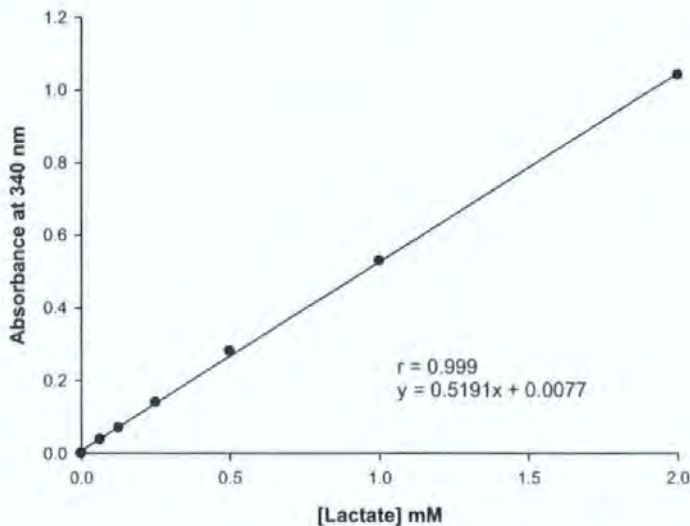


Fig 2. 10 Standard curve of modified lactate assay. Lactate standards (0 to 2 mM) were prepared in  $\text{H}_2\text{O}$ . The curve was obtained by linear regression.

## **2.5 VEGF ELISA Application**

### **2.5.1. Enzyme Linked ImmunoSorbent Assay**

Enzyme Linked ImmunoSorbent Assay (ELISA) was first described by Engvall and Perlman (1971), and soon became a popular technique for detecting and quantifying substances such as peptides, proteins, antibodies and hormones. The principle of ELISA is immobilizing the antigen of interest to a solid surface (commonly a 96-well polystyrene plate) and an enzyme-linked antibody is then bound to the antigen (commonly used enzymes are horseradish peroxidase and alkaline phosphatase); and finally a substrate for the enzyme antibody conjugate is added to produce a product detectable by spectrophotometer, fluorometer or luminometer. The most crucial requirement in this technique is a highly specific antibody-antigen interaction.

Mouse VEGF (VEGF-A) is the product of a single gene containing eight exons. By alternative splicing, three isoforms of mature VEGF containing 120, 164 and 188 amino acid (aa) residues that differ in their heparin binding ability exist. The 164 aa isoform of mouse VEGF shares 98% and 82% aa sequence identity with its rat and human homologs, respectively. Among VEGF family members, VEGF also shares 35%, 37% and 37% aa sequence identity with mouse VEGF-B, -C and -D, respectively. The Quantikine mouse VEGF Immunoassay is a 4.5 hour solid phase ELISA designed to measure mouse VEGF in cell culture supernates, tissue homogenates, mouse serum and plasma. This assay recognizes both the 164 and 120 amino acid residue forms of mouse VEGF. It is calibrated against a highly purified Sf 21-expressed recombinant mouse VEGF produced at R&D Systems and this disulfide-linked homodimeric glycosylated recombinant mouse VEGF contains two 164 amino acid residue subunits. This immunoassay shows no significant cross-reactivity or interference was observed with VEGF-B/C/D. This mouse ELISA kit

(R&D system, MMV00) has been confirmed for cross-reactivity with rat species and is able to measure the rat VEGF accurately (<http://www.rndsystems.com/pdf/mmv00.pdf>).

### **2.5.2. VEGF ELISA Measurement of Rat Aorta Segment Samples**

Tissue crude homogenate was obtained by homogenizing about 15 mg of rat aorta tissue in 0.6 ml hypotonic Tris buffer (pH 7.4, 20 mM Tris, 1mM EDTA) in the presence of protease inhibitors (Sigma P-2714, according to recommended usage). Tissues were then homogenized on ice using a TD20 rotor of CAT-X5 20 D homogenizer at 16,000 rpm and using  $3 \times 10$  second bursts to avoid frictional heating in the samples.

VEGF levels in tissue homogenate and medium were measured using the commercially available mouse VEGF immunoassay kit (R&D system, MMV00). Because the kit has not been used before for blood vessel homogenates; we optimised and validated sample volume and first binding incubation time at 50  $\mu$ l for 2 h at 25 °C for rat aorta homogenates. Assays were performed in duplicate and optical density was determined using an OPTImax tunable microplate reader set to 450 nm. Absorbance at 540 nm ( $A_{540}$ ) was also measured at the same time, and subtract readings at 540 nm from the reading at 450 nm was done as kit manual suggested to correct the optical imperfections in the plate. The quantities of VEGF in samples were determined by comparison with a standard curve generated each time the ELISA was performed (Fig 2.11).

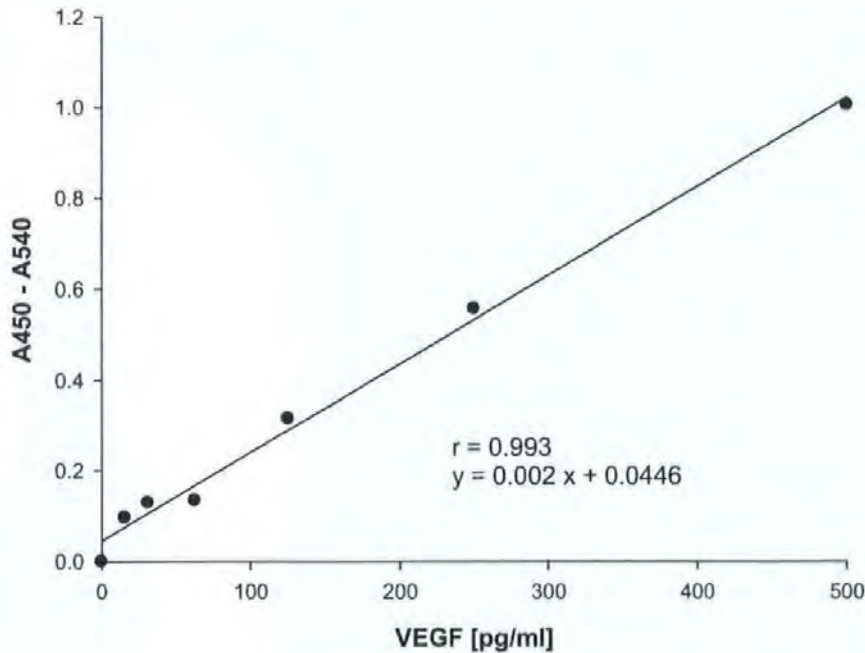


Fig 2. 11 Standard Curve of VEGF ELISA assay. VEGF standards (0 to 500 pg/ml) were prepared as described in the kit manual. The curve was obtained by linear regression, and the correlation coefficient is 0.993.

### 2.5.3. Protein Content Measurement

A semi-microplate method for protein measurement has been developed based on the Hartree (1972) modification of the Lowry protein assay. This assay has been used to monitor perfusate protein levels in perfused rat hearts and fish intestine preparations in our lab, and here works well with rat aorta tissue homogenates.

First, 1 ml of protein standard solution (up to 200 pg/ml), or diluted sample (25  $\mu$ l of homogenate from 2.5.2 needs to be diluted with 1 ml distilled water) was mixed with 0.9 ml of solution A (mixing 0.2 g potassium sodium tartrate, 10g  $\text{Na}_2\text{CO}_3$  and 50 ml of 1M NaOH for per 100 ml) incubate at 50  $^\circ\text{C}$  for 10 min. Secondly, 0.1 ml of solution B (mixing 0.2g potassium sodium tartrate, 0.1 g  $\text{CuSO}_4$  and 1 ml of 1M NaOH for per 10 ml) was added at room temperature and incubated for another 10 min. Thirdly, 3 ml of 6.25% [v/v] of fresh made Folin Ciocalteau reagent was added and incubated at 50  $^\circ\text{C}$  for 15 min.

Finally, 300  $\mu$ l of reaction sample was dispensed in to a well of 96-well microtitre plate and absorbance at 630 nm was measured in a Dynatech Laboratories MRX plate reader (Billingshurst, UK). Protein concentrations were converted to pg/ml against standard curve in the range 0-200 pg/ml (Fig 2.12).

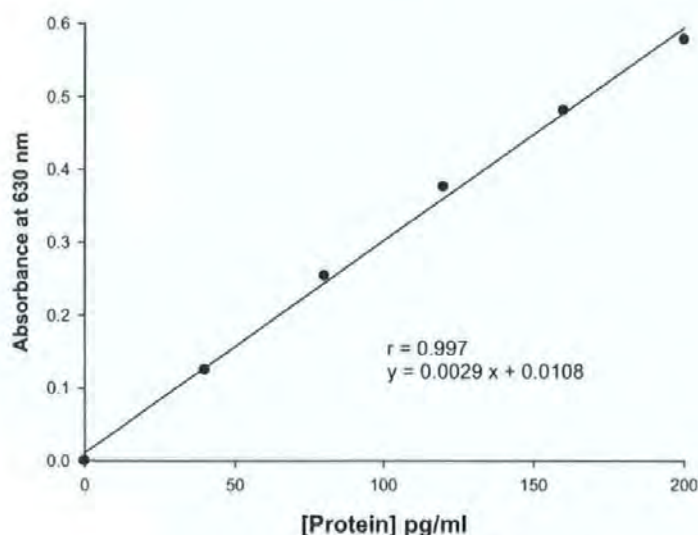


Fig 2. 12 Standard curve of modified protein assay. Bovine serum albumin standard solutions (0 to 200 pg/ml) were prepared in H<sub>2</sub>O. The curve was obtained by linear regression, and the correlation coefficient is 0.997.

## 2.6 Summary

In this chapter, an *in vitro* rat aorta segment model was set up. The tissues were demonstrated intact and healthy for up to 8 h exposure to normobaric air at 37 °C through LDH release measurement and histological examination.

Next, we presented a modified fluorescence method for *in situ* H<sub>2</sub>O<sub>2</sub> measurement in 2.2.1 and a modified NO<sub>x</sub> assay using *Aspergillus niger* nitrate reductase and Griess reaction in 2.2.2. As reactive species, H<sub>2</sub>O<sub>2</sub> and NO are known difficult to evaluate; however, both of our modified assays work well with our samples, which made the time and effort well worth spending on optimization and validation of the assays to suit our specific research interests and aims.

Another important biological marker, glutathione (GSH) is discussed in 2.3.1 as an indicator for oxidative stress. The principle and protocol of total glutathione measurement are subsequently addressed in 2.3.2 and 2.3.3, respectively. The lactate assay is a relatively easy adopted assay, and its detailed procedure is described in 2.4. Finally, the ELISA VEGF assay is presented, which includes the tissue homogenisation, protein content assay and optimization of VEGF measurements for rat aorta tissue homogenates in 2.5.

All the assays we have presented gave linear standard curves covering the range of concentrations present in our sample and applied for the investigation in Chapter 3 and Chapter 4.

## Chapter 3

# Effect of Hyperbaric Oxygen on Blood

## *Vessel in Vitro*

### 3.1 Introduction

Normal wound healing is a highly regulated process, which may be disrupted and delayed by diverse factors and develops to chronic wound. Hyperbaric oxygen (HBO) therapy promotes new vessel formation in granulation tissue, which in turn facilitates chronic wound healing. However, the underlying mechanisms of how HBO exert its effects are far from elucidation. On the other hand, toxic effects of HBO have been described in some cases. Although the mechanisms responsible for the toxicity are still not fully understood, increased formation of reactive oxygen species (ROS) especially at some extreme high pressure (e.g. 5 ATA) was suggested to be implicated in HBO-induced toxicity (Piantadosi and Tatro 1990; Elayan et al., 2000). Therefore, therapeutic HBO strategies (e.g. pressure and duration) for human exposure should be purposely selected to minimize possible adverse effects and guarantee clinical benefits. Paradoxically, at moderate level ROS may also exert as a signal to modulate diverse physiological processes including regulation of angiogenesis factors such as vascular endothelial growth factor (VEGF). VEGF is the most important growth factors known so far in regulating angiogenesis and endothelial cell function. Nevertheless, controversial results of HBO-

induced VEGF production have been presented by *in vitro* cellular studies and *in vivo* wound studies.

The angiogenesis is initiated from the existing blood vessel, but to our knowledge there are no studies that investigate the direct effect of HBO on the blood vessel *in vitro*. Thus, the aim of this study is to investigate the response of oxidative stress, reactive oxygen species and VEGF of blood vessels to a single HBO treatment.

## **3.2 Material and Methods**

### **3.2.1. Animals and Tissue Preparations**

Male Sprague Dawley rats (350 - 400 g; n = 20) were purchased from Harlan UK Ltd. Experiments were conducted in accordance with ethical approval. Aorta was obtained as described in 2.2.1, and sectioned into 7 segments (1 cm long), and then randomly placed in individual wells of Nunclon Delta SI 6-well tissue culture plates (Nunc, InterMed, Denmark) containing 6 ml Krebs-Ringer solution (composition in mM: NaCl 118.6, KCl 4.7, CaCl<sub>2</sub> 2.5, MgSO<sub>4</sub> 1.2, KH<sub>2</sub>PO<sub>4</sub> 1.2, NaHCO<sub>3</sub> 25.1, Hepes 10, glucose 10, pH 7.4).

### **3.2.2. Experimental Design**

After incubation in the above Krebs-Ringer solution for 30 min, one segment of aorta and medium were collected as a pre-treatment control. The other 6 aorta segments were randomly divided into 3 different treatment groups. The air groups (Air) remained exposed to room air at ambient pressure (1 ATA); the oxygen only groups exposed to 100% oxygen at 1 ATA (NBO) and hyperbaric oxygen treatment groups (HBO) were treated with 100% oxygen at 2.2 ATA. Treatment lasted for 90 min, and then culture dishes of all groups were left in air at 1 ATA to follow a 4 h recovery from treatment. Tissue and medium samples from each group were collected immediate after treatment and after a further 4 h

incubation. All experiments were conducted at 37 °C. All tissue and medium samples were snap-frozen in liquid nitrogen, and stored at -80 °C until used for analysis.

One series of experiments were also performed to monitor the generation of hydrogen peroxide, using the protocol above, with the method described in 2.2.1 to enable the measurement of low levels of hydrogen peroxide generation *in situ*.

### 3.2.3. Biochemical Analysis

Several biochemical parameters were measured during the study. Lactate dehydrogenase (LDH) release to the medium was used as a routine marker of tissue leakiness or injury, whilst lactate accumulation in the medium was used to assess anaerobic metabolism. The possibility of oxidative stress during oxygen exposure was monitored by following hydrogen peroxide (H<sub>2</sub>O<sub>2</sub>) concentration and total glutathione levels in medium. Total content of nitrite and nitrate in the medium was measured as a surrogate for NO production by the tissue. Since NO, H<sub>2</sub>O<sub>2</sub> and lactate are potential stimulatory factors for VEGF production, the level of VEGF in both the medium and the tissue were tested. The optimization and validation of all the biochemical assays have been described in Chapter 2.

### 3.2.4. Histological Examination

Partial of tissue samples (2 – 3 mm) were sectioned for histological examination using the method described in 2.1.2. For each specimen, at least 3 representative images were taken using Nikon E990 digital camera at a magnification of ×400 with Leica DM1RB light microscope, and the thickness of the tunica intima and tunica media were then determined in triplicate using Image J software (Image processing and analysis in Java). The endothelium index was calculated as:

$$\text{Endothelium index} = \frac{\text{thickness of tunica intima}}{\text{thickness of tunica intima} + \text{tunica media}} \quad \text{Eq.3. 1}$$

### **3.2.5. Statistics**

All biochemical results are normalized by tissue fresh weight (tw) and are presented as the means  $\pm$  S.E.M of the replicates ( $n = 8 - 10$ ). Statistical analysis was performed by one-way ANOVA followed by Tukey-Kramer multiple comparisons test or unpaired t-test for time and treatment differences. And the Pearson correlation test was performed among the biochemical indexes measured. The significant difference was accepted at  $P < 0.05$ .

## **3.3 Results**

### **3.3.1. Histological Examination of Aorta**

In Fig 3.1, high power ( $\times 400$ ) showed the details of layers in the walls of rat aorta. The wall of rat aorta consists of three basic layers: tunica intima (innermost layer) composed of an endothelial cell lining, tunica media (middle layer) containing largely of smooth muscle cells and tunica adventitia (outer layer in blue colour) composed mainly of connective tissue. All the three layers remained structurally intact and cell morphology was normal over the experiment. There was no evidence of tissue damage such as oedema, haemorrhage, epithelial lifting or necrosis from the histology examination.

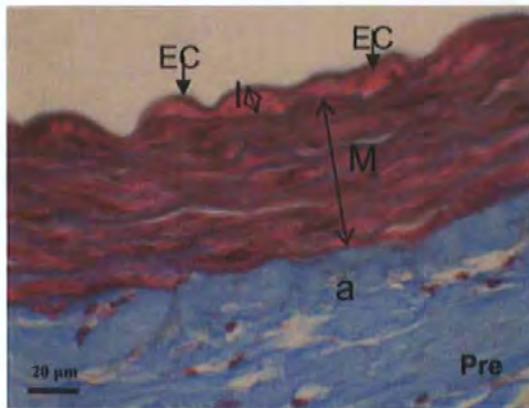
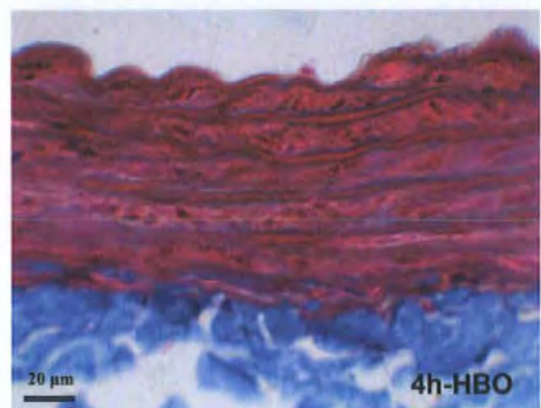
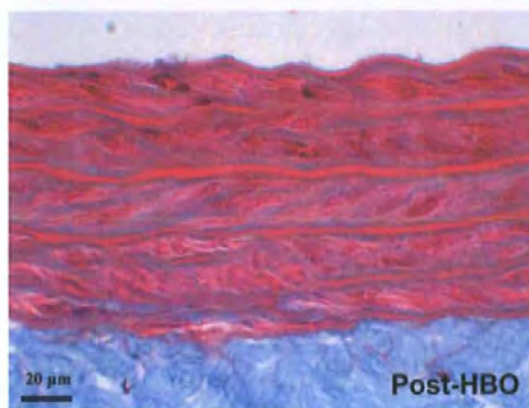
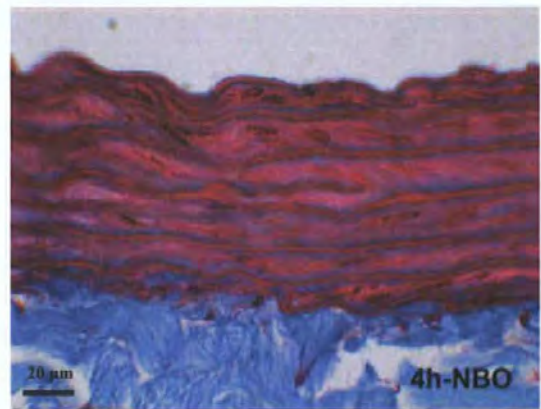
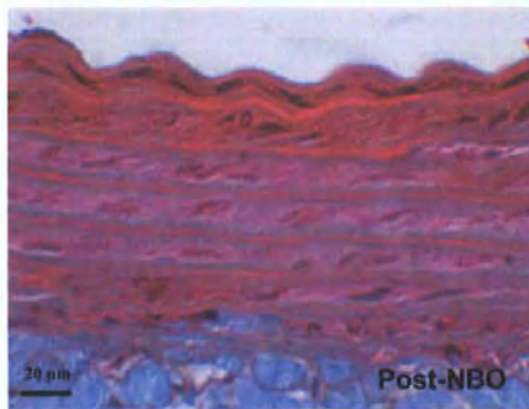
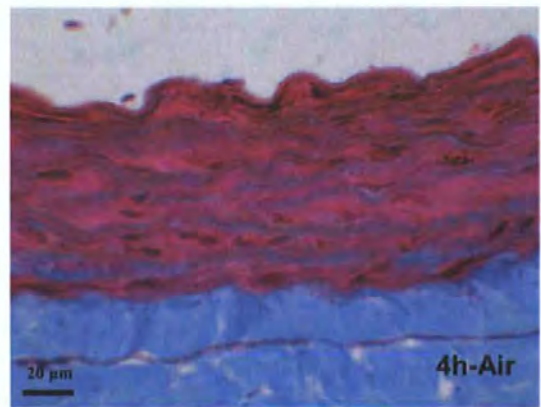
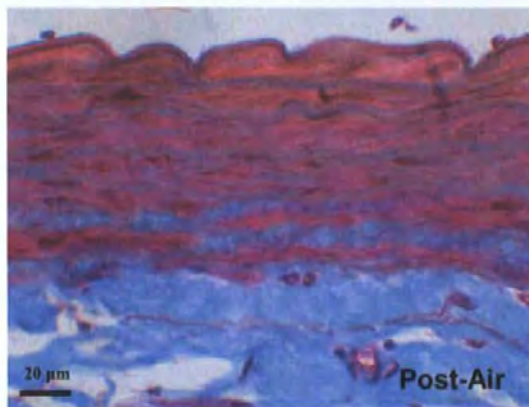


**Fig 3. 1** Histological images of aorta segments during experiments (Mallory's trichrome stain X400). Pre, Post and 4h are before, immediate and 4h after exposing to 90 min of air, 100% oxygen (NBO) and hyperbaric oxygen (HBO) treatments. Aorta wall is composed of tunica intima (I), media (M) and adventitia (a). Tunica intima is composed of endothelial cells (ECs, arrows). The endothelium index was calculated by the thickness ratio of I : (I+M).



The endothelium index is presented in Table 3.1. Although there is a tiny diversity of the results, no significant differences were observed between treatment groups.

Table 3. 1 The endothelium index of aorta segment

Treatment \ Time-point	Air	NBO	HBO
Immediate post exposure	2.97 ± 0.31%	2.59 ± 0.27%	2.45 ± 0.31%
4 h post exposure	2.86 ± 0.19%	2.36 ± 0.22%	2.46 ± 0.37%

Note: The endothelium index was calculated by the ratio of thickness of tunica intima to the total thickness of tunica intima and tunica media (%). The pre-treatment endothelium index was 2.83 ± 0.24%. Values are means ± SEM of five rats. No statistical differences were observed ( $P = 0.31$ , One-way ANOVA).

### 3.3.2. LDH Release

Overall, tissues showed low levels of LDH leak into the medium over time compared to the maximal LDH content in tissue ( $190 \pm 20$  Us  $g^{-1}$  tw of six replicates) (Fig 3.2). The pre-treatment baseline level of LDH was  $10.3 \pm 2.3$  Us  $g^{-1}$  tw, LDH level in the media at immediate and 4h post Air, NBO and HBO treatment showed no treatment-dependent nor time-dependent effects ( $P = 0.26$ , One-way ANOVA).

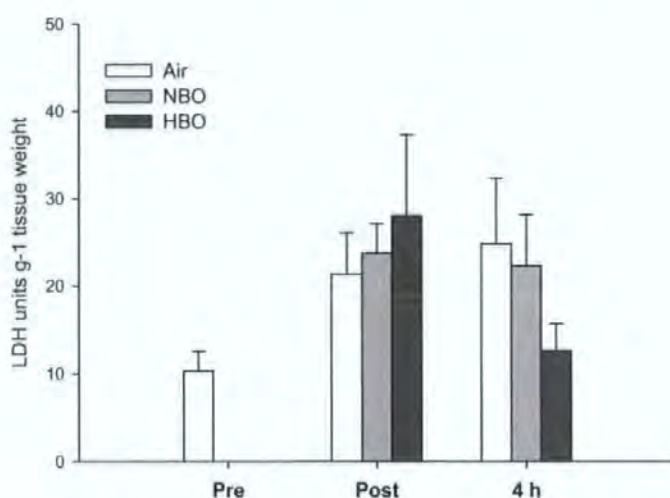


Fig 3. 2 LDH release from aorta segment tissue into the medium in Air (white bars), NBO (grey bars) and HBO (dark grey bars) groups on pre, post and 4h after treatment. Pre is at the start of the experiment after tissue allowed resting for 30 min; Post is immediately after 90 min treatment and 4h is at the end of 4h incubation after treatment. Data expressed as means ± SEM LDH units of per gram tissue of nine rats. One-way ANOVA test showed that  $P = 0.26$ .

### 3.3.3. Lactate Release

Lactate level increased over time within groups in Fig 3.3 ( $P < 0.001$ , Tukey-Kramer multiple comparisons test), but no significant difference was found between Air, NBO and HBO treatment throughout the experiment. There was a trend of decreased lactate production in HBO treatment. Immediately after treatment, lactate concentration was  $4.32 \pm 0.42 \mu\text{M mg}^{-1} \text{ tw}$  and  $3.52 \pm 0.49 \mu\text{M mg}^{-1} \text{ tw}$  in Air and HBO group. After 4 h incubation, the lactate concentration in HBO group was  $11.32 \pm 1.12 \mu\text{M mg}^{-1} \text{ tw}$ , and was  $15.72 \pm 2.34$  and  $14.17 \pm 1.11 \mu\text{M mg}^{-1} \text{ tw}$  in Air and NBO group, respectively ( $P = 0.16$ , one-way ANOVA).

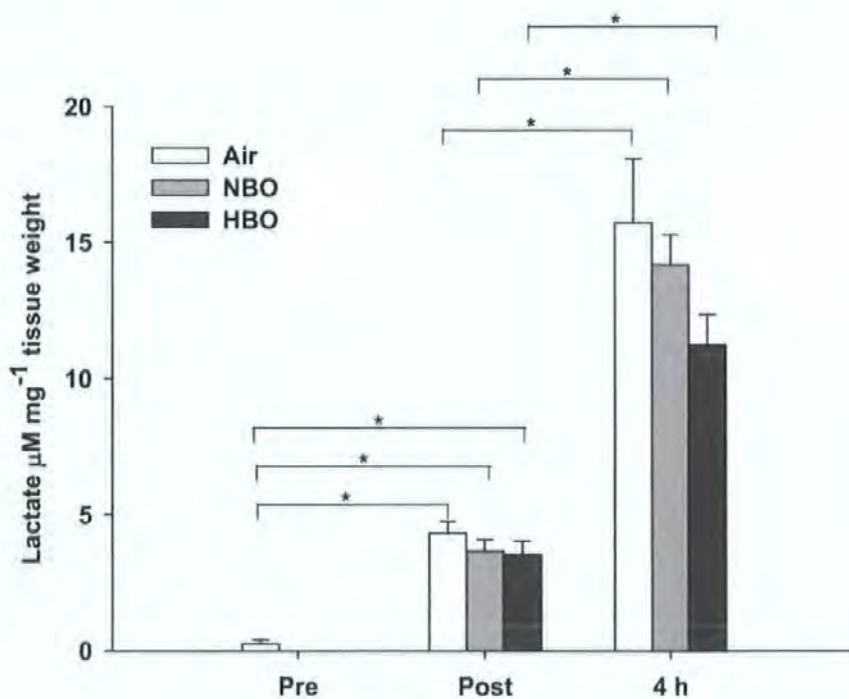


Fig 3. 3 Lactate concentration in the medium in Air (white bars), NBO (grey bars) and HBO (dark grey bars) groups on pre, post and 4h after treatment. Pre is at the start of the experiment after tissue allowed resting for 30 min; Post is immediately after 90 min treatment and 4h is at the end of 4h incubation after treatment. Data expressed as means  $\pm$  SEM  $\mu\text{M}$  lactate per mg tissue of nine rats and the pre-treatment baseline level of lactate in medium is  $0.25 \pm 0.15 \mu\text{M mg}^{-1} \text{ tw}$ . \*  $P < 0.05$  (Tukey-Kramer multiple comparisons test) showed significant differences.

### 3.3.4. Hydrogen Peroxide in Medium

Hydrogen peroxide ( $H_2O_2$ ) concentrations in the medium are shown in Fig 3.4. Before the treatments, the levels of  $H_2O_2$  in the media were at picomolar levels.  $H_2O_2$  production showed significant increase to  $0.24 \pm 0.06$ ,  $0.20 \pm 0.04$  and  $0.19 \pm 0.04$  nmoles  $mg^{-1}$  tw immediate after 90 min of Air, NBO and HBO treatments ( $P < 0.01$ , Tukey-Kramer multiple comparisons test). At the end of 4h incubation,  $H_2O_2$  level was  $0.13 \pm 0.03$ ,  $0.10 \pm 0.03$  and  $0.12 \pm 0.03$  nmoles  $mg^{-1}$  tw, respectively ( $P < 0.05$ , Tukey-Kramer multiple comparisons test when compare to pre-treatment levels). But no treatment difference was found among Air, NBO or HBO treatments throughout the experiment ( $P = 0.71$  and  $0.83$  at immediate post and 4h post exposure, respectively, One-way ANOVA).

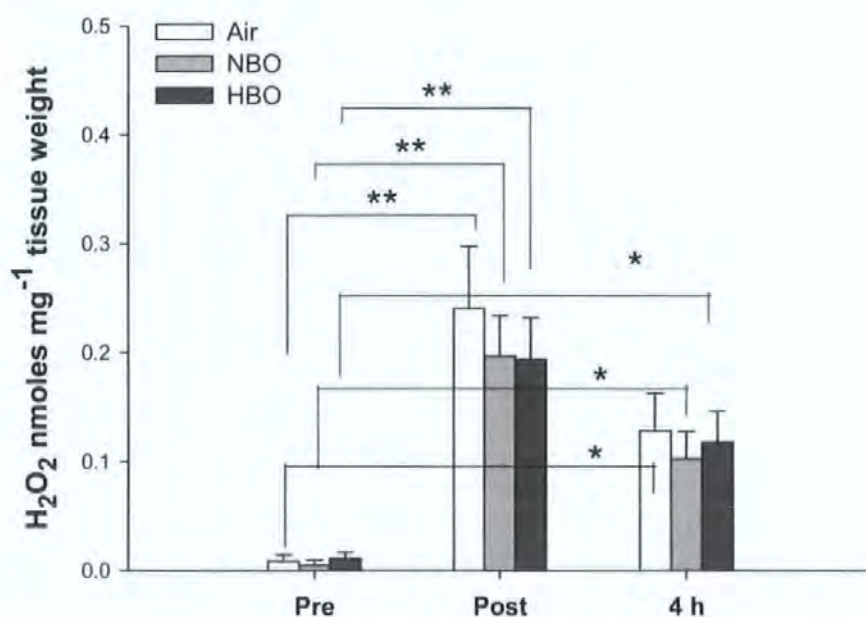


Fig 3. 4 Hydrogen peroxide levels in the medium in Air (white bars), NBO (grey bars) and HBO (dark grey bars) groups on pre, post and 4h after treatment. Pre is at the start of the experiment after tissue allowed resting for 30 min; Post is immediately after 90 min treatment and 4h is at the end of 4h incubation after treatment. Data expressed as means  $\pm$  SEM nM  $H_2O_2$  per mg tissue of eight rats. \*\*  $P < 0.01$ , \*  $P < 0.05$  (Tukey-Kramer multiple comparisons test) showed significant difference.

### 3.3.5. Total Glutathione Levels in Medium

There were low and stable levels of total glutathione release in the medium as showed in Fig 3.5. The pre-treatment baseline level of glutathione in medium was about  $13.3 \pm 1.3$  nM  $\text{mg}^{-1}$  tw. Exposure to Air, NBO or HBO did not affect the glutathione level in the medium. At immediate after exposure, the glutathione level in the medium was  $14.4 \pm 1.4$ ,  $15.5 \pm 1.8$ , and  $15.7 \pm 2.1$   $\text{mg}^{-1}$  tw of Air, NBO and HBO groups, respectively ( $P = 0.87$ , One-way ANOVA). Further incubation in air did not shown any changes of glutathione levels of Air, NBO and HBO groups ( $15.5 \pm 1.9$ ,  $15.4 \pm 1.1$  and  $16.0 \pm 1.7$   $\text{mg}^{-1}$  tw, respectively,  $P = 0.95$ , One-way ANOVA).

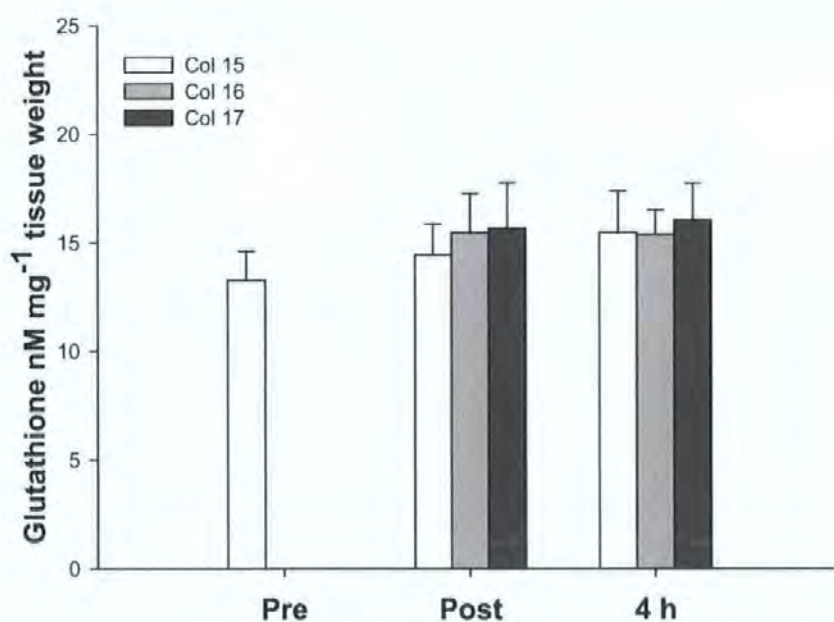
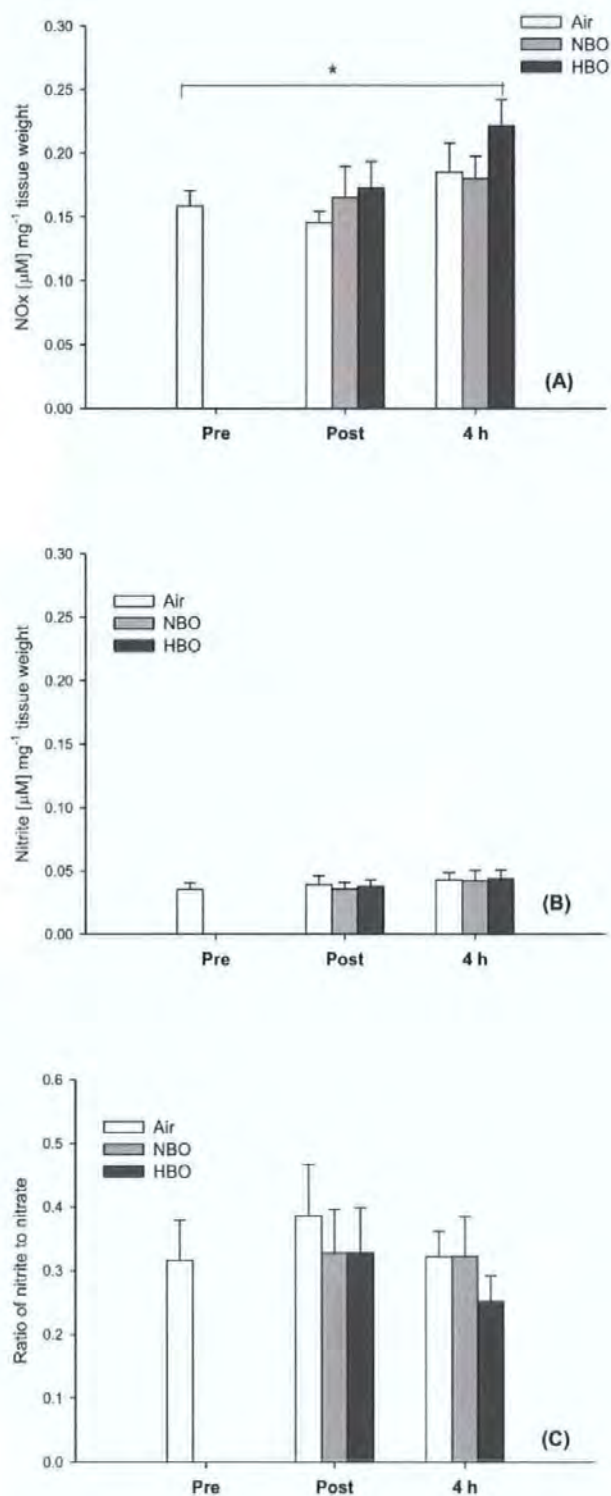


Fig 3. 5 Total glutathione concentration in the medium in Air (white bars), NBO (grey bars) and HBO (dark grey bars) groups on pre, post and 4h after treatment. Pre is at the start of the experiment after tissue allowed resting for 30 min; Post is immediately after 90 min treatment and 4h is at the end of 4h incubation after treatment. Data expressed as means  $\pm$  SEM glutathione nM per mg tissue of nine rats. One-way ANOVA analysis presented a P value at 0.92.

### 3.3.6. Nitric Oxide Production of Aorta segment

Nitric oxide production of aorta segment tissue was evaluated by its direct oxidative products nitrite and nitrate concentration in the media (Fig 3.6). In Fig 3.6A, the baseline level of NO<sub>x</sub> was  $0.19 \pm 0.04 \mu\text{M mg}^{-1} \text{ tw}$ , HBO exposure demonstrated the highest NO<sub>x</sub> concentration of the three treatments at each timepoints:  $0.21 \pm 0.04 \mu\text{M mg}^{-1} \text{ tw}$  at immediate post ( $P = 0.48$ , unpaired t-test), and a significant 37% increase at 4h post exposure ( $0.26 \pm 0.05 \mu\text{M mg}^{-1} \text{ tw}$ ,  $P = 0.02$ , unpaired t-test). However, there was no treatment effects were found of NO<sub>x</sub> levels between Air, NBO and HBO exposure. Unlike NO<sub>x</sub>, nitrite level in media remained quite stable throughout the experiments ranged between  $0.035 \pm 0.01$  (pre-treatment) and  $0.044 \pm 0.01$  (4h post HBO)  $\mu\text{M mg}^{-1} \text{ tw}$ , and neither time nor treatments affects on the nitrite level were observed throughout the experiment ( $P = 0.93$ , One-way ANOVA). Interestingly, the media contained much more nitrate than nitrite, and the ratio of nitrite to nitrate is shown in Fig 3.6C. The pre-treatment baseline of the ratio was  $31.6 \pm 6.4\%$ . Immediate after air exposure, the ratio was  $38.6 \pm 8.1\%$  of Air groups and then returned to  $32.1 \pm 4.0 \%$  at 4h after incubation. In NBO groups, the ratio kept at 32% during and after exposure. Whereas, the ratio was  $32.8 \pm 7.0 \%$  immediate post HBO treatment and then  $25.1 \pm 4.0 \%$  after 4h air recovery. Like the nitrite level, the ratio of nitrite to nitrate showed neither time nor treatments affects throughout the experiment ( $P = 0.88$ , One-way ANOVA).



**Fig 3.** 6 NOx changes in the medium in Air (white bars), NBO (grey bars) and HBO (dark grey bars) groups on pre, post and 4h after treatment. Pre, Post and 4h are at the start, immediately after 90 min treatment and at the end of 4h incubation. (A) total nitrite and nitrate level (NOx); (B) nitrite level; and (C) nitrite/(NOx-nitrite)%. Data expressed as means  $\pm$  SEM  $\mu\text{M}$  per mg tissue or percentage ratio of nine rats. \*  $P < 0.05$  (unpaired t-test) showed significant difference.

### 3.3.7. VEGF Production

Vascular endothelial growth factor (VEGF) concentration in both medium and tissue were measured. VEGF concentration was at or below the detectable limit ( $3 \text{ pg ml}^{-1}$ ) in the media, while it was easily detected in the tissue homogenates. A time dependent significant increase in VEGF was evident in tissue homogenates, but there was no treatment-dependent effect (Fig 3.7). The pre-treatment baseline level of VEGF in aorta segment homogenate was  $0.27 \pm 0.08 \text{ ng mg}^{-1}$  protein. And VEGF content were  $0.43 \pm 0.15 \text{ ng mg}^{-1}$  protein,  $0.36 \pm 0.08 \text{ ng mg}^{-1}$  protein and  $0.45 \pm 0.11 \text{ ng mg}^{-1}$  protein at immediate after Air, NBO and HBO exposure, respectively. After 4 h incubation, VEGF content attained the highest values at  $0.82 \pm 0.09 \text{ ng mg}^{-1}$  protein (Air),  $0.89 \pm 0.08 \text{ ng mg}^{-1}$  protein (NBO) and  $0.88 \pm 0.19 \text{ ng mg}^{-1}$  protein (HBO) which all showed significant difference to the pre level ( $P < 0.01$ , Tukey-Kramer multiple comparisons test) and to immediate post-treatment levels ( $P < 0.05$ , unpaired t-test). However, no significant difference was seen between Air, NBO and HBO treatments either at immediate post ( $P = 0.83$ , One-way ANOVA) or 4 h after treatment ( $P = 0.92$ , One-way ANOVA).

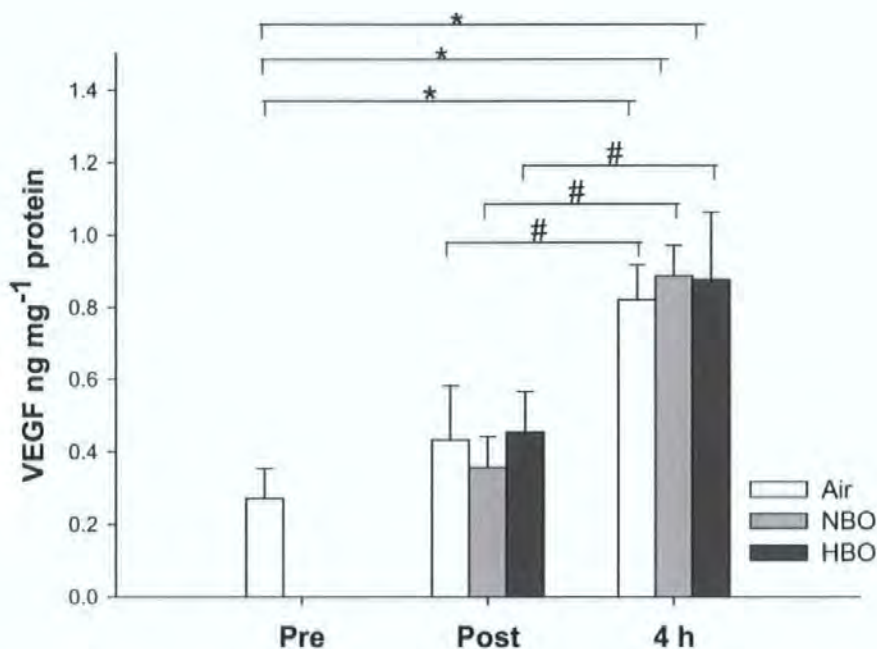


Fig 3. 7 VEGF content in aorta tissue homogenates in Air (white bars), NBO (grey bars) and HBO (dark grey bars) groups on pre, post and 4h after treatment. Pre is at the start of the experiment after tissue allowed resting for 30 min; Post is immediately after 90 min treatment and 4h is at the end of 4h incubation after treatment. Data expressed as means  $\pm$  SEM VEGF ng per mg protein of eight rats. \*  $P < 0.01$  (Tukey-Kramer multiple comparisons test) showed significant difference; and #  $P < 0.05$  (unpaired t-test) showed significant difference.

### 3.3.8. Correlation Test

Pearson correlation tests were performed among the biochemical indexes measured in this experiment (Table 3.2). The lactate concentration in the medium showed to be the most relevant factor to cellular VEGF content ( $P < 0.001$ ), nitrite concentration also showed a very significant correlation with VEGF content ( $P = 0.004$ ), and cumulative  $H_2O_2$  level showed a significant correlation with VEGF content ( $P = 0.04$ ). The factors correlated with LDH release included total glutathione in the medium ( $P = 0.001$ ), cellular VEGF content ( $P = 0.022$ ), and lactate in the medium ( $P = 0.036$ ). Interestingly, besides related with LDH release level, total glutathione level showed significant correlation with both  $NO_x$  ( $P = 0.001$ ) and nitrite ( $P = 0.046$ ).

Table 3. 2 The correlation test results

Index		VEGF	Lac- tate	H2O2	NOx	Nitrite	NO2: NO3	LDH	Gluta- thione
VEGF	r	1	.639	-.265*	.197	.379**	.210	.305*	.191
	P	.	.000	.048	.145	.004	.121	.022	.159
	n	56	56	56	56	56	56	56	56
Lactate	r	.639	1	-.175	.152	.215	.065	.265*	.066
	P	.000	.	.197	.235	.090	.612	.036	.605
	n	56	63	56	63	63	63	63	63
H2O2	r	-.265*	-.175	1	-.049	-.165	-.091	-.091	-.012
	P	.048	.197	.	.718	.224	.504	.506	.928
	n	56	56	56	56	56	56	56	56
NOx	r	.197	.152	-.049	1	.526**	-.196	-.117	.363**
	P	.145	.235	.718	.	.000	.124	.361	.003
	n	56	63	56	63	63	63	63	63
Nitrite	r	.379**	.215	-.165	.526**	1	.687**	.135	.252*
	P	.004	.090	.224	.000	.	.000	.292	.046
	n	56	63	56	63	63	63	63	63
NO2/NO3	r	.210	.065	-.091	-.196	.687**	1	.238	-.022
	P	.121	.612	.504	.124	.000	.	.061	.864
	n	56	63	56	63	63	63	63	63
LDH	r	.305*	.265*	-.091	-.117	.135	.238	1	.402**
	P	.022	.036	.506	.361	.292	.061	.	.001
	n	56	63	56	63	63	63	63	63
Glutathione	r	.191	.066	-.012	.363**	.252*	-.022	.402**	1
	P	.159	.605	.928	.003	.046	.864	.001	.
	n	56	63	56	63	63	63	63	63

Note: Pearson's correlation tests were performed between each two biochemical indexes using SPSS 11.0 for Windows software (SPSS Inc, Chicago, Illinois, USA). r represents correlation coefficient and ranges from -1 to 1. When r = Zero means that the two variables do not vary together at all; r = positive fraction means that the two variables tend to increase or decrease together; r = negative fraction means that one variable increases as the other decreases; r = 1.0 (or -1.0) means that the two variables are perfect (negative or inverse) correlation. P value represents the level (2-tailed) of significance and if the P value is small (as  $P < 0.05$ ), then the correlation is not a coincidence and more than 95% of the true population r lies within the confidence interval range. n represents the total number of points have been calculated in this statistic analysis. \*\* Correlation is significant at the 0.01 level (2-tailed) and \* Correlation is significant at the 0.05 level (2-tailed).

### 3.4 Discussion

In this study, we present evidence that the tissue is not overtly injured by a single treatment of HBO and there is no evidence to show that HBO treatment induces oxidative stress. Furthermore, a single HBO treatment has no effect on nitric oxide and VEGF production of blood vessel tissues.

### 3.4.1. The Viability of Aorta Segments during HBO Treatment

Once cell damage occurs, cell membrane is not intact any more. The LDH assay, trypan blue uptake assay and other cell survival assay are all based on this principle. The LDH assay measured the leakage of the enzyme into the medium; while the trypan blue assay distinguish cell survival as that living cell excludes trypan blue dye and dead cell uptake this dye. For our model, we need to evaluate the injury of blood vessel tissue. Thus, LDH assay is better for this purpose. The LDH level was at low percentage (less than 20%) compared to maximum LDH content in the tissue throughout the experiments (Fig 3.2). In addition, histological examination of rat aorta showed intact tissue structure and normal cell morphology (Fig 3.1). Therefore, neither pure oxygen treatment nor the HBO treatment had adverse effects on aorta segments.

### 3.4.2. Oxidative Stress and HBO Treatment

HBO treatment, as expose to high concentration of oxygen, will arguably produce more reactive oxidative species (ROS), and excessive ROS may induce oxidative stress which damage cells or tissue. For example, when vascular smooth muscle cells from rats thoracic aorta were exposed to a series of concentrations of  $H_2O_2$  (0.2-0.6 mM) for 6 h, there was severe leakage of intracellular LDH with apparent incremental cell death in a dose-dependent pattern, with 50 % cell viability at 0.5 mM  $H_2O_2$  (Zhang et al., 2002). Ram & Hiebert (2001) also reported a 50% viability of porcine aortic endothelium occurred at 1 mM of  $H_2O_2$  incubation, and 50% viability of bovine aorta endothelium while incubated with more than 6 mM of  $H_2O_2$ . Those studies have confirmed that at high concentration (in mM), ROS are toxic and lead to a remarkable cell damage which was indicated by survival rate and LDH leakage. In our model, although there was an increase in  $H_2O_2$  production occurred after treatments, the extracellular concentrations of  $H_2O_2$

were very low and only at nM levels (Fig 3.4). On the other side, LDH level and tissue histology showed no evidence of cell or tissue damage occurred during experiment.

A variety of vascular cells, including endothelial cells, smooth muscle cells, and fibroblasts, have demonstrated the ability to produce superoxide anion and  $H_2O_2$ . Studies have shown that superoxide anion, generated through the membrane-associated NAD(P)H oxidase(s), directly attenuates the biological activity of endothelium-derived nitric oxide (NO), and the net balance between superoxide and NO results in vasoconstriction or vasodilation (Mohazzab et al., 1994; Griendling et al., 1994; Rajagopalan et al., 1996). But on the other hand, the short half-life and radius of diffusion of superoxide drastically limit the role of this ROS as an important paracrine hormone in vascular biology. In contrast, the superoxide metabolite,  $H_2O_2$ , has been increasingly viewed as an important cellular signalling agent in its own right, capable of modulating both contractile and growth-promoting pathways with more far-reaching effects (Griendling et al., 2000; Sen, 2002; Ardanaz and Patrick., 2006). Yasuda et al (1999) found that the maximum rate of the tube formation of angiogenesis in cultured bovine thoracic aorta endothelial cells was seen when cells were incubated with 1  $\mu$ M  $H_2O_2$  for 30 min; and at micromolar level (0.1 and 1  $\mu$ M),  $H_2O_2$  was able to stimulate endothelium proliferation and migration. Comparing with the previous studies, the concentration of  $H_2O_2$  in our medium is far less than associated with normal ROS signalling in cells; it seems that a single 90 min exposure to hyperoxia may not be sufficient to evoke the blood vessel tissues to produce a signalling level of ROS.

GSH is oxidised to GSSG when  $H_2O_2$  is presented, and GSSG is then reduced back to GSH in cell to maintain the intracellular redox condition. The glutathione redox cycle is an important antioxidant system in cells, and its balance is critical for cell integrity and function. Under oxidative stress, excessive GSSG are transported outside the cell temporarily to keep redox balance of intracellular glutathione pool. But when the cell is

challenged with large amount of ROS and oxidative stress is overwhelming, cell damage or cell death will occur, and the glutathione and other intracellular enzymes will release from damaged cells. This explains the significant positive correlation of total glutathione level and LDH release in the medium existed in our study (Table 3.2). The total glutathione in medium is derived from the efflux of glutathione from the cells, which reflects the oxidized status in cell or tissue as well as the level of cell damages. The total glutathione concentration in medium remained quite stable at nM level throughout the experiment with no time and treatment differences (Fig 3.5). These results are consistent with the H<sub>2</sub>O<sub>2</sub> results. Overall, there is no evidence to show that a single 90 min HBO treatment at 2.2 ATA induce oxidative stress in aorta segment. The clinical application of HBOT never exceeds 3 ATA and usually does not last longer than 90 min, which keeps the ROS generation at safe level and lets the adaptive antioxidant system work efficiently to minimize oxidative stress.

### **3.4.3. Response of Lactate in Aorta Metabolism of HBO Treatment**

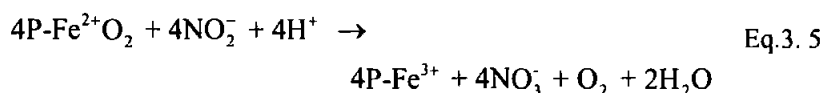
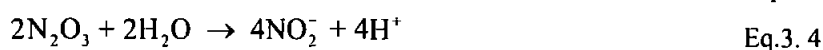
Cellular energy supply mostly depends on the oxidation of glucose. Only when oxygen supply is limited, for example during an instant reduction of blood supplying in tissue injury, cells will rely on anaerobic glycolysis to produce ATP. Therefore, lactate level reflects a consequence of hypoxia level and energy metabolism in tissue and cell. That is why lactate in the medium increased throughout the experiments and showed correlation with LDH level in the medium ( $P = 0.04$ ). Notably, there is a very significant correlation of lactate level in the medium and VEGF level in tissue ( $P < 0.001$ ), which may suggest that lactate could be involved in the VEGF regulation in blood vessel tissue.

Healing wounds were found to produce and accumulate large concentrations (10-15 mM) of lactate (Hunt et al., 1978). The lactate at the wound site is mainly produced by

leukocytes as a by-product of the “oxidative burst” for eliminating foreign invaders such as bacteria (Allen et al., 1997). Upon phagocytosis, the NAD(P)H-linked oxidase of leukocytes is activated to consume as much as 50- to 100-fold more oxygen than at rest and almost all oxygen is converted to superoxide anion. The energy of the initial conversion comes from anaerobic glycolysis and thus leukocytes actively maintain the high lactate (10 - 25 mM) at wounds (Hunt et al., 1985; Im & Hoopes, 1970). Thus, when oxygen concentration rises, lactate production rises as well in the phagocytic environment. That is part of the mechanisms that HBO treatment benefits chronic wound with severe infections. Studies demonstrated that high concentration of lactate in wound site (10-15 mM) is important to initiate angiogenesis via ADPr/pADPr system (Trabold et al., 2003). ADPr/pADPr is a post-translational modification of protein during which the adenosine diphosphoribose (ADRP) moiety from  $\text{NAD}^+$  is enzymatically transferred onto acceptor proteins and modifies their structures and functions. Lactate is relevant to mono/polyADP ribosylation (ADPr/pADPr) process in cells due to its ability of regulating  $\text{NAD}^+$  pool. The initiation role of lactate in angiogenesis may be performed through the induction of VEGF production. Sheikh et al (2000) found that HBO did not affect the high concentration of lactate (range 2.0-10.5 mM) in wound site as VEGF levels significantly increase with HBO by approximately 40% 5 days following wounding and decrease to control levels 3 days after exposures are stopped. Further study by Constant et al (2000) showed that increased VEGF production by exposing macrophages to hypoxia and/or lactate, each alone and more so together (at least an additive effect). These studies may help partially explain the role of lactate in the regulation of VEGF and wound healing. We believe that further studies to investigate the synergetic effect of HBO and high lactate concentration on aorta tissue will help to explain this phenomenon in vascular tissue.

### 3.4.4. Nitric Oxide, VEGF and HBO Treatment

NO is continuously produced at nanomoles (nM) concentration and is responsible for a wide range of physiological functions. In our study, we investigate the changes of nitrite and nitrate, which are the oxidizing products of NO. In aerobic aqueous solution, NO is rapidly and spontaneously autooxidize to nitrite (Eq.3. 2 - Eq.3. 4) and it has been definitively demonstrated that the only stable product formed by the spontaneous autoxidation of NO in oxygenated solutions is nitrite ( $\text{NO}_2^-$ ) (Pogrebnyaya et al., 1975; Pires et al., 1994; Goldstein and Czapski, 1995). However, when there is certain oxyhemoproteins ( $\text{P-Fe}^{2+}\text{O}_2$ ) such as oxyhemoglobin or oxymyoglobin, nitrite derived from NO autooxidation is rapidly converted to nitrate ( $\text{NO}_3^-$ ) (Eq.3. 5) (Ignarro et al., 1993). The rate law for NO autooxidation is second order with respect to NO and first order with respect to molecular oxygen, with a rate constant of approximately  $8 \times 10^6 \text{ M}^{-2} \cdot \text{s}^{-1}$  (Ford et al., 1993). On the other hand, the reaction of nitrite with hemoproteins is quite slow, requiring 2-3 h (Ignarro et al., 1993)



The proportion of nitrite in the medium was less than 40% compared to nitrate in our study, which was similar to the report from Privat et al (1997). They investigated NOx accumulation in cultured medium of HUVECs and indicated a nitrite plus nitrate cumulated basal production even for a relatively short incubation time (5 min); and the basal production was 10 times higher when nitrates instead of nitrites were measured.

Although HBO treatment did not increase NO release from blood vessels in our study (Fig 3.6), HBO modulated NO production has been shown in other investigations. HBO

increases nNOS-mediated NO production, which may contribute to oxygen toxicity in the central nerve system (Oury et al., 1992; Wang et al., 1998; Chavko et al., 2001; Demchenko et al., 2003). On the other hand, therapeutic HBO treatment has shown to reduce iNOS-mediated NO production induced by zymosan, lipopolysaccharide or in other pathological conditions (Kurata et al., 1995; Luongo et al., 1998; Imperatore et al., 2004; Huang et al., 2005; Chu et al., 2006; Chang et al., 2006). In the vascular system, NO plays important roles in regulating vascular tone and endothelial functions. North et al (1996) noted that increased oxygen tension in normobaric pressure (exposing to PO<sub>2</sub> 150 mmHg for 48 h) lead to an induction of 2.7-fold greater eNOS mRNA and protein expression for up to 24 hours in early passage of ovine fetal intrapulmonary artery endothelial cells (PAEC). Buras et al (2000) also showed that HBO induced the synthesis of eNOS in HUVECs and bovine aortic endothelial cells. But Hink et al (2006) used contractile and vasodilatory responses in rat aortic rings as an indirect measure of vascular NO production/release and reported that in vitro HBO expose decreased endothelial NO bioavailability, but activated non-endothelial vascular NO production.

VEGF is considered to play a consistent and prolonged angiogenic function during wound healing due to its ability to stimulate all the required steps in angiogenesis. In our study, the VEGF concentration rise with time, but this increase is unaffected by treatments. Therefore, the VEGF increase was unmodified by a single HBO treatment. It is known that hypoxia induces VEGF production, and also increases VEGF gene transcription and up-regulates its translation (Stein et al., 1995 and 1998). Direct evidence has shown that hypoxia inducible factor-1 (HIF-1) is implicated in the activation of the VEGF gene transcription during hypoxia (Forsythe et al., 1996). HIF-1 acts as a master transcription switch known to be activated within the physiological range of oxygen concentration, and mediates gene transcription in response to reduced cellular oxygen tension in order to

maintain oxygen homeostasis. Interestingly, studies have found that higher oxygen concentration (hyperoxia) may also regulate VEGF production. Cultured macrophages increase production of VEGF when exposed to oxygen at high tensions of about 300 mm Hg (Gimbel and Hunt, 1999). Sheikh et al (2000) administered HBO therapy for 90 minutes, twice daily at 2.1 ATA for 7 days after the rats' injury. Wound oxygen increased from nearly 0 mm Hg to as high as 600 mm Hg. The peak level occurs at the end of the 90 min treatment, and hyperoxia persists for approximately 1 hour. The VEGF levels significantly increase with HBO by approximately 40% 5 days following wounding and decrease to control levels 3 days after the exposures were stopped. Kang et al (2004) found VEGF levels in propagated human dermal fibroblasts slightly increased on day 1 of HBO treatment. While Lin (2002) investigated in vitro human umbilical vein endothelial cells exposed to HBO showed no effect of HBO on VEGF expression. Therefore, it seems that both hypoxia and hyperoxia regulate VEGF production. Further investigation suggested that the reactive oxidative species (ROS) generated during hypoxia/hyperoxia may be involved in this regulation. H<sub>2</sub>O<sub>2</sub> increasing VEGF production has been found in macrophages and vascular smooth muscle cell (Ruef et al., 1997; Cho et al., 2001). Richard et al (2000) demonstrated that the non-hypoxia induction of the HIF-1 transcription factor is triggered by a dual mechanism: one is a PKC-mediated increase in HIF-1 $\alpha$  transcription and the other is ROS -dependent activation of PI3K that increases the translation of HIF-1 $\alpha$ . Sen et al (2002) demonstrated that at  $\mu$ M concentrations oxidant induces VEGF expression and that oxidant-induced VEGF expression is independent of HIF-1 and dependent on Sp1 activation. In addition, studies have indicated that NO may use similar components, pathways and/or modifications to evoke HIF-1 $\alpha$  accumulation as exposure of various cells to NO under normoxic conditions induced HIF-1 $\alpha$  accumulation and HIF-1-DNA binding (Kimura et al. 2000; 2001), which may then activate the

downstream target gene expression (e.g. VEGF) (Brune and Zhou, 2003). On the other hand, lactate also showed the ability to induce VEGF production under normoxic conditions (as described above). So while hypoxia remains the undisputed ubiquitous inducer of HIF-1 and VEGF, other factors could also modulate VEGF increases under normoxic even hyperoxic conditions, which could be dependent/independent of HIF-1.

Correlation tests showed that VEGF content in the tissues were significantly related to lactate and LDH level in the medium. As the lactate and LDH levels are both biochemical indicator for cell stress, this correlation with VEGF may represents an adaptive changes in cell for damaging.

### **3.5 Summary**

In this chapter, we exposed an in vitro model of rat aorta segment to normobaric air, normobaric 100% oxygen and hyperbaric oxygen at 2.2 ATA for 90 min, and investigated the treatments effect at immediate post exposure and 4h post exposure. Overall, we find that the tissue is not injured by a single treatment of either oxygen or HBO. Meanwhile there is no oxidative stress induced by a single HBO treatment as measure the total glutathione and hydrogen peroxide production in the media. And there is no evidence to show that HBO treatment induces NO and VEGF productions and VEGF content in the tissue showed a positive correlation with the lactate and LDH level in the media, which may represents that VEGF production is a cell adaptation to stress.

## **Chapter 4**

### **Effects of HBO on Blood Vessel under**

### **Pathological Condition or with Arginine**

### **Supplement *in Vitro***

#### **4.1 Introduction**

In Chapter 3, we demonstrated that a single exposure of rat aorta segment to normobaric oxygen (NBO) or hyperbaric oxygen (HBO at 2.2 ATA) for 90 min did not damage the tissues of aorta segment, and in addition, there was no evidence of oxygen-induced oxidative stress when compared to normobaric air exposure (Air). Furthermore, time effects were observed on angiogenesis factors such as lactate, NO<sub>x</sub> and VEGF production, especially in HBO-exposed group, but no treatment differences were seen throughout the experiment among Air, NBO and HBO exposures. Interestingly, statistic tests suggested that the VEGF content in the tissue had a positive correlation with the lactate, nitrite, LDH and H<sub>2</sub>O<sub>2</sub> level in the medium.

In our study of Chapter 3, the aorta segments were incubated with modified Krebs-Ringer solution, which is a physiological salt solution commonly used in vascular research. This solution provides the essential physiological environment for blood vessel, and our study has successfully provided evidence on the changes and responses of oxidative stress and angiogenic factors of blood vessel to Air, Oxygen or HBO exposure under

physiological conditions. But in reality, HBO therapy is only applied to patients with clinical problems. Most of the chronic wound patients who benefit from HBO therapy are characterised by impaired oxygen supply, high levels of blood lactate, and combined with severe infection (Niinikoski, 2001; Zamboni et al., 2003). With such pathophysiological changes, HBO treatment may induce very different reactions in the vascular system when considering oxidative stress levels and the response to angiogenesis factors. It would therefore be worth testing the reactions of blood vessel under pathological condition, and so some experiments performed in Chapter 3 are repeated here, but with high lactate concentrations in the medium to reflect those found in a wound. In addition the Krebs-Ringer solution used in Chapter 3 did not contain L-arginine. The relative low and unresponsive nitric oxide production observed in Chapter 3 may due to the deprivation of L-arginine supply in Krebs-Ringer solution, while in contrast, blood would normally contains micromoles level of L-arginine which serves as a physiological precursor for NO formation in blood vessels (Kirk et al., 1993; Abbott and Schachter, 1994; Tsuchida et al., 1995). HBO treatment may require some L-arginine as a substrate to induce NO production in our system. In this Chapter, we add L-arginine as well as lactate to Krebs-Ringer solution, which mimics one aspect of chronic wound status, and the supplement of L-arginine will help to explain the NO regulation in physiological as well as pathological environment.

## **4.2 Material and Methods**

### **4.2.1. Experimental Protocol**

Male Sprague Dawley rats (350 - 400 g; n = 40) were purchased from Harlan UK Ltd. Experiments were conducted in accordance with ethical approval. Aorta was obtained as

described in 2.2.1, and sectioned into 7 segments (1 cm), and then randomly placed in individual wells of Nunclon Delta SI 6-well tissue culture plates (Nunc, InterMed, Denmark) containing 6 ml of Krebs-Ringer solution in the presence of either 100  $\mu$ M L-arginine (Arg), or 15 mM sodium L-lactate (Lac), or both (Arg + Lac). The composition of Krebs-Ringer solution (KRS) was (in mM): NaCl 118.6, KCl 4.7, CaCl<sub>2</sub> 2.5, MgSO<sub>4</sub> 1.2, KH<sub>2</sub>PO<sub>4</sub> 1.2, NaHCO<sub>3</sub> 25.1, Hepes 10, glucose 10, and pH 7.4.

Segments of aorta from one rat were used for each medium, and three rats were used simultaneously to incubate in Arg, Lac or Arg+Lac medium, respectively, in each trial. The treatment protocol is the same as in 3.2.2. Briefly, aorta segments were allowed to equilibrate in individual medium for 30 min before exposure. And then aorta segments were randomly exposed to air at 1 ATA (Air), 100% oxygen at 1 ATA (NBO) or 100% oxygen at 2.2 ATA (HBO). After 90 min exposure, a four hour recovery in normobaric air was introduced. All experiments were conducted at 37 °C. Tissue and medium samples were collected at the end of 30 min equilibration, immediate post 90 min exposure and 4h recovery as pre-treatment control, immediate post-treatment and 4h post-treatment respectively. All tissue and medium samples were snap-frozen in liquid nitrogen, and stored at -80 °C until used for analysis.

One series of experiments were performed to monitor the generation of hydrogen peroxide, using the protocol above, with the method described in 2.2.1 to enable the measurement of low levels of hydrogen peroxide generation in situ.

#### **4.2.2. Biochemical Analysis**

Cumulative lactate dehydrogenase (LDH) release into the medium was measured as a routine marker of tissue injury, and expressed as LDH Units g<sup>-1</sup> tissue weight (tw). The oxidative stress levels were monitored by following cumulative hydrogen peroxide (H<sub>2</sub>O<sub>2</sub>)

level and the total glutathione concentration in the media, and expressed as  $\text{H}_2\text{O}_2$  nmoles  $\text{mg}^{-1}$  tw and glutathione nM  $\text{mg}^{-1}$  tw, respectively. Concentration of NOx (nitrite + nitrate), nitrite in the medium was measured as  $\mu\text{M}$   $\text{mg}^{-1}$  tw, whilst the ratio of nitrite to nitrate was calculated as [nitrite]: ([NOx]-[nitrite]). The level of VEGF and protein content in the tissue homogenate was analysed, and expressed as VEGF  $\text{pg}$   $\text{mg}^{-1}$  tissue protein (tp). A twenty-time dilution was required when measuring the lactate level in the Lac and Arg+Lac medium. The lactate production was expressed as  $\mu\text{M}$   $\text{mg}^{-1}$  tw for the results of Arg medium, and for the Lac and Arg+Lac groups, after subtracting the background level of added lactate in the medium (15 mM) before normalized with tissue weight. All the biochemical assays have been described in Chapter 2, and the data obtained were normalized with fresh tissue weight.

### 4.2.3. Statistic Analysis

For each medium, nine replicated experiments were done, and all biochemical results are presented as the means  $\pm$  S.E.M of the replicates. Statistical analysis was performed by one-way ANOVA for time, treatment and chemical supplement differences. If P value achieved less than 0.05, Tukey-Kramer multiple comparisons test or unpaired t-test was used subsequently for further analysis. Correlation test were performed with Pearson correlation test among the interested biochemical indexes. For all the tests, the significant difference level was accepted at  $P < 0.05$ .

## 4.3 Results

### 4.3.1. LDH Release

In control Krebs-Ringer solution (KRS), LDH release remained at low level throughout the experiment, and there were no difference between Air, NBO and HBO treatment at either immediate or 4h post treatment. Supplement of L-arginine (Arg) and/or sodium L-lactate (Lac) to the KRS affect LDH release, but the effects showed differences within treatments. When exposure to normobaric air (Air), it was until 4h post treatment that LDH level increased in Arg and Arg+Lac media ( $P < 0.01$  and  $P < 0.05$  compared to KRS, respectively, Turkey-Kramer multiple test) but not in Lac medium. The NBO and HBO exposures caused significant increase of LDH release at immediate post-treatment in all three specific media ( $P < 0.01$  compared to KRS, respectively, Turkey-Kramer multiple test). After 4h incubation, the HBO-treated groups showed significant increase of LDH in all three specific media compared to control KRS ( $P < 0.01$ , Turkey-Kramer multiple test), and NBO-treated groups showed increase in both Arg and Arg+Lac media ( $P < 0.05$ , Turkey-Kramer multiple test), but not in Lac medium.

The LDH release from aorta segments into all Arg, Lac and Arg+Lac media tended to increase throughout the experiments (in Fig 4.1). The pre-treatment LDH level was  $15.0 \pm 3.3$ ,  $12.3 \pm 2.0$  and  $14.5 \pm 3.2$  Units  $g^{-1}$  tw in Arg, Lac and Arg+Lac media, respectively ( $P = 0.78$ , One-way ANOVA). Time effects were observed mainly in NBO and HBO treated groups at both immediate and 4h post treatments in all three media ( $P < 0.001$ , Turkey-Kramer multiple test) when compared with their pre-treatment levels. For Air treatment, LDH level increases were only seen at 4h post treatment in Arg and Arg+Lac media ( $P < 0.05$ , Turkey-Kramer multiple test). In Arg medium, NBO and HBO treatments induced nearly a 2-fold increase in LDH release compared to that of Air treatment ( $51.9 \pm 8.5$ ,

---

104.3 ± 16.1 and 97.1 ± 15.5 Units g<sup>-1</sup> tw of Air, NBO and HBO treated medium samples, respectively, P<0.05, Turkey-Kramer multiple test). But during 4h recovery, only HBO-treated samples showed higher level than that of Air-treated samples (P = 0.04, unpaired t-test) (74.5 ± 11.1, 105.1 ± 17.2 and 115.0 ± 14.9 Units g<sup>-1</sup> tw of Air, NBO and HBO treated Arg media, respectively). Similar oxygen effects were seen in Lac and Arg+Lac media. Interestingly, LDH level of the Air-treated group in Lac medium (42.5 ± 6.1 Units g<sup>-1</sup> tw) was significantly less than that of Arg medium (74.5 ± 11.1 Units g<sup>-1</sup> tw, P = 0.02, unpaired t test) after 4h recovery. Throughout the experiment, NBO and HBO treatments showed no differences on inducing LDH release in Arg and/or Lac media.

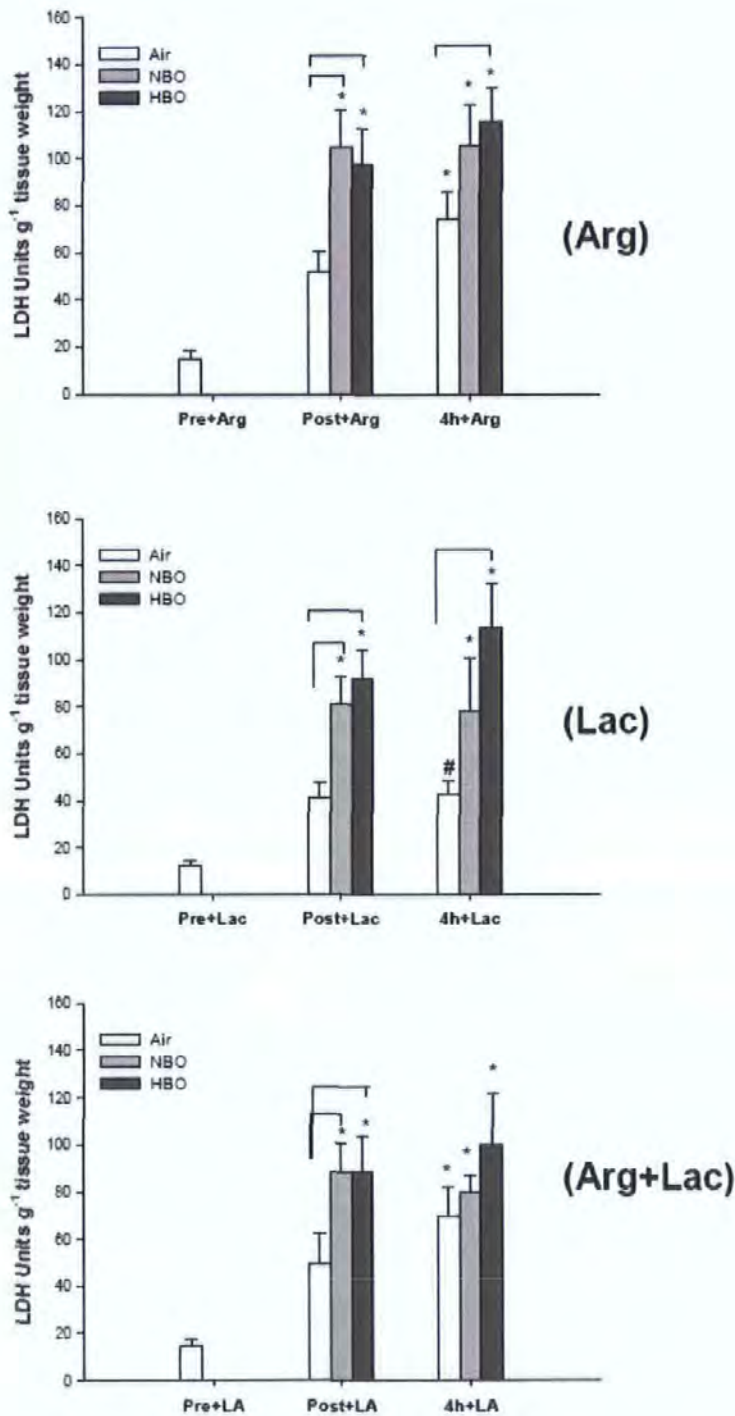


Fig 4. 1 Cumulative LDH release from segments of aorta into specific media under normobaric air (Air, white bar), normobaric 100% oxygen (NBO, grey bar) or hyperbaric 100% oxygen (HBO, dark grey bar) at Pre-treatment (Pre), Immediate post 90 min treatment (Post); and 4h after treatment (4h). Tissue was kept in Krebs-Ringer buffer in the presence of 100  $\mu$ M L-Arginine (Arg), 15 mM sodium L-lactate (Lac) or both (Arg+Lac). Data are expressed as means  $\pm$  SEM of nine rats. One-way ANOVA test was performed, and followed by Tukey-Kramer multiple test or unpaired t-test. Brackets indicates significant difference ( $P < 0.05$ ) between observations; \*  $P < 0.05$  significant difference vs. LDH pre-treatment level. #  $P < 0.05$  significant difference vs. LDH level in Arg medium.

### 4.3.2. H<sub>2</sub>O<sub>2</sub> Production and Total Glutathione Level in the Media

#### 4.3.2.1. Cumulative H<sub>2</sub>O<sub>2</sub> Level in the Media

In KRS, H<sub>2</sub>O<sub>2</sub> production increased during treatments, which tended to decline to level ranging of 0.10 to 0.13 nmoles mg<sup>-1</sup> tw at the end of experiments. Although the pre-treatment H<sub>2</sub>O<sub>2</sub> levels in KRS, Arg, Lac and Arg+Lac media showed no differences, Arg or/and Lac supplement increased H<sub>2</sub>O<sub>2</sub> levels during and after treatments when comparing with that in KRS.

In Arg media, the H<sub>2</sub>O<sub>2</sub> levels were higher than that in KRS at the same timepoint with NBO and HBO treatments but not with Air treatment. At immediately post-treatments, the H<sub>2</sub>O<sub>2</sub> levels were 0.61 ± 0.05 (P<0.01 vs 0.20 ± 0.04 in KRS) and 0.46 ± 0.05 (P<0.05 vs 0.19 ± 0.04 in KRS) nmoles mg<sup>-1</sup> tw in NBO and HBO-treated groups, respectively; and 0.58 ± 0.07 of Air-treated group (P>0.05 vs 0.24 ± 0.06 in KRS). After 4h recovery, the H<sub>2</sub>O<sub>2</sub> level remained at high level of 0.77 ± 0.13 nmoles mg<sup>-1</sup> tw of NBO- and 0.61 ± 0.06 nmoles mg<sup>-1</sup> tw of HBO-treated groups, which showed significant differences to that in KRS at the same timepoints (P<0.01 vs 0.10 ± 0.02 and 0.12 ± 0.03 in KRS of NBO and HBO treatment, respectively, Turkey-Kramer multiple test), whereas no difference was seen of Air-treated groups between Arg and KRS (0.44 ± 0.10 vs 0.13 ± 0.03 nmoles mg<sup>-1</sup> tw, P >0.05, Turkey-Kramer multiple test). In Lac containing media (Lac and Arg+Lac media), increased H<sub>2</sub>O<sub>2</sub> level were observed throughout the experiment in all three treatment groups (P<0.01 or P <0.001 vs corresponding H<sub>2</sub>O<sub>2</sub> level in KRS, Turkey-Kramer multiple test).

In Fig 4.2, the H<sub>2</sub>O<sub>2</sub> levels generated in Arg, Lac and Arg+Lac media were shown. The background levels of H<sub>2</sub>O<sub>2</sub> (pre-treatment levels) in the three specific media were less than 0.1 nmoles mg<sup>-1</sup> tw in all trails (P = 0.90, One-way ANOVA). Significant time effects were seen in all runs, such that H<sub>2</sub>O<sub>2</sub> level increased significantly (P < 0.001 compared to

pre-treatment level, One-way ANOVA) in the media during Air, NBO or HBO exposure and a further increasing trend of H<sub>2</sub>O<sub>2</sub> were seen in oxygen-treated groups but not in Air-treated group during the following 4h recovery. But overall, no treatment differences were found between Air, NBO and HBO exposure (P = 0.32, One-way ANOVA). Thus, Air, NBO or HBO treatment equally induced H<sub>2</sub>O<sub>2</sub> generation from aorta segments in these three specific media.

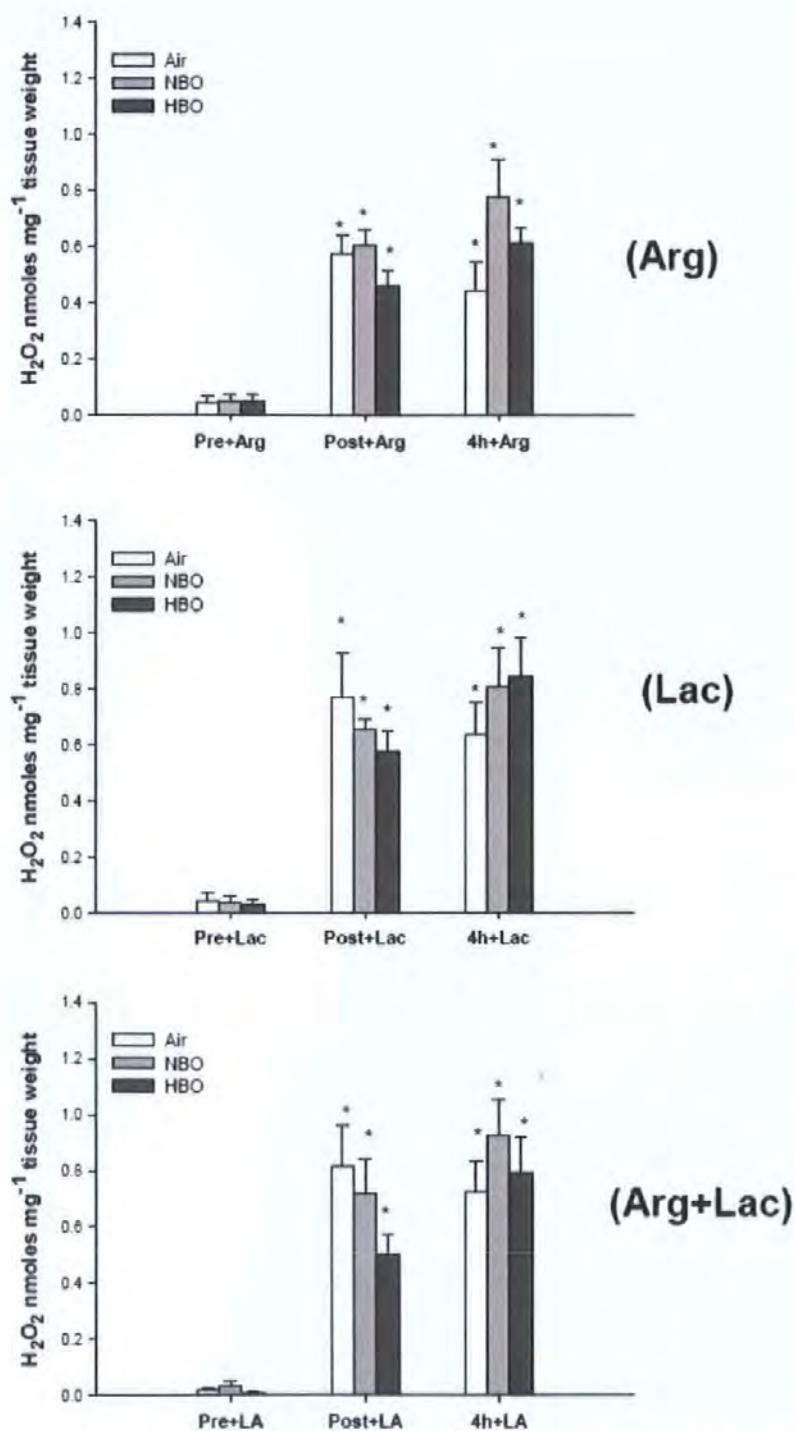


Fig 4.  $2 H_2O_2$  generation of aorta segments in specific media under normobaric air (Air, white bar), normobaric 100% oxygen (NBO, grey bar) or hyperbaric 100% oxygen (HBO, dark grey bar) at Pre-treatment (Pre), Immediate post 90 min treatment (Post); and 4h after treatment (4h). Tissue was kept in Krebs-Ringer buffer in the presence of 100  $\mu M$  L-Arginine (A), 15 mM sodium L-lactate (B) or both (C). Data are expressed as means  $\pm$  SEM of eight to ten replicates. One-way ANOVA test was performed, and followed by Turkey-Kramer multiple test or unpaired t-test. \*  $P < 0.05$  significant difference vs. pre-treatment level.

#### 4.3.2.2. Total Glutathione Level in the Media

In KRS, there was no difference between Air, NBO and HBO treatment throughout the experiment. However, in Arg, Lac and Arg+Lac media, oxygen treatments (both NBO and HBO) showed higher glutathione levels when comparing to control KRS with regard to the same timepoints; whilst normobaric air (Air) treatment showed less effect than only in Arg+Lac media at immediate post-Air treatment, the glutathione level was significantly higher than that in KRS ( $P < 0.05$ , Tukey-Kramer multiple comparisons test). On the other hand, the NBO treatment increased the glutathione level of 113% ( $P < 0.01$ ), 66% ( $P < 0.05$ ), and 86% ( $P < 0.05$ ) at immediate post treatment; and 120% ( $P < 0.001$ ), 86% ( $P < 0.01$ ), and 80% ( $P < 0.05$ ) at 4h post treatment when aorta segment was incubated in Arg, Lac and Arg+Lac media than that in KRS ( $15.4 \text{ nM mg}^{-1} \text{ tw}$ ), respectively. The HBO treatment showed the most significant increase in the three specific media that the glutathione levels were more than 2-fold than that in KRS at both immediate ( $P = 0.003$ , One-way ANOVA and then  $P < 0.01$ , respectively, Tukey-Kramer multiple comparisons test) and 4h post treatment ( $P < 0.001$ , One-way ANOVA and then  $P < 0.001$ , respectively, Tukey-Kramer multiple comparisons test).

In Arg media of Fig 4.3, NBO ( $32.0 \pm 5.1 \text{ nM mg}^{-1} \text{ tw}$ ,  $P = 0.04$ , unpaired t-test) and HBO ( $33.6 \pm 3.8 \text{ nM mg}^{-1} \text{ tw}$ ,  $P = 0.005$ , unpaired t-test) treatments induced distinct increases of glutathione levels when comparing with Air treatment ( $20.2 \pm 1.5 \text{ nM mg}^{-1} \text{ tw}$ ). The oxygen effects remained until the end of 4h recovery, when the glutathione level was  $33.3 \pm 4.1 \text{ nM mg}^{-1} \text{ tw}$  of NBO-treated group ( $P = 0.15$ , unpaired t-test) and  $38.0 \pm 4.2 \text{ nM mg}^{-1} \text{ tw}$  of HBO-treated group ( $P = 0.03$ , unpaired t-test) when comparing with  $26.0 \pm 2.6 \text{ nM mg}^{-1} \text{ tw}$  of the Air-treated group. There was no differences found between NBO and HBO treatment in Arg media ( $P = 0.81$  and  $P = 0.43$  at immediate and 4h post-treatment respectively, unpaired t-test).

In Lac media of Fig 4.3, the HBO treatment induced notably more glutathione release into the media than either NBO or Air treatment. The glutathione level of HBO-treated groups ( $33.9 \pm 3.7$  nM mg<sup>-1</sup> tw) were 65% ( $P = 0.006$ , unpaired t-test) and 33% ( $P = 0.045$ , unpaired t-test) higher than that of Air- and NBO-treated groups ( $20.5 \pm 2.2$  and  $25.5 \pm 1.3$  nM mg<sup>-1</sup> tw, respectively) at immediate post-treatment. And after 4h recovery, the glutathione level of HBO-treated groups ( $40.9 \pm 3.7$  nM mg<sup>-1</sup> tw) were 60% ( $P = 0.015$ , unpaired t-test) and 43% ( $P = 0.019$ , unpaired t-test) higher than that of Air- and NBO-treated groups, respectively ( $25.5 \pm 4.3$  and  $28.6 \pm 3.0$  nM mg<sup>-1</sup> tw). No difference was shown between Air- and NBO-treated groups throughout experiment in Lac medium.

In Arg+Lac media of Fig 4.3, although no treatment differences were found at immediate post-treatment ( $24.6 \pm 3.4$ ,  $28.6 \pm 3.8$  and  $33.2 \pm 2.5$  nM mg<sup>-1</sup> tw of Air, NBO and HBO-treated groups respectively,  $P = 0.20$ , One-way ANOVA), HBO-treated groups ( $36.7 \pm 2.8$  nM mg<sup>-1</sup> tw) showed a significantly higher level of glutathione than that of either Air-treated ( $27.4 \pm 3.4$  nM mg<sup>-1</sup> tw,  $P = 0.049$ , unpaired t-test) or NBO-treated ( $27.2 \pm 1.0$  nM mg<sup>-1</sup> tw,  $P = 0.005$ , unpaired t-test) groups after 4h recovery.

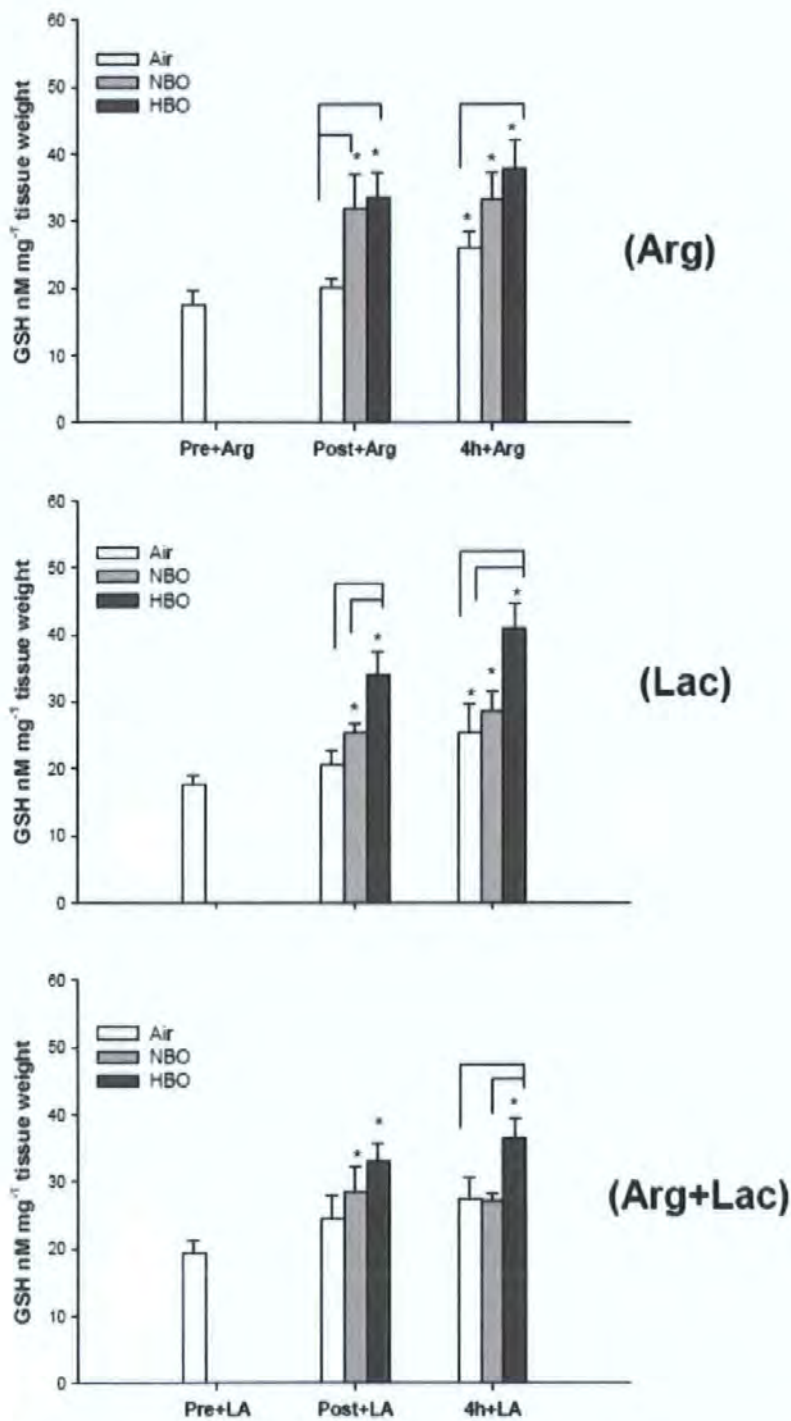


Fig 4. 3 Total Glutathione concentration released from aorta segments into specific media under normobaric air (Air, white bar), normobaric 100% oxygen (NBO, grey bar) or hyperbaric 100% oxygen (HBO, dark grey bar) at Pre-treatment (Pre), Immediate post 90 min treatment (Post); and 4h after treatment (4h). Tissue was kept in Krebs-Ringer buffer in the presence of 100  $\mu$ M L-Arginine (A), 15 mM sodium L-lactate (B) or both (C). Data are expressed as means  $\pm$  SEM of nine rats. One-way ANOVA test was performed, and followed by Tukey-Kramer multiple test or unpaired t-test. \*  $P < 0.05$  significant difference vs. pre-treatment level. Brackets indicate significant difference ( $P < 0.05$ ) between observations.

### 4.3.3. Nitric Oxide Production

When comparing with the values of NO<sub>x</sub> (nitrite + nitrate) ( $0.16 \pm 0.01 \mu\text{M mg}^{-1} \text{ tw}$ ), nitrite ( $0.035 \pm 0.005 \mu\text{M mg}^{-1} \text{ tw}$ ) and their ratio ( $31.6 \pm 6.4\%$ ) in KRS, supplement of Arg or/and Lac to KRS affected NO production. The NO<sub>x</sub> in the three specific media were significantly higher when compared to control KRS with respect treatments and timepoints ( $P < 0.05$ , unpaired t-test), whilst the nitrite levels and the ratio of nitrite to nitrate in three specific media were much less than that in KRS with respect treatments and timepoints ( $P < 0.001$ , Tukey-Kramer multiple comparison test).

In the three specific media, the NO<sub>x</sub> concentration varied slightly and no time effects were shown. However, the nitrite concentration and ratio of nitrite to nitrate increased during and after Air, NBO and HBO treatments in some of the groups (Fig 4.4).

In Arg medium, the NO<sub>x</sub> concentration at pre-treatment was  $0.47 \pm 0.08 \mu\text{M mg}^{-1} \text{ tw}$ , which remained at the same level in all treatments throughout experiments ( $0.30 \pm 0.03$  and  $0.45 \pm 0.10$ ,  $0.45 \pm 0.09$  and  $0.40 \pm 0.08$ ,  $0.43 \pm 0.07$  and  $0.43 \pm 0.05$  of Air-, NBO- and HBO-treated groups at immediate post and 4h post treatment, respectively). The nitrite level in Arg medium showed a increasing trend till the 4h post treatment with Air-treated group showed significance to its pre-treatment level and NBO-treated group showed significance to its immediate post-treatment level ( $P = 0.046$ , unpaired t-test). The ratio of nitrite to nitrate changed similarly as nitrite. No treatment effects were seen with NO<sub>x</sub>, nitrite and their ratio.

In Lac medium, the NO<sub>x</sub> level showed neither time nor treatment differences during and after the experiment. Time effects of nitrite levels were seen in NBO and HBO groups until 4h post treatment which were higher than pre-treatment and their immediate post-treatment levels ( $P < 0.05$ , Tukey-Kramer multiple comparison test). In addition, the ratio of nitrite to nitrate presented time effect in Air-treated group at immediate post-treatment

and in all three treatments groups at 4h post-treatment ( $P < 0.05$ , Tukey-Kramer multiple comparison test). Treatment effect was shown at immediate post-treatment that the ratio of Air-treated group was higher than that of both oxygen-treated groups. The ratio of nitrite to nitrate during treatments was  $2.1 \pm 0.2\%$  of Air-treated group, which was 233% ( $0.9 \pm 0.3\%$ ) and 263% ( $0.8 \pm 0.3\%$ ) of that of NBO- and HBO-treated groups respectively ( $P < 0.05$  and  $P < 0.01$ , Tukey-Kramer multiple comparison test). After 4h recovery, the ratios were  $4.1 \pm 0.5\%$ ,  $3.0 \pm 0.6\%$  and  $3.5 \pm 0.4\%$  of Air, NBO and HBO groups, and no difference were found ( $P = 0.35$ , One-way ANOVA).

In Arg+Lac medium, the NO<sub>x</sub> levels showed no time and treatment effects. Significant higher nitrite than pre-treatment level was found in Air-treated groups at both immediate and 4h post treatment. At 4h post treatment, oxygen-treated groups also showed higher level of nitrite than pre-treatment level and their immediate post-treatment level ( $P < 0.01$ , Tukey-Kramer multiple comparison test). Treatment effects were found at immediate post-treatment. The Air treatment induced  $0.008 \pm 0.001 \mu\text{M mg}^{-1} \text{ tw}$  of medium nitrite, which was 2-fold higher than the  $0.004 \pm 0.001 \mu\text{M mg}^{-1} \text{ tw}$  measured in the NBO- and HBO-treated groups ( $P < 0.05$ , Tukey-Kramer multiple comparison test). But this Air effect disappeared after 4h recovery when the medium nitrite level was  $0.013 \pm 0.003$ ,  $0.014 \pm 0.002$  and  $0.017 \pm 0.003 \mu\text{M mg}^{-1} \text{ tw}$  of Air, NBO and HBO groups in Arg+Lac medium, respectively ( $P = 0.59$ , One-way ANOVA). Consequently, the ratio of nitrite to nitrate during treatments was  $3.0 \pm 0.5\%$  for the Air-treated group, which was 176% ( $1.7 \pm 0.5\%$ ,  $P = 0.08$ , unpaired t-test) and 263% ( $1.1 \pm 0.4\%$ ,  $P = 0.01$ , unpaired t-test) of that in NBO- and HBO-treated groups respectively. After 4h recovery, the air effects diminished when the ratio of nitrite to nitrate increased to  $4.3 \pm 0.5\%$ ,  $4.1 \pm 0.4\%$  and  $4.4 \pm 0.6\%$  of Air, NBO and HBO groups ( $P = 0.89$ , One-way ANOVA).

---

Incubation of aorta segments in Arg media generated more nitrite and nitrate ( $0.47 \pm 0.08$  and  $0.008 \pm 0.002 \mu\text{M mg}^{-1}$  tw of pre-treatment NOx and nitrite levels), which were significant higher than that in Lac media ( $0.27 \pm 0.03$  and  $0.002 \pm 0.001 \mu\text{M mg}^{-1}$  tw,  $P = 0.03$ , unpaired t-test, respectively) but not than that in Arg+Lac media ( $0.32 \pm 0.03 \mu\text{M mg}^{-1}$  tw of NOx,  $P = 0.07$ , unpaired t-test; and  $0.003 \pm 0.001 \mu\text{M mg}^{-1}$  tw of nitrite,  $P = 0.05$ , unpaired t-test). The ratio of nitrite to nitrate of Arg medium was not different from Lac or Arg+Lac media at pre-treatment ( $1.8 \pm 0.5\%$ ,  $0.9 \pm 0.5\%$  and  $1.1 \pm 0.4\%$ ,  $P = 0.35$ , One-way ANOVA).

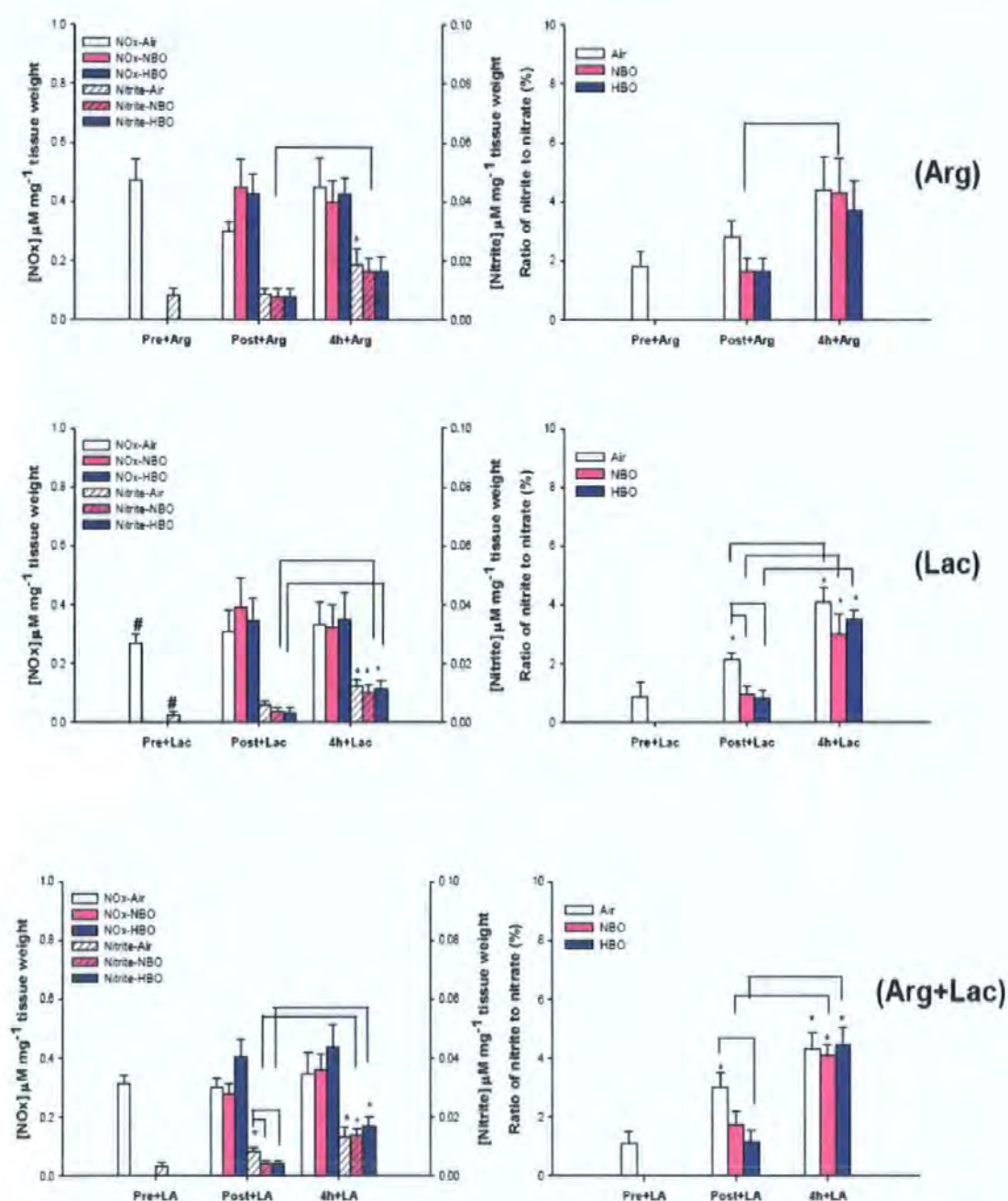


Fig 4. 4 Concentration of NOx and Nitrite, and their ratio in specific media under normobaric air (Air, white bar), normobaric 100% oxygen (NBO, pink bar) or hyperbaric 100% oxygen (HBO, blue bar) at Pre-treatment (Pre), Immediate post 90 min treatment (Post); and 4h after treatment (4h). Tissue was kept in Krebs-Ringer buffer in the presence of 100  $\mu\text{M}$  L-Arginine, 15 mM sodium L-lactate or both. Data are expressed as means  $\pm$  SEM, nine rats were used for groups in Arg and Arg+Lac mediums, eight rats were used for groups in Lac medium. NOx (blank columns) and nitrite (diagonal columns) level were plotted into the left figures with left and right Y axis corresponding to the level of NOx and nitrite in  $\mu\text{M mg}^{-1}$  fresh tw, and the ratio of nitrite to nitrate were plotted into the right figures. Statistic analysis was performed with One-way ANOVA test followed by Tukey-Kramer multiple comparison test or unpaired t-test. \*  $P < 0.05$  significant difference vs. pre-treatment level; #  $P < 0.05$  significant difference vs. level of group in Arg medium; and brackets indicate significant difference ( $P < 0.05$ ) between observations.

#### 4.3.4. Angiogenic Factor: VEGF Changes in Tissue Homogenates

The supplement of Arg or/and Lac to KRS showed a trend to decrease VEGF production of aorta segments. During treatment, the VEGF level in specific media were not significant difference from that in KRS ( $P = 0.67, 0.88$  and  $0.23$  of Air, NBO and HBO treatment respectively, One-way ANOVA). But at the end of 4h recovery, the VEGF level in NBO- and HBO-treated group in specific media were significant lower than that in Krebs-Ringer solution ( $P = 0.04$  and  $0.02$  of NBO and HBO treatment respectively, One-way ANOVA). Further investigation found that VEGF content of NBO-treated samples in Arg, Lac and Arg+Lac medium was only 72% ( $P = 0.03$ , unpaired t-test), 73% ( $P = 0.12$ , unpaired t-test) and 63% ( $P = 0.004$ , unpaired t-test) of that of NBO-treated samples in KRS ( $0.88 \pm 0.08 \text{ ng mg}^{-1} \text{ tp}$ ,  $n = 8$ ). In addition, the HBO-treated samples in Arg, Lac and Arg+Lac medium was only 72% ( $P = 0.21$ , unpaired t-test), 57% ( $P = 0.05$ , unpaired t-test) and 51% ( $P = 0.036$ , unpaired t-test) of that of HBO-treated samples in Krebs-Ringer solution ( $0.88 \pm 0.19 \text{ ng mg}^{-1} \text{ tp}$ ,  $n = 8$ ).

In Arg and/or Lac media, VEGF level of aorta segments increased over time. After 4h recovery, VEGF level showed statistically significant differences when comparing with either the pre-treatment level or their post-treatment values in all runs (Fig 4.5). The pre-treated VEGF level in aorta segments in Arg, Lac and Arg+Lac medium was  $0.25 \pm 0.05$ ,  $0.30 \pm 0.04$  and  $0.28 \pm 0.04 \text{ ng mg}^{-1} \text{ tp}$ , respectively. In Arg medium, Air, NBO and HBO treatment induced similar levels of VEGF production ( $0.40 \pm 0.05$ ,  $0.38 \pm 0.04$  and  $0.36 \pm 0.04 \text{ ng mg}^{-1} \text{ tp}$  respectively,  $P = 0.88$ , One-way ANOVA), and after 4h recovery, their VEGF levels were  $0.72 \pm 0.08$ ,  $0.63 \pm 0.07$  and  $0.63 \pm 0.06 \text{ ng mg}^{-1} \text{ tp}$ , respectively ( $P = 0.59$ , One-way ANOVA). And at 4h post-treatment, the VEGF levels in all three treatment groups were higher than that of pre-treatment levels and their post-treatment levels ( $P < 0.05$ , unpaired t-tests). But there were no differences of VEGF levels among Air, NBO or HBO

treatment when aorta segment incubated in Arg medium. In Lac and Arg+Lac media, similar changes were found. Notably, after 4h recovery, the VEGF level of HBO-treated groups showed difference between Arg and Arg+Lac medium that the VEGF level in Arg+Lac medium ( $0.45 \pm 0.06 \text{ ng mg}^{-1} \text{ tp}$ ) was 30% less than that its corresponding value in Arg medium ( $P=0.046$ , unpaired test).

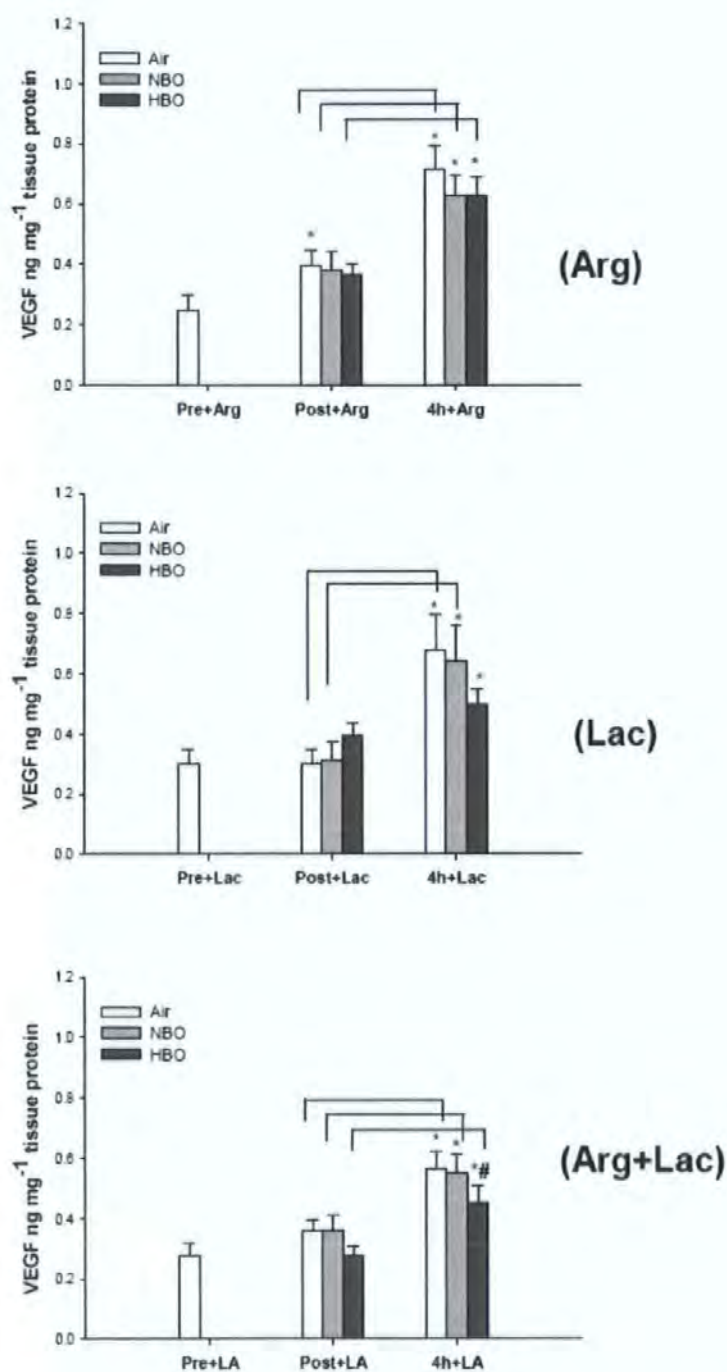


Fig 4. 5 VEGF content of aorta segment homogenate in specific media under normobaric air (Air, white bar), normobaric 100% oxygen (NBO, grey bar) or hyperbaric 100% oxygen (HBO, dark grey bar) at Pre-treatment (Pre), Immediate post 90 min treatment (Post); and 4h after treatment (4h). Tissue was kept in Krebs-Ringer buffer in the presence of 100  $\mu$ M L-Arginine (A), 15 mM sodium L-lactate (B) or both (C). Data are expressed as means  $\pm$  SEM ng mg<sup>-1</sup> protein of nine rats. One-way ANOVA test was performed, and followed by Tukey-Kramer multiple test or unpaired t-test. \* P < 0.05 significant difference vs. pre-treatment level, # P < 0.05 significant difference vs. level in Arg medium, and brackets indicate significant difference (P < 0.05) between observations.

#### 4.3.5. Lactate Level in the Media

Supplement of Arg significantly increased the lactate levels when comparing with that in Krebs–Ringer solution ( $P < 0.0001$ , One-way ANOVA). The lactate concentration in Arg media showed a significant time effect throughout the experiments (Fig 4.6-Arg). The lactate pre-treatment level in Arg media was  $1.0 \pm 0.2 \mu\text{M mg}^{-1} \text{ tw}$ , which had a distinct 6-fold increase during treatments ( $6.8 \pm 1.1$ ,  $6.3 \pm 1.0$  and  $5.5 \pm 0.6 \mu\text{M mg}^{-1} \text{ tw}$  of immediate after Air, NBO and HBO treatment respectively), and a further significant increase was seen in all treated groups during 4h recovery to  $26.0 \pm 2.5$ ,  $19.5 \pm 1.6$  and  $16.7 \pm 1.5 \mu\text{M mg}^{-1} \text{ tw}$  respectively. Treatment effects were not seen at immediate after treatment, but at 4h after treatment, when NBO-treated groups showed 25% ( $P = 0.04$ , unpaired t-test) and HBO-treated groups showed 36% ( $P < 0.01$ , unpaired t-test) less lactate level than that of the Air-treated groups.

Supplement of Lac into the media significantly increased lactate concentration compared to the Arg media. Although neither time nor treatment differences were seen ( $P = 0.30$ , One-way ANOVA), the lactate level in all groups was significant higher than that of corresponding level in Arg media ( $P < 0.0001$ , One-way ANOVA) (Fig 4.6-Lac). The lactate level in Arg+Lac media were significantly higher than that in either Arg or Lac media ( $P < 0.0001$ , One-way ANOVA), but no treatment difference was seen (Fig 4.6-Arg+Lac). The pre-treatment lactate level in Arg+Lac media was  $42.7 \pm 9.7 \mu\text{M mg}^{-1} \text{ tw}$ , which became  $50.0 \pm 6.6$ ,  $46.2 \pm 10.6$  and  $60.5 \pm 9.3 \mu\text{M mg}^{-1} \text{ tw}$  at immediate after Air, NBO and HBO treatment respectively, and increased during 4h recovery to  $70.9 \pm 10.0$ ,  $68.6 \pm 10.4$  and  $85.4 \pm 15.9 \mu\text{M mg}^{-1} \text{ tw}$ , respectively.

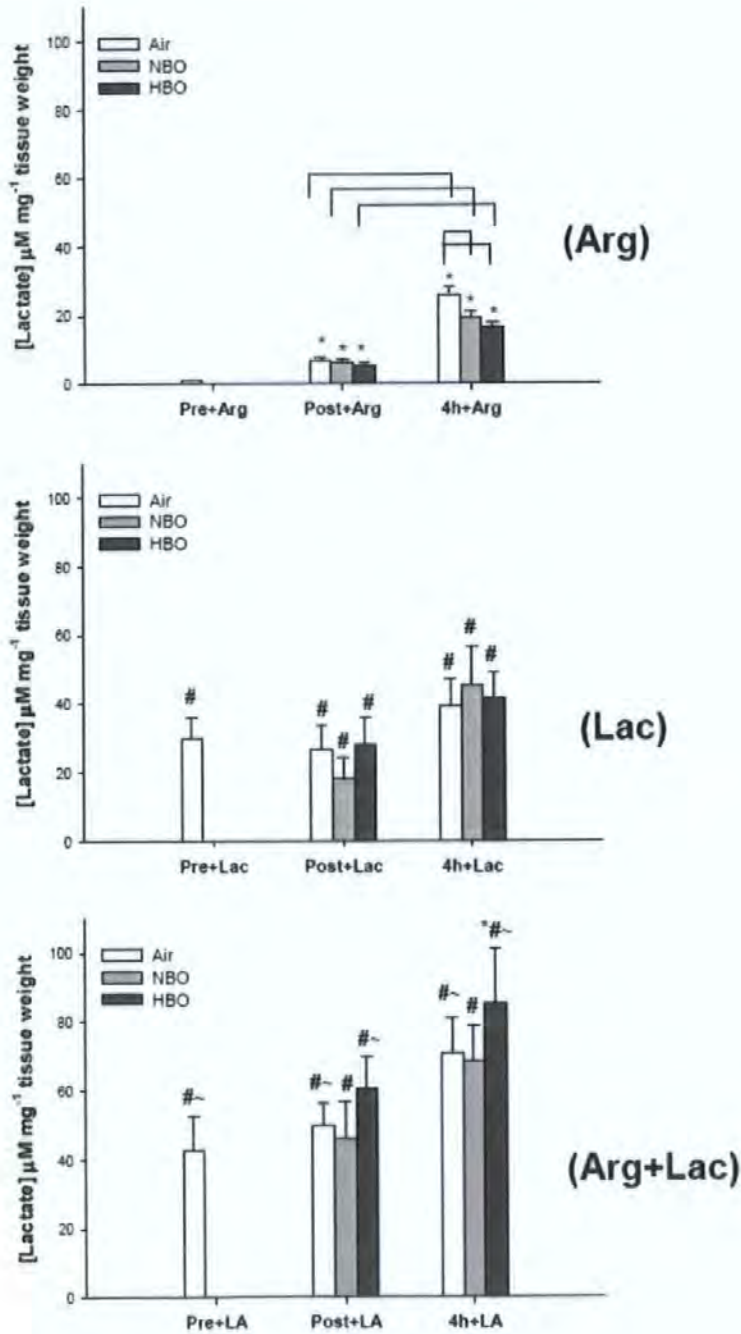


Fig 4. 6 Lactate concentration in specific media of aorta segments under normobaric air (Air, white bar), normobaric 100% oxygen (NBO, grey bar) or hyperbaric 100% oxygen (HBO, dark grey bar) at Pre-treatment (Pre), Immediate post 90 min treatment (Post); and 4h after treatment (4h). Tissue was kept in Krebs-Ringer buffer in the presence of 100  $\mu\text{M}$  L-Arginine (A), 15 mM sodium L-lactate (B) or both (C). Data of (A) are expressed as means  $\pm$  SEM  $\mu\text{M mg}^{-1}$  tw of nine rats and data of (B) and (C) have been subtracted added lactate (15 mM) before normalized by tissue weight. One-way ANOVA test was performed, and followed by Tukey-Kramer multiple test or unpaired t-test. \*  $P < 0.05$  significant difference vs. pre-treatment level. #  $P < 0.05$  significant difference vs. Arg medium, and ~  $P < 0.05$  significant difference vs. Lac medium. Brackets indicate significant difference ( $P < 0.05$ ) between observations.

## 4.4 Discussion

In this study, we investigated the effects of HBO on oxidative stress and angiogenic factors in aorta segments incubated in specific media which either mimic pathological condition or offset the possible limitation in normal physiological saline. First of all, supplement of L-arginine or/and sodium L-lactate to Krebs-Ringer solution significantly increased the release of LDH, H<sub>2</sub>O<sub>2</sub> and glutathione in NBO and HBO treatment groups than that in KRS only, which indicates synergic effects of oxygen and supplement ingredients in inducing oxidative stress and cell damage. Secondly, L-arginine and sodium L-lactate supplements increase NO production as more nitrite and nitrate were observed in Arg/Lac media than that in KRS; but no evidence has shown that HBO induce more NO production in either Arg or Lac media. Finally, unlike other parameters, there is no evidence shown that Arg/Lac supplement induce more VEGF production than that in KRS throughout experiments. On the contrary, after 4h recovery, less VEGF levels were observed in NBO or/and HBO treatments in Arg/Lac media than that in KRS, which may due to the high levels of cell damages and oxidative stress.

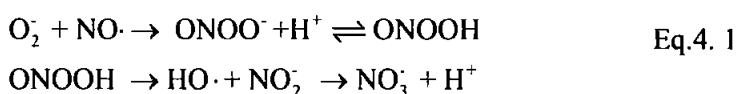
### 4.4.1. L-arginine Supplement and HBO Treatment

NO is produced continuously at nanomolar concentrations by nitric oxide synthase (NOS) in the human body, this enzyme catalyses the conversion of L-arginine into citrulline and NO with consumption of NADPH and oxygen. The fact that NO is responsible for vasodilatation has make NO an important factor in angiogenesis research. And in addition, NO is also widely involved in natural immune defences and the regulation of growth factors (Akimoto et al., 2000; Arany et al., 1996; Droge, 2002; Dulak, 2003). More and more studies have confirmed that HBO treatment affect NO production as well

as NOS expression. When applying HBO at high pressure (over 5 ATA), increased NO production and NOS expression in the central nervous system has been suggested to be relevant to oxygen toxicity (Oury et al., 1992; Wang et al., 1998 and Chavko et al., 2001). But at lower pressure (less than 4 ATA), limited or no oxygen toxicity were seen in several studies (Zhang et al., 1995; Zhiliaev et al., 2002; and Moskvin et al., 2003). Studies on the immune cells have demonstrated that HBO at treatment pressure is able to decrease NO production induced by pathogenic factors such as lipopolysaccharide (Kurata et al., 1995; Sunakawa and Yusa, 1997; Huang et al., 2005; Chu et al., 2006; Chang et al., 2006) and zymosan (Luongo et al., 1998; Imperatore et al., 2004). Furthermore, HBO helps to control some syndromes of chronic wound by suppressing expression and activity of NOS (Rachmilewitz et al., 1998; Yuan et al., 2004; Gajendrareddy et al., 2005). The complicated NO regulation during HBO treatment therefore reflects the multi-function nature of NO as well as the complexity of organisms. L-arginine is a natural physiological precursor in the NO synthesis pathway and there was about 100  $\mu\text{M}$  of L-arginine found in rat plasma (Osowska et al., 2004), but the Krebs-Ringer solution contained no L-arginine in our previous study. L-arginine has been proven to play a central role in NO synthesis of cultured endothelial cells which depend upon the L-arginine content of the media (Palmer et al., 1988). NO synthesis is also blocked by L-arginine analogues (Gross, et al., 1990) and supplemental L-arginine improves endothelial function (Chin-Dusting et al., 1996). In our previous study, a low and unchanged NO level was shown with HBO treatment when aorta segment was incubated in physiological salt solution without L-arginine (Fig 3.5). The depletion of L-arginine could be a reason why low NO level was found, and at such low levels it is hard to show any treatment-related changes.

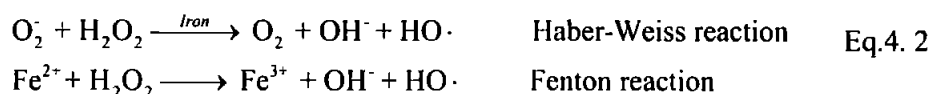
In the current chapter, L-arginine (100  $\mu\text{M}$ ) was added to Krebs-Ringer solution and increased NO production was found as both nitrate and nitrite levels were higher when

comparing with the Krebs-Ringer solution used in Chapter 3. And interestingly, in Arg medium, nitrate was the dominant NO end product as the nitrite to nitrate ratio ranged between 1 ~ 5%, whilst in the Krebs-Ringer medium this ratio ranged between 25 ~ 40%. It is believed that in aqueous phase, when free of biological material, NO exclusively autoxidizes to nitrite (Pogrebnaya et al., 1975; Pires et al., 1994; Goldstein and Czapski., 1995). However, NO also contains an unpaired electron and is paramagnetic, it rapidly reacts with superoxide ( $O_2^-$ ) to form peroxynitrite anion ( $ONOO^-$ ) in high yield when oxygen and nitrogen species co-exist in the same aqueous solution (Blough and Zafiriou., 1985). The  $ONOO^-$  can either spontaneously rearrange to form nitrate ( $NO_3^-$ ) or undergo cleavage to generate hydroxyl ( $OH^\cdot$ )-like radicals and nitrite ( $NO_2^-$ ). The peroxynitrite has a pKa of  $7.49 \pm 0.06$  at 37 °C and rapidly decomposes once protonated with a half-life of 1.9 sec at pH 7.4 (Beckman et al., 1990) (Eq 4.1). The peroxynitrite generation and its metabolism may explain the nitrate in the medium.



Although superoxide anion ( $O_2^-$ ) levels were not measured in our study, hydrogen peroxide ( $H_2O_2$ ) as the direct dismutation product of superoxide increased in the oxygen-treated group in Arg medium than that in KRS. The supplement of L-arginine into the medium increased NO production from aorta segment and meanwhile oxygen treatment promoted generation of oxygen and nitrogen radicals. Therefore, the production of peroxynitrite could be facilitated and nitrate became the dominant NO end-product in Arg medium. In these terms, the value of nitrite to nitrate ratio may lead to new insights regarding the oxidative environment when studying cell damage caused by the interactions of NO with other active molecules (Marzinzig et al., 1997).

Among the reactive oxidative species, the OH $\cdot$  are considered the major toxic radical form. In biological systems, the formation of OH $\cdot$  and OH $\cdot$ -like radicals are often considered to originate from the interaction of iron with enzymatically and/or non-enzymatically generated superoxide (Haber-Weiss reaction) and/or hydrogen peroxide (Fenton reaction) (Eq 4.2), and via peroxynitrite reaction (Eq 4.1).

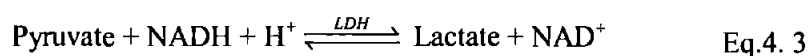


It is noteworthy that Fenton and Haber-Weiss reactions require the presence of H<sub>2</sub>O<sub>2</sub> as well as iron to produce OH $\cdot$ , but there is not much iron existed in our reaction system. So if the production of peroxynitrite increased, more OH $\cdot$ -like radicals will be produced simultaneously. Previous studies have shown that increased OH $\cdot$ -like radicals and enhanced cell damage occur at the same time as a sharp drop in intracellular GSH content (Shu et al., 1997). LDH, a common indicator for cell or tissue damage, showed higher levels in oxygen-treated groups than air groups in Arg media. This suggests synergic effect of oxygen and arginine on cell damage, or at least LDH leak. Another line of evidence to support the notion of oxidative stress is the simultaneous appearance of high level of total glutathione released into the Arg medium in oxygen-treated groups.

The lactate level in Arg medium was higher than that in Krebs-Ringer solution. The oxygen treatments reduced the lactate level in Arg medium as well as in Krebs-Ringer solution as expected, which confirmed that less anaerobic glycolysis but more aerobic oxidation to supply ATP in hyperoxia conditions (e.g. NBO and HBO treatments). There is no evidence shown that Arg supplement along or synergically with HBO treatment promotes VEGF production from aorta segments in any of the treatments in spite the fact that VEGF increased over time during experiments in Arg medium.

#### 4.4.2. Sodium L-lactate Supplement and HBO Treatment

Lactate is produced from pyruvate in a reaction catalysed by lactate dehydrogenase under anaerobic conditions in all tissues (Eq. 4.3). This reaction is rapid so that pyruvate and lactate are always in an equilibrium situation and the ratio of lactate to pyruvate is 10 to 1 in cells. The balance between lactate and pyruvate determines the ratio  $[NADH]$  to  $[NAD^+]$  and this ratio is also used to denote the redox state within the cytoplasm (Kruse and Carlson., 1987).



Chronic wounds suffer from insufficient oxygen supply, which cause large concentrations of lactate (10-25 mM) accumulated at the wound sites (Hunt et al., 1985; Im & Hoopes, 1970). Interestingly, lactate is also present in well-oxygenated wounds because of accumulation of leukocytes, fibroblasts. Relatively lacking mitochondria, all these cells rely on anaerobic glycolysis for energy recruitment. As a consequence, lactate levels increase in wounds under normoxic conditions as well (Tandara and Mustoe, 2004). This high level of lactate not only represents the anaerobic glycolysis energy supply in wound sites for cells, but also serves as an angiogenesis initiator to regulate the production of growth factors such as VEGF (Jensen et al., 1985; Zabel et al., 1996; Constant et al., 2000).

HBO treatment did not affect the high concentration of lactate as there were no differences found between Air, NBO and HBO treatments throughout the experiment in Lac-added media. Sheikh et al (2000) also showed a similar finding that lactate (range 2.0-10.5 mM) in wound site was not affected by HBO treatment. But higher level of LDH,  $\text{H}_2\text{O}_2$  and glutathione were found in oxygen-treated groups of Lac media than that in KRS. The stress and cell damage may due to the change of cell redox status induced by the high level of lactate via affecting the ratio of  $[NADH]$  to  $[NAD^+]$ . In Lac media, the nitrate level were lower than that in Arg media but higher than that in Krebs-Ringer solution, it seems

that high level of lactate also promote nitric oxide production. Hein et al (2006) exposed retinal arterioles to lactate *in vitro* and found that the vessels dilated in a dose-dependent manner in response to neutralized L-lactate (0.01-10 mM) and blockade of monocarboxylate transporters, nitric oxide synthase, soluble guanylyl cyclase, and ATP-sensitive potassium channels nearly abolished lactate-induced vasodilation. They suggested that uptake of lactate by vascular cells via monocarboxylate transporters caused retinal arteriolar dilation predominantly via stimulation of nitric oxide synthase and subsequent activation of guanylyl cyclase. Even with this evidence, the relationship of lactate, nitric oxide and HBO treatment needs further investigation to establish the possible signalling pathway.

Several studies have shown that high concentration of lactate facilitated VEGF production in macrophages (Zabel et al. 1996; Constant et al., 2000), and HBO treatment increased VEGF production in wound with high concentration of lactate (Sheikh et al., 2000). However, capillary endothelial cells and fibroblasts did not show increasing secretion of this angiogenesis factor when cultured under hypoxic conditions or in high concentrations of lactate (Jensen et al., 1986). In our study, neither the high lactate supplement nor HBO treatment increased VEGF level; there was no evidence of any synergic effect of HBO and lactate on VEGF production in aorta segment. Therefore, Lactate-induced VEGF production may be specific to macrophages.

#### **4.4.3. L-Arginine, Sodium L-lactate Supplement and HBO Treatment**

The same as Arg and Lac media, oxygen (NBO and HBO) treatments induced more damage and oxidative stress of aorta segments in Arg+Lac media as similar high level of LDH, H<sub>2</sub>O<sub>2</sub> and glutathione were observed. The NO<sub>x</sub>, nitrite level in Arg+Lac medium was not increased when compared with Arg or Lac medium, which implies that there is no

synergic effects of L-arginine and sodium L-lactate supplements on NO production. VEGF of NBO- and HBO-treated group in Arg+Lac media were less than that in KRS after 4h recovery, which indicates that no synergic effects of lactate, NO and HBO on promoting VEGF production, and on the contrary, reduces endogenous VEGF production from vascular tissues.

In Krebs-Ringer solution, the aorta segment was incubated in physiological saline, which showed the ability to maintain its redox balance under either normobaric oxygen or hyperbaric oxygen treatments. However, the Arginine supplement facilitated NO generation and the Lactate supplement changed the redox status, so the incubation environment had changed. Under these unfavorable circumstances, oxygen treatments especially HBO treatment induced more ROS, which may overcome the protection of antioxidant defence system in cells and induce cell damage. Our results supported this hypothesis. Comparing to that in KRS, oxygen treatments (NBO and HBO) induced higher level of oxidative stress and more cell damage in Arg or/and Lac supplemented media reflexed as higher release levels of LDH, hydrogen peroxide and total glutathione in the media. The mechanisms of the synergic results of Arg/Lac and oxygen were not clear, it could possible via the formation of peroxynitrite and hydroxyl ( $\text{OH}\cdot$ )-like radicals and nitrite ( $\text{NO}_2^-$ ) or unbalance the ratio of  $[\text{NADH}]$  to  $[\text{NAD}^+]$ . Thus, further investigation is needed. On the other hand, no synergic effects were found on promoting NO and VEGF production of Arg/Lac and oxygen. Under oxidative condition, NO is presented in the form of nitrate other than nitrite, so the nitrite to nitrate ratio is somehow reflecting the oxidative environment. Interestingly, recent study suggests that *in situ* VEGF production may related with the cell redox status as well. Sreekumar et al (2006) found significant induction of secretion and expression of VEGF and its receptors in human retinal pigment epithelial cells under conditions of oxidative stress induced by glutathione (GSH) depletion.

And Grasselli et al (2005) also indicated that a 'pro-oxidant' state was possibly involved in the stimulation of VEGF production to induce angiogenesis. But in our study, VEGF level in NBO or HBO-treated groups was decreased in Arg/Lac media after 4h recovery, which may due to the high level of cell damage interfered the cell autocrine function to generate more VEGF. The high cell damage level may represent the fact that HBO treatment helps to eliminate the wounded tissue and cells and at the same time to deliver signals to surrounding cells to generate growth factors to promote cell grow and wound healing. This hypothesis will need more experiments to support and verify.

## Chapter 5

# Oxygen Regulates $[Ca^{2+}]_i$ in Human Umbilical Vein Endothelial Cells

### 5.1 Abstract

Cytosolic free calcium is a ubiquitous intracellular signal responsible for many endothelial cell functions. In this study; intracellular  $Ca^{2+}$  changes of human umbilical vein endothelial cells (HUVECs) under different oxygen conditions were investigated. The HUVECs were loaded with Fura-2 AM ester, and then exposed to 95% air + 5%  $CO_2$  (air), 95%  $N_2$  + 5%  $CO_2$  (hypoxia), 95%  $O_2$  + 5%  $CO_2$  (hyperoxia), or 100%  $O_2$  at 2.2 ATA for 90 mins. The levels of  $[Ca^{2+}]_i$  were recorded at pre-treatment, and up to 1h continually post-treatment. All the treatments increased  $[Ca^{2+}]_i$  than their pre-treatment levels, whilst HBO treatment evoked higher level of  $[Ca^{2+}]_i$  than that of air treatment.  $[Ca^{2+}]_i$  showed no differences either among air, hypoxia and hyperoxia treatments; or among hypoxia, hyperoxia and HBO treatments. No evidence has been shown that HBO treatment caused cell injury, which may indicate that HBO-induced  $[Ca^{2+}]_i$  increases are likely to serve as a signalling messenger for hyperbaric oxygen treatment.

### 5.2 Introduction

Cell proliferation is a complex process, tightly regulated by a set of diffusible factors including hormones, peptidic growth factors, lipidic compounds, and other molecules

(Munaron, 2002). These factors act via autocrine and/or paracrine mechanisms and exert their effects interacting with high affinity receptors located in the plasma-membrane, triggering a cascade of intracellular reactions, finally leading to DNA synthesis and cell duplication (Schlessinger, 2000). Researches have suggested that change of intracellular free calcium concentration ( $[Ca^{2+}]_i$ ) is a ubiquitous intracellular signal responsible for controlling numerous cellular processes (Ermak and Davies, 2001; Bootman et al., 2002; Dawson et al., 2006). The  $Ca^{2+}$  signalling network has been described as four functional units by Berridge et al (2000): First, stimuli bind to variety of cell-surface receptors including G-protein-coupled receptors (GPCRs) and receptor tyrosine kinases (RTKs), which triggers  $Ca^{2+}$ -mobilizing signals e.g. inositol-1,4,5-trisphosphate ( $InsP_3$ ), cyclic ADP ribose (cADPR), nicotinic acid-adenine dinucleotide phosphate (NAADP), and sphingosine 1-phosphate (S1P). And then the  $Ca^{2+}$ -mobilizing signals activate  $Ca^{2+}$  channels to feed  $Ca^{2+}$  into the cytoplasm. The net  $Ca^{2+}$  influx are through plasma membrane  $Ca^{2+}$  channels, and intracellular  $Ca^{2+}$ -channels on the membrane of endoplasmic reticulum (ER) that includes the  $InsP_3$  receptor, ryanodine receptor (RyR), NAADP receptor, and sphingolipid  $Ca^{2+}$  release-mediating protein. Thirdly,  $Ca^{2+}$  activates different  $Ca^{2+}$  sensors, which augment a wide range of  $Ca^{2+}$ -sensitive processes such as contraction, proliferation, crosstalk with other signalling pathway, enzyme secretion, ATP synthesis, apoptosis and etc, which depending on cell type and context. Finally, the OFF mechanisms pump  $Ca^{2+}$  out of the cytoplasm: the  $Na^+/Ca^{2+}$  exchanger and the PMCA pumps  $Ca^{2+}$  out of the cell and the SERCA pumps it back into the ER/SR to restore resting state of  $Ca^{2+}$  concentration. The free cytosolic calcium increases are due either to release from the finite internal store, the endoplasmic reticulum (ER) or the equivalent organelle, sarcoplasmic reticulum (SR) of muscular cell, or to the influx from the infinite supply of extracellular medium through the opening of calcium-permeable channels (Berridge 1997). These two

pathways are not exclusive and can coexist in response to the stimulation with the same agonist. Mitochondrion is another important component of the calcium signalling system in that it sequesters  $\text{Ca}^{2+}$  rapidly during the development of the  $\text{Ca}^{2+}$  signal and then releases it back slowly during the recovery phase. Both intracellular and extracellular sources are triggered by a multitude of stimuli including signalling molecules, pH, calcium-induced calcium release, voltage, oxygen tension and mechanical stress. Given the complexity of the regulation of cellular  $\text{Ca}^{2+}$  and  $\text{Ca}^{2+}$ -signaling processes, it is not surprising that disruption of these control mechanisms has been linked to the pathogenesis of diseases and cytotoxic events (Kass and Orrenius, 1999). Actually, works from several laboratories have showed that a perturbation of  $\text{Ca}^{2+}$  homeostasis is a common and final event responsible for drug-induced cell death. The cytotoxic chemicals or their metabolites can inhibit  $\text{Ca}^{2+}$  transport mechanisms (e.g. the PMCAs and SERCAs); and the cells are exposed to a prolonged elevation of  $[\text{Ca}^{2+}]$ . Increased  $[\text{Ca}^{2+}]$  activates several catabolic processes catalyzed by  $\text{Ca}^{2+}$ -activated proteases (calpains), phospholipases, and endonucleases, which in turn lead to cell death (Kass et al., 1996; Jewell et al., 1982; Nicotera et al., 1986; Orrenius et al., 1992; Trump and Berezsky, 1996).

Various transmitters, such as acetylcholine, histamine, kinins (bradykinin), angiotensin, ATP, ADP, the coagulation factor thrombin, growth factors, and mechanical stimuli (e.g. shear stress) have been used as stimuli to increase  $[\text{Ca}^{2+}]$  of endothelial cells (Nilius and Droogmans, 2001). And as non-excitabile cells,  $\text{Ca}^{2+}$  homeostasis in endothelial cells involves uptake and release of  $\text{Ca}^{2+}$  into intracellular organelles (particularly ER) as well as controlled influx from the extracellular environment (Putney et al., 2001; Bootman et al., 2002). The  $\text{Ca}^{2+}$  signalling system plays important roles for most of endothelial cells' vital functions as diverse as coagulation, inflammation, vessel permeability, angiogenesis, and vascular tone (Tran et al., 2000; Adam and Hill, 2004). For example, the

synthesis and/or release of vasoactive compounds (e.g. nitric oxide, prostacyclin, PAF, or tPA, PAI-1) is generally believed to depend on or can be modulated by changes in  $[Ca^{2+}]_i$  (Busse et al., 1991; Miller and Vanhoutte, 1992; Carter and Pearson, 1992; Peiretti et al., 1997; Emeis et al., 1997).

Particularly in relation to this thesis, intracellular calcium signalling is also invoked as a result of VEGF activation in endothelial cells, which is a key event in the initiation of vasodilation, hypermeability, and angiogenesis. In the vascular endothelium, VEGF is capable of binding to the extracellular domain of two receptor tyrosin kinases, namely VEGFR-1 and VEGFR-2. But most studies have pointed out that the role of VEGF in promoting endothelial cell proliferation and vascular hyperpermeability is mediated primarily by the VEGFR-2/flk-1/KDR receptor (Ferrara and Smyth, 1997). Ligation of VEGF to the VEGFR2 receptor leads to receptor dimerization and phosphorylation of the tyrosine kinase receptor, and associates with the recruitment of src-homology (SH)-2 domain-containing proteins (Guo et al., 1995). Phospholipase C $\gamma$ 1 (PLC $\gamma$ 1) is one of several SH2-containing proteins and is capable of binding to VEGFR-2 after receptor autophosphorylation (He et al., 1999). Activation of PLC $\gamma$ 1 by VEGF leads to the production of diacylglycerol (DAG) and inositol 1,4,5 triphosphate (IP $_3$ ), an important regulator of calcium channels in the endoplasmic reticulum (ER) membrane. IP $_3$  opens ligand-operated channels in the ER, and subsequently empties intracellular calcium stores into the cytosol (Otun et al., 1996). IP $_3$  and its breakdown products may also contribute to extracellular calcium influx through IP $_3$  receptor channels in the plasma membrane as well (Vaca and Kunze., 1995). Faehling et al (2002) found that VEGF induced a biphasic  $[Ca^{2+}]_i$  signal and also increased the level of intracellular inositol 1,4,5-trisphosphate (IP $_3$ ), which suggests that VEGF-A releases  $Ca^{2+}$  from IP $_3$ -sensitive stores and induces store-operated calcium influx. Reduction of either extracellular or intracellular free  $Ca^{2+}$

inhibited VEGF-induced proliferation. Dawson et al (2006) found that VEGF<sub>165</sub> elicited a rapid rise in cytosolic calcium followed by a slower decline toward control values in HUVECs. The VEGF<sub>165</sub>-mediated  $[Ca^{2+}]_i$  rise is eliminated by inhibitors of VEGFR-2, tyrosine kinase, src kinase, inositol-1,4,5 triphosphate-operated calcium channels; and inhibition of plasmalemmal calcium channels also diminished the magnitude and duration of the calcium spike. They suggested that the calcium extracellular calcium influx, secondary to stores release, is a significant component of the calcium spike; and the VEGFR-2/src kinase/PLC $\gamma$ 1/IP<sub>3</sub> axis plays a critical role in governing endothelial calcium response to VEGF. Although VEGF may enhance eNOS activity via PI3K/Akt/PKB pathway, the elevated  $[Ca^{2+}]_i$  is the primary stimulus for NO production and calcium-dependent NO formation may represent a link between calcium signalling and proliferation. Kohn et al (1995) found that CAI, a blocker of ligand-stimulated  $Ca^{2+}$  influx, inhibits EC proliferation, adhesion, and invasion into the basement membrane of EC. Jobin et al (2003) reported that VEGF promotes rapid mobilization of intracellular calcium throughout the regions of the cell in which eNOS was distributed, and this distribution parallels the localization of agonist-induced intracellular calcium changes.

It is notable that hypoxic and ischemic conditions mediate  $[Ca^{2+}]_i$  levels of endothelial cells. Arnould et al (1992) reported that HUVECs showed a decrease in ATP content and then an increase in  $[Ca^{2+}]_i$  during 2 h of severe hypoxia. And Hu and Ziegelstein (2000) presented similar  $[Ca^{2+}]_i$  increase of human aortic endothelial cells in hypoxic condition. The  $[Ca^{2+}]_i$  increase under hypoxia may be mediated via extracellular calcium entry and calcium release from calcium-sensitive intracellular stores (Berna et al., 2002; Peers et al., 2006). During hypoxia, reactive oxidative species (ROS) seem to be involved in calcium regulation. Ikeda et al (1997) pointed out that anoxia induced elevation of  $[Ca^{2+}]_i$  in the brain capillary endothelial cells and the elevation depends on superoxide and peroxynitrite

generation. Peers et al (2006) found that hypoxia can evoke  $\text{Ca}^{2+}$  release from intracellular stores of human saphenous vein endothelial cells via a mechanism involving ROS generation from mitochondria. In addition, Aley et al (2005) defined two distinct pathways by which hypoxia regulate  $\text{Ca}^{2+}$  release from the ER. First is the mitochondrial pathway in which hypoxia evokes an increased production of ROS at the mitochondrion to trigger release of  $\text{Ca}^{2+}$  from the ER via RyRs, and second is the oxidase pathway, in which substrate limited reduction of ROS levels during hypoxia relieves tonic inhibitory influences of NADPH oxidase-derived ROS on  $\text{IP}_3$ -dependent  $\text{Ca}^{2+}$  release from the ER. There is also cross-talk between these two regulatory pathways; specifically, hypoxia-induced mitochondrial ROS production augments agonist-evoked  $\text{Ca}^{2+}$  release via mitochondrial, and oxidase regulation.

Mitochondria serve as the main source for ATP via oxidative phosphorylation and a consequence of this process is the production of ROS. Mitochondria are important containers of intracellular  $\text{Ca}^{2+}$  in endothelial cells, accounting for the remaining 25% of the cell's  $\text{Ca}^{2+}$  reserve (Tran et al., 2000; Wood et al., 1998). More evidence have shown that mitochondria were not simply a high-capacity, low-affinity  $\text{Ca}^{2+}$  storage pools that serve in states of  $\text{Ca}^{2+}$  overload as a life-rescuing mechanism by taking up the amount of  $\text{Ca}^{2+}$  that would otherwise overburden the ER (Gunter and Pfeiffer, 1990), they also excitable, capable of generating and conveying electrical and  $\text{Ca}^{2+}$  signals (Ichas et al., 1997).  $\text{Ca}^{2+}$  mobilizing stimulus generates mitochondrial ROS, which, in turn, facilitate  $[\text{Ca}^{2+}]_i$  signals. Similar to hypoxia, hyperoxia conditions such as anoxia/reoxygenation, normobaric high oxygen concentration or even HBO are able to produce ROS, so it is not surprising to see  $[\text{Ca}^{2+}]_i$  increases under hyperoxia conditions. Tirosh et al (2006) showed that acute normoxia increases  $[\text{Ca}^{2+}]_i$  and NO production in hypoxia-maintained fetal pulmonary artery endothelial cells via entry of extracellular calcium and subsequent  $\text{Ca}^{2+}$ -

induced calcium release from intracellular stores. Brueckl et al (2006) reported that exposure of lung capillary endothelial cells to normobaric 70% oxygen increased ROS and  $[Ca^{2+}]_i$ , and the ROS formation was initially originated from the mitochondrial electron transport chain, but subsequently involves activation of NAD(P)H oxidase by endothelial  $[Ca^{2+}]_i$  signaling and Rac1 activation. Wang et al (1998) found that HBO exposure at 0.5 MPa (5 ATA) increased the intrasynaptosomal  $[Ca^{2+}]_i$  by two or three folds, and suggested that neuronal  $Ca^{2+}$  overload during HBO exposure is a major factor in the pathogenesis of central nervous system  $O_2$  toxicity. Liu et al (1999) observed biphasic changes of  $[Ca^{2+}]_i$  in endothelial cells and smooth muscle cells during 0.2 MPa (2 ATA) and 0.3 MPa (3 ATA) HBO exposure, which first increased within 5 min, and then decreased throughout the exposures. It seems that both hypoxia and hyperoxia affect the homeostasis of  $[Ca^{2+}]_i$  and the oscillation is quite possibly coupled with ROS generation. This may suggest that calcium as an oxygen detector or at least as a second messenger involved in oxygen-induced responses during HBO treatment. Most of the previous studies are concerned on one aspect of  $[Ca^{2+}]_i$  changes at either hypoxia or hyperoxia condition and also there is lack of evidence on post-treatment changes. In this study, we aim to compare the real-time  $[Ca^{2+}]_i$  oscillation of non- or HBO-treated single endothelial cell in different oxygen environment, which was achieved by perfusion cells with hypoxic or hyperoxic buffers. Furthermore to back up the single cell measurement, we compare the  $[Ca^{2+}]_i$  changes in normobaric, hypoxic, hyperbaric and HBO conditions by using populations of HUVECs. And  $[Ca^{2+}]_i$  monitoring was continued for an hour to investigate the post-treatment effects. Moreover, cell viability test was performed to exclude the possibility of any cell injury.

Changes in calcium concentration are often monitored using fluorescence probes, which are notably very sensitive to any change in ion concentration and are relatively non-invasive; and can detect sudden changes in ion concentration. Depending on the

experimental requirements the same techniques can be used with different detector systems to obtain information on the time course of events, or the spatial localisation of events. Fura-2 and its acetoxymethyl (AM) ester derivatives are high affinity, intracellular calcium indicators that are ratiometric and UV light-excitable, which let them widely used in calcium detection for a wide variety of cells (Takahashi et al., 1999). The probe works by absorbing a short wavelength (ultra-violet) photon with high energy and then re-emitting a photon of lower energy. Binding of a calcium ion to the probe causes a change in the efficiency of the photon absorption, resulting in a higher rate of emission of photons. At low concentration of the indicator, use of the 340/380 nm excitation ratio allows accurate measurements of the  $[Ca^{2+}]_i$ ; and this ratio measurement considerably reduces the effects of uneven dye loading, leakage of dye, and photobleaching, as well as problems associated with measuring  $Ca^{2+}$  in cells of unequal thickness (Tsien et al., 1984).

## **5.3 Material and Methods**

### **5.3.1. Chemicals and Reagents**

The reagents used are all cell culture grade. Nutrient mixture Hams F-12, L-glutamine, gentamycin, heparin, and endothelial cell growth supplement from bovine neural tissue (ECGS), Pluronic F-127 and DMSO (Dimethyl Sulfoxide for molecular biology) were obtained from Sigma-Aldrich (Poole, UK); foetal bovine serum, 0.25% trypsin, Dulbecco's phosphate buffered saline (D-PBS) and Hanks' balanced salt solution contains 1.25 mM of  $Ca^{2+}$  (HBSS) were obtained from Invitrogen (Paisley, UK). And Fura-2 acetoxymethyl ester (Fura-2) was purchased from Molecular Probes (Eugene, OR, USA).

### 5.3.2. HUVECs Culture Protocol

The human umbilical vein endothelial cells (HUVECs) were kindly provided by Dr. Jackie Whatmore and her team, Cell and Molecular Biology, Peninsula Medical School, University of Plymouth and Exeter. Two solutions were used for routine HUVECs culture: (1) Standard Ham's solution: Ham's F-12 contains 0.68 mM of L-Glutamine and 50  $\mu\text{g ml}^{-1}$  of gentamycin; and (2) Complete Ham's solution: 40 ml of Foetal bovine serum and 4 ml of ECGS standard Ham's solution containing 1  $\text{mg ml}^{-1}$  of ECGS and 4.5  $\text{mg ml}^{-1}$  of Heparin were added into 156 ml standard Ham's solution to make a total volume of 200 ml complete Ham's solution.

HUVECs culture protocol was optimised from Jaffe et al (1974). Briefly, HUVECs were seeded in 25  $\text{cm}^2$  culture flask (Fisher, UK), and covered with 6 ml of complete Ham's solution. The flasks were placed in sealed cylinder gassed with air containing 5% carbon dioxide ( $\text{CO}_2$ ) and incubated in a 37 °C incubator. The complete Ham's solution was changed every second day. Once reaching confluence, cells were first rinsed twice with 5 ml of D-PBS, and then 0.5 ml of 0.25% trypsin was added to detach cells from culture surface. Finally, 6 ml of complete Ham's solution were added to deactivate trypsin and cell suspensions were transferred into three new flasks. Cells in 70 – 80% confluence in passages 3 to 5 were used for calcium experiments.

### 5.3.3. *In Situ* Recording of $\text{Ca}^{2+}$ Changes in Single HUVEC

#### 5.3.3.1 Apparatus for $[\text{Ca}^{2+}]_i$ Measurement

The recording chamber is composed of a rhombus-shaped Perspex block (10 mm  $\times$  5 mm in diameter, Warner Instruments heated bath RS22) and a glass coverslip. The glass coverslip was attached to the underside of the block using epoxy resin, which formed the base of the bath to hold the cell suspension on the stage. A drop of cell suspension was

placed at the bottom of the bath, and allowed to adhere to the coverslip for up to 30 min. The initial perfusion pump flow rate was set at  $0.5 \text{ ml min}^{-1}$  through the bath, and only cells that had attached firmly and stayed immobile under microscope were used. When the solution level and flow was stable, and just reached below the upper edge of the bath, a size-fitted coverslip was placed to cover the upper open surface of the Perspex block in order to prevent oxygen exchange during experiment. The maximal bath volume was about 0.5 ml and it took approximately 1 - 2 min for a fully solution replacement.

The recording chamber was mounted on the stage of a Nikon Diaphot Eclipse inverted microscope and the cells were viewed using a  $\times 40$  oil immersion lens (Nikon Plan Fluor X40 DLL). There was a stage heater to keep the stage at about  $37^\circ\text{C}$  during experiments. In experiments,  $[\text{Ca}^{2+}]_i$  was measured using a Cairn microspectrofluorimeter as previously described (Handy et al., 1996) using a spinning wheel filter (excitation/emission 340/380 nm) and a dichroic mirror with a 500 nm cut-off for emitted light (Cairn Research, Faversham, Kent). The average  $[\text{Ca}^{2+}]_i$  within the visual field containing the cell was indicated by the ratio of the 340/380 nm signal. Light emitted from areas of the field of view not occupied by the cell was reduced using a variable rectangular window on the side-port of the microscope. All imaging and data collection was observed and controlled by the Acquisition Engine software (Cairn Research, Faversham, Kent). The fluorescence intensity at wavelengths 340 nm and 380 nm were recorded every 4 seconds, and the intensity ratio of 340 to 380 nm was calculated as indication of  $[\text{Ca}^{2+}]_i$  changes.

### 5.3.3.2 Cell Preparation and Fura-2 Loading

When HUVECs achieved 70% - 80% confluences, cells were harvested by trypsinisation and resuspended in complete Ham's solution to obtain cell suspension at concentration of  $2 \times 10^5 \text{ cells ml}^{-1}$  (as outlined above). Fura-2 acetoxymethyl ester (Fura-2) was dissolved in 5% pluronic in DMSO solution to get 1 mM of final concentration. For

loading with Fura-2, 2  $\mu\text{l}$  of 1 mM Fura-2 solution was added to 1 ml of cell suspension, then cells were incubated for 1 h at 37 °C in dark with culture medium and Fura-2 at a final concentration of 2  $\mu\text{M}$ .

### 5.3.3.3 Experimental Protocol

The aim of this experiment was to test the responsiveness of cells to hypoxia or hyperoxia following HBO treatment. Cells that had not been treated with HBO were used as controls. After loading with Fura-2, cells were placed on the stage and the  $[\text{Ca}^{2+}]_i$  of a single HUVEC was initially recorded during perfusion with HBSS (gassed with 95% air + 5%  $\text{CO}_2$ ) for half an hour as a control to demonstrate that each cell had a stable intracellular  $[\text{Ca}^{2+}]_i$  in normal saline. The next stage was to investigate the effect of hypoxia or hyperoxia on each cell. This was achieved by first recording cell with control perfusion and then switched to perfusate of hypoxic or hyperoxic HBSS solution as appropriate. Solutions were made hypoxic or hyperoxic by continuous bubbling with 95%  $\text{N}_2$  + 5%  $\text{CO}_2$  or 95%  $\text{O}_2$  + 5%  $\text{CO}_2$  for at least 30 min prior to perfusion of cells, and during the appropriate part of the perfusions, respectively. For each series of calcium recordings, the same batch of Fura-2 loaded cells was exposed to HBO treatment at 2.2 ATA for 90 min at 37 °C. Immediate after HBO exposure, the  $[\text{Ca}^{2+}]_i$  was recorded as outlined above. Identical batches of cells from the same culture plates were used as the non-HBO treated controls, and similarly subject to either hypoxia or hyperoxia perfusions.  $\text{pO}_2$  (partial oxygen pressure) was measured in the solution before it applied to the perfusion system using a MLT1120 Micro-Oxygen Electrode (ADInstruments Ltd, Oxfordshire, UK). For each procedure, 4 – 6 cells were recorded. The recording process was performed at 37 °C. In our experiment, calcium signal recording was terminated when the cell shape start to change (if at all) to ensure functional responses were recorded.

### 5.3.4. $[Ca^{2+}]_i$ Measurement Using Fluorescence Plate Reader

#### 5.3.4.1. Experiment Protocol

In addition to recordings  $[Ca^{2+}]_i$  changes from single cells, some experiments were also performed using population of cells in microplates, and the fluorescence recorded on a plate reader instead. Briefly, confluent HUVECs monolayer (70% - 80%) were trypsinised and resuspended in 6 ml of fresh complete Ham's culture medium. Two thirds of cell suspension (4 ml) was loaded with Fura-2 at a final concentration of 2  $\mu$ M. For loading with Fura-2, cells were incubated for 1 h at 37 °C in dark in a humidified atmosphere gassed with air and 5% CO<sub>2</sub>. The one third of cell suspension (2 ml) was not loaded with Fura-2 and served as a blank control. After incubation, cells were washed to remove excess dye by centrifugation for 10 min at 1,000 rpm and resuspended in HBSS to give a final concentration of  $2.0 \times 10^5$  cells ml<sup>-1</sup>. And then 0.2 ml of control and the Fura-2 loaded cell suspension was added in triplicate into wells of 96-well cell culture plates at  $4.0 \times 10^4$  cells per well. The plate was again incubated at 37 °C in a humidified atmosphere gassed with air and 5% CO<sub>2</sub> for 1 hour to let all the cells attach to the plate bottom.

The plates containing the same batch of cells were exposed to normobaric air + 5% CO<sub>2</sub> (Control), normobaric 95% N<sub>2</sub> + 5% CO<sub>2</sub> (Hypoxia), normobaric 95% O<sub>2</sub> + 5% CO<sub>2</sub> (Hyperoxia) and 100% O<sub>2</sub> at 2.2 ATA (HBO) for 90 min at 37 °C.  $[Ca^{2+}]_i$  measurement was performed at 30 min and 0 min prior to exposures to show the pre-treatment  $[Ca^{2+}]_i$  levels; treatment and post-treatments effects were observed at immediate post exposures and at 5, 10, 30 and 60 min post exposures, respectively.  $[Ca^{2+}]_i$  measurement of HUVECs was done using a PerSeptive Biosystems CytoFluor<sup>lm</sup>II Fluorometer (GMI, Ramsey, MN, U.S.A.) equipped with dual injectors. The excitation filters were setting at 320/20 nm and 380/20 nm, when gain was set to 80% and 60% respectively of resting baseline intensity to ensure consistency between wells after calibration. The emission filter was setting at

508/20 nm. The fluorescence intensity ratio at 340nm and 380nm was calculated to represent intracellular calcium concentration.

#### **5.3.4.2. Neutral Red Retention Assay for HUVECs**

The  $[Ca^{2+}]_i$  is believed to be relevant to cell damage, so cell viability was tested with the neutral red retention assay, which was adapted from Mori and Wakabayashi (2000). To exclude the possible effect of Fura-2 loading on cells neutral red intake, Fura-2 loaded cells were performed neutral red retention assay along with non-loaded cells (as blank control cells) for each experiment before expose to treatment. To investigate the treatment effects on neutral red intake of cells, the neutral red retention assay was performed after the last reading, which was at the end of 60 min incubation after different oxygen exposure. Briefly, cells were washed twice with D-PBS, and 0.2 ml phenol red-free HBSS solution containing  $10 \mu\text{g ml}^{-1}$  neutral red was added to each well. Then the plates were incubated at  $37^\circ\text{C}$  to allow cells to uptake neutral red for 3 hours. After incubation, the cells were fixed with 1% formal saline (containing 1%  $\text{CaCl}_2$ ) for 5 min to enhance cell attachment to the substrate. Finally, the neutral red dye was extracted by adding 0.2 ml of 1% acetic acid in 50% ethanol to each well and read the plate at 540nm using a spectra-photometric microplate reader (Optimax, Sunnyvale, USA). The neutral red intake content in Fura-2 loaded untreated cells and Fura-2 loaded treated cells was expressed as percentage to blank control cells from the same batch.

#### **5.3.4.3. $[Ca^{2+}]_i$ Calibration in Plate Reader Measurement**

The fluorescence intensity ratio of 340nm to 380nm need to be converted to  $[Ca^{2+}]_i$ , which was achieved by creating a calibration curve from graded concentration of free calcium buffers with the same measurement condition as outlined above. The calcium buffers used to produce low stabilised concentrations of  $\text{Ca}^{2+}$  were made by mix equal

volume of serials concentration of  $\text{CaCl}_2$  with 4 mM of ethylene glycol bis ( $\beta$ -aminoethyl ether)- $N,N'$ -tetraacetate (EGTA) at pH 7.4.

The free calcium concentrations in these Ca-EGTA buffers were calculated via “Free calcium calculator” (<http://entropy.brneurosci.org/cgi-bin/egta>) and assumed that no magnesium were added to the buffer solution (Table 5.1).

Table 5. 1 Free calcium concentration calculation of Ca-EGTA buffers

Total $[\text{Ca}^{2+}]$ (M)	Total EGTA (M)	Free $[\text{Ca}^{2+}]$ (M)
$2.4 \times 10^{-3}$	$2.0 \times 10^{-3}$	$3.99 \times 10^{-4}$
$2.2 \times 10^{-3}$	$2.0 \times 10^{-3}$	$1.99 \times 10^{-4}$
$2.1 \times 10^{-3}$	$2.0 \times 10^{-3}$	$9.93 \times 10^{-5}$
$2.0 \times 10^{-3}$	$2.0 \times 10^{-3}$	$8.16 \times 10^{-6}$
$1.6 \times 10^{-3}$	$2.0 \times 10^{-3}$	$1.34 \times 10^{-7}$
$1.2 \times 10^{-3}$	$2.0 \times 10^{-3}$	$5.02 \times 10^{-8}$
$0.8 \times 10^{-3}$	$2.0 \times 10^{-3}$	$2.23 \times 10^{-8}$
$0.4 \times 10^{-3}$	$2.0 \times 10^{-3}$	$8.37 \times 10^{-9}$

## 5.4 Results

### 5.4.1. Intracellular Calcium Changes of Single HUVEC

#### 5.4.1.1 Single HUVEC Locating and Recording

When cells settled on to the bottom of the bath, we were able to observe and locate single HUVEC. The healthy cell varied in size and appeared round in shape (typical of a healthy cell just removed from a culture flask). The nucleus was centrally located, and organelles and cytoplasm looked evenly distributed around the nucleus inside the cell. The cell membrane appeared to be smooth and intact. The cells showed good contrast with the background, which made it easy to locate recording area for a single cell (Fig 5.1A). As

some of the experiments continued, some cells started to change shape and blebs appeared on cell surface, although at first cells still maintain their size (Fig 5.1B), and then the cell became swollen and irregular shape (Fig 5.1C). Finally, the cell membrane broke with cell content releasing from the cell and cell death occurs (Fig 5.1D). The HUVECs were generally round at the start of the perfusion, and only good cells were selected for recordings. However, even healthy cells eventually showed membrane blebs after 1-2 hours in the bright UV light of the microscope/vibration of flowing solution. But this was not a problem for experiments, because most recordings were made in 30 min or less.

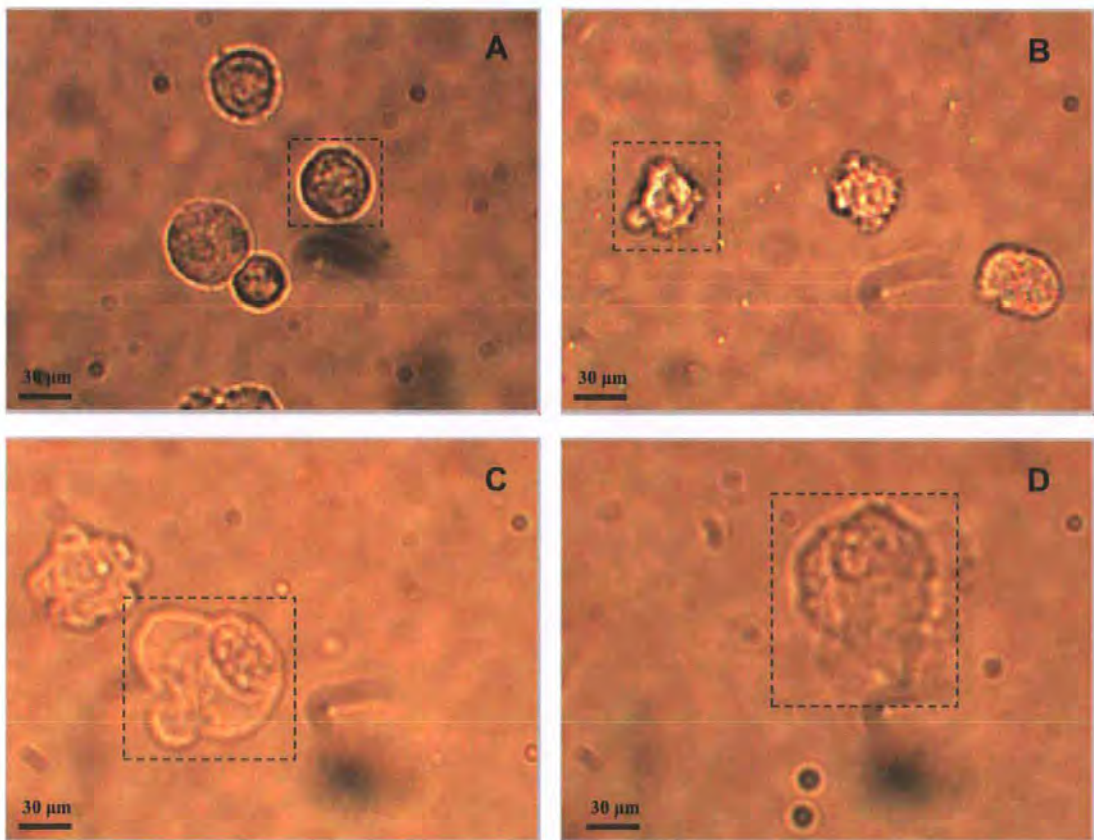


**Fig 5. 1** Photomicrographes of Fura-2 loaded HUVECs during perfusion ( $\times 400$ ). The cells are attached to the bath bottom and perfuse with HBSS gassed with air + 5%  $\text{CO}_2$ . Cells show different morphology during perfusion: at the beginning, all cells are in round shape with an intact and distinct cell membrane (A); when perfusion persists for more than 2 hours, cells show variety of morphological changes such as (B) blebs appeared on surface but cell size and intact membrane was maintained; (C) bigger and more obvious blebs, cell swelling; and (D) cell membrane break and cell contents released from the cell. Calcium measurement of single cell was performed by recording only the setting area: the dashed rectangular area in (A) and (B). When the cell was observed start change shape as in (B), recordings were terminated.

#### 5.4.1.2 Intracellular Calcium Measurements in non-HBO-treated Single HUVEC during Perfusion with Solutions of Different Oxygen Content

The intracellular calcium level of non-HBO treated HUVEC was kept stable throughout the 30 min of control perfusion (HBSS gassed with 95% air + 5% CO<sub>2</sub>). The fluorescence intensity ratio of 340 to 380 nm ranged between 0.35 – 0.55, which gave an average value of  $0.45 \pm 0.05$  (means  $\pm$  SD) of five cells from different batches (Fig 5.2). The pO<sub>2</sub> of HBSS bubbled with 95% air + 5% CO<sub>2</sub> was at about 150 - 200 mm Hg.

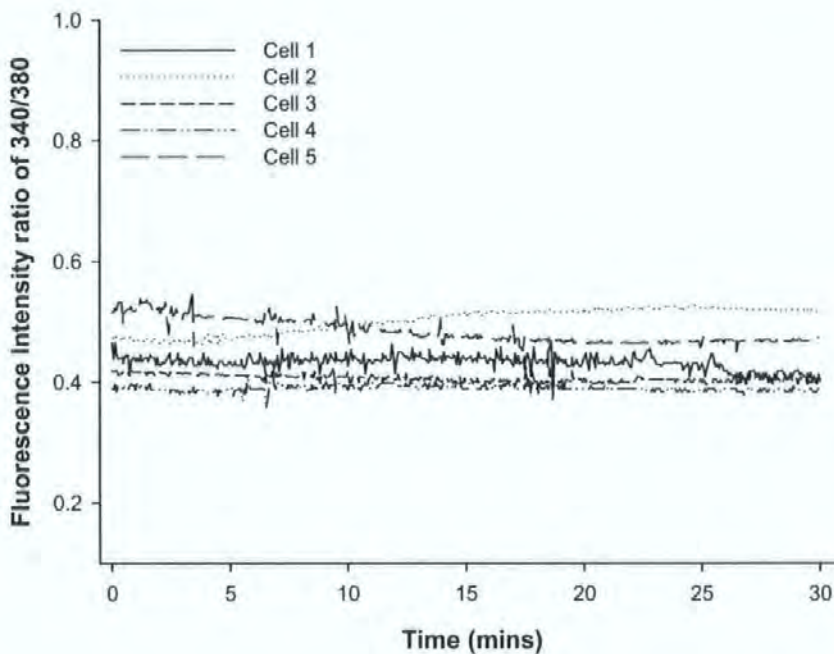
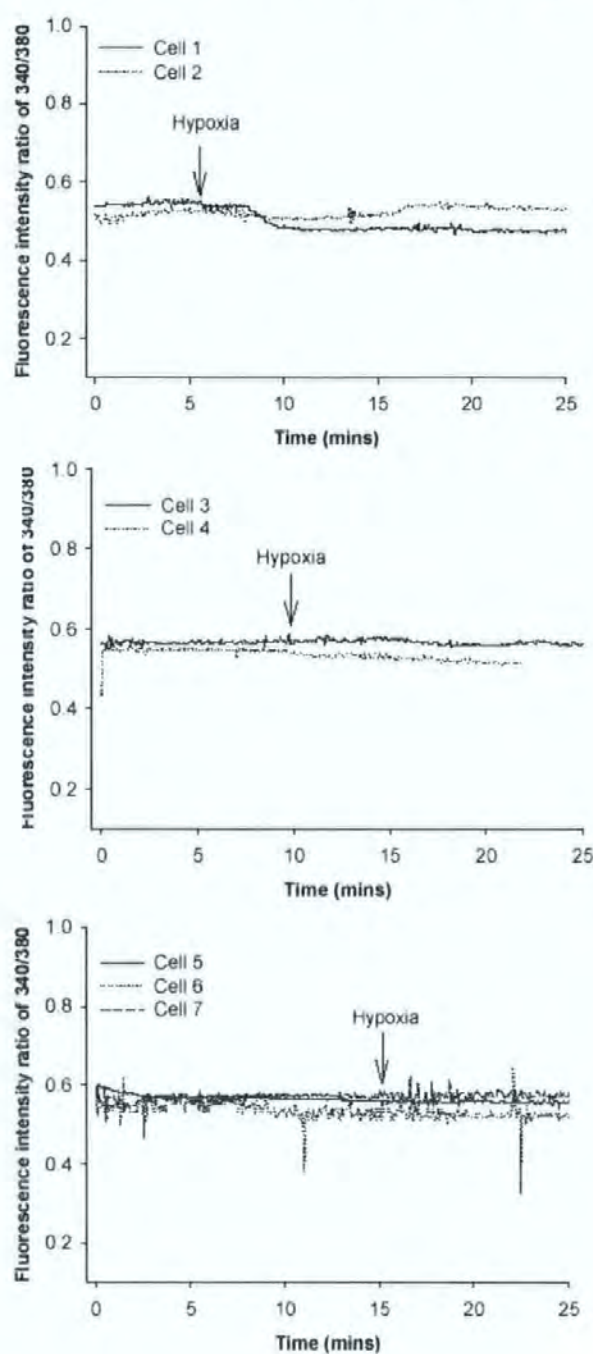


Fig 5. 2 Fluorescence intensity ratio at 340nm to 380nm of HUVEC perfusion with control solution (HBSS gassed with air + 5% CO<sub>2</sub>). Five cells from different batches have been recorded for half hour respectively.

When cells were perfused with control solution, it varied between a couple of minutes to about 10 minutes to get clear stable recordings, and any cell that was not stable was discarded. Once a stable recording was observed, hypoxic solution was applied to the cells. In Fig 5.3, seven cells from different batch were recorded for a total at least 20 min. There was only one cell (Cell 1) that showed a slight decrease in fluorescence ratio after

switching to the hypoxic solution, the other six cells remained at the same level when considering the fluorescent intensity ratio of 340 to 380 nm. The  $pO_2$  of HBSS bubbled with 95%  $N_2$  + 5%  $CO_2$  was at about 10 - 25 mm Hg.



**Fig 5. 3** Ratio of fluorescence intensity at 340nm to 380nm of HUVEC perfusion with control solution and then switched to hypoxia solution (HBSS gassed with 95%  $N_2$  + 5%  $CO_2$ ). The hypoxic solution switch happened after 5 min control perfusion for Cell 1 and 2; 10 min for Cell 3 and 4; and 15 min for Cell 5 to 7.

In Fig 5.4, five cells from different batches were recorded in control + hyperoxia perfusate. Two cells showed a slow decrease in fluorescence ratio and then it returned to its control perfusion level in 10 min during hyperoxic solution perfusion (Cell 1 and Cell 5); whilst one cell showed a sharp increase in fluorescence ratio and then returned to its control perfusion level in less than 3 min after switch (Cell 3); the fluorescence ratio of the other two cells (Cell 2 and 4) remained unchanged from control perfusion level. All the five cells remained intact morphology during the experiments and the pO<sub>2</sub> of HBSS bubbled with 95% O<sub>2</sub> + 5% CO<sub>2</sub> was ranged at 600 - 800 mm Hg.

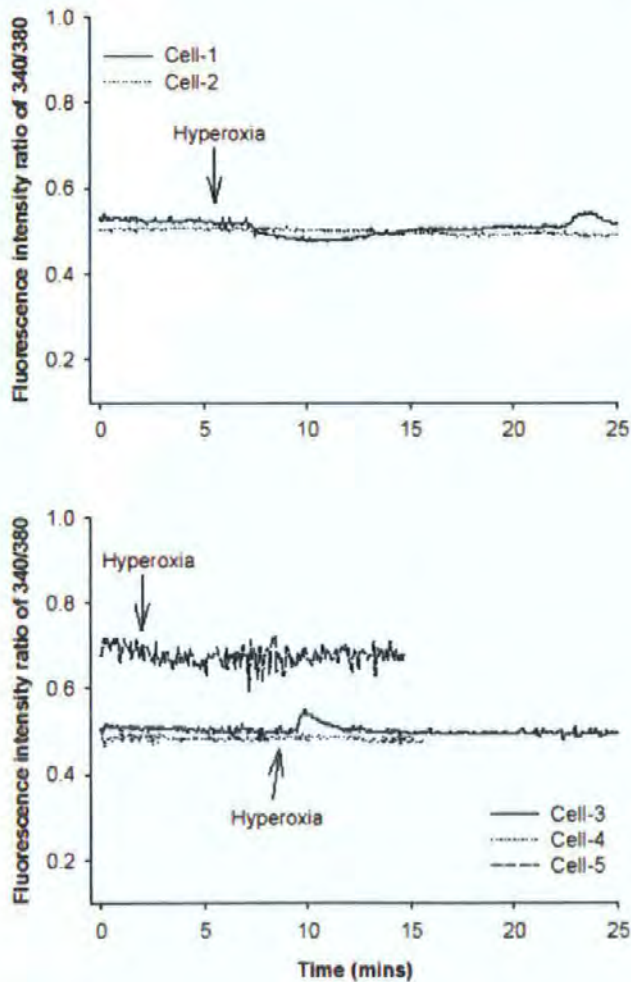


Fig 5. 4 Ratio of fluorescence intensity at 340nm to 380nm of HUVEC perfusion with control solution and then switched to hyperoxia solution (HBSS gassed with 95% O<sub>2</sub> + 5% CO<sub>2</sub>). The hyperoxic solution switch happened after 5 min control perfusion for Cell 1 and 2; 10 min for Cell 3 and 4; and 4 min for Cell 5.

### 5.4.1.3 Intracellular Calcium Measurement of HBO-treated HUVEC during Perfusion with Solutions of Different Oxygen Content

The fluorescence intensity ratio of HBO-treated cells varies greatly. In Fig 5.5, at immediate after loading HBO-treated cells, the highest ratio recorded was 1.2 (Cell 1), whilst the lowest ratio was 0.55 (Cell 6), which gave an average of  $0.74 \pm 0.27$  (means  $\pm$  SD) of six cells from different batches and was 64% higher than that of control non-HBO treated cells. When perfusion with control solution, the HBO-treated cells start to release intracellular calcium as the fluorescence intensity ratio decreased as each perfusion persisted. The decrease was different among the cells, with some cell showing a rapid fall in fluorescence ratio, especially the cells with high fluorescence intensity ratios at the start. Other cells showed slower decreases of fluorescence intensity ratio. But at the end of each trial, all the cells maintained a similar fluorescence ratio with an average of  $0.51 \pm 0.04$  (means  $\pm$  SD) of six cells from different batches, which was 32% less than that of immediate post-HBO value in the same cells.

The background variation of the fluorescence ratio in HBO-treated cells, and the lack effect of hypoxia or hyperoxic perfusion on non-HBO treated cells, suggested that any effect of hyperoxia/hypoxia on an already low fluorescence ratio in the HBO-treated cells would not be detected. Observations on two HBO-treated cells with either hypoxia (Fig 5.6) or hyperoxia (Fig 5.7) solution showed a slight decrease of fluorescence ratio but no different effects were seen from the control solution recording, so it seems unnecessary to further investigate the response of HBO-treated cells to hypoxia or hyperoxia solution as original planed.

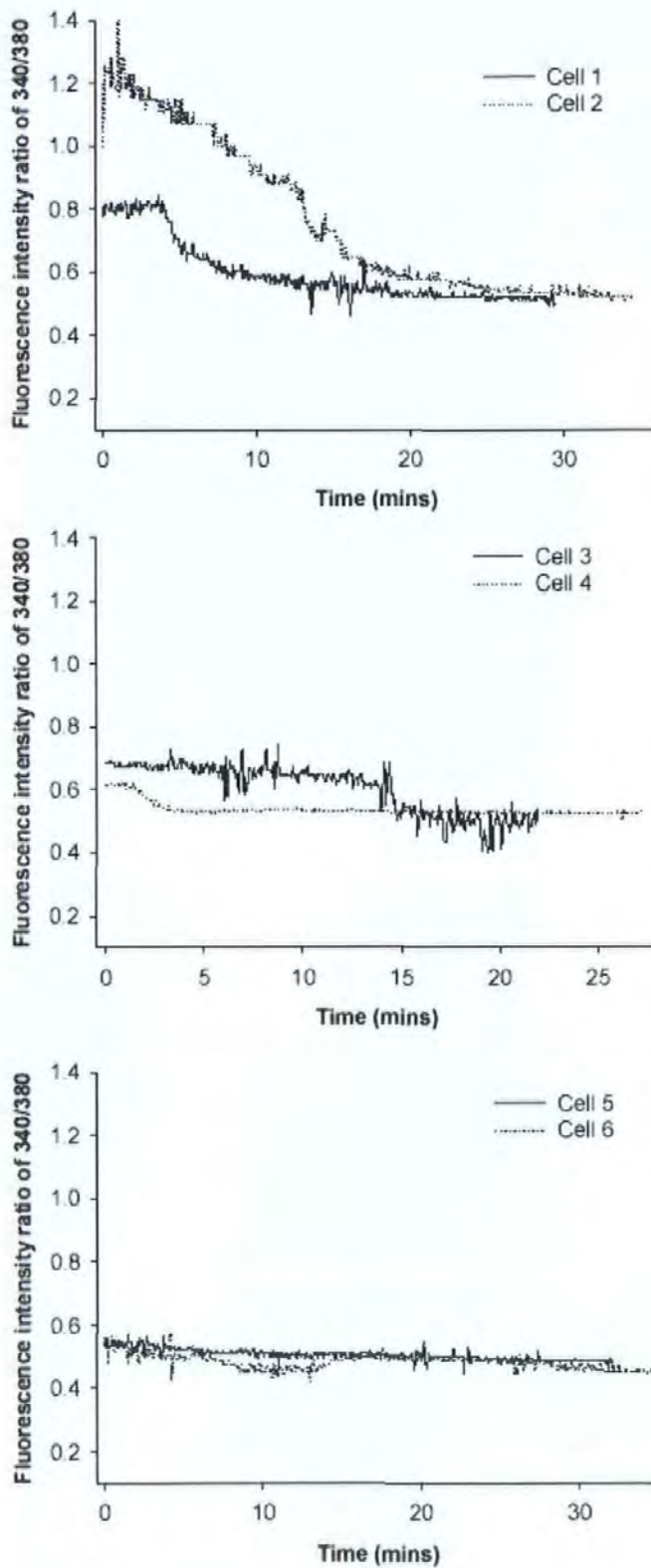


Fig 5. 5 Fluorescence intensity ratio of 340nm to 380nm of HBO-treated HUVEC perfusion with control solution (HBSS gassed with air + 5% CO<sub>2</sub>). Six cells from different batches have been recorded for up to 35 min respectively.

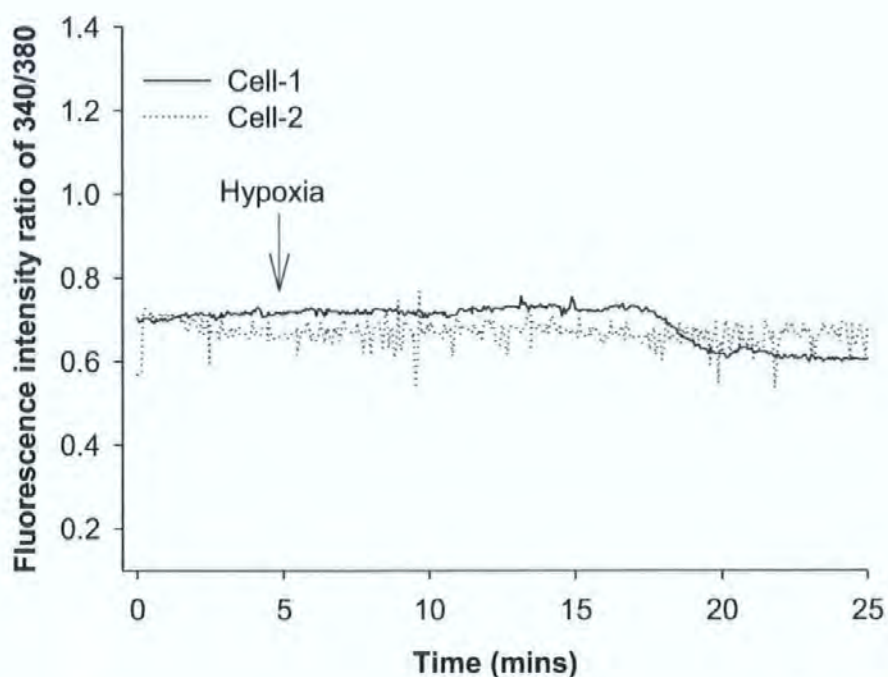


Fig 5. 6 Ratio of fluorescence intensity at 340nm to 380nm of HBO-treated HUVEC perfusion with hypoxia solution (HBSS gassed with 95% N<sub>2</sub> + 5% CO<sub>2</sub>).

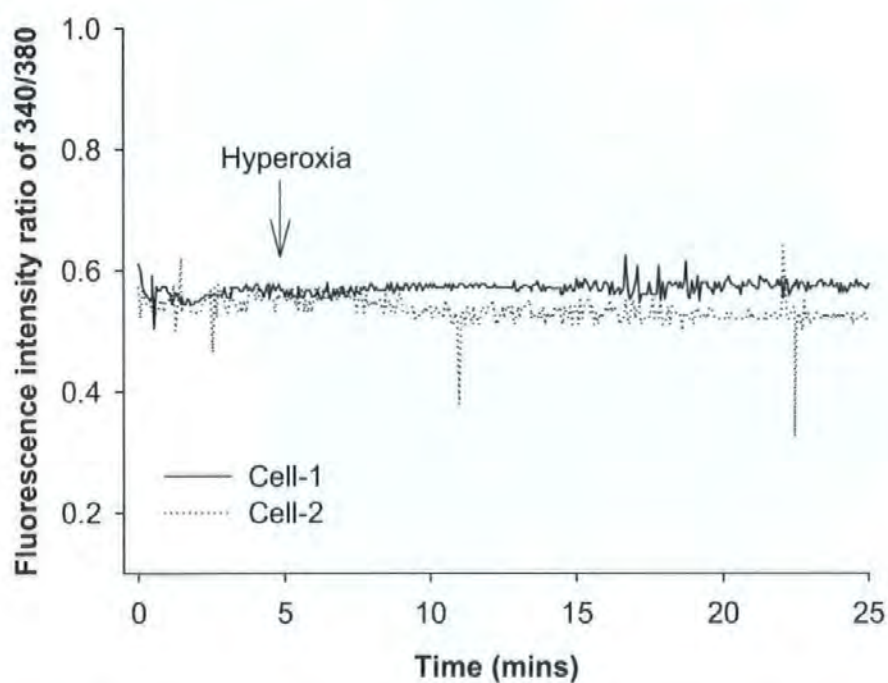


Fig 5. 7 Ratio of fluorescence intensity at 340nm to 380nm of HBO-treated HUVEC perfusion with hyperoxia solution (HBSS gassed with 95% O<sub>2</sub> + 5% CO<sub>2</sub>).

### 5.4.2. Oxygen Effects on $[Ca^{2+}]_i$ in Population of HUVECs

In addition to recording the real-time  $[Ca^{2+}]_i$  changes of single HUVEC with or without HBO treatment to different concentration of oxygen perfusates, we also investigated the  $[Ca^{2+}]_i$  response in population of cells to different concentration of oxygen.

#### 5.4.2.1 Oxygen Effects on Intracellular Calcium of HUVECs

The cells were allowed to rest in a microplate for 1 hour to attach to the microplate and achieving a stable reading of  $[Ca^{2+}]_i$  prior to treatments.  $[Ca^{2+}]_i$  measurements were taken at 30 min and 0 min before treatment, and the fluorescent intensity ratio remained stable and there was no difference between treatment groups. The per-treatment level of average ratio ranged of 0.30 ~ 0.32 as shown in Fig 5.8.

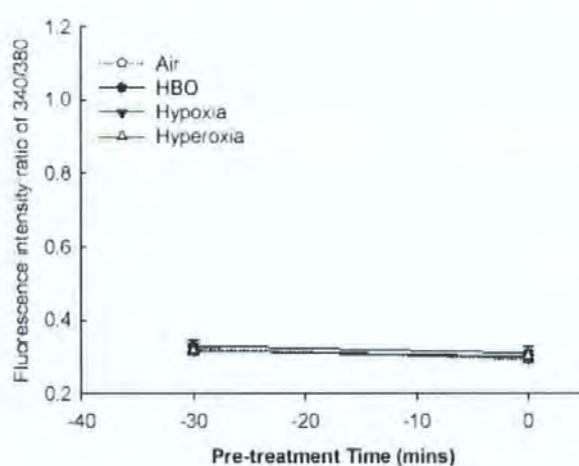


**Fig 5. 8** Fluorescence intensity ratio at 340nm/380nm of population of HUVECs at 30 min and 0 min prior to treatments. Data were presented as means  $\pm$  SEM of at least 8 replicates. Recordings are from populations of cells made on a plate reader.

Once a stable pre-treatment  $[Ca^{2+}]_i$  level had reached, the plates were exposed to control Air, Hypoxia, Hyperoxia or HBO treatment for 90 min at 37 °C as described. Interestingly, all the four kinds of exposures increased the fluorescence intensity ratio significantly in the population of HUVECs, and the ratio remained at relatively higher levels for up to 60 min post-treatment. However, the  $[Ca^{2+}]_i$  of HUVECs showed a slightly different response to each treatment. Exposure of HUVECs to the control Air (95% air +

5% CO<sub>2</sub>) increased the ratio value to  $0.58 \pm 0.06$  (n = 7) at immediate post exposure, which showed a slight shift during 60 min incubation and gave a value of  $0.51 \pm 0.03$  (n = 9) at the end of incubation (Fig 5.9). When population of HUVECs exposed to hypoxic environment (95% N<sub>2</sub> + 5% CO<sub>2</sub>), a higher fluorescence intensity ratio was shown than that of Air exposure. The immediate post-treatment level was  $0.68 \pm 0.06$  (n = 9), which decreased slowly throughout 60 min incubation to  $0.63 \pm 0.04$  (n = 8) (Fig 5.9A). Although the ratio level in the hypoxic group was kept higher than that of air group, there was no significant differences seen (P = 0.23, One-way ANOVA). The fluorescence intensity ratio increases of HUVECs during high concentration of oxygen were bigger than either control air or hypoxic exposure. The normobaric 95% O<sub>2</sub> + 5% CO<sub>2</sub> exposure increased the ratio to  $0.74 \pm 0.07$  (n = 8), which is 27% higher than that of Air group (P = 0.11, unpaired t-test). The ratio in hyperoxic group decreased relatively quickly especially in the last 20 min of observed incubation time and it was  $0.61 \pm 0.05$  (n = 7) at the end of incubation (Fig 5.9B). Although a total P = 0.02 (One-way ANOVA) was shown when comparing the value of hyperoxia groups to air groups, there was no significant difference was found at each corresponding time-points. HBO treatment presented the highest level of fluorescence intensity ratio among the four treatments (Fig 5.9C). At immediate post-treatment, the ratio was  $0.75 \pm 0.05$  (n = 8), which is similar to that of hyperoxia group, but 29% higher than that of Air group (P = 0.04, unpaired t-test). Unlike hyperoxia group, the ratio decreased very slowly and a nearly even line was observed during 60 min incubation and was  $0.69 \pm 0.06$  (n = 7) at the end of the incubation. This change was similar to that observed in hypoxia group. The ratio in the HBO group remained significant higher than that of control air group and a P < 0.05 (unpaired t-test) was seen at each corresponding time-points. However, there was no statistic difference shown between hypoxia, hyperoxia or HBO treatments, nor within each group of the post-treatment changes.

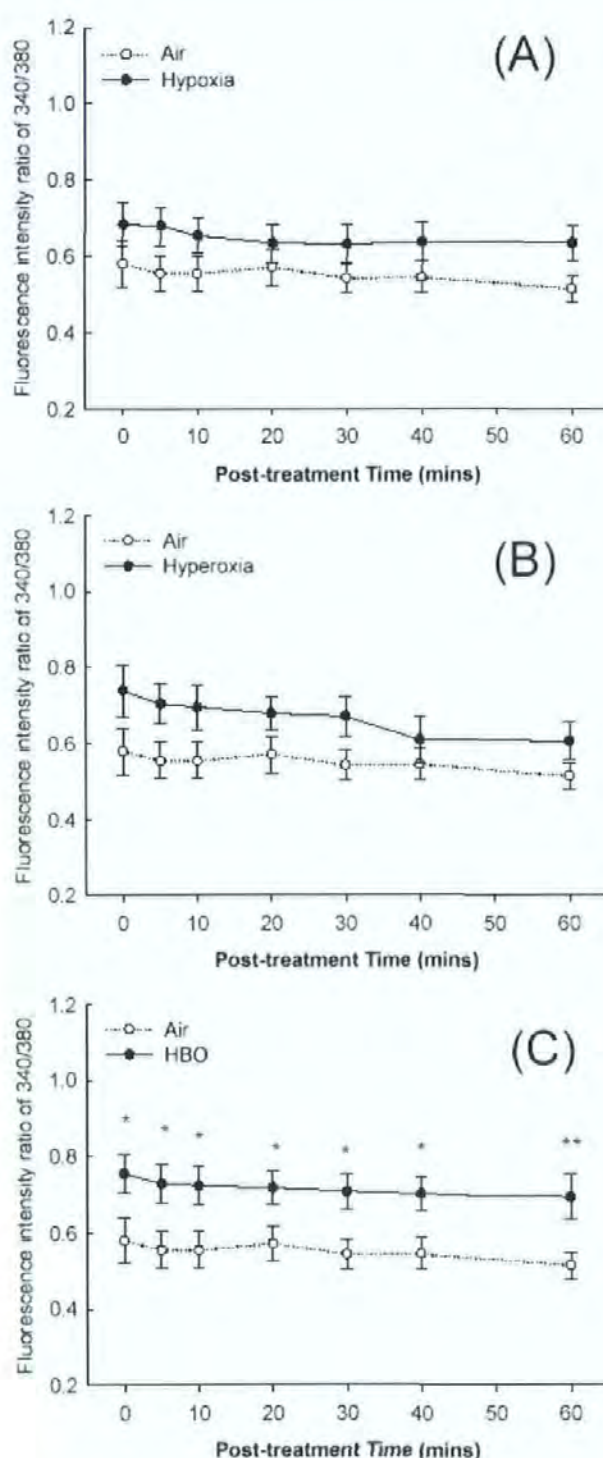
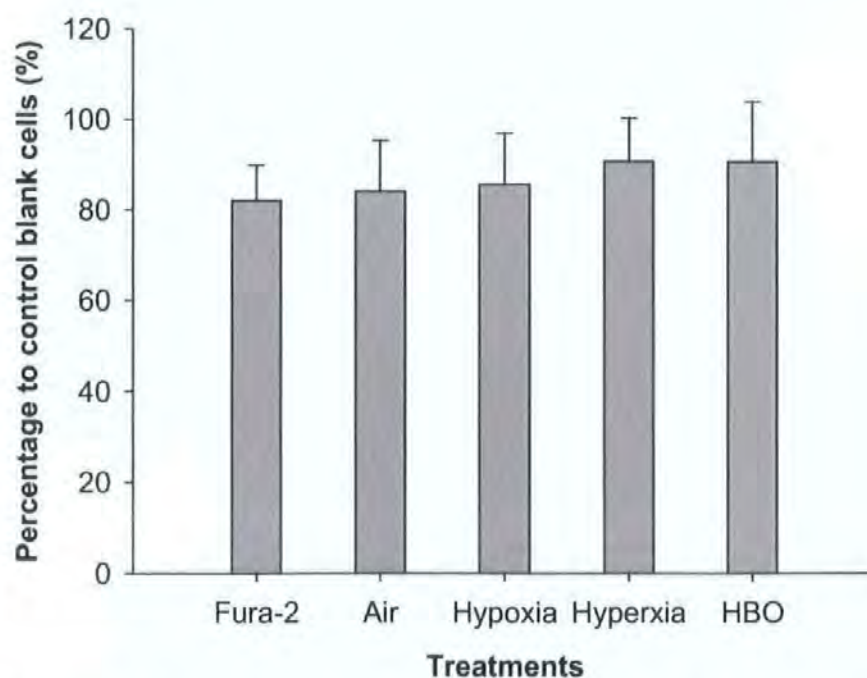


Fig 5. 9 Changes of fluorescence intensity ratio at 340nm to 380nm of HUVECs during 60 min post treatment. HUVECs were exposed to normobaric 95% air + 5% CO<sub>2</sub> (Air) as control, normobaric 95% N<sub>2</sub> + 5% CO<sub>2</sub> (Hypoxia) in (A), normobaric 95% O<sub>2</sub> + 5% CO<sub>2</sub> (Hyperoxia) in (B) and 100% O<sub>2</sub> at 2.2 ATA (HBO) in (C) for 90 min at 37 °C. Intracellular calcium measurement were performed at immediate, 5min, 10min, 20min, 30min, 40min and 60min post treatments. Data were presented as means ± SEM of at least 7 replicates. And \* P < 0.05, \*\* P < 0.01 (unpaired t-test) when compared with control level in Air treatment group.

#### 5.4.2.2 Cell Viability in Different Oxygen Treatments

In order to find out if calcium disturbances induced more cell damage, the neutral red assay was performed (healthy cells uptake more neutral red dye than damaged cells). HUVECs loading with Fura-2 AM showed a slight less neutral red uptake as  $82 \pm 8\%$  ( $n = 5$ ) than that of blank control cells without Fura-2. None of the treatments affect the neutral red uptake percentage when measured at the end of each experiment, which presented as  $84 \pm 11\%$  ( $n = 5$ ),  $87 \pm 11\%$  ( $n = 5$ ),  $91 \pm 10\%$  ( $n = 7$ ), and  $91 \pm 13\%$  ( $n = 5$ ) to that of blank control cells in air, hypoxic, hyperoxic and HBO-treated group respectively (Fig 5.10). There were neither statistical differences between the four groups ( $P = 0.97$ , One-way ANOVA), nor with the blank control group ( $P = 0.84$ , One-way ANOVA).



**Fig 5. 10** Relative absorbance intensity of treated HUVECs to blank healthy control cells in neutral red intake ability. Blank control cells were healthy HUVECs without Fura-2 loading and showed above 99% viability as counted with Eosin Y stain, and their neutral red absorbance intensity at 540 nm was  $7.5 \pm 1.0$  per  $10^5$  cells (means  $\pm$  SEM,  $n = 6$ ). Fura-2 represents cells loaded with Fura-2 before any treatment. Air, Hypoxia, Hyperoxia and HBO represent cells loaded with Fura-2 and exposed to 95% air + 5%  $\text{CO}_2$  (control Air), 95%  $\text{N}_2$  + 5%  $\text{CO}_2$  (Hypoxia), 95%  $\text{O}_2$  + 5%  $\text{CO}_2$  (Hyperoxia) and 100%  $\text{O}_2$  at 2.2 ATA (HBO) for 90 min at 37 °C respectively, and then incubated for a further 60 min in air. The reading for the later four groups was at the end of 60 min incubation. Data were expressed as means  $\pm$  SEM of more than 5 replicates. One-way ANOVA test was performed for group difference.

### 5.4.2.3 $[Ca^{2+}]_i$ Calculation from Fluorescence Intensity Ratio of 340 to 380 nm

Calculation of fluorescence intensity ratio to  $[Ca^{2+}]_i$  was performed with the plate reader measurement. A standard curve of  $[Ca^{2+}]_i$  to fluorescence intensity ratio of Fura-2 was obtained and showed as Fig 5.11. At very low concentration between 8.4 to 22.3 nM, the fluorescence intensity ratio increased slightly from  $0.17 \pm 0.005$  to  $0.23 \pm 0.002$ . When raising  $[Ca^{2+}]_i$  higher than 22.3 nM, there was a nearly linear sharp increase as the corresponding ratio was  $0.49 \pm 0.03$  at 50.2 nM and  $1.22 \pm 0.05$  at 134 nM. Our  $[Ca^{2+}]_i$  measurement of HUVECs were in the range between 35 nM and 85 nM, which corresponding to ratio of 0.30 and 0.80 respectively. Once the  $[Ca^{2+}]_i$  raised up to  $\mu M$  level, the fluorescence intensity ratio stop increasing and became a stable line. At  $8.16 \mu M$  of  $[Ca^{2+}]_i$ , the ratio was  $2.16 \pm 0.01$ , while increase  $[Ca^{2+}]_i$  to  $400 \mu M$ , the ratio only increased to  $2.42 \pm 0.01$ .

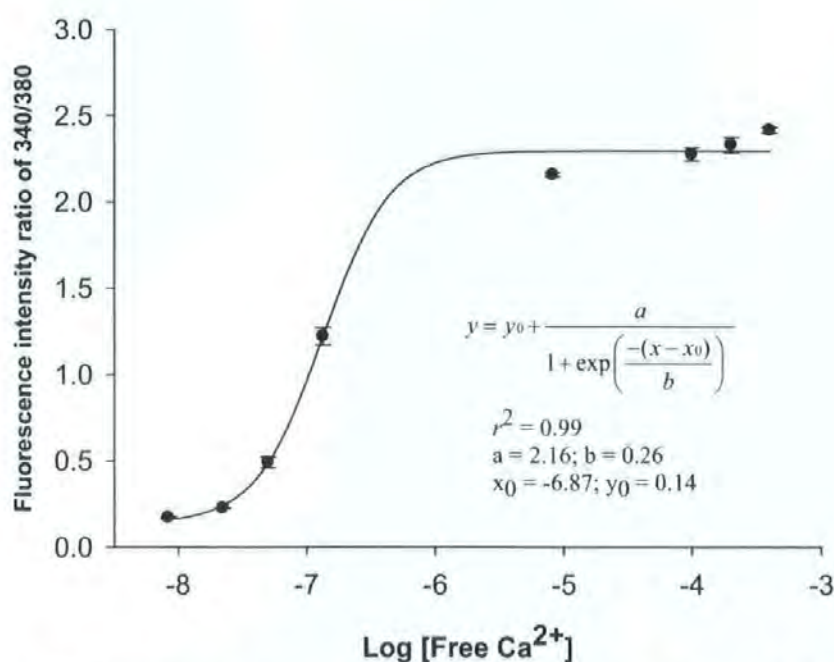


Fig 5. 11  $[Ca^{2+}]_i$  calibrations from fluorescence intensity ratio of 340 to 380 nm with Fura-2 AM loading. Graded concentration of free calcium solution was made from Ca-EGTA buffer at pH 7.4. The data was means  $\pm$  SEM of five replicates at each concentration, and nonlinear regression equation of Sigmoid was used with Sigmaplot 10.0, and  $r^2 = 0.99$ .

## 5.5 Discussion

Using a Cairn microspectrofluorimeter, we have successfully recorded the real-time  $[Ca^{2+}]_i$  changes of single cultured HUVEC during different oxygen concentration perfusion. The non-HBO treated cell presented a stable fluorescence intensity ratio (340 to 380 nm) during control solution perfusion, and switching to hypoxic or hyperoxic solution showed no effects on the ratio. The HBO-treated cell showed a higher initial fluorescence intensity ratio, but the variable ratio decrease during perfusion covered the possible effects to be observed when perfusion with different solutions. However, when population of HUVECs were exposed to hypoxic, hyperoxic and HBO conditions for 90 min, the HBO treated cells showed significant higher level of  $[Ca^{2+}]_i$  than that of control air treated cells, and this effect lasted for 60 min post-treatment under observation. There was no evidence shown that oxygen treatment affect cell viability as confirmed by neutral red cell retention assay. And finally, a standard curve of fluorescence intensity ratio of 340 to 380 nm versus a serial concentration of free calcium was set up, which allows us to calculate the actual corresponding intracellular calcium concentration.

The resting basal  $[Ca^{2+}]_i$  in our study was at about 40 nM. In previous studies, the basal intracellular free calcium concentrations ( $[Ca^{2+}]_i$ ) of endothelial cells varies with the precise origin of the cells and cell cycles, and a range of  $[Ca^{2+}]_i$  of 30 – 100 nM in cultured HUVECs have been reported (Dolor et al., 1992; Arnould et al., 1992; Berna et al., 2002). Our measurement is right in the range of previous studies, which confirms that the calcium measurements were successful. Exposure cells to hypoxia for 90 min,  $[Ca^{2+}]_i$  increased two fold of the pre-treatment and showed an increasing trend when comparing to air-exposed cells in our study. In previous studies, the amplitude and the spatio-temporal patterns of hypoxia-induced  $[Ca^{2+}]_i$  varied. Arnould et al (1992) reported that during the first 30 min

of hypoxic incubation of HUVECs,  $[Ca^{2+}]_i$  only showed a very slightly increase, and between 30 min and 120 min, the increase was constant and more pronounced, leading to a concentration of around 230 nM after 120 min which represented ten fold the concentration of control cells whilst still had 80% viability. The same research groups reported a four fold of  $[Ca^{2+}]_i$  increase (220 nM) after 120 min of hypoxia incubation (Berna et al., 2002). Using simultaneous hypoxic and  $Ca^{2+}$ -free perfusion to indicating  $Ca^{2+}$  release from an intracellular pool, Aley et al (2005) showed a small but discernible, transient rise of  $[Ca^{2+}]_i$  (about 30 - 40 nM) in 85% of measured human saphenous vein endothelial cells. The  $[Ca^{2+}]_i$  recording were from intact monolayers of endothelial cells in these hypoxia experiments, and were grown to confluence on glass coverslips. Due to the requirement of simultaneous perfusion, the specific design of our experimental system made it incompatible to put an extra glass coverslip on the microscope stage in our lab, therefore we are unable to perform calcium measurement from monolayer of cells grown on glass coverslips. Instead, we used cell suspension in our single and population of cells study. Although there was one report of unsatisfactory  $[Ca^{2+}]_i$  measurement in suspensions of endothelial cells (Wickham et al., 1988), considerable studies have been using suspensions of endothelial cells to examine  $[Ca^{2+}]_i$  response to variety of stimulus such as thrombin, calcium, ET-1 and etc (Jaffe et al., 1987; Nakayama and Matsuda, 2003; Jacques et al., 2005; Hadri et al., 2006). In our present study, hypoxia showed an increasing trend of  $[Ca^{2+}]_i$  when population of ECs were used, and no effect was observed with single cell recording. Similar results were found when exposing HUVECs to hyperoxia condition (95% oxygen). The reasons for the difference between single cell and the cell population in microplates are unclear, but perfusate flow rate and adhesion of the cell to the bath, the UV light intensity, and temperature control are factors that may contribute to the different results.

Although studies have shown that oxygen is able to regulate  $[Ca^{2+}]_i$  levels in endothelial cells, but the signalling pathway is not clear yet. Aley et al (2005) indicated local  $O_2$  tension is a major determinant of  $Ca^{2+}$  signalling in the vascular endothelium because hypoxia regulates intracellular  $Ca^{2+}$  signalling via two distinct pathways. Firstly, it modulates agonist-evoked  $Ca^{2+}$  liberation from ER primarily through regulation of ROS generation from NADPH oxidase. Secondly, hypoxia liberates  $Ca^{2+}$  from ER via ryanodine receptors, an effect requiring mitochondrial ROS generation. Consistently, Peers et al (2006) showed that hypoxia evoked liberation of  $Ca^{2+}$  from the ER via activation of the  $IP_3$  receptor and involves ROS generation from mitochondria because pre-treatment of endothelial cells with thapsigargin (an inhibitor for  $Ca^{2+}$ -ATPase of ER),  $IP_3$ -generating agonists, or antioxidants, abolished hypoxia-induced  $[Ca^{2+}]_i$  increase. Study on hyperoxia also pointed the involvement of ROS in calcium regulation. Brueckl et al (2006) found continuously yet reversibly increase ROS formation and  $[Ca^{2+}]_i$  when cells were exposed to 70% oxygen, which were blocked by the mitochondrial complex I inhibitor rotenone (inhibitors of NAD(P)H oxidase); and BAPTA (intracellular  $Ca^{2+}$  chelator) predominantly attenuated the late phase of the ROS increase after > 30 min. Thus, they implied that hyperoxia induces ROS formation in lung capillary ECs, which initially originates from the mitochondrial electron transport chain but subsequently involves activation of NAD(P)H oxidase by endothelial  $[Ca^{2+}]_i$  signalling. Therefore, it seems that the cross-talk between  $Ca^{2+}$  and ROS in either hypoxia or hyperoxia finely tunes the homeostasis and integrates functionality in different types of cells. On one side, calcium homeostasis components are modified by ROS (e.g. thiol oxidants increase the activity of  $IP_3$ ) (Bootman et al., 1992; Bultynck et al., 2004) and ryanodine receptors (Feng et al., 2000). The presence of sulfhydryl groups in these receptor channels enables them to respond to low levels of oxidants far below those achieved during pathological states or in extreme experimental

conditions (Camello-Almaraz et al., 2006). And on the other side, ROS participates in normal  $\text{Ca}^{2+}$  signalling as the blockade or scavenging of ROS can modify the  $\text{Ca}^{2+}$  signal (Hu et al., 2002; Xi et al., 2005; Camello-Almaraz et al., 2006). And functionally, the effect of oxidants on calcium signalling can vary from stimulating to repressive, depending on the type of oxidants, their concentrations, and the duration of exposure (Ermak and Davies, 2002).

In our study, significant increase of  $[\text{Ca}^{2+}]_i$  was observed in HBO-treated cells, and this increase last up to 60 min post-treatment. There were only two studies so far that investigated the HBO effects on  $[\text{Ca}^{2+}]_i$ . Wang et al (1998) found that after HBO exposure at 5 ATA, the  $[\text{Ca}^{2+}]_i$  increased two fold in rat hippocampus, and pre-treated with daurisoline (a putative P-type calcium channel blocker) reduced  $[\text{Ca}^{2+}]_i$  by 56 % as well as delayed the appearance of CNS oxygen toxicity and increased the survival rate. Liu et al (1999) measured  $[\text{Ca}^{2+}]_i$  changes of co-cultured endothelial cells (EC) and smooth muscle cells (SMC) in a specially designed miniature oxygen chamber. Under 1.0 MPa (1.0 ATA) of HBO treatment,  $[\text{Ca}^{2+}]_i$  kept stable for the first 3 min then declined; whilst under 2.0 ATA and 3.0 ATA,  $[\text{Ca}^{2+}]_i$  increased during the first 3 min and then declined; under 4.0 ATA,  $[\text{Ca}^{2+}]_i$  increased during the first 2 min and then declined, some cells showed membrane rupture. In Liu's experiment, HBO treatment lasted for 10 min and the required pressure were achieved in 1 min, which may cause great changes of cell properties, and then influence the  $[\text{Ca}^{2+}]_i$  measurement. In our study, cells were treated with HBO at 2.2 ATA for 90 min, slow pressure increases and decreases were selected to avoid manipulating the cells abruptly. Simultaneously, single cell recording and neutral red retention test have confirmed that HBO treatment did not affect the cell integrity or viability. Although studies all showed that HBO treatment induce  $[\text{Ca}^{2+}]_i$  increase, it is still not clear what causes this changes and what signalling pathway is involved. Considering

our results, the mechanical stress such as pressure during HBO may contribute to the  $[Ca^{2+}]_i$  increase as hyperoxia treatment did not show the same effect as HBO treatment. Coincidentally, Matsuo and Matsuo (1996) found that transient elevations or oscillations of the intracellular calcium concentration in response to the elevation of hydraulic pressure to 20-30 mm Hg. In addition, Sato et al (2006) presented up-regulated of  $Ca^{2+}$  regulatory proteins RyR and  $Ca^{2+}$ -ATPase and their genes expression in cardiac myocytes subjected to a high ambient pressure (200 mm Hg higher than normobaric pressure). On the other hand, due to the nature of generating ROS in HBO, it is still possible that ROS signalling may responsible for the  $[Ca^{2+}]_i$  increase. At present study, we conducted the preliminary investigation of  $[Ca^{2+}]_i$  changes in HBO treatment. The ability of HBO treatment to increase  $[Ca^{2+}]_i$  of HUVECs without damaging the cells imply that calcium may serve as an oxygen sensor or a second messenger in HBO-induced cell events. Moreover, mechanical stress such as pressure may be responsible for this induction. But due to the complex regulatory system on calcium and limited information from previous HBO research, further examination will be needed to investigate the calcium signalling pathway, as well as to distinguish the oxygen effect from mechanical stress effect (e.g. pressure, pH) during HBO treatment, which we believe will make a great contribution towards the understanding of the beneficial effects of HBO treatment.

## **Chapter 6**

# **Hyperbaric Oxygen Treatment Protects Endothelial Cells against H<sub>2</sub>O<sub>2</sub> - induced DNA Damage**

### **6.1 Abstract**

Hyperbaric oxygen (HBO) therapy has been reported to regulate and improve endothelial cell functions. However, studies have demonstrated that HBO exposure induces oxidative DNA damage in human lymphocytes, and the involvement of antioxidant defense system during this process varies from studies. In this chapter, we investigate the potential DNA-damaging effects of HBO treatment and further oxidative stress stimulation on human endothelial cells using comet assay for the first time. Meanwhile, changes of intracellular glutathione pool were examined to demonstrate the involvement of this important antioxidant scavenger. The results suggest that a single HBO exposure under therapeutic condition causes small but significant DNA migration extent change, and this change is totally repairable in HUVECs. In addition, HBO treatment protects the cells against H<sub>2</sub>O<sub>2</sub>-induced DNA damage, and the increase in antioxidant capacity as reflected in an increase in redox status of glutathione pool may be relevant to this protective response.

## 6.2 Introduction

There are over 74,000 damage incidences occur in DNA per cell per day, mostly by oxidation, hydrolysis, alkylation, radiation or toxic chemicals that directly damage one of the 3 billion bases contained in DNA or create breaks in the phosphodiester backbone that the bases sit on (Lodish et al., 2004). The common types of DNA damages include: (1) Base modifications by methylation, oxidation; (2) Mispairs: mistakes in DNA synthesis; (3) Cross-linked nucleotides: intrastrand, interstrand covalent links; (4) single-stranded or double-stranded DNA breaks; (5) pyrimidine intrastrand dimer (cyclobutane); and (6) hydrolysis: de-amination of base (Watson et al., 2004). To protect the genetic integrity, cells have developed efficient mechanisms to repair DNA damage: DNA repair enzymes; and multiple processes such as base- and nucleotide-excision pathways exist that continuously monitor chromosomes to correct and repair the wide range of DNA damage (Friedberg et al., 2006). If the damage in a cell is too severe, the cell will be eliminated via committing programmed cell death (apoptosis, Friedberg et al., 2006).

Oxidative DNA damage, caused by reactive oxidative species (ROS) attack, is the most frequent type encountered by aerobic cells. Oxidative DNA damage can produce a multiple modifications in DNA including base and sugar lesions, single or double strand breaks, alkali labile sites, and various species of oxidized purines and pyrimidines (Joenje, 1989). Notably, oxidative DNA damage can be eliminated or repaired accurately and efficiently by strand break rejoining and base excision repair. But if left unrepaired, oxidative DNA damage can lead to detrimental biological consequence including cell death, mutations and transformation of cells to malignant cells, which is believed largely contributed to cancer and aging (Feig et al., 1994; Wilson and Bohr, 2006).

In 1984, Swedish scientists Östling and Johanson first introduced a microgel electrophoresis technique for direct visualization of DNA damage in individual cells, which is later called “the single gel assay (SCG) or comet assay”. In 1988, Singh and co-workers modified an alkaline comet assay based on its initial version of neutral lysis and electrophoresis conditions, which increased the sensitivity and broadened the applicability of comet assay. The advantages of comet assay include: (1) the sensitivity for detecting low levels of DNA damage; (2) the requirement for small numbers of cells per samples; (3) flexibility; (4) low costs; (5) ease of application; and (6) the relatively short time period (a few days) needed to complete an experiment (Tice et al., 2000).

In comet assay, the cells were embedded in a thin agarose gel on a microscope slide and lysed by non-ionic detergents and high salts to deplete all cell protein, and the remaining nucleoid DNA were characterised of intact, negatively supercoiled and circular. DNA nucleoids were subsequently allowed unwinding under either alkaline or neutral conditions. Following unwinding the DNA is electrophoresed which was like that the electric current simply pulled the DNA halo to one side in electrophoretic field. After staining with fluorescent DNA binding dye, a cell under a microscope displayed the appearance of a comet, with a head (the nuclear region) and a tail containing DNA fragments or strands migrating in the direction of the anode. The extent of DNA liberated from the head of the comet was directly proportional to the DNA damage (Collins, 2004). And the relative tail intensity, presented the relative fluorescence intensity of head and tail, normally expressed as a percentage of DNA in tail (% DNA in tail), is a common way to evaluate and quantify DNA damage by image analysis. This parameter is relatively unaffected by threshold settings, and also allows discrimination of damage over the widest possible range (in theory, from 0 to 100% DNA in tail). In addition, it bears a linear relationship to DNA break frequency up to about 80 % in tail, as well as gives a very clear

indication of what the comets actually looked like (Collins, 2004). Nowadays, with the help of lesion-specific enzymes that digest a particular recognised kind of damage, it is possible to convert the enzyme sensitive sites to additional DNA breaks which increase tail intensity in comet assay. The endonuclease III detects oxidized pyrimidines (Collin et al., 1993); formamidopyrimidine DNA glycosylase (FPG) detects the major purine oxidation product 8-oxoguanine as well as other altered purines (Collin et al., 1996). The endonuclease III or FPG treatment has made comet assay more specific and sensitive to measure oxidative DNA damage.

Comet assay has been widely used for studies on genotoxic agents, ecological monitoring, DNA repair (Collins, 2004). Using comet assay, HBO treatment has shown to induce DNA damage in whole blood samples, human lymphocytes and V79 Chinese hamster cells (Dennog et al., 1996; Speit et al., 1998 and 2000; Eken et al., 2005).

Although HBO therapy has been used successfully as a conjunctive treatment to patients suffering severe hypoxia or inflammatory problems, exposure to high concentration of oxygen always raise an issue of producing more ROS, which may cause oxidative stress and damage cell or tissue (Jamieson et al., 1986). In mammalian cells, the existing antioxidant defence system is always ready to protect cell and tissue from free radicals' attack. But under certain circumstance, ROS level may overcome the antioxidant defence, which consequently cause cell oxidative damage. There is evidence that HBO treatment can induce oxidative damage in cells. Both *in vivo* and *in vitro* studies have demonstrated that a single HBO exposure (2.5 ATA, 3 × 20 min) induces clear and reproducible DNA strand breaks of lymphocytes from healthy volunteers, and these breaks are due to the oxidative base damages (Dennog et al., 1996; Speit et al., 1998 and 2000). And they also indicated that HBO- induced lymphocyte DNA damage was reversible as DNA damage was not found 24 h after 1<sup>st</sup> HBO treatment and the following HBO

treatments; an increase of antioxidant defence in HBO-treated cells may contribute to these protective effects. Eken et al (2005) found similar changes in lymphocytes samples isolated from patients with hypoxia-related problems; however, they also observed a persistent DNA damage effect even after the 10<sup>th</sup> and 20<sup>th</sup> HBO treatment (2.5 ATA of 3 × 20 min for each treatment). It is suggested that HBO treatment affects antioxidant defence system; the response of antioxidants enzymes and scavengers to HBO treatments really varies between studies. Ozden et al (2004) addressed that HBO treatment benefit the redox state by increasing SOD activity, GSH and Zn levels; and Kudchodkar et al (2006) demonstrated the increased levels of GSH, glutathione reductase (GR), Se-dependent glutathione peroxidase (GPx) and catalase in chronic HBO treatment. But other studies showed no changes or even decreased activity in some antioxidant enzyme after HBO exposure (Muth et al., 2004; Eken et al., 2005). Till now, whole blood or lymphocytes have been used in most HBO studies and other cell types have rarely been investigated. Lymphocytes are a part of white blood cell and work together with other types of white blood cells to build the natural defence system in human. They are supposed to be more resistant to oxidative stress than any other types of cells because of their congenital properties. Therefore, it is vital to investigate how other types of human cells conflict with HBO treatment. Endothelial cells comprise the innermost surface of blood vessels, and are exposed to various sources of stress. HBO therapy has been documented for benefiting some patients with chronic wounds by improving endothelial cell functions and angiogenesis in the wound site (Sheikh et al., 2000). In this chapter, we aim to study the effects of a single HBO treatment on DNA damage in human endothelial cells, which have not been investigated before. Cultured human umbilical vein cells (HUVECs) were used in our study because it enabled precise control of the experimental conditions and provided the opportunity to manipulation the media for other factors. The experimental approach

included positive controls to explore the sensitivity of comet assay to detect DNA damage of HUVECs induced by hydrogen peroxide ( $H_2O_2$ ), which has been a frequently used reference toxicant to assess DNA damage in many cell types (Aruoma et al., 1989). The DNA migration of cell comet images to HBO treatment were then detected immediately, and 24 h after HBO treatment to observe the DNA damage level and repairable capability. Meanwhile, immediate and 24h post HBO-treated cells were further exposed to  $H_2O_2$  to investigate the potential effect of HBO treatment on oxidants-induced DNA damage. Along with all the DNA damage measurement, we also looked at the changes of glutathione pool in these cells to investigate the involvement of these important antioxidant proteins. Glutathione (GSH) is among the most important antioxidant in cells, being used in enzymatic reactions to eliminate peroxides and in nonenzymatic reactions to maintain ascorbate and  $\alpha$ -tocopherol in their reduced and functional forms. In these reactions, GSH is oxidized to its disulfide form, GSSG. The balance of glutathione pool (GSH to GSSG) provides a dynamic indicator of oxidative stress as well as redox signaling and control (Johes, 2002). Thus, both GSH and GSSG levels of HUVECs were measured in our study, and the ratio of GSH to GSSG was calculated.

## **6.3 Material and Methods**

### **6.3.1. Cell Culture**

HUVECs were cultivated in 3 ml of complete Ham's solution (refer back to 5.3.2 where the culture is described) in Nunclon Delta SI 6-well tissue culture plates (Nunc, InterMed, Denmark) and maintained in a humidified incubator at 37 °C (5%  $CO_2$  + 95% air). The cells were used when reaching 80 - 90% confluences in the 2nd to 5th passage.

### 6.3.2. Response of HUVECs to H<sub>2</sub>O<sub>2</sub> Treatment

Cells were exposed to a serial concentration of H<sub>2</sub>O<sub>2</sub> in order to find out the sensitivity of HUVECs to oxidative stress. Briefly, cells were harvested with 0.25% trypsin and resuspended with complete Ham's solution to obtain final concentration of  $2 - 5 \times 10^4$  cells ml<sup>-1</sup>. The cell viability was checked by Eosin Y stain as over 98% cells were alive. H<sub>2</sub>O<sub>2</sub> were then added to 1 ml of cell suspension to obtain final H<sub>2</sub>O<sub>2</sub> concentrations ranging 0 - 0.5 mM. After incubated for 15 min at 37 °C, cells were centrifuged at 1,000 rpm for 5 min and washed twice with 0.3 ml of PBS. Comet assay was conducted, and four replicates experiments were performed for data analysis. H<sub>2</sub>O<sub>2</sub> induced a dose-dependent change in HUVECs' DNA migration pattern. And subsequently, two concentration of H<sub>2</sub>O<sub>2</sub> (0.1 and 0.2 mM, respectively) approximately at the start and end of the linear range of H<sub>2</sub>O<sub>2</sub>-induced DNA damage were selected and applied to investigate and compare the acute and potential influence of HBO treatment on H<sub>2</sub>O<sub>2</sub>-induced DNA response.

### 6.3.3. HBO Treatment and Subsequent H<sub>2</sub>O<sub>2</sub> Incubation

HBO exposure was performed in a hyperbaric chamber incubated at 37 °C. Intact HUVECs monolayers cultured in 6-well plates were exposed to 100% oxygen at 2.2 ATA (HBO) for 90 min, and cells from the same batch exposed to normobaric air (Air) were set as control. After exposures, cells were transferred to normal culture conditions for a further 24 h recovery. At immediate post exposures and 24h post recovery, cells were collected by gently trypsinization and resuspended in complete Ham's solution to obtain final concentration of  $2 - 5 \times 10^4$  cells ml<sup>-1</sup>.

For detection the HBO-induced DNA damages, one microliter of HBO-treated and Air-treated cell suspensions were examined by comet assay right away at immediate post and 24h post exposure. In order to explore the effects of HBO treatment on oxidative

stress-induced DNA damage, another one microliter of above cell suspensions were treated with 0.1 mM and 0.2 mM of H<sub>2</sub>O<sub>2</sub>, respectively, at 37 °C for 15 min, and then examined by comet assay as well. Prior to each comet assay examination, 50 µl of cell suspension was taken and stain with 5 µl of 2 mg ml<sup>-1</sup> stock Eosin Y solution, the total number of cells and the stained number of cells (dead cells) were counted with a hemocytometer to give a percentage of cell viability.

#### **6.3.4. Glutathione Pool Measurement**

Cells collected at the time points above were also analysed for total glutathione and oxidized glutathione content using the glutathione reductase (GR)-DTNB recycling assay described in 2.3.2. Briefly, cell suspension from above treatments was centrifuged at 1,000 rpm for 5 min, and cell pellet was quickly mixed with 250 µl of 3.5 % 5-sulfosalicylic acid to lysis cells. The acid-cell solution was aliquot into 100 µl each of two microcentrifuge tubes. To conjugate GSH, 2-vinylpyridine was added to one of the aliquots to a final concentration of 0.35 M and mixed vigorously (Vandeputte et al, 1994). All samples were stored at -20 °C until used for glutathione measurement.

For glutathione and protein content measurements, all the samples were thawed on ice and centrifuged at 10,000 rpm for 5 min at 4 °C. The protein-free supernant was collected for glutathione measurement. Briefly, 20 µl supernant was mixed with 20 µl of 10 mM 5,5'-dithiobis-(2-nitrobenzoic acid) (DTNB) each well of 96-well plate, followed by adding 280 µl of assay mixture consist of 0.17 U of glutathione reductase and 0.078 µmol NADPH solved in phosphate buffer (100 mM potassium phosphate, pH 7.5, containing 5 mM potassium EDTA). The change of the absorbance was read at 412 nm for 5 min at 1 min intervals using Kinetic function on plate reader. The absolute values of GSH were determined during each measurement with a standard curve created from 20 µl of standard

amount of GSH solution (0 to 10  $\mu$ M) in 3.5% 5-sulfosalicylic acid. The precipitated protein was measured using Bio-Rad protein assay with bovine album protein as standard.

### **6.3.5. Detecting HUVECs DNA Damage Using Alkaline Comet Assay**

#### **6.3.5.1. Chemicals and Solutions**

All the chemicals are purchased from Sigma-Aldrich (Poole, UK). Solutions to make before comet assay include:

- (1) LMP agarose: 0.1g low melting agarose is melt in 10 ml PBS solution.
- (2) HMP agarose: 0.1g high melting agarose is melt in 10 ml PBS solution.
- (3) Lysis solution contains 2.5 M NaCl, 0.1 M EDTA, 10 mM Tris, and 1% N-Lauroylsarcosine sodium salt, pH 10, and stored at 4 °C.
- (4) Electrophoresis solution contains 0.3M NaOH, 1mM EDTA, and pH >13.
- (5) Neutralising buffer contains 0.4M Tris, pH 7.5; and stored at 4 °C.

#### **6.3.5.2. Comet Assay Protocol**

The alkaline comet assay has been modified and optimised for endothelial cells and the general schematic flow is shown in Fig 6.1.

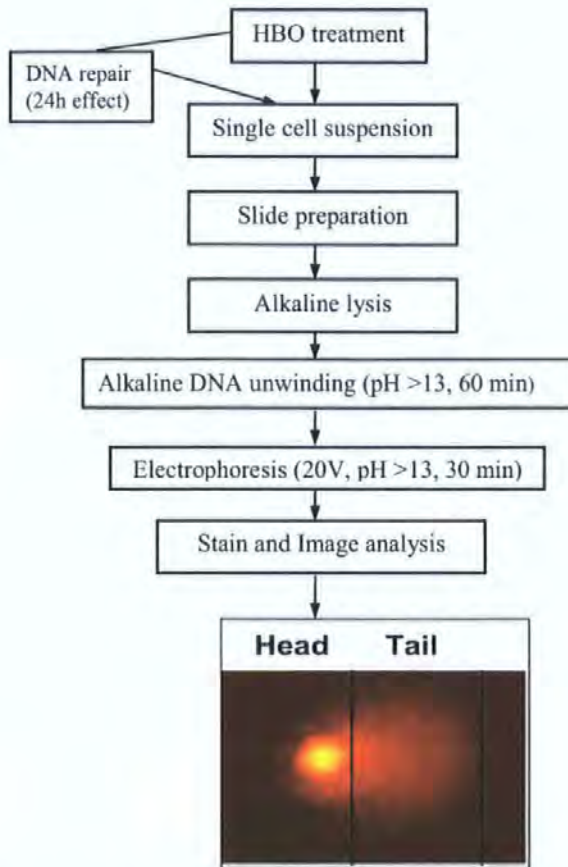


**Fig 6. 1** General schematic flow of the alkaline comet assay protocol for HUVECs.

One microlitre of cell suspension from 6.3.1 was centrifuged at 1,000rpm for 5 min, and the supernants was discarded. The cell pellet was mixed well with 180  $\mu$ l of LMP agarose. Two drops of 80  $\mu$ l cell-LMP agarose suspension were placed directly onto a HMP agarose pre-coated slide, and quickly covered each with an 18  $\times$ 18 mm coverslip. The slides were kept at 4  $^{\circ}$ C for 10 min to allow solidification of the agarose. Each slide was then lysed for 1 hr at 4  $^{\circ}$ C in lysis solution ( 2.5 M NaCl, 0.1M EDTA, 10 mM Trizma base, 1% N-Lauroylsarcosine, with 1% Triton X-100 and 10% DMSO added just prior to use). Next, the slides were placed in the electrophoresis solution for 40 min of alkali denaturation and followed by 30 min electrophoresis at 20 V using an electrophoresis compact power supply at 4 $^{\circ}$ C. The slides were neutralized by rinsing in neutralising buffer

(pH 7.5) for 20 min at 4°C. Finally, the slides were stained with ethidium bromide (20  $\mu\text{g ml}^{-1}$ ) for the visualisation. To score of comet DNA, pictures of 100 randomly selected cells per slide were captured at  $\times 400$  magnifications under fluorescence microscope and examined with Komet 5.0 image analysis software, which is able to automatically analyse % DNA in tail for each comet image.

### 6.3.6. Statistical Analysis

Four cohorts of cultured HUVECs were used to evaluate  $\text{H}_2\text{O}_2$  dose effect on DNA damage. 100 comet images were scored per slide for each concentration of  $\text{H}_2\text{O}_2$  (0 – 0.5 mM) and mean % DNA in the tail ( $\pm$  SD) were calculated from the respective values of the four replicates. The  $\text{EC}_{50}$  was calculated by applying curve fitting function (Equation: Sigmoidal, Logistic, 4 Parameter) of Sigmaplot 8.0 (Systat Software Inc). DNA damages of HUVECs were scored by % DNA in tail and expressed as means  $\pm$  SEM of replicates at immediate post Air or HBO treatment as well as 24 h post treatments. The content of cellular glutathione were presented as reduced glutathione (GSH  $\text{nmol mg}^{-1}$  protein), oxidatised glutathione (GSSG  $\text{nmol mg}^{-1}$  protein). And the glutathione ratio (% of GSH to GSSG) was calculated based on individual GSH and GSSG value. The means of % DNA in tail, GSH, GSSG and their ratio ( $\pm$  SEM of replicates) were analysed by One-way ANOVA test, then followed by Tukey-Kramer multiple comparisons test or unpaired t-test for comparisons of HBO or/and  $\text{H}_2\text{O}_2$  effects. Pearson's correlation tests were used to compute the correlation coefficient between DNA damage and glutathione (GSH, GSSG and their ratio) level. For all statistical analysis, a P value  $< 0.05$  was accepted as a statistically significant difference.

## 6.4 Results

### 6.4.1. HUVECs' Comet Images

As shown in Fig 6.2, the alkaline comet assay worked very well with cultured HUVECs. The images obtained under fluorescent microscope appeared in comet pattern with a bright fluorescent head and a less fluorescent tail. The extent of DNA migration in tail can be easily distinguished and scored by the Komet 5.0 software. Healthy HUVEC formed a well defined circle in the gel as no tail discriminated by human eye, while the computer program evaluated as less than 5% of DNA in tail. As more DNA breaks occurred, comet tail increased in length as well as fluorescent intensity and it became more easily viewed by human eye. When the tail DNA reached more than 90%, comet image showed an indistinct fluorescent head with a long and bright DNA tail.

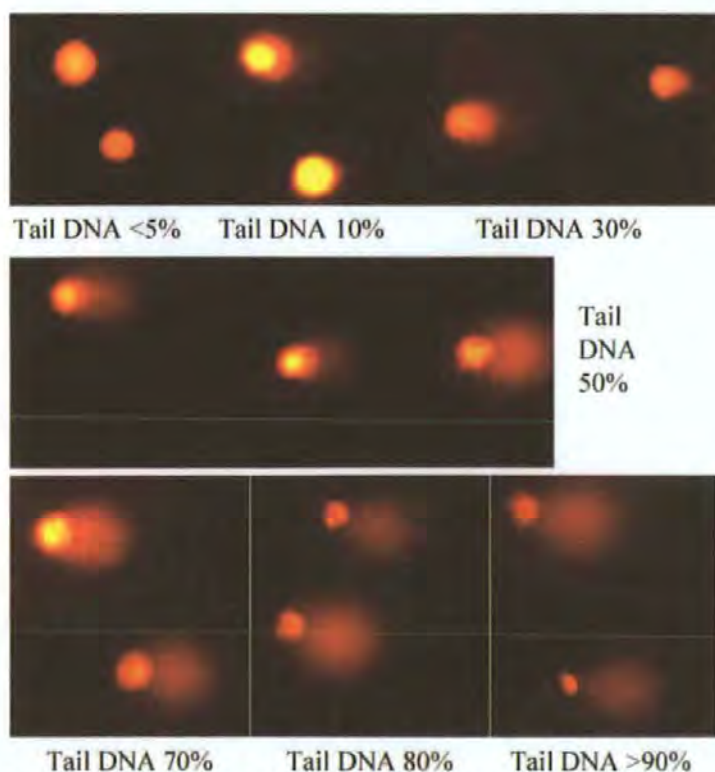


**Fig 6. 2** H<sub>2</sub>O<sub>2</sub>-induced DNA migration patterns of HUVECs. The comet images were scored as % DNA in tail by Komet 5.0 image analysis software. Pictures were taken under the Zeiss fluorescent microscope with the setting at 400 × magnification.

### 6.4.2. Response of HUVECs to Different Dose of H<sub>2</sub>O<sub>2</sub>

Expose HUVECs to exogenous H<sub>2</sub>O<sub>2</sub> induced a dose-dependent increase of DNA tail migration (Fig. 6.3 and Fig. 6.4). Although no visible DNA tail were viewed by eye in non H<sub>2</sub>O<sub>2</sub> treated control cells, computer scored the percentage of DNA in tail was  $4.26 \pm 0.42$  % (Means  $\pm$  SD, n = 5). Incubation the cells with 0.05 mM of H<sub>2</sub>O<sub>2</sub>, caused little effect of tail DNA migration as very few cell showed comet tail and only quantified as  $6.26 \pm 1.12$  % DNA in tail (Means  $\pm$  SD, n = 3). When increase concentration of H<sub>2</sub>O<sub>2</sub>, visible DNA fluorescent tail were seen more frequently. The curve of % DNA in tail showed a quickly rise as it ascended to  $15.84 \pm 6.44$  % (Means  $\pm$  SD, n = 5) at 0.1 mM of H<sub>2</sub>O<sub>2</sub> and an even steeper increase to  $46.23 \pm 6.72$  % (Means  $\pm$  SD, n = 5) when H<sub>2</sub>O<sub>2</sub> concentration reached 0.2 mM. Both of them showed statistical significances when compared with DNA migration level of control cells (P<0.05 and P<0.001 respectively). The increase of DNA migration slowed to a plateau at about  $78.65 \pm 6.11$ % (Means  $\pm$  SD, n = 4) when the concentration of H<sub>2</sub>O<sub>2</sub> reached 0.5 mM. Incubation the HUVECs at a higher concentration of H<sub>2</sub>O<sub>2</sub> (1 mM), the extent of DNA damage in comet was too great to permit an accurate measurement. By curve fitting calculation, the EC<sub>50</sub> for H<sub>2</sub>O<sub>2</sub> was estimated to be 0.19 mM. The concentrations between 0.05 mM to 0.2 mM of H<sub>2</sub>O<sub>2</sub> had significant effects on HUVECs DNA damage. The rapid increase of % DNA in tail between these concentrations were nearly lineal, which provided good working doses for investigating HUVECs' physiological response to oxidative stress and their radical scavenging capabilities.

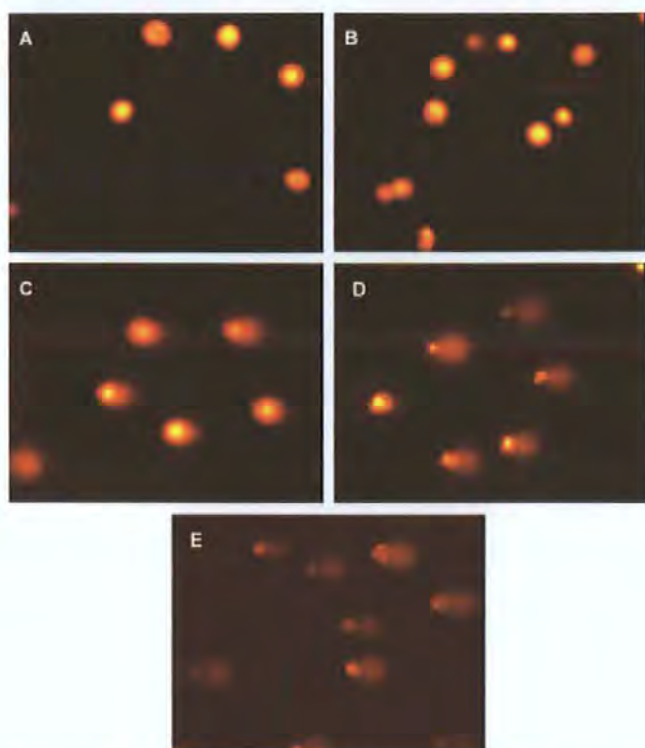


Fig 6. 3 Comet images of HUVECs response to different dose of  $\text{H}_2\text{O}_2$  as A: non- $\text{H}_2\text{O}_2$  treated control cells; B: 0.05 mM of  $\text{H}_2\text{O}_2$  ; C: 0.1 mM of  $\text{H}_2\text{O}_2$  ; D: 0.2 mM of  $\text{H}_2\text{O}_2$  ; and E: 0.5 mM of  $\text{H}_2\text{O}_2$  ; For a better field viewing, pictures were taken before scoring using Komet 5.0 software with 200 $\times$  magnification setting to fluorescent microscope.

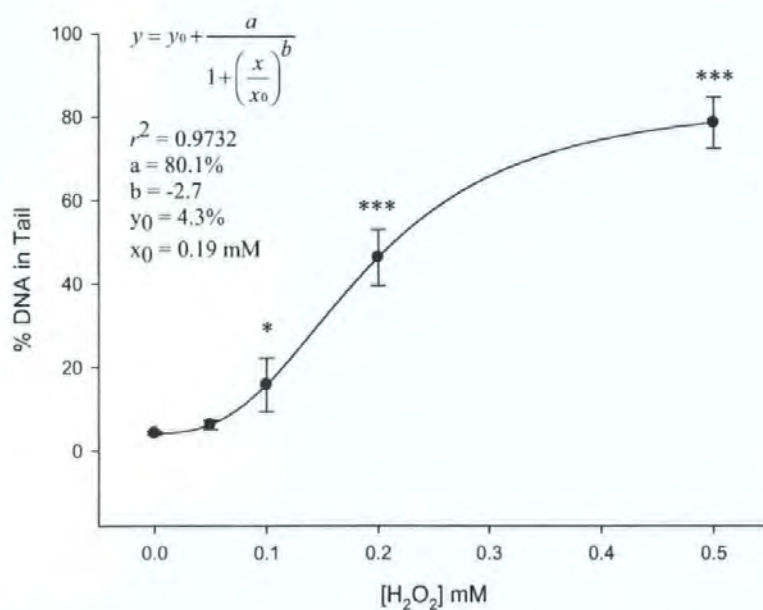


Fig 6. 4  $\text{H}_2\text{O}_2$ -dependent response in DNA of HUVECs. Each point represents the means ( $\pm$  SD) of more than 3 replicate experiments of graded concentration  $\text{H}_2\text{O}_2$ . One-way ANOVA test followed by Tukey-Kramer multiple comparisons test were used for statistic analysis. \* ( $P < 0.05$ ) and \*\*\* ( $P < 0.001$ ) indicate significantly different from control data at 0 mM  $\text{H}_2\text{O}_2$ . The curve was obtained with sigmoidal analysis with Sigmaplot 10.0;  $r^2$  was 0.97 and  $\text{EC}_{50}$  for  $\text{H}_2\text{O}_2$  was calculated to be 0.19 mM.

### 6.4.3. DNA Migrations of HUVECs to HBO Treatment and Subsequent H<sub>2</sub>O<sub>2</sub> Incubation

#### 6.4.3.1. Cell Viability

It is essential to check that satisfactory cell viability is achieved (sub-lethal not lethal effects), so there are many representative cells available for the comet assay. The cell viability was tested using Eosin Y stain method prior to each comet assay. All the samples had reached that above 95% of cell viability, and less than 5% differences were shown between matching experimental samples in our study as in Table 6.1.

Table 6. 1 The cell viability

Treatment \ Viability (%)	Air	HBO
Immediate post exposure	98.8 ± 0.6% (n = 9)	98.7 ± 1.0% (n = 10)
Post + 0.1 mM H <sub>2</sub> O <sub>2</sub>	99.5 ± 0.5% (n = 4)	98.6 ± 1.4% (n = 4)
Post + 0.2 mM H <sub>2</sub> O <sub>2</sub>	99.5 ± 0.5% (n = 6)	99.0 ± 1.0% (n = 6)
24 h post exposure	99.6 ± 0.4% (n = 10)	99.0 ± 0.7% (n = 11)
24 h + 0.1 mM H <sub>2</sub> O <sub>2</sub>	98.3 ± 1.2% (n = 4)	99.0 ± 1.0% (n = 6)
24 h + 0.2 mM H <sub>2</sub> O <sub>2</sub>	99.0 ± 1.0% (n = 6)	98.8 ± 1.2% (n = 6)

Note: The cell viability was examined using Eosin Y stain prior to conduction comet assay. Values are expressed as means ± SEM of replicates, and no statistical differences were observed (P = 0.98, One-way ANOVA).

#### 6.4.3.2. Response of HUVECs to HBO and Subsequent H<sub>2</sub>O<sub>2</sub> Incubation

A single 90 min HBO treatment at 2.2 ATA was able to induce more DNA strand breaks than a coordinate Air treatment that more HUVECs presented visible holo patterns in B1 than in A1 of Fig 6.5. The means of % DNA in tail of HBO-treated cells (6.8 ± 0.8 %, n = 8) was significant higher than the 4.6 ± 0.2 % (n = 8) of control air-exposed cells (P < 0.05, unpaired t-test). However, 24 h after exposure, HBO-treated cells showed the same level of % tail DNA as the control cells (4.9 ± 0.2 % and 4.6 ± 0.3 %, n = 6 and 9, respectively) (Fig 6.5C1, D1 and Fig 6.6).

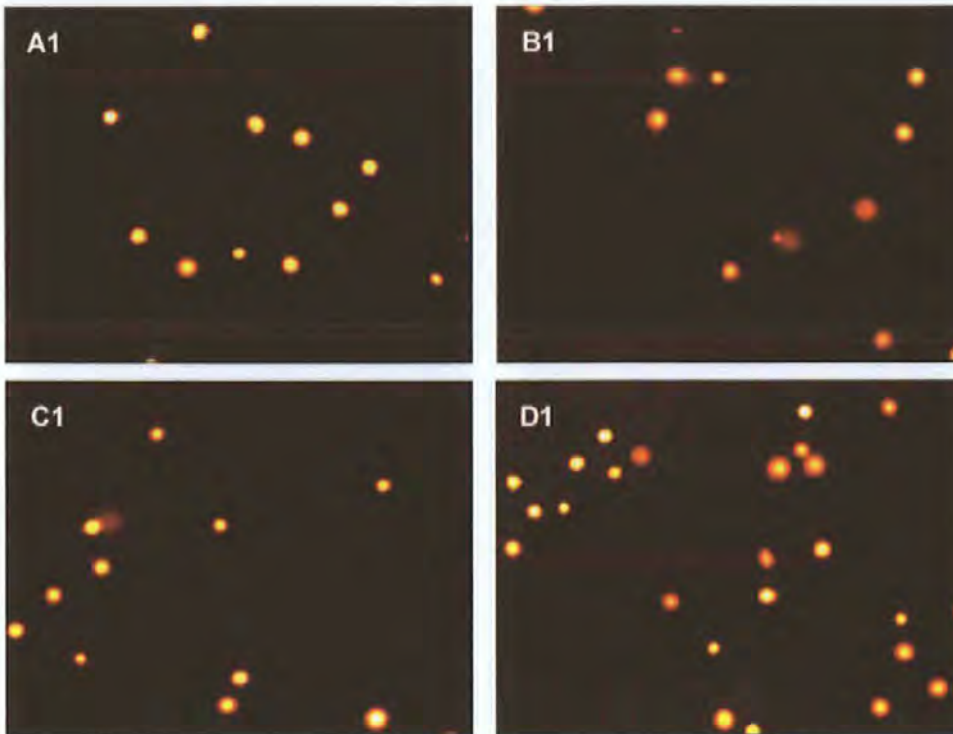


Fig 6. 5 HUVECs' comet images with HBO or Air treatment only. Cells were exposed to 100% oxygen at 2.2 ATA (HBO) or norbobaric air (Air) for 90 min, and followed by a 24 h recovery at normal culture condition. The images (200× magnification) represented DNA immigration at: immediate post Air treatment (A1) and HBO treatment (B1); 24h post Air treatment (C1) and HBO treatment (D1).

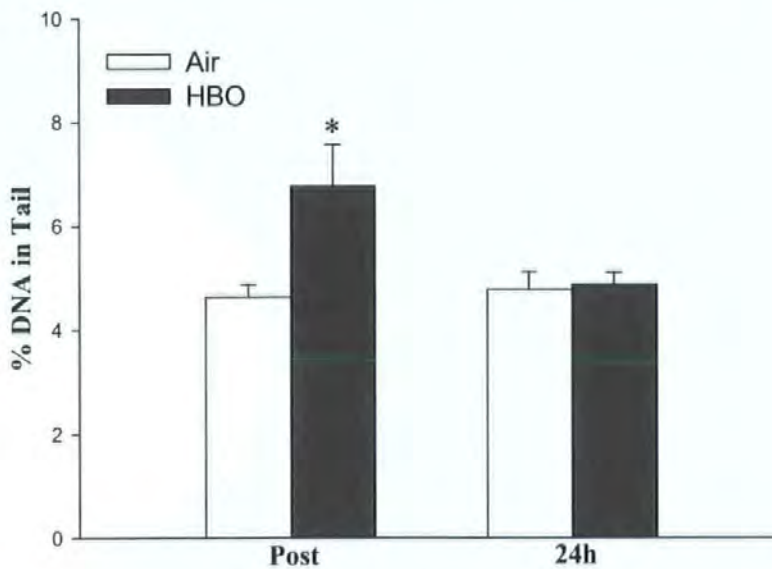
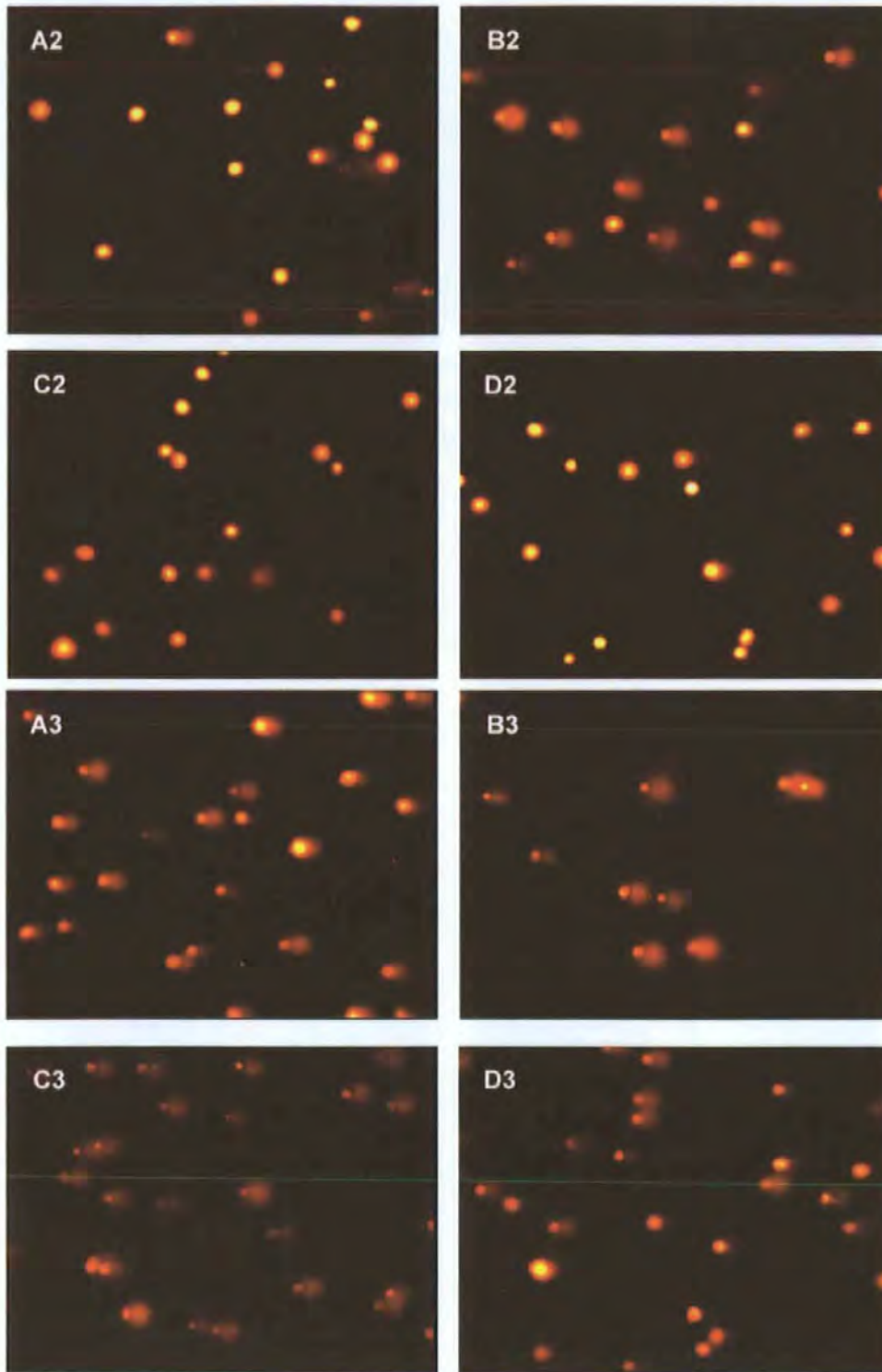


Fig 6. 6 Extent of DNA migration (% DNA in tail) in HUVECs after HBO (dark grey column) or Air (white column) exposure only. Cells were exposed to 100% oxygen at 2.2 ATA (HBO) or norbobaric air (Air) for 90 min, and followed by a 24 h recovery at normal culture condition. DNA damage was evaluated at immediate post and 24h post treatments and expressed of means  $\pm$  SEM of replicates. Unpaired T-test was performed between Air and HBO treatment immediate and 24h after treatments respectively, and \* ( $P < 0.05$ ) indicates significant differences to the control air treated cells.

As shown in Figs. 6.7 and 6.8, the HBO-treated cells were more vulnerable to oxidative stress at immediate post HBO treatment, but not after 24h recovery. Interestingly, the responses of HBO-treated HUVECs seem having dose difference. Immediately after Air or HBO treatment, incubation with 0.1 mM H<sub>2</sub>O<sub>2</sub> caused significant 66% more DNA strand breaks of HBO-treated cells ( $31.5 \pm 4.0\%$  DNA in tail,  $n = 4$ ) than that of Air-treated cells ( $18.9 \pm 2.7\%$  DNA in tail,  $n = 5$ ;  $P = 0.03$ , unpaired t-test); and consistently incubation with 0.2 mM H<sub>2</sub>O<sub>2</sub> induced a significant 26.4% increase of DNA strand breaks in HBO-treated cells than that in Air-treated cells ( $66.6 \pm 2.7\%$  DNA in tail,  $n = 5$ ; and  $52.7 \pm 1.2\%$  DNA in tail,  $n = 5$ ;  $P = 0.002$ , unpaired t-test). However, 24h post recovery, different DNA migration patterns were seen between additional H<sub>2</sub>O<sub>2</sub> incubations. The 0.1 mM of H<sub>2</sub>O<sub>2</sub> incubation induced similar levels of DNA strand breaks in Air- and HBO-treated cells ( $P = 0.54$ , unpaired t-test); whilst the 0.2 mM of H<sub>2</sub>O<sub>2</sub> incubation induced 22% less strand breaks in HBO-treated cells ( $44.0 \pm 1.6\%$  tail DNA,  $n = 9$ ) than that of Air-treated HUVECs ( $56.3 \pm 2.6\%$  tail DNA,  $n = 9$ ;  $P = 0.001$ , unpaired t-test). Another fact need to mention is that HBO-treated cells are more likely to be protected from additional oxidative stress. Additional H<sub>2</sub>O<sub>2</sub> incubation at 0.2 mM led much less of tail DNA levels in 24h post HBO-treated cells than that in immediate post HBO-treated cells ( $P < 0.001$ , unpaired t-test); whereas additional exposure of Air-treated cells to H<sub>2</sub>O<sub>2</sub> showed no differences on DNA migration patterns between immediate and 24h post treatment time points ( $P = 0.34$  of 0.2 mM of H<sub>2</sub>O<sub>2</sub> incubations, unpaired t-test).



**Fig 6. 7** Comet images with HBO or Air-treated cells after further incubation with 0.1 mM (A2-D2) and 0.2 mM of H<sub>2</sub>O<sub>2</sub>(A3-D3) The treatments were 90 min exposure to 100% oxygen at 2.2 ATA (HBO) or norbaric air (Air), and then transferred to normal culture condition for a following 24h recovery. The images (200× magnification) represented DNA immigration of the treated cells after further treated with 0.1 mM and 0.2 mM of H<sub>2</sub>O<sub>2</sub> at: immediate post Air treatment (A2 and A3) and HBO treatment (B2 and B3); 24h post Air treatment (C2 and C3) and HBO treatment (D2 and D3), respectively.

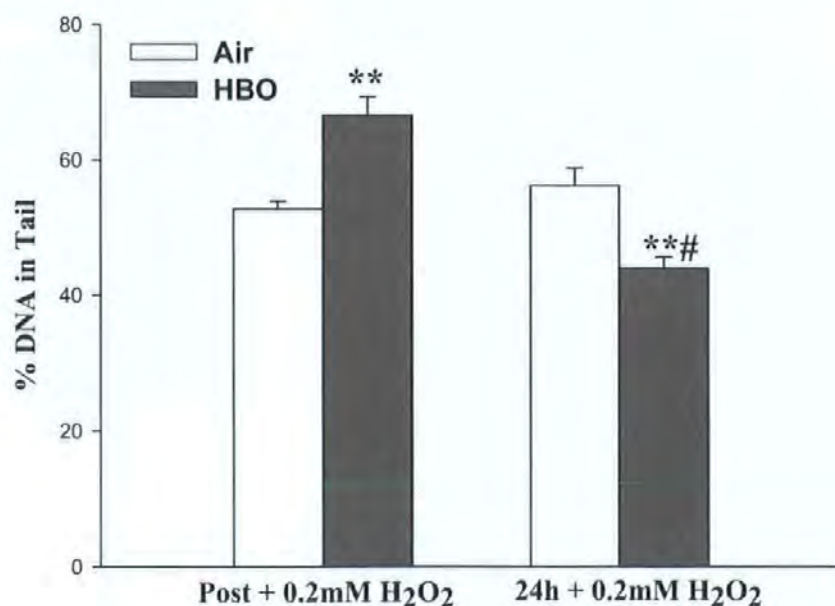
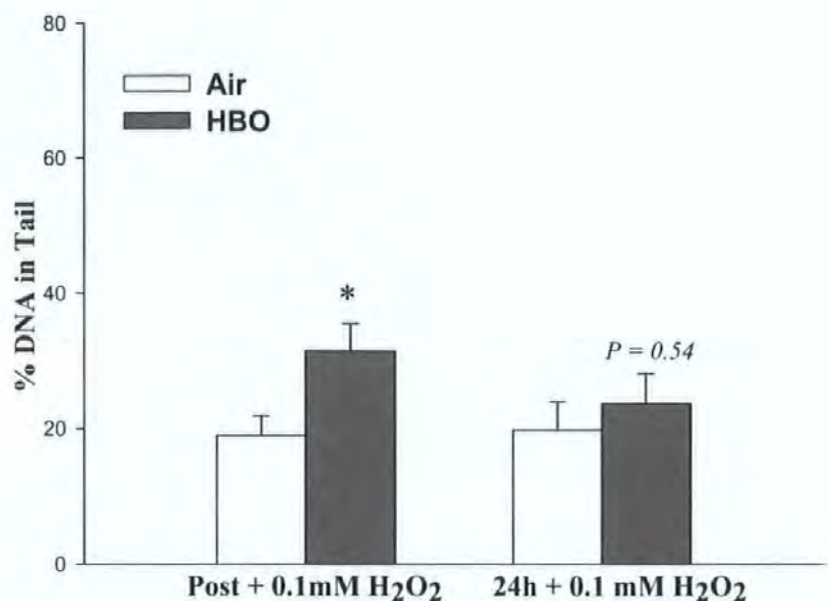


Fig 6. 8 Effects on DNA migration after subsequent incubation with 0.1 mM and 0.2 mM of H<sub>2</sub>O<sub>2</sub> of HBO- or Air-treated HUVECs. The treatments were 90 min exposure to 100% oxygen at 2.2 ATA (HBO) or norbaric air (Air), and then transferred to normal culture condition for a following 24h recovery. DNA damage was evaluated at immediate post (post + 0.1mM H<sub>2</sub>O<sub>2</sub>; post + 0.2mM H<sub>2</sub>O<sub>2</sub>) and 24h post (24h+ 0.1mM H<sub>2</sub>O<sub>2</sub>; 24h+ 0.2mM H<sub>2</sub>O<sub>2</sub>) treatments, and expressed of means  $\pm$  SEM of replicates, respectively. Unpaired T-test was performed, and \* (P<0.05) and \*\* (P<0.01) indicates significant differences to control air-treated cells; # (P<0.001) indicates very significant differences immediate HBO-treated cells, respectively.

#### 6.4.4. Glutathione Pool Changes of HUVECs

The overall response of glutathione pool to HBO treatment was loss of intracellular contents of GSH and GSSG during treatment, but after 24h recovery the glutathione pool was able to return to its pre-treatment levels. Meanwhile, the ratio of GSH to GSSG was not affected by HBO treatment. Post-incubation with H<sub>2</sub>O<sub>2</sub> further reduced the GSH and GSSG contents as expected; but importantly, HBO-treated cell showed much higher GSH to GSSG ratio when incubation with H<sub>2</sub>O<sub>2</sub> at 24h after treatment, and significance dose-effects were found between the 0.1 mM and 0.2 mM of H<sub>2</sub>O<sub>2</sub> incubations.

##### 6.4.4.1. Glutathione Changes of HUVECs with Treatments

In Fig 6.9, a single HBO treatment reduced the GSH and GSSG content of HUVECs. The GSH contents of air-exposed cells was  $10.5 \pm 1.7$  nmol mg<sup>-1</sup> protein (n = 10), which was more than 2-fold that of the  $4.8 \pm 0.6$  nmol mg<sup>-1</sup> protein (n = 10) of HBO-exposed cells (P < 0.05, Tukey-Kramer multiple comparison test). The GSSG level showed a similar significant decrease (P < 0.05, Tukey-Kramer multiple comparison test) so that HBO-exposed cells ( $0.7 \pm 0.1$  nmol mg<sup>-1</sup> protein) had about 47% less GSSG content of the air-treated cells ( $1.5 \pm 0.4$  nmol mg<sup>-1</sup> protein). As both GSH and GSSG level decreased, the ratio of GSH to GSSG showed no difference between Air ( $7.7 \pm 1.3$ ) and HBO treatment ( $7.7 \pm 1.1$ ). However, after 24h post-treatment culture, the intracellular level of GSH and GSSG recovered and no differences were seen between Air ( $9.6 \pm 0.8$  and  $1.0 \pm 0.2$  nmol mg<sup>-1</sup> protein of GSH and GSSG, n = 11) and HBO treated cells ( $9.2 \pm 1.3$  and  $1.0 \pm 0.3$  nmol mg<sup>-1</sup> protein of GSH and GSSG, n = 11). The glutathione ratio of 24 h post HBO-treated cells ( $16.7 \pm 3.7$ ) was about 2-fold of that of immediate HBO-treated cells (P = 0.04, unpaired t-test).

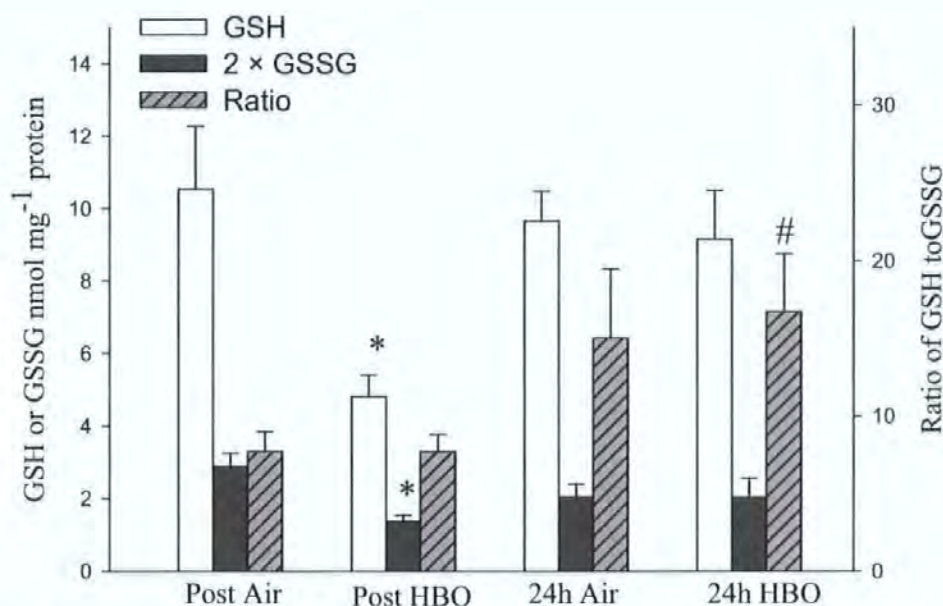


**Fig 6. 9** Glutathione pool changes of HUVECs after HBO or Air treatment only. The treatments were 90 min exposure to 100% oxygen at 2.2 ATA (HBO) or norobaric air (Air), and then transferred to normal culture condition for a following 24h recovery. Samples were collected at immediate post and 24h post treatment for intracellular GSH and GSSG analysis, and expressed in nmol mg<sup>-1</sup> protein. For clear view, GSSG values are 2-fold of actual GSSG value. Data were plotted as means  $\pm$  SEM of more than 10 replicates. Left Y axis corresponds to level of GSH (white column) and GSSG (grey column) in nmol mg<sup>-1</sup> protein, and right Y axis corresponds to ratio of GSH to GSSG (grey diagonal column). Statistic analysis was performed with One-way ANOVA test followed by Tukey-Kramer multiple comparison test or unpaired t-test. \*  $P < 0.05$  indicates significant difference from Air-treated cells; and #  $P < 0.05$  indicates significant difference from that of immediate post HBO-treated cells.

#### 6.4.4.2. Glutathione Changes of Treated HUVECs to Subsequent H<sub>2</sub>O<sub>2</sub> Incubation

Immediately after treatments, subsequent incubation of Air- or HBO-treated HUVECs to either 0.1 mM or 0.2 mM of H<sub>2</sub>O<sub>2</sub> resulted in a consistent decrease of GSH and GSSG content; and the HBO-treated cells showed more decrease than that of Air-treated cells (Fig 6.10). The GSH and GSSG level were  $5.5 \pm 0.7$  and  $1.1 \pm 0.1$  nmol mg<sup>-1</sup> protein ( $n = 4$ ) of Air-treated cells and  $3.8 \pm 0.3$  and  $0.6 \pm 0.1$  nmol mg<sup>-1</sup> protein ( $n = 6$ ) of HBO-treated cells with 0.1 mM of H<sub>2</sub>O<sub>2</sub> incubation (Fig. 6.10A). And cellular GSH and GSSG levels decreased more in 0.2 mM of H<sub>2</sub>O<sub>2</sub> incubation (Fig. 6.10B) to  $6.1 \pm 0.8$  and  $1.3 \pm 0.4$  nmol mg<sup>-1</sup> protein ( $n = 4$ ) in Air-treated cells; and  $3.5 \pm 0.3$  and  $0.8 \pm 0.1$  nmol mg<sup>-1</sup> protein ( $n = 6$ ) in HBO-treated cells. The GSH and GSSG levels showed significant treatment differences in both H<sub>2</sub>O<sub>2</sub> incubations ( $P < 0.05$ , Tukey-Kramer multiple comparison test),

---

the ratio of GSH to GSSG in both H<sub>2</sub>O<sub>2</sub> incubations appeared no differences between Air and HBO treatments.

After 24h recovery, H<sub>2</sub>O<sub>2</sub> incubation showed dose differences on glutathione pool changes. In 0.1 mM of H<sub>2</sub>O<sub>2</sub> incubation, no significant difference was shown in either GSH or GSSG level between Air- and HBO-treated cells ( $P = 0.86$  and  $0.51$  of GSH and GSSG, respectively, unpaired t-tests), but significant lower levels of GSH and GSSG in HBO-treated cells were found in 0.2 mM of H<sub>2</sub>O<sub>2</sub> incubation ( $P < 0.01$  and  $P < 0.05$  of GSH and GSSG, respectively, Tukey-Kramer multiple comparison test). In addition, both the Air-treated cells and HBO-treated cells showed more decreased glutathione ratio values in 0.2 mM H<sub>2</sub>O<sub>2</sub> incubation ( $14.4 \pm 3.5$ ,  $n = 5$  of HBO-treated cells and  $6.2 \pm 1.4$ ,  $n = 4$  of Air-treated cells) than that in 0.1 mM H<sub>2</sub>O<sub>2</sub> incubation ( $23.5 \pm 8.0$ ,  $n = 6$  of HBO treatment and  $13.5 \pm 6.9$ ,  $n = 4$  of Air treatment). But more importantly, the glutathione ratio in HBO cells was 74% higher with 0.1 mM H<sub>2</sub>O<sub>2</sub> incubation, and significantly 134% higher than that in Air cells with 0.2 mM H<sub>2</sub>O<sub>2</sub> incubation ( $P = 0.56$  and  $P = 0.04$ , respectively, unpaired t-test). Furthermore, the ratios of 24h HBO-treated cells were 4-fold and 3-fold ( $P = 0.08$  and  $P = 0.04$ , unpaired t-tests) as to immediately HBO-treated cells within subsequent 0.1 mM and 0.2 mM of H<sub>2</sub>O<sub>2</sub> incubation. Meanwhile, there were no time differences in Air-treated cells ( $P = 0.35$  and  $0.69$  of 0.1 mM and 0.2 mM of H<sub>2</sub>O<sub>2</sub> incubation, respectively).

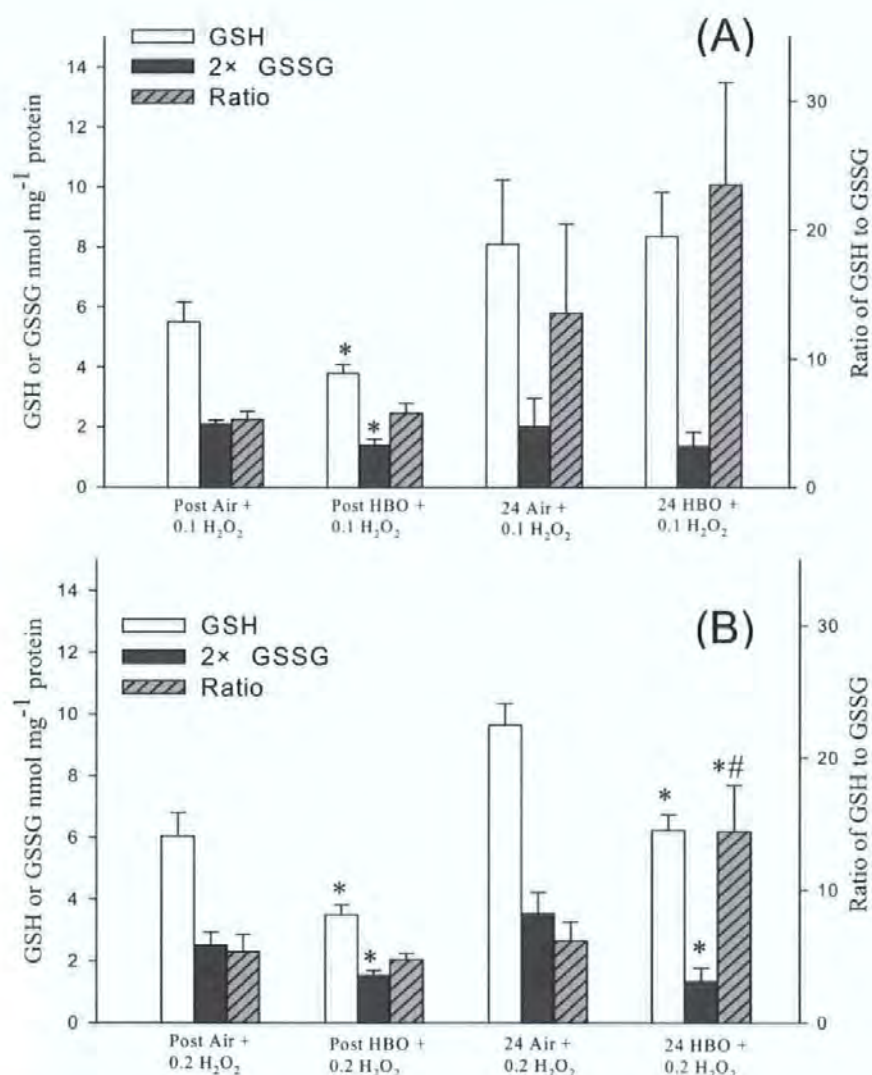


**Fig 6. 10** Glutathione pool responses to subsequent incubation with 0.1 (A) and 0.2 (B) mM of H<sub>2</sub>O<sub>2</sub> of Air or HBO treated HUVECs. The treatments were 90 min exposure to 100% oxygen at 2.2 ATA (HBO) or norbarobaric air (Air), and then transferred to normal culture condition for a following 24h recovery. Air or HBO treated HUVECs were subsequently incubated with 0.1 or 0.2 mM of H<sub>2</sub>O<sub>2</sub> at 37 °C for 15 min at immediate post treatment and 24h post treatment. Intracellular GSH and GSSG are expressed in nmol mg<sup>-1</sup> protein. For clear view, GSSG values are 2-fold of actual GSSG value. Data were plotted as means  $\pm$  SEM of more than 4 replicates ( $n = 4 - 6$ ). Left Y axis corresponded to level of GSH (white column) and GSSG (grey column) in nmol mg<sup>-1</sup> protein, and right Y axis corresponded to ratio of GSH to GSSG (grey diagonal column). Statistic analysis was performed with One-way ANOVA test followed by Tukey-Kramer multiple comparison test and unpaired t-test. \*  $P < 0.05$  significant difference from Air-treated cells at the same time point; and #  $P < 0.05$  significant difference from that of immediate post-treated cells.

### 6.4.5. Correlations of DNA Migration Levels and Glutathione Pool

Correlation analysis was performed using Pearson's correlation test. In Table 6.2, GSH and the ratio of GSH to GSSG showed significant correlation with % DNA in tail ( $P < 0.01$  and  $P < 0.05$ , respectively). However, no significant correlation was found between GSSG level and % DNA in tail ( $P = 0.16$ ).

Table 6. 2 The correlation test results

<i>Index</i>	<i>r</i>	<i>P</i>
GSH	-.429*	.000
GSSG	-.174	.155
GSH:GSSG	-.292**	.013

Note: Pearson's correlation tests were performed between DNA migration level (% DNA in tail) and any of glutathione pool indexes using SPSS 11.0 for Windows software (SPSS Inc, Chicago, Illinois, USA). *r* represents correlation coefficient and ranges from -1 to 1. When *r* = Zero means that the two variables do not vary together at all; *r* = positive fraction means that the two variables tend to increase or decrease together; *r* = negative fraction means that one variable increases as the other decreases; *r* = 1.0 (or -1.0) means that the two variables are perfect (negative or inverse) correlation. *P* value represents the level (2-tailed) of significance and if the *P* value is small (as  $P < 0.05$ ), then the correlation is not a coincidence and more than 95% of the true population *r* lies within the confidence interval range. \* and \*\* correlation is significant at the 0.05 and 0.01 level (2-tailed), respectively.

## 6.5 Discussions

### 6.5.1. HBO-induced Repairable DNA Migration Changes in HUVECs

Using the comet assay, HBO treatment has been shown to induce genotoxic effects with human whole blood, isolated human lymphocytes, V79 Chinese hamster cells, and mouse lymphoma L5178Y cells line (Speit et al., 2002). For the first time, we have successfully applied the comet assay to measure HBO-induced DNA migration changes and repair in cultured HUVECs. The clear comet images we got can be easily recognised and scored by Komet 5.0 image analysis software. Our data demonstrated that a single HBO treatment at 2.2 ATA for 90 min had a small but significant increase on DNA migration extent of HUVECs (to 6.8% DNA in tail) (Fig 6.5). Nevertheless, an average 50% increase of tail DNA in HBO-treated HUVECs than that of Air-treated control cells seems

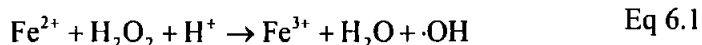
relatively very small effect comparing to other studies. Speit and his colleagues reported an average of 5-fold increase in DNA migration pattern of human lymphocytes after a HBO exposure at 2.5 ATA for 3×20 min (Dennog et al., 1996) and Rothfuss et al (2002) presented a 6-fold increase in DNA migration of V79 cells after 1 hour HBO exposure at 3.0 ATA. The differences among studies may indicate that HBO-induced DNA migration varies between HBO strategies as well as cell types.

By comparing the extent of DNA migration at different time points, we were able to monitor DNA repair capability with the comet assay. At 24h after exposure, the HBO-treated cells had the same level of % DNA in tail as the air-treated control cells, indicating a complete repair of the induced DNA strand breaks (Fig 6.5). Our finding was consistent with *in vivo* studies where blood taken 6 h or 24 h after HBO shown no effect of DNA migration (Speit et al., 1998). Actually, the higher DNA migration level in human leukocytes from healthy volunteers after HBO exposure (2.5 ATA for 3×20 min) has been confirmed due to oxidative DNA base damage (Dennog et al., 1996); and further studies showed that HBO-induced DNA strand breaks and oxidative base modifications were rapidly repaired, after 1 or 2 h the repair efficiency could be more than 50% and no difference were found between *in vivo* or *in vitro* exposure (Dennog et al., 1996; Speit et al., 1998).

### 6.5.2. Protective Effect of HBO on H<sub>2</sub>O<sub>2</sub>-induced DNA Damage

H<sub>2</sub>O<sub>2</sub> is a common intermediate in a variety of oxidative stress and can efficiently oxidize iron-sulfur clusters and protein thiols (Flint et al., 1993; Storz and Imlay, 1999). But H<sub>2</sub>O<sub>2</sub> does not directly interact with DNA to produce oxidative lesions (Brawn and Fridovich., 1981). In fact, when cells are exposed to external H<sub>2</sub>O<sub>2</sub>, the H<sub>2</sub>O<sub>2</sub> rapidly

diffuses inside and oxidizes ferrous iron, thereby forming hydroxyl radicals that cause oxidative DNA damage (Eq 6. 1).



The hydroxyl radical is powerful enough to react at diffusion-limited rates with either the base or sugar residues of DNA (Aruoma et al., 1989), producing base modifications, sites of base loss (AP site), and strand breaks, which can be captured by the comet assay.

$\text{H}_2\text{O}_2$  has been frequently used as a reference toxicant in comet assay to assess oxidative DNA damage in many cell types, and the dose responses of  $\text{H}_2\text{O}_2$  vary in cell types and origins (Aruoma et al., 1989; Visvardis et al., 1997). In our study, the DNA migration of human umbilical vein endothelial cells showed a dose-dependent effect, too. Incubation with 0.1 mM and 0.2 mM of  $\text{H}_2\text{O}_2$  induced 16% and 46% of DNA in tail, those concentrations are the start and the end concentration points to induce a nearly linear DNA migration/damage curve (Fig 6.4). Although we have not found a study using endothelial cells to generate an  $\text{EC}_{50}$  calculation curve,  $\text{H}_2\text{O}_2$  dose effects have been investigated in a couple of different cell types using comet assay. Collin et al (1995) found that when incubated with 50  $\mu\text{M}$   $\text{H}_2\text{O}_2$ , Hela (human transformed epithelial) cells and GM1899A (human lymphoblastoid) cells suffered considerable DNA breakage with virtually all or most comets in class 4 (equal to 80% DNA in tail approximately); in contrast, fresh isolated human lymphocytes were less severely damaged with more than 60% of comets in class 0 (equal to 5% DNA in tail approximately) at the same concentration of 50  $\mu\text{M}$   $\text{H}_2\text{O}_2$ , and even at 200  $\mu\text{M}$   $\text{H}_2\text{O}_2$ , almost half of the comets were still in class 0. But in another study that fresh isolated human lymphocyte was less resistant to  $\text{H}_2\text{O}_2$  with  $\text{EC}_{50}$  at 20  $\mu\text{M}$  that led to unwinding in alkali of 50% of the DNA (Schraufstatter et al., 1988). Clearly, because of the variety of cell responses and experimental conditions of comet assay on measuring  $\text{H}_2\text{O}_2$ -induced DNA damages, it is essential to validate the dose effects before

---

individual experiment, which not only optimise working condition for specific cell type, but also set a positive control for the following experiments.

Additional incubation with  $H_2O_2$ , HBO-treated cells showed more DNA migration than that of Air-treated cells (Fig 6.7 and 6.8). The evidence that HBO treatment caused oxidative DNA base damage (Dennog et al., 1996) may help to explain the higher DNA damage level in HBO-treated cells when further incubated with  $H_2O_2$ . Immediate post HBO treatment, the cells have been exposed to oxidative stress, so in theory, the cells are more vulnerable to further oxidative stress. Nevertheless, the beneficial effect of therapeutic HBO treatment may count on the adaptive protective mechanism triggered by HBO exposure against further  $H_2O_2$  attack. Because in our study, with 0.2 mM of  $H_2O_2$  incubation, HBO-treated cells had shown a significant 22% less DNA migration than that of Air-treated cells after 24 h recovery. The human lymphocyte had also shown similar protective effects against  $H_2O_2$  at both 4 h and 24 h post initial HBO treatment with 10  $\mu$ M and 20  $\mu$ M of  $H_2O_2$  induction *in vitro* (Rothfuss et al., 2001). Interestingly, in our experiment, incubation 24 h post HBO-treated cells with 0.1 mM of  $H_2O_2$  was not shown the protection effects. In Rothfuss' study (2001), treatment with  $H_2O_2$  alone induced a clear and dose-dependent DNA migration effect of freshly isolated human lymphocytes as measured with comet assay; and pre-exposure with HBO efficiently dramatically minimized both 10  $\mu$ M and 20  $\mu$ M  $H_2O_2$ -induced DNA effects. The diminishing effect was bigger in 20  $\mu$ M of  $H_2O_2$  incubation group at 4 h than 24 h after initial HBO treatment; and in 10  $\mu$ M of  $H_2O_2$  incubation group at 24 h than 4 h after initial HBO treatment. Another interesting thing to note is that the lymphocytes 24 h after isolation showed somewhat lower extent of  $H_2O_2$ -induced DNA damage than cells 4 h after isolation in the comet assay. The study indicates that some unknown mechanisms may exist to influence  $H_2O_2$ -induced DNA damage, especially when it is measured with comet assay. Therefore, it is

possible cell specificities or experimental conditions influenced the H<sub>2</sub>O<sub>2</sub>-induced DNA damage in HUVECs and contributed to the diverse protective effects in our study.

### 6.5.3. Glutathione: Possible Mechanism for HBO Protective Effect

Although studies have shown the protective effects of HBO treatment, little is known about the underlying mechanisms and molecular basis. It is commonly recognized that prior to DNA damage, ROS has to overwhelm the cellular threshold of antioxidant capacity. The antioxidant capacity is created by the presence of antioxidant enzymes, scavenger molecules or the removal of the altered molecules by turnover (Gutteridge., 1994; Remacle et al., 1995; Anderson, 1996). Reduced glutathione (GSH), the most abundant cellular thiol (0.5-10 mM), plays an important role in antioxidant defence system as well as regulating the intracellular redox environment (Cotgreave and Gerdes, 1998). Under oxidative stress, GSH is utilised directly as a proton donor to detoxify H<sub>2</sub>O<sub>2</sub> and other organic peroxides to oxidized glutathione (GSSG) by glutathione peroxidase (GPx). Measurement of intracellular glutathione redox pool is therefore a useful dynamic indicator of oxidative stress as well as a monitor of antioxidant effectiveness.

The GSH and GSSG content of HUVECs we measured was approximately at 10 nmol mg<sup>-1</sup> protein and 1 nmol mg<sup>-1</sup> protein, respectively, which were at the range of previous report: 5.88 to 12.1 nmol mg<sup>-1</sup> protein of GSH (Andreoli et al., 1986); and 10 – 25 nmol mg<sup>-1</sup> protein of GSH and 0.2 – 1.2 nmol mg<sup>-1</sup> protein of GSSG (Carlisle et al., 2002). The ROS generated during HBO exposure facilitated consumption of GSH storage in HUVECs, thus a lower level of intracellular GSH was presented of immediate post HBO cells (Fig 6.9). Unlike GSH, GSSG is usually present in cells in much smaller concentration, and because the activity of GPx is coupled to NADPH-dependent glutathione reductase (GR), which recycled GSSG back to GSH, the increase of GSSG during oxidative stress are

generally transient. The relatively rapid GSSG reduction and an active ATP-dependent GSSG export mechanism decrease intracellular GSSG content to maintain the glutathione balance (Sharma et al., 1990). It is crucial for cells to maintain the redox balance of GSH to GSSG, studies have confirmed that changes in the ratio of intracellular GSH to GSSG can affect signalling pathways that participate in various physiological responses from cell proliferation to gene expression (Suzuki et al., 1998; Kim et al., 2004; Rahman et al., 2005); but excessive changes such as depletion of intracellular GSH by cytotoxic stimuli has been shown to lead to cell apoptosis and/or necrosis (Teramoto et al., 1999; Merad-Boudia et al., 1998; Lin et al., 2007). Therefore, in non-lethal stress, as in HBO treatment, although GSH was consumed through reactions to remove and alter deleterious compounds, GSSG level was also reduced to maintain an unchanged glutathione ratio (Fig 6.9). However, the temporary depletion of GSH must be reversed to avoid further damages. Restoration of GSH can easily be accomplished by GR or by *de novo* GSH synthesis (Dickinson et al., 2003). In our study, during 24h recovery, the HBO-treated cells were able to recover original glutathione pool as the GSH, GSSG content returned to the same levels of control cells, with the ratio remained the same. The changes of glutathione pool during and after HBO treatment indicate that HBO treatment may be able to regulate 'functional alteration' of glutathione pool without damage the cells. Recently, GSH content and metabolism changes have been related with signaling pathways, probably through alteration of the redox state (Dickinson et al., 2003). It is due to the fact that many proteins have a highly conserved cysteine (sulfhydryl) sequence in their active/regulatory sites, which are primary targets of oxidative modifications and thus important components of redox signalling. And recent data suggest that multiple modifications of cysteine residues may occur and leading to different outcomes in signal transduction (e.g. kinase pathways, transcription factors nuclear factor- $\kappa$ B, and ryanodine receptors (Cooper et al., 2002;

---

Rahman et al., 2005). Thus, the adaptive response to non-toxic oxidative stress as in HBO treatment may lead to another aspect in understanding HBO benefits.

Another important finding in our study is the protective effects of HBO treatment on oxidative stress-induced DNA damage in HUVECs. The corresponding glutathione pool showed that 24h HBO-treated cells maintained much higher GSH to GSSG ratio than that of Air-treated cells after exposing to H<sub>2</sub>O<sub>2</sub> (Fig 6.10); and the GSH content and the ratio also showed significantly correlation with the DNA migration level (Table 6.2). It seems that the glutathione pool regulation during HBO treatment may responsible for the protective mechanism against oxidative stress. The nontoxic stress-induced glutathione adaptive response within the cell has been proposed to be relevant to the improved capacity to withstand a subsequent stress that would otherwise have been lethal (Rahman et al., 2005). The glutathione adaptive response could appear in higher intracellular levels of GSH itself, and/or an increased capacity for rapid synthesis. For example, pre-exposure macrophages and endothelial cells to oxidized low density lipoprotein leads to the induction of GSH and protection against oxidative stress (Shen and Sevanian, 2001; Moellerin et al., 2002); and pre-treatment with NO also elicit GSH synthesis and thus lead to protect against a subsequent oxidative stress (Dickinson et al., 2003). In our cases, although GSH level was not seen obvious increase, the ratio of GSH to GSSG in HBO-treated cells did show a significant higher levels than control cells. So it is possible that a single HBO treatment may alter the glutathione redox status other than only increase GSH content. The effects of HBO treatment on glutathione content and metabolic enzymes varies amongst *in vivo* studies. Ozden et al (2004) and Kudchodkar et al (2006) addressed that chronic HBO treatment increased GSH, GR, and GPx levels. Eken and colleagues (2005) reported unchanged erythrocyte GPx levels at the end of the 1st HBO therapy and

the prolonged HBO exposure; which was supported by Muth's findings that unaffected GSH, GSSG levels and an even decreased GPx activity after HBO exposure (Muth et al., 2004). Thus, the effect of HBO treatment on intracellular glutathione regulation may differ between *in vitro* or *in vivo* experiments. Since HBO treatment provides an ideal model for non-cytotoxic oxidative stress study and is capable to regulate glutathione pool; it will be informative to continue the *in vitro* endothelial cells study on glutathione and its metabolic enzymes (e.g. GPx, GR) response with different HBO strategies, and research of these aspects in clinical trials will also be very helpful for a better understanding of the antioxidants' functions in HBO treatment.

## 6.6 Conclusion

In this chapter, using alkaline comet assay, we demonstrated that H<sub>2</sub>O<sub>2</sub> induced DNA damage in HUVECs showed a dose-dependent effect. Secondly, a single 90 min HBO treatment at 2.2 ATA induced a small but detectable increase in DNA migration pattern, and this change was totally recovered after 24h incubation in normal culture conditions, indicating an efficient DNA repair after therapeutic HBO treatment. Thirdly, pre-HBO exposure showed a protective effect on HUVECs against subsequent H<sub>2</sub>O<sub>2</sub>-induced DNA damage, which may be concentration-related and more investigation is needed. The HBO treatment is able to regulate glutathione pool in HUVECs, which is especially demonstrated in the ratio of GSH to GSSG. The GSH content and the ratio of GSH to GSSG showed consistent changes with DNA migration pattern. The increase in the glutathione ratio may reflect the increased antioxidant capacity after HBO treatment, which is quite possible contribute to the protective response.

## **Chapter 7**

# **General Discussions and Future Work**

In this chapter, the thesis is concluded with a summary of the main results and achievements obtained from this project. Furthermore, the limitations of the work are identified, and the perspectives for future work are presented.

### **7.1 Summary of the Project**

Hyperbaric oxygen therapy (HBOT) is a medical treatment during which the patients are placed in an airtight chamber at more than one atmospheric pressure and are usually breathing 100 percent pure oxygen. This treatment either as a primary or adjunctive treatment has proven relatively effective for a number of different medical and surgical conditions. Although nowadays HBOT has been clinically accepted and used, it seems that scientific explanation for the benefits of HBOT lags behind the booming application of HBOT. Hence, more scientific research is required to provide sound evidence for clinical application, and more importantly to explore the underlying mechanisms of HBOT in order to benefit more patients by improving and directing HBOT strategy.

As a matter of fact, one of the successful applications that HBOT has achieved is to facilitate problem or chronic wound healing as a conjunctive treatment to traditional therapies. Chronic wounds are common and present a health problem with significant effect on quality of life. The application of HBOT has been shown to reduce the costs involved with wound management and decreases the incidence of amputations (Kranke et al., 2003). Wound healing is a highly regulated and complex process involving several

main medical conditions such as inflammation, angiogenesis, proliferation, and remodelling process. Angiogenesis, the formation of new blood vasculature from pre-existing vessels, is crucial for granulation tissue formation and proper wound healing. Appropriate oxygen levels are required for angiogenesis so that the cells involved can generate ATP and perform multiple physiological functions. However, the various pathologies of chronic wounds may cause tissue breakdown, including poor blood supply resulting in inadequate oxygenation of the wound bed. HBOT has been suggested to reverse local wound hypoxia and set up beneficial oxygen gradients across the wound space to promote wound angiogenesis and therefore improve their healing. Although both *in vivo* and *in vitro* studies have demonstrated that HBOT accelerates wound angiogenesis, the mechanisms are far from elucidated.

Regulation of angiogenesis factors is a key field in HBO studies. HBO treatments are able to experimentally manipulate the production of angiogenesis factors at the molecular and cellular levels, but the effects (positive/negative) are dependent on the wound model being used, cell types, as well as the details of the HBO strategies. During the past twenty years, with the development of cellular and molecular techniques, researchers have been able to find out more about the physiological and pathological properties of ROS and oxidative stress. For a long time it was believed that ROS and oxidative stress would damage tissue and cell, even cause cell death. Thus, recent studies have confirmed that mild oxidative stress and oxidant challenge can serve as signalling messenger and then enhance cell functional activity. This recognition is consistent with the clinical and scientific evidence that HBO at very high pressure (over 5 ATA) causes more side effects, while at therapeutic pressure HBOT brings more beneficial effects. Therefore, in this project, we focus our study on the response of ROS, oxidative stress, angiogenesis factors and cell injury during and after a single therapeutic HBO treatment. First of all, at tissue

level, direct effects of HBO treatment were investigated on blood vessel *in vitro*; and the ROS and oxidative stress initiation and angiogenesis factor responses were evaluated in both physiological and pathological conditions. Secondly, at cellular level, response of cultured endothelial cells to HBO treatment was measured. Changes of intracellular calcium concentration were investigated during HBO treatment with both single cells, and populations of cells. Next, HBO-induced DNA damage and the potential effects of HBO treatment against further oxidative stress were measured; meanwhile, response of glutathione pool in the process were examined. In all the studies, the possible damaging effects of HBO were investigated.

### **7.1.1. Main Findings of the Project**

The main findings of tissue treatment are:

- A single therapeutic HBO treatment (at 2.2 ATA for 90 min) does not damage blood vessels tissues in physiological conditions (Fig 3.1 and 3.2); while in pathological condition, HBO treatment induced more cell injury (Fig 4.1).
- In physiological conditions (blood vessel incubated in physiological salt solution), HBO treatment does not induce oxidative stress as the total glutathione and hydrogen peroxide production was very low in the medium (Fig 3.4 and 3.5). However, in pathological condition (blood vessel incubated in high lactate-contained physiological salt solution), HBO treatment induced more ROS generation and oxidative stress as  $H_2O_2$  and total glutathione levels showed significantly higher values than that of either the air treatment or to the controls in physiological solution (Fig 4.2 and 4.3).
- Although supplements of L-arginine and/or sodium L-lactate to the incubation buffer increased nitric oxide production, there was no evidence shown that HBO

treatment alone or synergically promoted NO production in either physiological or pathological conditions (Fig 3.6 and Fig 4.4).

- VEGF content was not affected by HBO treatment in either physiological or pathological conditions (Fig 3.7 and Fig 4.5).
- Exposure of blood vessel to normobaric pure oxygen showed similar effects as HBO treatment on the above indexes.

The main findings of endothelial cell treatment are:

- A single HBO treatment (at 2.2 ATA for 90 min) does not induce cytotoxic damage of human umbilical vein endothelial cells (Fig 5.10 and Table 6.1). However, measured with comet assay, HBO treatment causes small but significant change in DNA migration extent at immediate post treatment, but this change is repaired after 24 hours (Fig 6.6).
- HBO treatment induces sustained increase of cytosolic free calcium level in HUVECs (Fig 5.9).
- HBO treatment successfully protects HUVECs against H<sub>2</sub>O<sub>2</sub>-induced DNA damage as measured with comet assay (Fig 6.8). An increase in antioxidant capacity as reflected in an increase in redox status of glutathione pool (Fig 6.10) may be relevant to this protective response.

### 7.1.2. Technical Contributions

This project not only provides *in vitro* scientific evidence to enrich basic research of HBO treatment, but also makes contributions to biological experimental techniques.

To our knowledge, we are the first to successfully establish an *in vitro* blood vessels model to HBO treatment. Meanwhile, biochemistry methods for measurement of *in situ* H<sub>2</sub>O<sub>2</sub> generation, total glutathione release and ELISA measurement of vascular VEGF are

all modified and optimized to apply in the *in vitro* blood vessel model. Secondly, we successfully recorded real-time calcium changes in single HUVEC; and also accomplished calcium measurements on populations of HUVECs with a fluorescent plate reader. Thirdly, using the comet assay, for the first time we demonstrated the dose effect of hydrogen peroxide-induced DNA damage in HUVECs; and showed the HBO treatment effect on DNA migration extents in HUVECs as well.

### 7.1.3. General Discussion

The vascular system distributes in every tissue and organ of the human body, besides delivers nutrients and oxygen to tissue, it also experiences local physiological and pathological environmental changes and adapts simultaneously to protect and repair affected cell and tissue. One of these adaptations is to generate new vasculature. The angiogenesis process is regulated by many growth factors from various kinds of cells, and the VEGF seems the critical one in all sorts of angiogenesis studies. The regulation of VEGF production is complex, although hypoxia is conventionally accepted as a VEGF regulator, more and more evidence have shown that ROS and lactate are able to regulate VEGF as well. Interestingly, nitric oxide (NO) is not only considered as a free radical, but also works as an angiogenesis regulator, which is particularly involved in the VEGF-regulated angiogenesis pathway. Since therapeutic HBO treatment demonstrates the beneficial effects on chronic wound angiogenesis, the mechanisms involved have drawn scientific attention, especially to the relationship between HBO treatment, ROS, NO and VEGF. *In vitro* and *in vivo* studies have provided controversial results on this subject, the literature remind us that a major breakthrough should be on the diversity of ROS formation in HBO treatment. From the day that high concentration of oxygen was first used for clinical purpose, there was argument about the therapeutic effects and side effects. The

reactive oxygen species (ROS) generation in HBO treatment has long been considered as the deteriorative factors to induce unexpected damage to tissues and cells. But recent scientific developments in ROS research have shown that the ROS level is balanced with antioxidant defence systems, and this balance is important to the cell redox state and redox signalling systems. So at a moderate level, ROS is able to regulate multi-functions in cell physiological activity, which includes angiogenesis regulation.

In our initial study, we investigated the effects of a single therapeutic HBO treatment on the responses of oxidative stress and angiogenesis factors in an established healthy *in vitro* blood vessel experimental system. Preliminary experiment showed that it is safe to incubate aorta segments in our physiological salt solution for up to 8 hours. Therefore, the comparison experiment was done by exposing aorta segment to a single 90 min treatment of normobaric air, normobaric pure oxygen or hyperbaric oxygen (2.2 ATA) and followed by 4 hours recovery in this solution. The histological and biochemical index (LDH release) examination confirmed that aorta segments were not damaged throughout HBO treatment, and HBO treatment induced neither oxidative stress, nor more nitric oxide and VEGF production of aorta segments. Interestingly, VEGF level was significantly correlated with concentration of lactate and nitrite; and the cumulative H<sub>2</sub>O<sub>2</sub> and LDH levels in the medium, which may indicate that VEGF generation is responding to levels of damage in cell or tissues and redox status changes. The Krebs-ringer solution used in initial experiment met the basic physiological requirement of blood vessels. However, elimination of the naturally existed precursor for nitric oxide production, L-arginine, may gloss over some potential effects amongst NO, VEGF production and HBO treatment. Meanwhile, adding sodium L-lactate to the incubation medium will mimic the pathological environment of chronic wounds and simulate reactions of blood vessel to HBO treatment in these adverse conditions. Thus, in the following experiments, we added L-arginine

or/and sodium L-lactate to the medium. In these specific media, we found that HBO treatment induced more ROS and oxidized glutathione production, which was accompanied by more LDH release. So, under pathological conditions, HBO treatment showed the ability to induce more oxidative stress of aorta segment, which in turn damaged the tissue. The high level of tissue damage quite possibly interferes with the autocrine mechanisms in blood vessels as well, because L-arginine or/and sodium L-lactate supplement decreased VEGF level in HBO-treated samples after 4h recovery. On the other hand, although the oxidative state may reduce VEGF production in blood vessel cells, the damaging signals may cause paracrine mechanisms to increase VEGF generation from other types of cells in the wound sites. For example, studies on macrophages, fibroblasts and *in vivo* chronic wound models have reported that HBO treatment increase VEGF production (Sheikh et al., 2000; Gimbel and Hunt. 1999; Kang et al., 2004). The oxidative state not only affects growth factor secretion, it also regulates NO production. The administration of L-arginine increased NO production, and increased NO production was accompanied by a high level of tissue damage in our study. In the case of oxidative stress, NO is known to react with  $O_2^-$  to generate more toxic  $ONOO^-$  and  $OH^-$ , that may explain the high level of tissue damage of aorta segment in L-arginine media to HBO as well as normobaric pure oxygen treatment. In our study, no synergic effect on NO production was found with HBO treatment and the L-arginine supplement. A number of previous studies showed that HBO treatment was able to affect NO production in controversial ways. Increase of NO levels are suspected to be involved in HBO-induced toxic effect in central nerve system, and alternatively, inhibition of NO in some pathophysiological conditions is believed to contribute to the anti-inflammatory effect of HBO treatment (Oury et al., 1992; Wang et al., 1998; Demchenko et al., 2003; Kurata et al., 1995; Sunakawa and Yusa, 1997; Huang et al., 2005; Chu et al., 2006; Chang et al., 2006). Therefore, the controversial effect

of HBO treatment on NO production reflects the controversial roles of HBO in the particular circumstances, and the decisive factors may be the HBO strategies and the NO origination. This concept may also apply to the controversial effect of HBO treatment on VEGF regulation. The physiological condition is like the surrounding healthy area of the wound, therapeutic HBO induces rational level of ROS formation, which is within the control range of antioxidant systems, so no harm is observed in tissue and cells. While the pathological condition is like the centre of wound site, HBO treatment induces more ROS formation, although it is toxic to part of the cells, the ROS is effective in antibacterial actions; and alternatively, the signal of oxidative state and metabolic gradient may pass to surrounding healthy tissue and cells to initiate all kinds of protective and proliferate activities (e.g. immune responses and angiogenesis). In clinical experiments, the re-vascularisation pattern in wound centre site seems to support the above ROS signalling transfer theory. Myers and Marx (1990) observed that although the tissue in the peripheral non-wounded field had a stable level of oxygen supply and vascular structure throughout HBO treatment, the centre site of wound showed no measurable angiogenesis but reflected capillary budding, which is defined as the lag phase of angiogenesis. Then a rapidly growing new vessel followed. During this period of rapid change, an increase to 82% of oxygen-supply in the non-wounded surrounding tissue was observed, and the geometric rise in oxygenation was due to capillary budding from pre-existing vessels in adjacent tissues. When neovascularisation is accomplished, the centre wound field has been converted from hypovascular tissue to a more vascular tissue area. Finally, a plateau phase is presented when the  $TcO_2$  measurement levels of at 80 - 85% of the level in non-wounded surrounding tissue.

Now consider the response in segments of aorta: the aorta segment is composed of endothelial cells, smooth muscle cells and connective tissues, as shown by histological

morphology (Fig 2.1). The investigation of aorta segment represents an integral response of blood vessel to HBO treatment, and we are unable to distinguish the respective cellular events with our measurements. However, an intact blood vessel model does allow angiogenesis factors via intracellular signalling messengers to deliver proliferative information to endothelial cells of blood vessels. And then a complex series of cellular events can occur, such as penetration and migration of endothelial cells into the extracellular matrix, proliferation of endothelial cells to form tubes, and finally smooth muscle cells migrate and associate with these tubes to accomplish the micro-vessel formation (Folkman and Shing., 1992; Risau., 1997; Beck and D'Amore, 1997). So, subsequently, studies on endothelial cell with HBO treatment seems necessary to follow up the findings in blood vessel tissue.

Intracellular free calcium, as a ubiquitous intracellular signal, is responsible for many endothelial cell functions (Berridge et al., 2000). Oxygen level seems to regulate  $\text{Ca}^{2+}$  signals via a mechanism that involves ROS (Ermak and Davies, 2002). To get it started, we established a real-time single cell  $\text{Ca}^{2+}$  recording system. At first, a stable fluorescence ratio (as an expression of  $[\text{Ca}^{2+}]_i$ ) was obtained, but further exposure of cells to hypoxic or hyperoxic solutions did not shown any effects on  $[\text{Ca}^{2+}]_i$ . The unaffected  $[\text{Ca}^{2+}]_i$  during either hypoxia or hyperoxia may be a genuine response, or could due to cell diversity or the perfusion system, which will need more investigation. Meanwhile, HBO-treated cells showed a higher average  $[\text{Ca}^{2+}]_i$  than that of non-treated control cells. Besides the single cell recording, we also recorded the  $[\text{Ca}^{2+}]_i$  changes of populations of endothelial cells with fluorescent plate reader. In the later study,  $[\text{Ca}^{2+}]_i$  increased after exposing to hypoxic, hyperoxia and HBO treatments, which lasted for at least 60 min. More importantly, only HBO treatment showed the significant higher level of  $[\text{Ca}^{2+}]_i$  than that of air treatment. To exclude the conventional theory that  $[\text{Ca}^{2+}]_i$  increase was responsible for cell injury, we

checked the cell viability and confirmed neither of the treatments induced cytotoxic effects. To our knowledge, there have not been a study comparing the  $[Ca^{2+}]_i$  response to different oxygen levels. Although there is only two studies investigated the changes of  $[Ca^{2+}]_i$  during HBO treatment, several studies have shown that the elicit of  $[Ca^{2+}]_i$  in hypoxia has related with ROS pathways (Ikeda et al., 1997; Aley et al., 2005; Peers et al., 2006) and mechanical factors such as pressure were able to increase  $[Ca^{2+}]_i$  as well (Matsuo and Matsuo., 1996; Sato et al., 2006). Due to the fact that HBO treatment contains both effects from high oxygen tension and high pressure, it is quite possible that the calcium increase observed can be due to either of these two factors. Therefore, further investigation is needed to work on this aspect.

In spite of the fact that HBO treatment increased  $[Ca^{2+}]_i$  without inducing cytotoxic effects, it does not mean there is absolute no potential damage to endothelial cells such as effects at genome level. Other studies have shown that HBO treatment induced genotoxic damage in lymphocytes as well as other cell types (Dennog et al., 1996; Speit et al., 1998 and 2002). Thus, we used the comet assay to investigate the genotoxic effect of HBO treatment on endothelial cells (which have not been done before). Our results indicated that HBO treatment induce repairable DNA modification because a slight but significant migration changes in DNA of endothelial cells were seen at immediate after HBO treatment, which were totally reversed after 24 hours. To further investigate the potential adaptive or damaging effects of HBO treatment on endothelial cells, we exposed HBO-treated cells to subsequent oxidative stress. HBO-treated cells showed less DNA damage than non HBO-treated cells, which indicates protective mechanisms occurred. Examination of the intracellular glutathione pool suggested that the redox glutathione balance may be responsible for the protective effect. With the data presented throughout the studies in this

project, we hope to provide scientific *in vitro* evidence to support clinical application and contribute to the mechanism research of hyperbaric oxygen therapy.

## **7.2 Limitations of the Current Work**

Although every effort has been taken to ensure a comprehensive work, we are aware of the following limitations, some of which may be addressed in the future work.

### **7.2.1. Limited Considerations on Pathological Conditions**

Most of the chronic wounds are mainly characterised by hypoxia, low pH and containing high level of lactate. In our study to mimic the pathological wound conditions, we have investigated one aspect of pathological conditions with high level of lactate supplement. Because of lack of sealed chamber and unable/difficult to control the experimental conditions, we were unable to proceed other independent experiments to investigate the HBO effects on blood vessel in other pathological conditions.

### **7.2.2. Limited Validation of ROS Functions**

In our study, the ROS formation has been directly detected and the relationship amongst ROS, cell damage and angiogenesis factors was analysed, but the role of ROS was more like to be deduced from our data and previous references, and direct validation is needed to provide more experimental evidence.

### **7.2.3. Limited Work of *in vivo* Investigation**

This thesis is based on *in vitro* experiment to study the HBO treatment, due to the time restriction and long procedure to get ethical approval; we are unable to investigate the effects of *in vivo* HBO treatment. For example, studies on the biochemical indexes and

genotoxic effects of HBO treatment to patients with chronic wounds will greatly help to partially fulfil the gap between clinical trial and basic scientific research.

## **7.3 Future Work**

In light of the limitations of the current work and the possible extensions, the following selected projects may be undertaken as future work.

### **7.3.1. Effects of HBO Treatment on Hypoxia Condition**

Hypoxia, is an important factor to delay healing in chronic wound and it is well known to regulate angiogenesis process. Study to investigate the effects of HBO treatment on acute or chronic hypoxia tissue or cells samples will help to understand another important aspect of pathophysiological changes in chronic wounds.

### **7.3.2. Antioxidants Implication to Validate ROS Function**

Another natural extension of the current work is to further explore the ROS function using direct experimental methods such as implication of antioxidants in our experimental system. Furthermore, it is worthy examining the antioxidant enzymes changes during and after HBO treatment, which may provide extra evidence of the HBO function to antioxidant defence system.

### **7.3.3. Calcium Changes in HBO Treatment**

In Chapter 5, we have demonstrated that HBO treatment elevate intracellular calcium concentration. However, it is desirable to devise experiment to find out the resource and the possible mechanism of the correlation of calcium changes with the ROS formation in HBO treatment. And in addition, the association of the calcium signalling system with cellular events during HBO treatment also deserves further study.

### **7.3.4. *In vivo* Experiment of HBO Treatment**

In Chapter 6, we have demonstrated that *in vitro* HBO treatment induces repairable DNA damage, and more importantly, it provides protective effects against subsequent oxidative stress. Although similar findings have been reported with *in vivo* HBO treatment to healthy volunteers, it is necessary to investigate in patients with chronic wounds for the acute as well as long-term effects of HBO treatment on DNA damage, which will provide valuable information for HBO therapy protocol selection.

## **7.4 Conclusion**

In this thesis, we have shown a systematic study on the effects of HBO treatment. The numerical results and analyses have indicated that a single therapeutic HBO treatment showed different effects on oxidative stress and tissue toxicity to blood vessel in physiological and pathological conditions. In physiological condition, HBO treatment induces neither oxidative stress nor toxic effect; while in pathological condition, HBO treatment induces oxidative stress and toxic effect. No evidence from our studies has shown that a single HBO treatment is able to induce vascular endothelial growth factor and nitric oxide production in blood vessel tissue. In another aspect, a single therapeutic HBO treatment elevates intracellular calcium levels in endothelial cells without injury to the cells, and more importantly, HBO treatment is able to protect cells from subsequently oxidative stress. The intracellular glutathione pool changes may contribute to this protective effect.

This project contributes to the pioneering work of a serial hyperbaric oxygen therapy research supported by Diving Diseases Research Centre, Plymouth and the University of Plymouth. With little preliminary work to reference in this field, we expect that our work

through this project has advanced the knowledge of understanding the physiological roles of HBO treatment and contributed to the scientific basis of HBO therapy.

# Bibliography

## [A]

- Abbott, R. E. & Schachter, D. 1994. Regional differentiation in rat aorta: L-arginine metabolism and cGMP content in vitro. *AJP - Heart and Circulatory Physiology*, 266(6): H2287-H2295.
- Adams JD Jr, L. B. M. J. 1983. Plasma glutathione and glutathione disulfide in the rat: regulation and response to oxidative stress. *J Pharmacol Exp Ther.*, 227(3): 749-54.
- ADAMS, D. J. & HILL, M. A. 2004. Potassium Channels and Membrane Potential in the Modulation of Intracellular Calcium in Vascular Endothelial Cells. *Journal of Cardiovascular Electrophysiology*, 15(5): 598-610.
- Agren, A and Arnqvist, HJ. Influence of diabetes on enzyme activities in rat aorta. *Diabete Metab.* 7(1): 19-24. 1981.
- Akimoto, M., Hashimoto, H., Shigemoto, M., Yamashita, K., & Yokoyama, I. 2000. Changes of nitric oxide and growth factors during gastric ulcer healing. *J Cardiovasc Pharmacol.*, 36(5 Suppl 1): S282-S285.
- Al-Waili, N. & Butler, G. 2006. Effects of hyperbaric oxygen on inflammatory response to wound and trauma: possible mechanism of action. *ScientificWorldJournal.*, 6: 425-441.
- Albelda, S. & Buck, C. 1990. Integrins and other cell adhesion molecules. *The FASEB Journal*, 4(11): 2868-2880.
- Albina, J., Mills, C., Henry, W. J., & Caldwell, M. 1990. Temporal expression of different pathways of L-arginine metabolism in healing wounds. *J Immunol.*, 144(10): 3877-3880.
- Albina, J., Mastrofrancesco, B., Vessella, J., Louis, C., Henry, W. J., & Reichner, J. 2001. HIF-1 expression in healing wounds: HIF-1 $\alpha$  induction in primary inflammatory cells by TNF- $\alpha$ . *Am J Physiol Cell Physiol.*, 81(6)(C1971): C1977.
- Aley, P. K., Porter, K. E., Boyle, J. P., Kemp, P. J., & Peers, C. 2005. Hypoxic Modulation of Ca<sup>2+</sup> Signaling in Human Venous Endothelial Cells: MULTIPLE ROLES FOR REACTIVE OXYGEN SPECIES. *Journal of Biological Chemistry*, 280(14): 13349-13354.
- Allen, D., Maguire, J., Mahdavian, M., Wicke, C., Marcocci, L., Scheuenstuhl, H., Chang, M., Le, A., Hopf HW, & Hunt, T. 1997. Wound hypoxia and acidosis limit neutrophil bacterial killing mechanisms. *Arch Surg.*, 132(9): 991-996.
- Alleva R, Nasole E, Di Donato F, Borghi B, Neuzil J, and Tomasetti M. 2005.  $\alpha$ -Lipoic acid supplementation inhibits oxidative damage, accelerating chronic wound healing in patients undergoing hyperbaric oxygen therapy. *Biochemical and Biophysical Research Communications*, 333(2): 404-410.
- Amadeu, T. & Costa, A. 2006. Nitric oxide synthesis inhibition alters rat cutaneous wound healing. *J Cutan Pathol.*, 33(7): 465-473.
- Anderson, D. Antioxidant defences against reactive oxygen species causing genetic and other damage. *Mutat Res.* 350(1): 103-108. 19-2-1996.
- Anderson, M. 1998. Glutathione: an overview of biosynthesis and modulation. *Chem Biol Interact*, 111-112: 1-14.
- Andrea, A. T. & Thomas, A. M. 2004. Oxygen in Wound Healing: More than a Nutrient. *World Journal of Surgery*, V28(3): 294-300.
- Andreoli, SP, Mallett, CP, and Bergstein, JM. Role of glutathione in protecting endothelial cells against hydrogen peroxide oxidant injury. *J Lab Clin Med.* 108(3): 190-198. 1986.
- Arany, I., Brysk, M., Brysk, H., & Tying, S. 1996. Regulation of inducible nitric oxide synthase mRNA levels by differentiation and cytokines in human keratinocytes. *Biochem Biophys Res Commun.*, 220(3): 618-622.
- Ardanaz, N. & Pagano, P. 2006. Hydrogen Peroxide as a Paracrine Vascular Mediator: Regulation and Signaling Leading to Dysfunction. *Experimental Biology and Medicine*, 231(3): 237-251.
- Arikan, S., Adas, G., Barut, G., Toklu, A., Kocakusak, A., Uzun, H., Kemik, O., Daduk, Y., Aydin, S., & Purisa, S. 2005. An evaluation of low molecular weight heparin and hyperbaric oxygen treatment in the prevention of intra-abdominal adhesions and wound healing. *Am J Surg.*, 189(2): 155-160.
- Arnould, T, Michiels, C, Alexander, I, and Remacle, J. Effect of hypoxia upon intracellular calcium concentration of human endothelial cells. *J Cell Physiol.* 152(1), 215-221. 1992.
- Arrigo, A. 1999. Gene expression and the thiol redox state. *Free Radic Biol Med.*, 27(9-10): 936-944.

- Arroyo, C. & Kohno, M. 1991. Difficulties encountered in the detection of nitric oxide (NO) by spin trapping techniques. A cautionary note. *Free Radic Res Commun.*, 14(2): 145-155.
- Aruoma, O., Halliwell, B., Gajewski, E., & Dizdaroglu, M. 1989. Damage to the bases in DNA induced by hydrogen peroxide and ferric ion chelates. *Journal of Biological Chemistry*, 264(34): 20509-20512.
- Asahara, T., Chen, D., Takahashi, T., Fujikawa, K., Kearney, M., Magner, M., Yancopoulos, G., & Isner, J. 1998. Tie2 receptor ligands, angiopoietin-1 and angiopoietin-2, modulate VEGF-induced postnatal neovascularization. *Circ Res.*, 83(3): 233-240.
- Aw, Tak Yee. Cellular Redox: A Modulator of Intestinal Epithelial Cell Proliferation. *News in Physiological Sciences* 18[5], 201-204. 1-10-2003.

## [B]

- Baatar, D., Jones, M., Tsugawa, K., Pai, R., Moon, W., Koh, G., Kim, I., Kitano, S., & Tarnawski, A. 2002. Esophageal ulceration triggers expression of hypoxia-inducible factor-1 alpha and activates vascular endothelial growth factor gene  
Implications for angiogenesis and ulcer healing. *American Journal of Pathology*, 161(4): 1449-1457.
- Babior, B., Kipnes, R., & Curnutte, J. 1973. Biological defense mechanisms. The production by leukocytes of superoxide, a potential bactericidal agent. *J Clin Invest.*, 52(3): 741-744.
- Bacuerle, P., Rupec, R., & Pahl, H. 1996. Reactive oxygen intermediates as second messengers of a general pathogen response. *Pathol Biol (Paris)*. 1996 Jan; 44(1): 29-35.
- Balentine, J. 1973. Selective vulnerability of the central nervous system to hyperbaric oxygen. *Adv Exp Med Biol.*, 37A: 293-298.
- Bano, D. & Nicotera, P. 2007. Ca<sup>2+</sup> signals and neuronal death in brain ischemia. *Stroke*, 38(2): 674-676.
- Barleon, B.; Sozzani, S.; Zhou, D.; Weich, H.A.; Antovani, A.; Arne, D. 1996. Migration of human monocytes in response to vascular endothelial growth factor (VEGF) is mediated via the VEGF receptor flt-1. *Blood.*, 87(8): 3336-3343.
- Bates, D. & Jones, R. 2003. The role of vascular endothelial growth factor in wound healing. *Lower Extremity Wounds*, 2(2): 107-120.
- Baumgartner, I., Pieczek, A., Manor, O., Blair, R., Kearney, M., Walsh, K., & Isner, J. 1998. Constitutive expression of phVEGF165 after intramuscular gene transfer promotes collateral vessel development in patients with critical limb ischemia. *Circulation.*, 97(12): 1114-1123.
- Bayati, S., Russell, R., & Roth, A. 1998. Stimulation of angiogenesis to improve the viability of prefabricated flaps. *Plast Reconstr Surg.*, 101(5): 1290-1295.
- Bayati, S., Russell, R., & Roth, A. 1998. Stimulation of angiogenesis to improve the viability of prefabricated flaps. *Plast Reconstr Surg.*, 101(5): 1290-1295.
- Beckman, J., Beckman, T., Chen, J., Marshall, P., & Freeman, B. 1990. Apparent hydroxyl radical production by peroxynitrite: implications for endothelial injury from nitric oxide and superoxide. *Proc Natl Acad Sci U S A*, 87(4): 1620-1624.
- Benedetti, S., Lamorgese, A., Piersantelli, M., Pagliarani, S., Benvenuti, F., & Canestrari, F. 2004. Oxidative stress and antioxidant status in patients undergoing prolonged exposure to hyperbaric oxygen. *Clinical Biochemistry*, 37(4): 312-17.
- Bennett, N. T. and Schultz, G. S. Growth factors and wound healing: part II. Role in normal and chronic wound healing. *The American Journal of Surgery* 166, 74-81. 1993.
- Bennett, N. T. and Schultz, G. S. Growth factors and wound healing: biochemical properties of growth factors and their receptors. *The American Journal of Surgery* 165, 728-737. 1993.
- Berna, N., Arnould, T., Remacle, J., and Michiels, C. Hypoxia-induced increase in intracellular calcium concentration in endothelial cells: Role of the Na<sup>+</sup>-glucose cotransporter. *Journal of Cellular Biochemistry* 84 [1], 115-131. 2002.
- Berridge, M. 1997. Elementary and global aspects of calcium signalling. *J Physiol.*, 499 ( Pt 2): 291-306.
- Berridge, M., Lipp, P., & Bootman, M. 2000. The versatility and universality of calcium signalling. *Nat Rev Mol Cell Biol*, 1(1): 11-21.
- Berse, B., Brown, L., Van De Water, L., Dvorak, H., & Senger, D. 1992. Vascular permeability factor (vascular endothelial growth factor) gene is expressed differentially in normal tissues, macrophages, and tumors. *Mol Biol Cell.*, 3(2): 211-220.
- Blacher, S., Devy, L., Burbridge, M., Roland, G., Tucher, G., Noel, A., & Foidart, J. 2001. Improved quantification of angiogenesis in rat aortic ring assay. *Angiogenesis*, 4: 133-142.

- Blough, N. & Zafiriou, O. 1985. Reaction of superoxide with nitric oxide to form peroxonitrite in alkaline aqueous solution. *Inorganic Chemistry*, 24: 3502-3504.
- Bootman, M. D., Taylor, C. W., & Berridge, M. J. 1992. The thiol reagent, thimerosal, evokes Ca<sup>2+</sup> spikes in HeLa cells by sensitizing the inositol 1,4,5-trisphosphate receptor. *Journal of Biological Chemistry*, 267(35): 25113-25119.
- Bootman, M. D., Berridge, M. J., & Roderick, H. L. 2002. Calcium Signalling: More Messengers, More Channels, More Complexity. *Current Biology*, 12(16): R563-R565.
- Borle, A. 1981. Control, Modulation, and regulation of cell calcium. *Rev Physiol Biochem Pharmacol.*, 90.: 13-153.
- Bouloumie, A., Schini-Kerth, V. B., & Busse, R. 1999. Vascular endothelial growth factor up-regulates nitric oxide synthase expression in endothelial cells. *Cardiovascular Research*, 41(3): 773-780.
- Brakora, M. & Sheffield, P. 1995. Hyperbaric oxygen therapy for diabetic wounds. *Clin Pod Med Surg*, 12(1): 105-117.
- Brawn, K. & Fridovich, I. 1981. DNA strand scission by enzymically generated oxygen radicals. *Arch Biochem Biophys.*, 206(2): 414-419.
- Brogi, E., Wu, T., Namiki, A., & Isner, J. 1994. Indirect angiogenic cytokines upregulate VEGF and bFGF gene expression in vascular smooth muscle cells, whereas hypoxia upregulates VEGF expression only. *Circulation.*, 90(2): 649-652.
- Bueckl, C., Kaestle, S., Kerem, A., Habazettl, H., Krombach, F., Kuppe, H., & Kuebler, W. M. 2006. Hyperoxia-Induced Reactive Oxygen Species Formation in Pulmonary Capillary Endothelial Cells In Situ. *American Journal of Respiratory Cell and Molecular Biology*, 34(4): 453-463.
- Brune, B and Zhou, J. Hypoxia inducible factor-1 and angiogenesis. *Curr Med Chem* . 2003.
- Bultynck G, Szlufcik K, Kasri NN, Assefa Z, Callewaert G, Missiaen L, Parys JB, De Smedt H. 2007. Thimerosal stimulates Ca<sup>2+</sup> flux through inositol 1,4,5-trisphosphate receptor type 1, but not type 3, via modulation of an isoform-specific Ca<sup>2+</sup>-dependent intramolecular interaction. *Biochem J*. 2004 Jul 1; 381(Pt 1):87-96.
- Buras, J; Stahl, G; Svoboda, K; & Reenstra, W. 2000. Hyperbaric oxygen downregulates ICAM-1 expression induced by hypoxia and hypoglycemia: the role of NOS. *Am.J.Physiol.Cell Physiol.*, 278: C292-C302.
- Burke, P., Lehmann-bruinsma, K., & Powell, J. 1995. Vascular endothelial growth factor causes endothelial proliferation after vascular injury. *Biochem Biophys Res Commun.*, 207(1)(348): 354.
- Busse, R., Luckhoff, A., & Mulsch, A. 1991. Cellular mechanisms controlling EDRF/NO formation in endothelial cells. *Basic Res Cardiol.*, 86 Suppl 2: 7-16.

## [C]

- Camello-Almaraz MC, Pozo MJ, Murphy MP, Camello PJ. 2006. Mitochondrial production of oxidants is necessary for physiological calcium oscillations. *J Cell Physiol.*, 206(2):487-94.
- Camello-Almaraz, C., Gomez-Pinilla, P. J., Pozo, M. J., & Camello, P. J. 2006. Mitochondrial reactive oxygen species and Ca<sup>2+</sup> signaling. *AJP - Cell Physiology*, 291(5): C1082-C1088.
- Carlisle, R; Rhoads, CA; Aw, TY; Harrison, L. 2002. Endothelial cells maintain a reduced redox environment even as mitochondrial function declines. *AJP - Cell Physiology*, 283(6): C1675-C1686.
- Carter, T. D. & Pearson, J. D. 1992. Regulation of Prostacyclin Synthesis in Endothelial Cells. *News in Physiological Sciences*, 7(2): 64-69.
- Chang KY, Tsai PS, Huang TY, Wang TY, Yang S, Huang CJ. HO-1 Mediates the Effects of HBO Pretreatment Against Sepsis. *J Surg Res*. 136(1): 143-53. 2006.
- Chavko, M., Xing, G. Q., & Keyser, D. O. 2001. Increased sensitivity to seizures in repeated exposures to hyperbaric oxygen: role of NOS activation. *Brain Research*, 900(2): 227-233.
- Chin-Dusting, J., Alexander, C., Arnold, P., Hodgson, W., Lux, A., & Jennings, G. 1996. Effects of in vivo and in vitro L-arginine supplementation on healthy human vessels. *J Cardiovasc Pharmacol*, 28(1): 158-166.
- Cho, C. & Lo, J. 1998. Dressing the part. *Dermatol Clin.*, 16(1): 25-47.
- Cho, M., Hunt, T., & Hussain, M. 2001. Hydrogen peroxide stimulates macrophage vascular endothelial growth factor release. *AJP - Heart and Circulatory Physiology*, 280: H2357-H2363.
- Chu SJ, Li MH, Hsu CW, Tsai SH, Lin SH, Huang KL. Influence of hyperbaric oxygen on tumor necrosis factor-alpha and nitric oxide production in endotoxin-induced acute lung injury in rats. *Pulm Pharmacol Ther. Epub*. 2006.

- Chu, S. J., Li, M. H., Hsu, C. W., Tsai, S. H., Lin, S. H., & Huang, K. L. Influence of hyperbaric oxygen on tumor necrosis factor-[alpha] and nitric oxide production in endotoxin-induced acute lung injury in rats. *Pulmonary Pharmacology & Therapeutics*, In Press, Corrected Proof.
- Chun-Chung, L., Shu-Chen, C., Shio-Chwen, T., Bao-Wei, W., Ya-Chen, L., Horng-Mo, L., & Kou-Gi, S. 2006. Hyperbaric oxygen induces VEGF expression through ERK, JNK and c-Jun/AP-1 activation in human umbilical vein endothelial cells. *Journal of Biomedical Science*, V13(1): 143-156.
- Ciaravino ME, Friedell ML Kammerlocher TC. Is hyperbaric oxygen a useful adjunct in the management of problem lower extremity wounds? *Ann Vasc Surg*. 10(6): 558-562. 1996.
- Clauss, M., Weich, H., Breier, G., Knies, U., Rockl, W., Waltenberger, J., & Risau, W. 1996. The vascular endothelial growth factor receptor Flt-1 mediates biological activities. Implications for a functional role of placenta growth factor in monocyte activation and chemotaxis. *J Biol Chem.*, 271(30): 17629-17634.
- Collin, A., Duthie, S., & Dobson, V. 1993. Direct enzymic detection of endogenous oxidative base damage in human lymphocyte DNA. *Carcinogenesis.*, 14(9): 1733-1735.
- Collin, A., Ma, A., & Duthie, S. 1995. The kinetics of repair of oxidative DNA damage (strand breaks and oxidised pyrimidines) in human cells. *Mutat Res.*, 336((1):): 69-77.
- Collin, AR, Dusinska, M, Gedik, CM, and Stetina, R. Oxidative damage to DNA: do we have a reliable biomarker? *Environ Health Perspect*. 104 Suppl 3: 465-469. 1996.
- Collins, AR. The comet assay for DNA damage and repair: principles, applications, and limitations. *Mol Biotechnol*. 26[3], 249-261. 2004.
- Collins, A. 2005. Assays for oxidative stress and antioxidant status: applications to research into the biological effectiveness of polyphenols. *American Journal of Clinical Nutrition*, 81(1): 261S-267.
- Conconi, MT, Baiguera, S, Guidolin, D, Furlan, C, Menti, AM, Vigolo, S, Belloni, AS, Parnigotto, PP, and Nussdorfer, GG. Effects of hyperbaric oxygen on proliferative and apoptotic activities and reactive oxygen species generation in mouse fibroblast 3T3/J2 Cell line. *Journal of Investigative Medicine* 51(4), 227-232. 2003.
- Constant, J., Suh, D., Hussain, M., & Hunt, T. 1996. Wound healing angiogenesis: The metabolic basis of repair. In: M.E. Maragoudakis and North Atlantic Treaty Organization. Scientific Affairs Division, Eds. New York: Plenum Press, 1996:ix. In M. Margoudakis (Ed.), *Molecular, cellular, and clinical aspects of angiogenesis*: 298. New York and London: Plenum Publishing Corporation.
- Constant, J., Feng, J., Zabel, D., Yuan, H., Suh, D., Scheuenstuhl, H., Hunt, T., & Hussain, M. 2000. Lactate elicits vascular endothelial growth factor from macrophages: a possible alternative to hypoxia. *Wound Repair and Regeneration*, 8: 353-360.
- Cook, PR., Brazell, IA., & Jost, E. 1976. Characterization of nuclear structures containing superhelical DNA. *Journal of Cell Science*, 22(2): 303-324.
- Cooper, CE., Patel, RP., Brookes, PS., & rley-USmar, VM. 2002. Nanotransducers in cellular redox signaling: modification of thiols by reactive oxygen and nitrogen species. *Trends in Biochemical Sciences*, 27(10): 489-492
- Corral, C., Siddiqui, A., Wu, L., Farrell, C., Lyons, D., & Mustoe, T. 1999. Vascular endothelial growth factor is more important than basic fibroblastic growth factor during ischemic wound healing. *Arch Surg.*, 134(2): 200-205.
- Cotgreave, I. & Gerdes, R. 1998. Recent trends in glutathione biochemistry--glutathione-protein interactions: a molecular link between oxidative stress and cell proliferation? *Biochem Biophys Res Commun.*, 242(1):1-9.
- Crake T, Kirby MS, Poole-Wilson PA. 1987. Potassium efflux from the myocardium during hypoxia: role of lactate ions. *Cardiovasc Res.*, 21(12): 886-891.
- Crovetti G, Martinelli G, Issi M, Barone M, Guizzardi M, Campanati B, Moroni M, and Carabelli A. 2004. Platelet gel for healing cutaneous chronic wounds. *Transfusion and Apheresis Science*, 30(2): 145-151.

**[D]**

- D'Agnillo, F. & Alayash, A. I. 2000. Interactions of hemoglobin with hydrogen peroxide alters thiol levels and course of endothelial cell death. *AJP - Heart and Circulatory Physiology*, 279(4): H1880-H1889.
- D'Amours, D., Desnoyers, S., D'Silva, I., & Poirier, G. 1999. Poly(ADP-ribosyl)ation reactions in the regulation of nuclear functions. *Biochem J.*, 342 ( Pt 2): 249-268.
- Davis, JC. The use of adjuvant hyperbaric oxygen in treatment of the diabetic foot. *Clinics in Podiatric Medicine and Surgery* 4, 429-437. 1987.

- Dawson, NS., Zawieja, DC., Wu, MH., & Granger, HJ. 2006. Signaling pathways mediating VEGF165-induced calcium transients and membrane depolarization in human endothelial cells. *The FASEB Journal*, 20(7): 991-993.
- Demchenko, I. T., Boso, A. E., Bennett, P. B., Whorton, A. R., & Piantadosi, C. A. 2000. Hyperbaric Oxygen Reduces Cerebral Blood Flow by Inactivating Nitric Oxide. *Nitric Oxide*, 4(6): 597-608.
- Demchenko, IT., Atochin, DN., Boso, AE., Astern, J., Huang, PL., & Piantadosi, CA. 2003. Oxygen seizure latency and peroxynitrite formation in mice lacking neuronal or endothelial nitric oxide synthases. *Neuroscience Letters*, 344(1): 53-56.
- Dennog, C., Hartmann, A, Frey, G, and Speit, G. Detection of DNA damage after hyperbaric oxygen (HBO) therapy. *Mutagenesis*. 11(6): 605-609. 1996.
- Dennog, C., Gedik, C., Wood, S., & Speit, G. 1999. Analysis of oxidative DNA damage and HPRT mutations in humans after hyperbaric oxygen treatment. *Mutation Research/Fundamental and Molecular Mechanisms of Mutagenesis*, 431(2): 351-359.
- Dennog, C., Radermacher, P., Barnett, Y. A., & Speit, G. 1999. Antioxidant status in humans after exposure to hyperbaric oxygen. *Mutation Research/Fundamental and Molecular Mechanisms of Mutagenesis*, 428(1-2): 83-89.
- Detmar, M., Brown, L., Berse, B., Jackman, R., Elicker, B., Dvorak, H., & Claffey, K. 1997. Hypoxia regulates the expression of vascular permeability factor/vascular endothelial growth factor (VPF/VEGF) and its receptors in human skin. *J Invest Dermatol.*, 108(3): 263-268.
- Dickinson, DA, Moellering, DR, Iles, KE, Patel, RP, Levonen, AL, Wigley, A, Darley-Usmar, VM, and Forman, HJ. Cytoprotection against oxidative stress and the regulation of glutathione synthesis. *Biol Chem*. 384(4): 527-537. 2003.
- Dimitrijevič, S., Paranjape, S., Wilson, J., Gracy, R., & Mills, J. 1999. Effect of hyperbaric oxygen on human skin cells in culture and in human dermal and skin equivalents. *Wound Repair and Regeneration*, 7: 53-64.
- Dizdaroglu, M., Rao, G., Halliwell, B., & Gajewski, E. 1991. Damage to the DNA bases in mammalian chromatin by hydrogen peroxide in the presence of ferric and cupric ions. *Arch Biochem Biophys.*, 285(2): 317-324.
- Dolor, RJ., Hurwitz, LM., Mirza, Z., Strauss, HC., & Whorton, AR. 1992. Regulation of extracellular calcium entry in endothelial cells: role of intracellular calcium pool. *AJP - Cell Physiology*, 262(1): C171-C181.
- Drinkwater, S., Smith, A., Sawyer, B., & Burnand, K. 2002. Effect of venous ulcer exudates on angiogenesis in vitro. *Br J Surg.*, 89(6): 709-713.
- Droge, W. 2002. Free Radicals in the Physiological Control of Cell Function. *Physiological Reviews*, 82(1): 47-95.
- Duchen, M. R. 2000. Mitochondria and calcium: from cell signalling to cell death. *The Journal of Physiology Online*, 529(1): 57-68.
- Dulak, J., Jozkowicz, A., Dembinska-Kiec, A., Guevara, I., Zdzienicka, A., Zmudzinska-Grochot, D., Florek, I., Wojtowicz, A., Szuba, A., & Cooke, J. 2000. Nitric oxide induces the synthesis of vascular endothelial growth factor by rat vascular smooth muscle cells. *Arterioscler Thromb Vasc Biol.*, 20(3): 659-666.
- Dulak, J. & Jozkowicz, A. 2003. Regulation of vascular endothelial growth factor synthesis by nitric oxide: facts and controversies. *Antioxidants & Redox Signaling*, 5(1): 123-132.
- Dvorak, H. 1986. Tumors: wounds that do not heal. Similarity between tumor stroma generation and wound healing. *N Engl J Med*, 315: 1650-1658.

## [E]

- Eaton, D. L. & Bammler, T. K. 1999. Concise review of the glutathione S-transferases and their significance to toxicology. *Toxicological Sciences*, 49(2): 156-164.
- Edwards, R. & Harding, K. 2004. Bacteria and wound healing. *Curr Opin Infect Dis.*, 17(2): 91-96.
- Eken, A., Aydin, A., Sayal, A., Ustundag, A., Duydu, Y., & duNDAR, K. 2005. The effects of hyperbaric oxygen treatment on oxidative stress and SCE frequencies in humans. *Clin Biochem.*, 38(12): 1133-1137.
- Elayan, I. M., Axley, M. J., Prasad, P. V., Ahlers, S. T., & AuKER, C. R. 2000. Effect of Hyperbaric Oxygen Treatment on Nitric Oxide and Oxygen Free Radicals in Rat Brain. *Journal of Neurophysiology*, 83(4): 2022-2029.

- Eliceiri, B. & Chersesh, D. 1999. The role of alphav integrins during angiogenesis: insights into potential mechanisms of action and clinical development. *The Journal of Clinical Investigation*, 103: 1227-1231.
- Ellman, G. 1959. *Arch Biochem Biophys.*, 82: 70-77.
- Elson, D., Ryan, H., Snow, J., Johnson, R., & Arbeit, J. 2000. Coordinate up-regulation of hypoxia inducible factor 1a and HIF-1 target genes during multi-stage epidermal carcinogenesis and wound healing. *Cancer Research*, 60(Nov 1): 6189-6195.
- Emeis, J. J., Eijnden-Schrauwen, Y. v. d., Hoogen, C. M., Priester, W. d., Westmuckett, A., & Lupu, F. 1997. An Endothelial Storage Granule for Tissue-Type Plasminogen Activator. *The Journal of Cell Biology*, 139(1): 245-256.
- Engvall, E. & Perlman, P. 1971. Enzyme-linked immunosorbent assay (ELISA). Quantitative assay of immunoglobulin G. *Immunochemistry.*, 8(9): 871-874.
- Ermak, G. & Davies, K. J. A. 2002. Calcium and oxidative stress: from cell signaling to cell death. *Molecular Immunology*, 38(10): 713-721.
- Etlik, O, Tomur, A, Dundar, K, Erdem, A, & Gundogan, N. 1997. The effect of antioxidant vitamins E and C on lipoperoxidation of erythrocyte membranes during hyperbaric oxygenation. *J Basic Clin Physiol Pharmacol.*, 8(4): 269-77.

## [F]

- Fachling, M; kroll, J; Fohr, K; Fellbrich, G; Mayr, U; Trischler, G; Waltenberger, J. 2002. Essential role of calcium in vascular endothelial growth factor A-induced signaling: mechanism of the antiangiogenic effect of carboxyamidotriazole. *The FASEB Journal*, 16(13): 1805-1807.
- Faglia, E., Favales, F., Aldeghi, A., Calia, P., Quarantiello, A., Oriani, G., Michael, M., Campagnoli, P., & Morabito, A. 1996. Adjunctive systemic hyperbaric oxygen therapy in treatment of severe prevalently ischemic diabetic foot ulcer. A randomized study. *Diabetes Care.*, 19(12): 1338-1343.
- Feclisch, M. & Noack, E. A. 1987. Correlation between nitric oxide formation during degradation of organic nitrates and activation of guanylate cyclase. *European Journal of Pharmacology*, 139(1): 19-30.
- Feig, D. I., Reid, T. M., & Loeb, L. A. 1994. Reactive Oxygen Species in Tumorigenesis. *Cancer Research*, 54(7\_Supplement): 1890s-1894.
- Felder, C., MacArthur, L., Ma, A., Gusovsky, F., & Kohn, E. 1993. Tumor-suppressor function of muscarinic acetylcholine receptors is associated with activation of receptor-operated calcium influx. *Proc Natl Acad Sci U S A.*, 90(5): 1706-1710.
- Feng, W., Liu, G., Allen, P. D., & Pessah, I. N. 2000. Transmembrane Redox Sensor of Ryanodine Receptor Complex. *Journal of Biological Chemistry*, 275(46): 35902-35907.
- Ferrara, N. & vis-Smyth, T. 1997. The Biology of Vascular Endothelial Growth Factor. *Endocrine Reviews*, 18(1): 4-25.
- Fife, C., Buyukcakar, C., Otto, G., Sheffield, P., Warriner, R., Love, T., & Mader, J. 2002. The predictive value of transcutaneous oxygen tension measurement in diabetic lower extremity ulcers treated with hyperbaric oxygen therapy: a retrospective analysis of 1144 patients. *Wound Repair and Regeneration*, 10(4)(Jul-Aug): 198-207.
- Flint, D. H., Tuminello, J. F., & Emptage, M. H. 1993. The inactivation of Fe-S cluster containing hydrolyases by superoxide. *Journal of Biological Chemistry*, 268(30): 22369-22376.
- Folkman, J. 1997. Angiogenesis and angiogenesis inhibition: an overview. *EXS*, 79: 1-8.
- Ford, P. C., Wink, D. A., & Stanbury, D. M. 1993. Autoxidation kinetics of aqueous nitric oxide. *FEBS Letters*, 326(1-3): 1-3.
- Forsythe, J., Jiang, B., Iyer, N., Agani, F., Leung, S., Koos, R., & Semenza, G. 1996. Activation of vascular endothelial growth factor gene transcription by hypoxia-inducible factor 1. *Mol Cell Biol.*, 16(9): 4604-4613.
- Frank, S, Hubner, G, Breier, G, Longaker, MT, Greenhalgh, DG, and Werner, S. Regulation of vascular endothelial growth factor expression in cultured keratinocytes. *The Journal of Biological Chemistry* 270(21)[May 26], 12607-12613. 1995.
- Frank, S., Stallmeyer, B., Kampfner, H., Kolb, N., & Pfeilschifter, J. 1999. Nitric oxide triggers enhanced induction of vascular endothelial growth factor expression in cultured keratinocytes (HaCaT) and during cutaneous wound repair. *The FASEB Journal*, 13(14): 2002-2014.
- Fridovich, I. 1978. The biology of oxygen radicals. *Science.*, 201(4359): 875-880.
- Friedberg EC, Walker GC, Siede W, Wood RD, Schultz RA, Ellenberger T. 2006. DNA Repair and Mutagenesis.

Fusi, F., Saponara, S., Gagov, H., & Sgaragli, G. 2001. 2,5-Di-*t*-butyl-1,4-benzohydroquinone (BHQ) inhibits vascular L-type Ca<sup>2+</sup> channel via superoxide anion generation. *Br J Pharmacol*, 133(7): 988-996.

## [G]

- Gabb, G. & Robin, E. 1987. Hyperbaric oxygen. A therapy in search of diseases. *Chest.*, 92(6): 1074-1082.
- Gabbiani, G. 1996. The cellular derivation and the life span of the myofibroblast. *Pathol Res Pract.*, 192(7)(708): 711.
- Gajendrareddy, P. K., Sen, C. K., Horan, M. P., & Marucha, P. T. 2005. Hyperbaric oxygen therapy ameliorates stress-impaired dermal wound healing. *Brain, Behavior, and Immunity*, 19(3): 217-222.
- Ghani, Q., Wagner, S., & Hussain, M. 2003. Role of ADP-ribosylation in wound repair. The contributions of Thomas K. Hunt, MD. *Wound Repair Regen.*, 11(6): 439-444.
- Ghigo, D., Alessio, P., Foco, A., Bussolino, F., Costamagna, C., Heller, R., Garbarino, G., Pescarmona, G. P., & Bosia, A. 1993. Nitric oxide synthesis is impaired in glutathione-depleted human umbilical vein endothelial cells. *AJP - Cell Physiology*, 265(3): C728-C732.
- Gifford, S. M., Grummer, M. A., Pierre, S. A., Austin, J. L., Zheng, J., & Bird, I. M. 2004. Functional characterization of HUVEC-CS: Ca<sup>2+</sup> signaling, ERK 1/2 activation, mitogenesis and vasodilator production. *Journal of Endocrinology*, 182(3): 485-499.
- Gill, A. L. & Bell, C. N. A. 2004. Hyperbaric oxygen: its uses, mechanisms of action and outcomes. *QJM*, 97(7): 385-395.
- Gimbel, M. & Hunt, T. 1999. Wound healing and hyperbaric oxygenation. In H. Whelan & E. Kindwall (Eds.), *Hyperbaric Medicine Practice*: 169-207. Flagstaff, Ariz: Best Publishing Co.
- Giuliani, R., Bastaki, M., Coltrini, D., & Presta, M. 1999. Role of endothelial cell extracellular signal-regulated kinase1/2 in urokinase-type plasminogen activator upregulation and in vitro angiogenesis by fibroblast growth factor-2. *Journal of Cell Science*, 112(15): 2597-2606.
- Goldstein LJ, Gallagher KA Bauer SM Bauer RJ Baireddy V Liu ZJ Buerk DG Thom SR Velazquez OC. Endothelial progenitor cell release into circulation is triggered by hyperoxia-induced increases in bone marrow nitric oxide. *Stem Cells*. 24(10): 2309-18. 6.
- Goldstein, S. & Czapski, G. 1995. Kinetics of Nitric Oxide Autoxidation in Aqueous Solution in the Absence and Presence of Various Reductants. The Nature of the Oxidizing Intermediates. *J.Am.Chem.SOC.*, 117: 12078-12084.
- Gordillo, G. & Sen, C. 2003. Revisiting the essential role of oxygen in wound healing. *The American Journal of Surgery*, 186: 259-263.
- Granger DL, Taintor RR, Boockvar KS, Hibbs JB Jr. 1996. Measurement of nitrate and nitrite in biological samples using nitrate reductase and Griess reaction. *Methods Enzymol.*, 268: 142-151.
- Grasselli, F., Basini, G., Bussolati, S., & Bianco, F. 2005. Cobalt chloride, a hypoxia-mimicking agent, modulates redox status and functional parameters of cultured swine granulosa cells. *Reproduction, Fertility and Development*, 17(7): 715-720.
- Green LC, Wagner DA, Glogowski J, Skipper PL, Wishnok JS, Tannenbaum SR. 1982. Analysis of nitrate, nitrite, and [15N]nitrate in biological fluids. *Anal Biochem.*, 126(1): 131-138.
- Green, H. & Oldberg, B. 1964. Collagen and cell protein synthesis by established mammalian fibroblast line. *Nature*. 1964 Oct 24; 204: 347-349.
- Gregorevic P, L. G. W. DA. 2001. Hyperbaric oxygen modulates antioxidant enzyme activity in rat skeletal muscles. *Eur J Appl Physiol.*, 86(1): 24-27.
- Griendling, K., Minieri, C., Ollerenshaw, J., & Alexander, R. 1994. Angiotensin II stimulates NADH and NADPH oxidase activity in cultured vascular smooth muscle cells. *Circ Res.*, 74(6): 1141-1148.
- Griendling, K., Sorescu, D., Lassegue, B., & Ushio-Fukai, M. 2000. Modulation of protein kinase activity and gene expression by reactive oxygen species and their role in vascular physiology and pathophysiology. *Arteriosclerosis, Thrombosis, and Vascular Biology*, 20: 2175-2183.
- Griffioen, AW. & Molema, G. 2000. Angiogenesis: potentials for pharmacologic intervention in the treatment of cancer, cardiovascular diseases, and chronic inflammation. *Pharmacological Review*, 52(2): 237-268.
- Griffith, O. 1980. Determination of glutathione and glutathione disulfide using glutathione reductase and 2-vinylpyridine. *Anal Biochem.*, 106(1): 207-12.
- Grisham, M., Johnson, G., & Lancaster, J. J. 1996. Quantitation of nitrate and nitrite in extracellular fluids. *Methods Enzymol.*, 268: 237-246.

- Groger, M., Speit, G., Radermacher, P., & Muth, C. M. 2005. Interaction of hyperbaric oxygen, nitric oxide, and heme oxygenase on DNA strand breaks in vivo. *Mutation Research/Fundamental and Molecular Mechanisms of Mutagenesis*, 572(1-2): 167-172.
- Gross, S. S., Stuehr, D. J., Aisaka, K., Jaffe, E. A., Levi, R., & Griffith, O. W. 1990. Macrophage and endothelial cell nitric oxide synthesis: Cell-type selective inhibition by NG-aminoarginine, NG-nitroarginine and NG-methylarginine. *Biochemical and Biophysical Research Communications*, 170(1): 96-103.
- Gunter, T. & Pfeiffer, D. 1990. Mechanisms by which mitochondria transport calcium. *Am J Physiol*, 258: C755-C786.
- Guo, D., Jia, Q., Song, H. Y., Warren, R. S., Donner, D. B. (1995) Vascular endothelial cell growth factor promotes tyrosine phosphorylation of mediators of signal transduction that contain SH2 domains. Association with endothelial cell proliferation. *J. Biol. Chem.* 270,6729-6733
- Gutteridge, JM. Biological origin of free radicals, and mechanisms of antioxidant protection. *Chem Biol Interact.* 91(2-3): 133-140. 1994.
- Gutteridge, JMC and Halliwell, BARR. Free Radicals and Antioxidants in the Year 2000: A Historical Look to the Future. *Annals of the New York Academy of Sciences* 899[1], 136-147. 1-1-2000.
- [H]**
- Hadri L, Pavoine C, Lipskaia L, Yacoubi S, & Lompre AM 2006. Transcription of the sarcoplasmic/endoplasmic reticulum Ca<sup>2+</sup>-ATPase type 3 gene, ATP2A3, is regulated by the calcineurin/NFAT pathway in endothelial cells. *Biochem J.*, 394(Pt 1):27-33..
- Hagioka, S., Takeda, Y., Zhang, S., Sato, T., & Morita, K. 2005. Effects of 7-nitroindazole and N-nitro-l-arginine methyl ester on changes in cerebral blood flow and nitric oxide production preceding development of hyperbaric oxygen-induced seizures in rats. *Neuroscience Letters*, 382(3): 206-210.
- Handy, R. D., Gow, I. F., Ellis, D., & Flatman, P. W. 1996. Na-dependent Regulation of Intracellular Free Magnesium Concentration in Isolated Rat Ventricular Myocytes. *Journal of Molecular and Cellular Cardiology*, 28(8): 1641-1651.
- Harabin, AL., Braisted, JC., and Flynn, ET. Response of antioxidant enzymes to intermittent and continuous hyperbaric oxygen. *Journal of Applied Physiology* 69, 328-335. 1990.
- Haron, Z., Raleigh, J., Greenberg, C., & Dewhirst, M. 2000. Early wound healing exhibits cytokine surge without evidence of hypoxia. *Annals of Surgery*, 231(1): 137-147.
- Hartree, E. 1972. Determination of protein: a modification of the Lowry method that gives a linear photometric response. *Anal Biochem.*, 48(2): 422-427.
- He, H., Venema, V. J., Gu, X., Venema, R. C., Marrero, M. B., Caldwell, R. B. (1999) Vascular endothelial growth factor signals endothelial cell production of nitric oxide and prostacyclin through flk-1/KDR activation of c-Src. *J. Biol. Chem.* 274,25,130-25,135
- Heck, D., Laskin, D., Gardner, C., & laskin, J. 1992. Epidermal growth factor suppresses nitric oxide and hydrogen peroxide production by keratinocytes. Potential role for nitric oxide in the regulation of wound healing. *J Biol Chem.*, 267(30): 21277-21280.
- Hein, T. W., Xu, W., & Kuo, L. 2006. Dilation of Retinal Arterioles in Response to Lactate: Role of Nitric Oxide, Guanylyl Cyclase, and ATP-Sensitive Potassium Channels. *Investigative Ophthalmology Visual Science*, 47(2): 693-699.
- Hink, J., Thom, S. R., Simonsen, U., Rubin, I., & Jansen, E. 2006. Vascular reactivity and endothelial NOS activity in rat thoracic aorta during and after hyperbaric oxygen exposure. *AJP - Heart and Circulatory Physiology*, 291(4): H1988-H1998.
- Hiratsuka, S., Minowa, O., Kuno, J., Noda, T., & Shibuya, M. 1998. Flt-1 lacking the tyrosine kinase domain is sufficient for normal development and angiogenesis in mice. *Proc Natl Acad Sci U S A.*, 95(16): 9349-9354.
- Hood, J., Meininger, C., Ziche, M., & Granger, H. 1998. VEGF upregulates ecNOS message, protein, and NO production in human endothelial cells. *AJP - Heart and Circulatory Physiology*, 274: H1054-H1058.
- Hostikka, SL and Tryggvason, K. The complete primary structure of the  $\alpha 2$  chain of human type IV collagen and comparison with the  $\alpha 1(IV)$  chain. *J.Bio.Chem.* 263, 19488-19493. 1988.
- Howdieshell, T., Riegner, C., Gupta, V., Callaway, D., Grembowica, K., Sathyanarayana, & McNeil, P. 1998. Normoxia wound fluid contains high levels of vascular endothelial growth factor. *Annals of Surgery*, 228(5): 707-715.

- Howdieshell, T., Callaway, D., Webb, W., Gaines, M., Procter, C. J., Sathyanarayana, Pollock, J., Brock, T., & McNeil, P. 2001. Antibody neutralization of vascular endothelial growth factor inhibits wound granulation tissue formation. *Surg Res.*, 96(2): 173-182.
- Howdieshell, T., Webb, W., Sathyanarayana, & McNeil, P. 2003. Inhibition of inducible nitric oxide synthase results in reductions in wound vascular endothelial growth factor expression, granulation tissue formation, and local perfusion. *Surgery.*, 133(5): 528-537.
- Hu, Q. & Ziegelstein, R. C. 2000. Hypoxia/Reoxygenation Stimulates Intracellular Calcium Oscillations in Human Aortic Endothelial Cells. *Circulation*, 102(20): 2541-2547.
- Hu, Q., Yu, Z. X., Ferrans, V. J., Takeda, K., Irani, K., & Ziegelstein, R. C. 2002. Critical Role of NADPH Oxidase-derived Reactive Oxygen Species in Generating Ca<sup>2+</sup> Oscillations in Human Aortic Endothelial Cells Stimulated by Histamine. *Journal of Biological Chemistry*, 277(36): 32546-32551.
- Hua HT,Albadawi H,Entabi F,Conrad M,Stoner MC,Meriam BT,Sroufe R,Houser S,Lamuraglia M,Watkins MT. 2005. Polyadenosine diphosphate-ribose polymerase inhibition modulates skeletal muscle injury following ischemia reperfusion. *Arch Surg.*, 140(4): 344-351.
- Huang TY, Tsai PS Wang TY Huang CL Huang CJ. Hyperbaric oxygen attenuation of lipopolysaccharide-induced acute lung injury involves heme oxygenase-1. *Acta Anaesthesiol Scand.* 49(9): 1293-301. 2005.
- Hunt, T., Twomey, P., Zederfeldt, B., & Dunphy, JE. 1967. Respiratory gas tensions and pH in healing wounds. *American Journal of Surgery*, 114: 302-307.
- Hunt, T. & Pai, M. 1972. The effect of varying ambient oxygen tensions on wound metabolism and collagen synthesis. *Surgery, Gynecology & Obstetrics*, 135: 561-567.
- Hunt, TK, Linsey, M., Grislis, G., Sonne, M., and Jawetz, E. The effect of differing ambient oxygen tensions on wound infection. *Annals of Surgery* 181, 35-39. 1974.
- Hunt, T., Conolly, W., Aronson, S., & Goldstein, P. 1978. Anaerobic metabolism and wound healing: an hypothesis for the initiation and cessation of collagen synthesis in wounds. *Am J Surg*, 135: 328-332.
- Hunt, T., Banda, M., & Silver, I. 1985. Cell interaction in post-traumatic fibrosis. *Ciba Found Symp.*, 114: 127-149.
- Hunt, T. & Hussain, M. 1992. Wound microenvironment. In I. Cohen, R. diegelmann, & W. Lindblad (Eds.), *Wound healing: biochemical and clinical aspects.*: 274-281. Philadelphia: Saunders..
- Hussain, M., Ghani, Q., & Hunt, T. 1989. Inhibition of prolyl hydroxylase by poly(ADP-ribose) and phosphoribosyl-AMP. Possible role of ADP-ribosylation in intracellular prolyl hydroxylase regulation. *J Biol Chem.*, 264(14): 7850-7855.
- Hyslop PA,Hinshaw DB,Halsey WA Jr,Schraufstatter IU,Sauerheber RD,Spragg RG,Jackson JH,Cochrane CG. 1988. Mechanisms of oxidant-mediated cell injury. The glycolytic and mitochondrial pathways of ADP phosphorylation are major intracellular targets inactivated by hydrogen peroxide. *J Biol Chem.*, 263(4): 1665-1675.
- [I]**
- Ichas, F. & Mazat, J. 1998. From calcium signaling to cell death: two conformations for the mitochondrial permeability transition pore. Switching from low- to high-conductance state. *Biochim Biophys Acta.*, 1366(1-2): 33-50.
- Ichas, F., Jouaville, L. S., & Mazat, J. P. 1997. Mitochondria Are Excitable Organelles Capable of Generating and Conveying Electrical and Calcium Signals. *Cell*, 89(7): 1145-1153.
- Ignarro, L. J., Fukuto, J. M., Griscavage, J. M., Rogers, N. E., & Byrns, R. E. 1993. Oxidation of Nitric Oxide in Aqueous Solution to Nitrite but not Nitrate: Comparison with Enzymatically Formed Nitric Oxide From L-Arginine. *Proceedings of the National Academy of Sciences*, 90(17): 8103-8107.
- Ignarro, L. 2002. Nitric oxide as a unique signaling molecule in the vascular system: a historical overview. *J Physiol Pharmacol.*, 53(4 Pt 1): 503-514.
- Ikeda, E., Achen, M., Breier, G., & Risau, W. 1995. Hypoxia-induced transcriptional activation and increased mRNA stability of vascular endothelial growth factor in C6 glioma cells. *J Biol Chem*, 270(34): 19761-66.
- Im, M. & Hoopes, J. 1970. Enzyme activities in the repairing epithelium during wound healing. *J Surg Res.*, 10(4): 173-179.
- Imlay, J. & Linn, S. 1988. DNA damage and oxygen radical toxicity. *Science*, 240(4857): 1302-1309.
- Imperatore F,Cuzzocrea S,Luongo C,Liguori G,Scafuro A,De Angelis A,Rossi F,Caputi AP,Filippelli A. Hyperbaric oxygen therapy prevents vascular derangement during zymosan-induced multiple-organ-failure syndrome. *Intensive Care Med.* 30(6):1175-81. 2004.

Isner, J., Baumgartner, I., Rauh, G., Schainfeld, R., Blair, R., Manor, O., Razvi, S., & Symes, J. 1998. Treatment of thromboangiitis obliterans (Buerger's disease) by intramuscular gene transfer of vascular endothelial growth factor: preliminary clinical results. *J Vasc Surg.*, 28(6): 964-973.

## [J]

Jacques, D., Descorbeth, M., bdcl-Samad, D., Provost, C., Perreault, C., & Jules, F. 2005. The distribution and density of ET-1 and its receptors are different in human right and left ventricular endocardial endothelial cells. *Peptides*, 26(8): 1427-1435.

Jaffe, E. A., Grulich, J., Weksler, B. B., Hampel, G., & Watanabe, K. 1987. Correlation between thrombin-induced prostacyclin production and inositol trisphosphate and cytosolic free calcium levels in cultured human endothelial cells. *Journal of Biological Chemistry*, 262(18): 8557-8565.

Jaffe, EA, Nachman, RL, Becker, CG, and Minick, CR. Culture of human endothelial cells derived from umbilical veins: Identification by morphologic and immunologic criteria. *Journal of Clinical Investigation*. 52, 2745-2756. 1974.

Jamieson, D. & Cass, N. 1967. CNS and pulmonary damage in anesthetized rats exposed to hyperbaric oxygen. *J Appl Physiol.*, 23(2): 235-242.

Jamieson, D, Chance, B, Cadenas, E, and Boveris, A. The relation of free radical production to hyperoxia. *Annu Rev Physiol*. 48: 703-719. 1986.

Jen, C. J., Jhiang, S. J., & Chen, H. I. 2000. Cellular Responses to Mechanical Stress: Invited Review: Effects of flow on vascular endothelial intracellular calcium signaling of rat aortas ex vivo. *Journal of Applied Physiology*, 89(4): 1657-1662.

Jensen, J., Hunt, T., Scheuenstuhl, H., & Banda, M. 2006. Effect of lactate, pyruvate, and pH on secretion of angiogenesis and mitogenesis factors by macrophages. *Lab Invest*.1986 May;54(5):574-8..

Jewell SA,Bellomo G,Thorn P,Orrenius S,Smith MT. 1982. Bleb formation in hepatocytes duringdrug metabolism is caused by disturbances inthiol and calcium ion homeostasis. *Science*, 217: 1257-1259.

Jiang, B., Semenza, G., Bauer, C., & Marti, H. 1996. Hypoxia-inducible factor 1 levels vary exponentially over a physiologically relevant range of O<sub>2</sub> tension. *Am J Physiol.*, 271(4 Pt 1): C1172-C1180.

Jobin CM, Chen H Lin AJ Yacono PW Igarashi J Michel T Golan DE. Receptor-regulated dynamic interaction between endothelial nitric oxide synthase and calmodulin revealed by fluorescence resonance energy transfer in living cells. *Biochemistry*. 42(40), 11716-11725. 2003.

Joenje, H. 1989. Genetic toxicology of oxygen. *Mutat Res.*, 219(4): 193-208.

Jones, D. 2002. Redox potential of GSH/GSSG couple: assay and biological significance. *Methods Enzymol.*, 348: 93-112.

Jozkowicz, A., Cooke, J., Guevara, I., Huk, I., Funovics, P., Pachinger, O., Weidinger, F., & Dulak, J. 2001. Genetic augmentation of nitric oxide synthase increases the vascular generation of VEGF. *Cardiovascular Research*, 51: 773-783.

Juha, N. 2006. Physiologic Effects of Hyperbaric Oxygen on Wound Healing Processes.

Junod AF, J. L. P. H. 1989. Differential effects of hyperoxia and hydrogen peroxide on DNA damage, polyadenosine diphosphate-ribose polymerase activity, and nicotinamide adenine dinucleotide and adenosine triphosphate contents in cultured endothelial cells and fibroblasts. *J Cell Physiol.*, 140(1): 177-185.

Jurk, K. & Kehrel, B. 2005. Platelets: physiology and biochemistry. *Semin Thromb Hemost.*, 31(4): 381-392.

## [K]

Kagan, V., Serbinova, E., Bakalova, R., Stoytchev, T., Erin, A., Prilipko, L., & Evstigneeva, R. 1990. Mechanisms of stabilization of biomembranes by alpha-tocopherol. The role of the hydrocarbon chain in the inhibition of lipid peroxidation. *Biochem Pharmacol.*, 40(11):(2403): 2413.

Kang, TS, Gorti, GK, Quan, SY, Ho, M, and Koch, RJ. Effect of hyperbaric oxygen on the growth factor profile of fibroblasts. *Arch Facial Plast Surg*. 6(1), 31-35. 2004.

Kass Gen,Nicotera P,Orrenius S. 1996. Calcium-modulated cellular effects of oxidants.

Kass Gen,Wright JM,Nicotera P,Orrenius S.1988. The mechanism of 1-methyl-4-phenyl-1,2,3,6-tetrahydropyridine toxicity: role of intracellularcalcium. *Arch Biochem Biophys* 260:789-797.

Kass, G. & Orrenius, S. 1999. Calcium signaling and cytotoxicity. *Environ Health Perspect.*, 107 Suppl 1: 25-35.

Kawasaki, J., Hirano, K., Hirano, M., Nishimura, J., Nakatsuka, A., Fujishima, M., & Kanaide, H. 2000. Dissociation between the Ca<sup>2+</sup> signal and tube formation induced by vascular endothelial growth factor in bovine aortic endothelial cells. *European Journal of Pharmacology*, 398(1): 19-29.

- Kendall, R. & Thomas, K. 1993. Inhibition of vascular endothelial growth factor activity by an endogenously encoded soluble receptor. *Proc Natl Acad Sci U S A.*, 90: 10705-10709.
- Kessler, L., Bilbault, P., Ortega, F., Grasso, C., Passemard, R., Stephan, D., Pinget, M., and Schneider, F. Hyperbaric Oxygenation Accelerates the Healing Rate of Nonischemic Chronic Diabetic Foot Ulcers: A prospective randomized study. *Diabetes Care* 26[8], 2378-2382. 1-8-2003.
- Keyt, B., Nguyen, H., Berleau, L., Duarte, C., Park, J., Chen, H., & Ferrara, N. 1996. Identification of vascular endothelial growth factor determinants for binding KDR and FLT-1 receptors. Generation of receptor-selective VEGF variants by site-directed mutagenesis. *J Biol Chem.*, 271(10): 5638-5646.
- Kim, J. M., Kim, H., Kwon, S. B., Lee, S. Y., Chung, S. C., Jeong, D. W., & Min, B. M. 2004. Intracellular glutathione status regulates mouse bone marrow monocyte-derived macrophage differentiation and phagocytic activity. *Biochemical and Biophysical Research Communications*, 325(1): 101-108.
- Kimura, H., Weisz, A., Kurashima, Y., Hashimoto, K., Ogura, T., D'Acquisto, F., Addeo, R., Makuuchi, M., & Esumi, H. 2000. Hypoxia response element of the human vascular endothelial growth factor gene mediates transcriptional regulation by nitric oxide: control of hypoxia-inducible factor-1 activity by nitric oxide. *Blood.*, 95: 189-197.
- Kimura, H., Weisz, A., Ogura, T., Hitomi, Y., Kurashima, Y., Hashimoto, K., D'Acquisto, F., Makuuchi, M., & Esumi, H. 2001. Identification of hypoxia-inducible factor 1 ancillary sequence and its function in vascular endothelial growth factor gene induction by hypoxia and nitric oxide. *J Biol Chem.*, 276(3): 2292-2298.
- Kimura, H and Esumi, H. Reciprocal regulation between nitric oxide and vascular endothelial growth factor in angiogenesis. *Acta Biochimica Polonica* 50(1), 49-59. 2003.
- King, L. 2001. Impaired wound healing in patients with diabetes. *Nursing Standard*, 15(38 June 6): 39-45.
- Kirk SJ, Hurson M, Regan MC, Holt DR, Wasserkrug HL, Barbul A. 1993. Arginine stimulates wound healing and immune function in elderly human beings. *Surgery.*, 114(2): 155-160.
- Kirsner, R. & Eaglstein, W. 1993. The wound healing process. *Dermatol Clin.*, 11(4): 629-640.
- Kliche, S. & Waltenberger, J. 2001. VEGF receptor signaling and endothelial function. *IUBMB Life*, 52: 61-6.
- Knighton, DR, Silver, IA., and Hunt, TK. 1981. Regulation of wound-healing angiogenesis – effect of oxygen gradients and inspired oxygen concentration. *Surgery* 90(2), 262-269.
- Knighton, D., Hunt, T., Scheuenstuhl, H., Halliday, B., Werb, Z., & Banda, M. 1983. Oxygen tension regulates the expression of angiogenesis factor by macrophages. *Science.*, 221(4617): 1283-1285.
- Knighton, D., Halliday, B., & Hunt, T. 1984. Oxygen as an antibiotic. The effect of inspired oxygen on infection. *Arch Surg.*, 119(2): 199-204.
- Knighton, D., Halliday, B., & Hunt, T. 1986. Oxygen as an antibiotic. A comparison of the effects of inspired oxygen concentration and antibiotic administration on in vivo bacterial clearance. *Arch Surg.*, 121(2): 191-5.
- Knowles, R. & Moncada, S. 1994. Nitric oxide synthases in mammals. *Biochem J.*, 298 ( Pt 2): 249-258.
- Kohn, E. C., Alessandro, R., Spoonster, J., Wersto, R. P., & Liotta, L. A. 1995. Angiogenesis: Role of Calcium-Mediated Signal Transduction. *Proceedings of the National Academy of Sciences*, 92(5): 1307-11.
- Kohn, K. 1991. Principles and practice of DNA filter elution. *Pharmacol Ther.*, 49(1-2): 55-77.
- Konturek SJ, Brzozowski T, Majka J, Pytko-Polonczyk J, Stachura J. 1993. Inhibition of nitric oxide synthase delays healing of chronic gastric ulcers. *Eur J Pharmacol.*, 239(1-3): 215-217.
- Konturek, S., Brzozowski, T., Majka, J., Pytko-Polonczyk, J., & Stachura, J. 1993. Inhibition of nitric oxide synthase delays healing of chronic gastric ulcers. *Eur J Pharmacol.*, 239(1-3): 215-217.
- Kosower, NS and Kosower, EM. The glutathione status of cells. *Int Rev Cytol.* 54: 109-160. 1987.
- Kouric, J. I. 1998. Interaction of reactive oxygen species with ion transport mechanisms. *AJP - Cell Physiology*, 275(1): C1-24.
- Kroll, J. & Waltenberger, J. 1998. VEGF-A induces expression of eNOS and iNOS in endothelial cells via VEGF receptor-2 (KDR). *Biochem Biophys Res Commun.*, 252(3): 743-746.
- Kroll, J. & Waltenberger, J. 1999. A novel function of VEGF receptor-2 (KDR): rapid release of nitric oxide in response to VEGF-A stimulation in endothelial cells. *Biochem Biophys Res Commun.*, 265(3): 636-639.
- Kruse, J. & Carlson, R. 1987. Lactate metabolism. *Crit Care Clin*, 3(4): 725-746.
- Kudchodkar, B., Pierce, A., & Dory, L. 2006. Chronic hyperbaric oxygen treatment elicits an anti-oxidant response and attenuates atherosclerosis in apoE knockout mice. *Atherosclerosis.*, [Epub ahead of print].
- Kurata S, Yamashita U Nakajima H. 1995. Hyperbaric oxygenation reduces the cytostatic activity and transcription of nitric oxide synthetase gene of mouse peritoneal macrophages. *Biochim Biophys Acta* 1263(1): 35-38.

Kutchai, H, Geddis, LM, and Martin, MS. Mediated transport and metabolism of lactate in rat aorta. *Biochemica et biophysica Acta* 541, 312-320. 1978.

## [L]

Labinsky, N., Csiszar, A., Orosz, Z., Smith, K., Rivera, A., Buffenstein, R., & Ungvari, Z. 2006. Comparison of endothelial function, O<sub>2</sub>· and H<sub>2</sub>O<sub>2</sub> production, and vascular oxidative stress resistance between the longest-living rodent, the naked mole rat, and mice. *AJP - Heart and Circulatory Physiology*, 291(6): H2698-H2704.

Lee, P., Salyapongse, A., Bragdon, G., Shears II, L., Watkins, S., Edington, H., & Billiar, T. 1999. Impaired wound healing and angiogenesis in eNOS-deficient mice. *American Journal of Physiology*, 277: H1600-H1608.

Lee, R., Efron, D., Tantry, U., & Barbul, A. 2001. Nitric oxide in the healing wound: a time-course study. *J Surg Res.*, 101(1): 104-108.

Lerman, O., Galiano, R., Armour, M., Levine, J., & Gurtner, G. 2003. Cellular dysfunction in the diabetic fibroblast: impairment in migration, VEGF production, and response to hypoxia. *American Journal of Pathology*, 162(1): 303-312.

Leung, D., Cachianes, G., Kuang, W., G. D., & Ferrara, N. 1989. Vascular endothelial growth factor is a secreted angiogenic mitogen. *Science.*, 246(4935): 1306-1309.

Levy, A., Levy, N., & Goldberg, M. 1996. Post-transcriptional regulation of vascular endothelial growth factor by hypoxia. *J Biol Chem.*, 271(5): 2746-2753.

Liekens, S., De Clercq, E., & Neyts, J. 2001. Angiogenesis: regulators and clinical applications. *Biochem.Pharmacol.*, 61(2001): 253-270.

Lin, C., Huang, C., Wang, T., Wang, Y., & Lin, P. 2007. Disparity in the induction of glutathione depletion, ROS formation, poly(ADP-ribose) polymerase-1 activation, and apoptosis by quinonoid derivatives of naphthalene in human cultured cells. *Chemico-Biological Interactions*, 165(3): 200-210.

Lin, S., Shyu, K., Lee, C., Wang, B., Chang, C., Liu, Y., Huang, F., & Chang, H. 2002. Hyperbaric oxygen selectively induces angiopoietin-2 in human umbilical vein endothelial cells. *Biochemical and Biophysical Research Communications*, 296: 710-715.

Lin, S; Fagan, KA.; Li, KX; Shaul, PW.; Cooper,DMF.; Rodman, DM. 2000. Sustained Endothelial Nitric-oxide Synthase Activation Requires Capacitative Ca<sup>2+</sup> Entry. *Journal of Biological Chemistry*, 275(24): 17979-17985.

Liotta, LA, Tryggvason, K, Garbisa, S, Foltz, CM, and Shafie, S. Metastatic potential correlates with enzymatic degradation of basement membrane collagen. *Nature* 284, 67-68. 1980.

Lirk, P., Hoffmann, G., & Reider, J. 2002. Inducible nitric oxide synthase--time for reappraisal. *Curr Drug Targets Inflamm Allergy.*, 1(1): 89-108.

Liu L, Liu JC, Lin SL, Li B. 1999. Changes and its measurement of intracellular Ca<sup>2+</sup> during exposure to hyperbaric oxygen. *Space Med Med Eng (Beijing).*, 12(6): 410-413.

Lodish H, Berk A, Matsudaira P, Kaiser CA, Krieger M, Scott MP, Zipursky SL, Darnell J. 2004. *Molecular Biology of the Cell*. WH Freeman: New York, NY. 5<sup>th</sup> edition. P963

Loetscher, P, Alvarez-Gonzalez, R, and Althaus, FR. Poly(ADP-ribose) may signal changing metabolic conditions to the chromatin of mammalian cells. *Proc Natl Acad Sci U S A.* 84(5), 1286-1289. 1987.

Loomis, E. D., Sullivan, J. C., Osmond, D. A., Pollock, D. M., & Pollock, J. S. 2005. Endothelin mediates superoxide production and vasoconstriction through activation of NADPH oxidase and uncoupled NOS in the rat aorta. *Journal of Pharmacology And Experimental Therapeutics*, jpet.

Loscalzo, J. 2001. An experiment of nature: genetic l-arginine deficiency and NO insufficiency. *Journal of Clinical Investigation*, 108(5): 663-664.

Luo, Y., Henle, E. S., & Linn, S. 1996. Oxidative Damage to DNA Constituents by Iron-mediated Fenton Reactions. THE DEOXYCYTIDINE FAMILY. *Journal of Biological Chemistry*, 271(35): 21167-21176.

Luongo C, Imperatore F, Cuzzocrea S, Filippelli A, Scafuro MA, Mangoni G, Portolano F, Rossi F. Effects of hyperbaric oxygen exposure on a zymosan-induced shock model. *Crit Care Med.* 26(12):1972-6. 1998.

## [M]

Ma, L. & Wallace, J. 2000. Endothelial nitric oxide synthase modulates gastric ulcer healing in rats. *Am J Physiol Gastrointest Liver Physiol.*, 279(2): G341-G346.

Mader, J., Brown, G., Guckian, J., Wells, C., & Reinartz, J. 1980. A mechanism for the amelioration by hyperbaric oxygen of experimental staphylococcal osteomyelitis in rabbits. *J Infect Dis.*, 142(6): 915-922.

- Mader, J., Adams, K., & Sutton, T. 1987. Infectious diseases: pathophysiology and mechanisms of hyperbaric oxygen. *Journal of Hyperbaric Medicine*, 2(3): 133-140.
- Mader, J., Hicks, C., & Calhoun, J. 1989. Bacterial osteomyelitis. Adjunctive hyperbaric oxygen therapy. *Orthop Rev.*, 18(5): 581-585.
- Madri, J. & Marx, M. 1992. Matrix composition, organization and soluble factors: modulators of microvascular cell differentiation in vitro. *Kidney Int*, 41: 560-565.
- Madri, J., Sankar, S., & Romanic, A. 1996. Angiogenesis. In R. A. F. Clark (Ed.), *The molecular and cellular biology of wound repair*: 355-371. New York: Plenum Press.
- Maisonpierre, P., Suri, C., Jones, P., Bartunkova, S., Wiegand, S., Radziejewski, C., Compton, D., McClain, J., Aldrich, T., Papadopoulos, N., Daly, T., Davis, S., Sato, T., & Yancopoulos, G. 1997. Angiopoietin-2, a natural antagonist for Tie2 that disrupts in vivo angiogenesis. *Science*, 277(5322): 55-60.
- Malek, A. M., Jiang, L., Lee, I., Sessa, W. C., Izumo, S., & Alper, S. L. 1999. Induction of Nitric Oxide Synthase mRNA by Shear Stress Requires Intracellular Calcium and G-protein Signals and Is Modulated by PI 3 Kinase. *Biochemical and Biophysical Research Communications*, 254(1): 231-242.
- Malinski T, Mesaros S, Patton SR, Mesarosova A. 1996. Direct measurement of nitric oxide in the cardiovascular system. *Physiol Res.*, 45(4): 279-284.
- Mandriota, S. & Pepper, M. 1997. Vascular endothelial growth factor-induced in vitro angiogenesis and plasminogen activator expression are dependent on endogenous basic fibroblast growth factor. *J Cell Sci.*, 110 ( Pt 18): 2293-2302.
- Marletta, M. 1993. Nitric oxide synthase structure and mechanism. *J Biol Chem*. 1993 Jun 15; 268(17): 12231-12234.
- Martin, T. W. & Michaelis, K. C. 1990. Ca<sup>2+</sup>-dependent synthesis of prostaglandin I<sub>2</sub> and mobilization of arachidonic acid from phospholipids in cultured endothelial cells permeabilized with saponin. *Biochimica Et Biophysica Acta (BBA) - Molecular Cell Research*, 1054(2): 159-168.
- Martins, E. & Meneghini, R. 1990. DNA damage and lethal effects of hydrogen peroxide and menadione in Chinese hamster cells: distinct mechanisms are involved. *Free Radic Biol Med.*, 8(5): 433-440.
- Martins, E., Chubatsu, L., & Meneghini, R. 1991. Role of antioxidants in protecting cellular DNA from damage by oxidative stress. *Mutat Res.*, 250(1-2): 95-101.
- Martins, E. & Meneghini, R. 1994. Cellular DNA damage by hydrogen peroxide is attenuated by hypotonicity. *Biochem J.*, 299( Pt 1): 137-140.
- Marx, R., Ehler, W., Tayapongasak, P., & Pierce, L. 1990. Relationship of oxygen dose to angiogenesis induction in irradiated tissue. *AM J Surg* 1990 Nov; 160(5): 519-524.
- Marzinzig M, Nussler AK, Stadler J, Marzinzig E, Barthlen W, Nussler NC, Beger HG, Morris SM Jr, Bruckner UB. Improved methods to measure end products of nitric oxide in biological fluids: nitrite, nitrate, and S-nitrosothiols. *Nitric Oxide*. 1(2): 177-189. 1997.
- Matsuo T, Matsuo N. 1996. Intracellular calcium response to hydraulic pressure in human trabecular cells. *Br J Ophthalmol*. 80(6):561-6.
- Mazure, N., Chen, E., Laderoute, K., & Giaccia, A. 1997. Induction of vascular endothelial growth factor by hypoxia is modulated by a phosphatidylinositol 3-kinase/Akt signaling pathway in Ha-ras-transformed cells through a hypoxia inducible factor-1 transcriptional element. *Blood.*, 90(9): 3322-3331.
- Mazure, N., Brahimi-Horn, M., & Pouyssegur, J. 2003. Protein kinase and the hypoxia-inducible factor-1, two switches in angiogenesis. *Current Pharmaceutical Design*, 9: 531-541.
- McCurry, L. S. & Jacobson, M. K. 1981. Poly(ADP-ribose) synthesis following DNA damage in cells heterozygous or homozygous for the xeroderma pigmentosum genotype. *Journal of Biological Chemistry*, 256(2): 551-553.
- McGuigan, J., Luthi, D., & Buri, A. 1991. Calcium buffer solutions and how to make them: a do it yourself guide. *Can J Physiol Pharmacol.*, 69(11): 1733-1749.
- Mechine, A., Rohr, S., Toti, F., Aysoy, C., Schneider, F., Meyer, C., Tempe, J., & Bellocq, J. 1999. Wound healing and hyperbaric oxygen. Experimental study of the angiogenesis phase in the rat. *Ann Chir*, 53(4):307: 313.
- Merad-Boudia, M., Nicole, A., Santiard-Baron, D., Saille, C., & Ceballos-Picot, I. 1998. Mitochondrial impairment as an early event in the process of apoptosis induced by glutathione depletion in neuronal cells: relevance to Parkinson's disease. *Biochem Pharmacol*, 56:(645): 655.

- Mercandetti, M. Wound healing, healing and repair. 7-8-2002.
- Mignatti, P. & Rifkin, D. 1996. Plasminogen activators and matrix metalloproteinases in angiogenesis. *Enzyme Protein.*, 49(1-3): 117-137.
- Miles AM, Wink DA, Cook JC, Grisham MB. 1996. Determination of nitric oxide using fluorescence spectroscopy. *Methods Enzymol.*, 268: 105-120.
- Miller, V. & Vanhoutte, P. 1992. Endothelium-dependent vascular responsiveness: evolutionary aspects. In U. Ryan & G. Rubanyi (Eds.), *Endothelial Regulation of Vascular Tone.*: 3-20. New York: Marcel Dekker, Inc.
- Millington, J. & Norris, T. 2000. Effective treatment strategies for diabetic foot wounds. *J Fam Pract.*, 49(11 Suppl): S40-S48.
- Minchenko, A., Bauer, T., Salceda, S., & Caro, J. 1994. Hypoxic stimulation of vascular endothelial growth factor expression in vitro and in vivo. *Lab Invest.*, 71(3): 374-379.
- Missiaen L, T. C. B. MJ. 2007. Luminal Ca<sup>2+</sup> promoting spontaneous Ca<sup>2+</sup> release from inositol trisphosphate-sensitive stores in rat hepatocytes. *J Physiol.* 1992 Sep;455:623-40..
- Moellering, DR, Levonon, AL, Go, YM, Patel, RP, Dickinson, DA, Forman, HJ, and Darley-USmar, VM. 2002. Induction of glutathione synthesis by oxidized low-density lipoprotein and 1-palmitoyl-2-arachidonoyl phosphatidylcholine: protection against quinone-mediated oxidative stress. *Biochem J.* 362(Pt 1): 51-59.
- Mohazzab, K., Kaminski, P., & Wolin, M. 1994. NADH oxidoreductase is a major source of superoxide anion in bovine coronary artery endothelium. *Am J Physiol.*, 266(6 Pt 2): H2568-H2572.
- Morbidelli, L., Donnini, S., & Ziche, M. 2003. Role of nitric oxide in the modulation of angiogenesis. *Current Pharmaceutical Design*, 9: 521-530.
- Mori, M. & Wakabayashi, M. 2000. Cytotoxicity evaluation of synthesized chemicals using suspension-cultured fish cells. *Fisheries Science*, 66(5): 871-875.
- Moskvin AN, Zhilyaev SY Sharapov OI Platonova TF Gutsaeva DR Kostkin VB Demchenko IT. Brain blood flow modulates the neurotoxic action of hyperbaric oxygen via neuronal and endothelial nitric oxide. *Neurosci Behav Physiol.* 33(9)[883-8.]. 2003.
- Mueller, Cornelius F. H., Laude, Karine, McNally, J. Scott, and Harrison, David G. Redox Mechanisms in Blood Vessels. *Arteriosclerosis, Thrombosis, and Vascular Biology* 25[2], 274-278. 1-2-2005.
- Muhonen, A., Haaparanta, M., Gronroos, T., Bergman, J., Knuuti, J., Hinkka, S., & Happonen, R.-P. 2004. Osteoblastic activity and neoangiogenesis in distracted bone of irradiated rabbit mandible with or without hyperbaric oxygen treatment. *International Journal of Oral and Maxillofacial Surgery*, 33(2): 173-178.
- Munaron, L. Calcium signalling and control of cell proliferation by tyrosine kinase receptors (review). *Int J Mol Med.* 10(6): 671-676. 2002.
- Murakami, H., Liu, J. L., Yoneyama, H., Nishida, Y., Okada, K., Kosaka, H., Morita, H., & Zucker, I. H. 1998. Blockade of neuronal nitric oxide synthase alters the baroreflex control of heart rate in the rabbit. *AJP - Regulatory, Integrative and Comparative Physiology*, 274(1): R181-R186.
- Murohara T, Asahara T Silver M Bauters C Masuda H Kalka C Kearney M Chen D Symes JF Fishman MC Huang PL Isner JM. Nitric oxide synthase modulates angiogenesis in response to tissue ischemia. *J Clin Invest.* 101(11): 2567-2578. 1998.
- Mustoe, T. 2004. Understanding chronic wounds: a unifying hypothesis on their pathogenesis and implications for therapy. *The American Journal of Surgery*, 187(5)(Supplement 1.): S65-S70.
- Muth, C., Glenz, Y., Klaus, M., Radermacher, P., Speit, G., & Lerverve, X. 2004. Influence of an orally effective SOD on hyperbaric oxygen-related cell damage. *Free Radic Res.*, 38(9): 927-932.
- Mutsaers, S., Bishop, J., Mcgrouter, G., & Laurent, G. 1997. Mechanisms of tissue repair: from wound healing to fibrosis. *Int.J.Biochem.Cell Biol.*, 29(1): 5-17.
- Myers, R. & Marx, R. 1990. Use Of Hyperbaric Oxygen In Postradiation Head And Neck Surgery. *Nci Monographs*, Number 9, 151-157.
- Myllyla, R., Tuderman, L., & Kivirikko, K. 1977. Mechanism of the prolyl hydroxylase reaction. 2. Kinetic analysis of the reaction sequence. *Eur J Biochem.*, 80(2): 349-357.

**[N]**

- Nakayama, Y. & Matsuda, T. 2003. Photo-control of the interaction between endothelial cells and photo-generated water-soluble polymers. *Journal of Controlled Release*, 89(2): 213-224.
- Narkowicz, CK, Vial, JH, and McCartney, PW. Hyperbaric oxygen therapy increases free radical levels in the blood of humans. *Free Radic Res Commun.* 19(2): 71-80. 1993.

- Nicosia, R. & Ottinetti, A. 1990. Growth of microvessels in serum-free matrix culture of rat aorta. A quantitative assay of angiogenesis in vitro. *Lab Invest*, 63(1): 115-122.
- Nicosia, R., Nicosia, S., & Smith, M. 1994. Vascular endothelial growth factor, platelet-derived growth factor, and insulin-like growth factor-1 promote rat aortic angiogenesis in vitro. *Am J Pathol*, 145(5): 1023-9.
- Nicotera P, Hartzell P, Davis G, Orrenius S. 1986. The formation of plasma membrane blebs in hepatocytes exposed to agents that increase cytosolic  $Ca^{2+}$  is mediated by the activation of a non-lysosomal proteolytic system. *FEBS Lett*, 209: 139-144.
- Niinikoski, J. 1970. Effect of oxygen supply on wound healing and formation of experimental granulation tissue. *Acta Physiol Scand*, 78: 1-72.
- Niinikoski, J, Hunt, T. K., and Dunphy, J. E. Oxygen supply in healing tissue. *American Journal of Surgery* 123, 247-252. 1972.
- Niinikoski, J. 1980. Cellular and nutritional interactions in healing wounds. *Med Biol.*, 58(6): 303-309.
- Nilius, B. & Droogmans, G. 2001. Ion Channels and Their Functional Role in Vascular Endothelium. *Physiological Reviews*, 81(4): 1415-1459.
- Nishida, D., Harrison, D., Navas, J., Fisher, A., Dockery, S., Uematsu, M., Nerem, R., Alexander, R., & Murphy, T. 1992. Molecular cloning and characterization of the constitutive bovine aortic endothelial cell nitric oxide synthase. *J Clin Invest.*, 90(5): 2092-2096.
- Nissen, N., Polverini, P., Koch, A., Volin, M., Gamelli, R., & DiPietro, L. 1998. Vascular endothelial growth factor mediates angiogenic activity during the proliferative phase of wound healing. *Am J Pathol.*, 152(6): 1445-1452.
- North, A., Lau, K., Brannon, T., Wu, L., Wells, L., German, Z., & Shaul, P. 1996. Oxygen upregulates nitric oxide synthase gene expression in ovine fetal pulmonary artery endothelial cells. *Am J Physiol.*, 270(4 Pt 1): L643-L649.

## [O]

- Orrenius S, Burkitt M, Kass GEN, Dypbukt JM,; Nicotera P. 1992. Calcium ions and oxidative cell injury. *Ann Neurol* 32:S33-S42.
- Osovska, S., Moinard, C., Loi, C., Neveux, N., & Cynober, L. 2004. Citrulline increases arginine pools and restores nitrogen balance after massive intestinal resection. *Gut*, 53(12): 1781-1786.
- Ostling, O. & Johanson, K. 1984. Microelectrophoretic study of radiation-induced DNA damages in individual mammalian cells. *Biochem Biophys Res Commun.*, 123((1)): 291-298.
- Otun, H., Aidulis, D. M., Yang, J. M., Gillespie, J. I. (1996) Interactions between inositol trisphosphate and  $Ca^{2+}$  dependent  $Ca^{2+}$  release mechanisms on the endoplasmic reticulum of permeabilised bovine aortic endothelial cells. *Cell Calcium* 19, 315-325
- Oury, TD, Ho, YS, Piantadosi, CA, and Crapo, JD. Extracellular superoxide dismutase, nitric oxide, and central nervous system O<sub>2</sub> toxicity. *Proc Natl Acad Sci U S A.* 89(20): 9715-9719. 1992.
- Owens, C., Belcher, R.V. 1965. A colorimetric micro-method for the determination of glutathione. 94:705-11.
- Ozden, TA, Uzun, H, Bohlioli, M, Toklu, AS, Paksoy, M, Simsek, G, Durak, H, Issever, H, and Ipek, T. The effects of hyperbaric oxygen treatment on oxidant and antioxidants levels during liver regeneration in rats. *Tohoku J Exp Med.* 203(4): 253-265. 2004.

## [P]

- Paddon-Jones, D., Borsheim, E., & Wolfe, R. R. 2004. Potential Ergogenic Effects of Arginine and Creatine Supplementation. *Journal of Nutrition*, 134(10): 2888S-2894.
- Palmer, R. M. J., Rees, D. D., Ashton, D. S., & Moncada, S. 1988. L-arginine is the physiological precursor for the formation of nitric oxide in endothelium-dependent relaxation. *Biochemical and Biophysical Research Communications*, 153(3): 1251-1256.
- Papapetropoulos, Andreas, Garcia-Cardena, Guillermo, Madri, Joseph A., and Sessa, William C. Nitric Oxide Production Contributes to the Angiogenic Properties of Vascular Endothelial Growth Factor in Human Endothelial Cells. *Journal of Clinical Investigation* 100[12], 3131-3139. 15-12-1997.
- Papetti, M. & Herman, I. 2001. Mechanisms of normal and tumor-derived angiogenesis. *Am. J. Physiol. Cell Physiol.*, 282: C947-C970.
- Parfenova, H., Basuroy, S., Bhattacharya, S., Tcheranova, D., Qu, Y., Regan, R. F., & Leffler, C. W. 2006. Glutamate induces oxidative stress and apoptosis in cerebral vascular endothelial cells: contributions of HO-1 and HO-2 to cytoprotection. *AJP - Cell Physiology*, 290(5): C1399-C1410.

- Parola, M, Bellomo, G, Robino, G, Barrera, G, and Dianzani, MU. 4-Hydroxynonenal as a biological signal: molecular basis and pathophysiological implications. *Antioxid Redox Signal.* 1(3): 255-284. 1999.
- Peers, C and Kang P, Boyle JP Porter KE Pearson HA Smith IF Kemp PJ. Hypoxic regulation of Ca<sup>2+</sup> signalling in astrocytes and endothelial cells. *Novartis Found Symp.* 272, 119-127; discussion 127-40. 2006.
- Peiretti, F., Alessi, M. C., Henry, M., Anfosso, F., Juhan-Vague, I., & Nalbone, G. 1997. Intracellular Calcium Mobilization Suppresses the TNF- $\alpha$  Stimulated Synthesis of PAI-1 in Human Endothelial Cells : Indications That Calcium Acts at a Translational Level. *Arteriosclerosis, Thrombosis, and Vascular Biology*, 17(8): 1550-1560.
- Pekala, P., Marlow, M., Heuvelman, D., & Connolly, D. 1990. Regulation of hexose transport in aortic endothelial cells by vascular permeability factor and tumor necrosis factor-alpha, but not by insulin. *J Biol Chem.*, 265(30): 18051-18054.
- Pepper, M. & Montesano, R. 1990. Proteolytic balance and capillary morphogenesis. *Cell Differ Dev*, 32: 319-331.
- Pepper, M., Ferrara, N., Orci, L., & Montesano, R. 1991. Vascular endothelial growth factor (VEGF) induces plasminogen activators and plasminogen activator inhibitor-1 in microvascular endothelial cells. *Biochem Biophys Res Commun.*, 181(2): 902-906.
- Pepper, M., Ferrara, N., Orci, L., & Montesano, R. 1992. Potent synergism between vascular endothelial growth factor and basic fibroblast growth factor in the induction of angiogenesis in vitro. *Biochem Biophys Res Commun.*, 189(2): 824-831.
- Phillips, G., Stone, A., Jones, B., Schultz, J., Whitehead, R., & Knighton, D. 1995. Vascular endothelial growth factor (rh VEGF165) stimulates direct angiogenesis in the rabbit cornea. *In Vivo*, 8: 961-965.
- Piantadosi, C., Tatro, L., & Zhang, J. 1995. Hydroxyl radical production in the brain after CO hypoxia in rats. *Free Radical Biology and Medicine*, 18(3): 603-609.
- Pires, M., Rossi, M., & Ross, D. 1994. Kinetic and mechanistic aspects of the NO oxidation by O<sub>2</sub> in aqueous phase. *International Journal of Chemical Kinetics*, 26(12): 1207-1227.
- Plummer, D. 1971. *An introduction to practical biochemistry.* London: McGraw Hill.
- Pogrebnyaya, V., Usov, A., Baranov, A., Nesterenko, A., & Bez'yazychnyi, P. 1975. Liquid-phase oxidation of nitric oxide by oxygen. *J.Appl.Chem.USSR* 48 (Engl. Transl.), 1004.
- Pollock, J. S., Nakane, M., Buttery, L. D., Martinez, A., Springall, D., Polak, J. M., Forstermann, U., & Murad, F. 1993. Characterization and localization of endothelial nitric oxide synthase using specific monoclonal antibodies. *AJP - Cell Physiology*, 265(5): C1379-C1387.
- Portzehl, H; Caldwell, P; Rueegg, J. 1964. The dependence of contraction and relaxation of muscle fibres from the crab *maia squinado* on the internal concentration of free calcium ions. *Biochim Biophys Acta.*, 79: 581-591.
- Privat, C, Lantoinc, F, Bedioui, F, Millanvoye van Brussel E, Devynck, J, and Devynck, MA. 1997. Nitric oxide production by endothelial cells: comparison of three methods of quantification. *Life Sci.* 61(12), 1193-1202.
- Puri, M., Rossant, J., Alitalo, K., Bernstein, A., & Partanen, J. 1995. The receptor tyrosine kinase TIE is required for integrity and survival of vascular endothelial cells. *EMBO J.*, 14(23): 5884-5891.
- Putney, J. W., Jr., Broad, L. M., Braun, F. J., Lievreumont, J. P., & Bird, G. S. 2001. Mechanisms of capacitative calcium entry. *Journal of Cell Science*, 114(12): 2223-2229.

**[R]**

- Rachmilewitz D, Karmeli F Okon E Rubenstein I Better OS. Hyperbaric oxygen: a novel modality to ameliorate experimental colitis. *Gut.* 43(4): 512-8. 1998.
- Rahman I, B. S. J. L. T. M. F. HJ. 2005. Glutathione, stress responses, and redox signaling in lung inflammation. *Antioxid Redox Signal.*, 7(1-2):42-59..
- Rajagopalan, S., Kurz, S., Munzel, T., Tarpey, M., Freeman, B., Griending, K., & Harrison, D. 1996. Angiotensin II-mediated hypertension in the rat increases vascular superoxide production via membrane NADH/NADPH oxidase activation. Contribution to alterations of vasomotor tone. *J Clin Invest.*, 97(8): 1916-1923.
- Ranby, M. 1982. Studies on the kinetics of plasminogen activation by tissue plasminogen activator. *Biochim Biophys Acta.*, 704(3): 461-469.
- Reenstra-Buras, WR. Mechanisms of HBO<sub>2</sub> and wound healing. [The ninth annual advanced symposium Hyperbaric Medicine 2003], 1-19. 24-4-2003.

- Reeve, H. L., Tolarova, S., Nelson, D. P., Archer, S., & Weir, E. K. 2001. Redox control of oxygen sensing in the rabbit ductus arteriosus. *The Journal of Physiology Online*, 533(1): 253-261.
- Reichner, J., Meszaros, A., Louis, C., Henry, W. J., Mastrofrancesco, B., Martin, B., & Albina, J. 1999. Molecular and metabolic evidence for the restricted expression of inducible nitric oxide synthase in healing wounds. *Am J Pathol.*, 154(4): 1097-1104.
- Remacle, J., Raes, M., Toussaint, O., Renard, P., & Rao, G. 1995. Low levels of reactive oxygen species as modulators of cell function. *Mutat Res.*, 316((3)): 103-122.
- Remensnyder, J. & Majno, G. 1968. Oxygen gradients in healing wounds. *Am J Pathol.*, 52: 301-323.
- Richard, D., Berra, E., & Pouyssegur, J. 2000. Nonhypoxic pathway mediates the induction of hypoxia-inducible factor 1 alpha in vascular smooth muscle cells. *The Journal of Biological Chemistry*, 275(September 1): 26765-26771.
- Risau, W. 1997. Mechanisms of angiogenesis. *Nature*, 386(6626): 671-674.
- Roeckl, W., Hecht, D., Sztajer, H., Waltenberger, J., Yayon, A., & Weich, H. 1998. Differential binding characteristics and cellular inhibition by soluble VEGF receptors 1 and 2. *Exp Cell Res.*, 241: 161-170.
- Romano, D. P. S., Mangoni, A., Zambruno, G., Spinetti, G., Melillo, G., Napolitano, M., & Capogrossi, M. 2002. Adenovirus-mediated VEGF(165) gene transfer enhances wound healing by promoting angiogenesis in CD1 diabetic mice. *Gene Ther.*, 9(19): 1271-1277.
- Rothfuss, A., Dennog, C., & Speit, G. 1998. Adaptive protection against the induction of oxidative DNA damage after hyperbaric oxygen treatment. *Carcinogenesis.*, 19(11): 1913-1917.
- Rothfuss, A., Stahl, W., Radermacher, P., and Speit, G. Evaluation of mutagenic effects of hyperbaric oxygen (HBO) in vitro. *Environ Mol Mutagen.* 34(4): 291-296. 1999.
- Rothfuss, A., Radermacher, P., Speit, G. 2001. Involvement of heme oxygenase-1 (HO-1) in the adaptive protection of human lymphocytes after hyperbaric oxygen (HBO) treatment. *Carcinogenesis*, 22(12):1979-85.
- Rothfuss, A. & Speit, G. 2002. Investigations on the mechanism of hyperbaric oxygen (HBO)-induced adaptive protection against oxidative stress. *Mutation Research/Fundamental and Molecular Mechanisms of Mutagenesis*, 508(1-2): 157-165.
- Ruch, W., Cooper, P., & Baggiolini, M. 1983. Assay of H<sub>2</sub>O<sub>2</sub> production by macrophages and neutrophils with homovanillic acid and horse-radish peroxidase. *Journal of Immunological Methods.*, 63: 347-357.
- Ruef, J., Hu, Z., Hanson, S., Kelly, A., Harker, L., Rao, G., Runge, M., & Patterson, C. 1997. Induction of Vascular Endothelial Growth Factor in Balloon-Injured Baboon Arteries: A Novel Role for Reactive Oxygen Species in Atherosclerosis. *Circulation Research.*, 81: 24-33.

**[S]**

- Sapico, F., Witte, J., Canawati, H., Montgomerie, J., & Bessman, A. 1984. The infected foot of the diabetic patient: quantitative microbiology and analysis of clinical features. *Rev Infect Dis.*, 6 Suppl 1: S171-S176.
- Saran, M. & Bors, W. 1990. Radical reactions in vivo - an overview. *Radiation and Environmental Biophysics*, V29(4): 249-262.
- Sato T, Ohkusa T, Suzuki S, Nao T, Yano M, Matsuzaki M. 2006. High ambient pressure produces hypertrophy and up-regulates cardiac sarcoplasmic reticulum Ca<sup>2+</sup> regulatory proteins in cultured rat cardiomyocytes. *Hypertens Res.* 29(12):1013-20.
- Sato, T., Takeda, Y., Hagioka, S., Zhang, S., & Hirakawa, M. 2001. Changes in nitric oxide production and cerebral blood flow before development of hyperbaric oxygen-induced seizures in rats. *Brain Research*, 918(1-2): 131-140.
- Sato, T., Tozawa, Y., Deutsch, U., Wolburg-Buchholz, K., Fujiwara, Y., Gendron-Maguire, M., Gridley, T., Wolburg, H., Risau, W., & Qin, Y. 1995. Distinct roles of the receptor tyrosine kinases Tie-1 and Tie-2 in blood vessel formation. *Nature.*, 376(6535): 70-74.
- Savarese, DM, Russell, JT, Fatatis, A., and Liotta, LA. 1992. Type IV collagen stimulates an increase in intra-cellular calcium. Potential role in tumor cell motility. *Journal of Biological Chemistry*, 267(30): 21928-35.
- Savill, J. 1997. Apoptosis in resolution of inflammation. *J Leukoc Biol.*, 61(4): 375-380.
- Schaffer, M., Tantry, U., Gross, S., Wasserburg, H., & Barbul, A. 1996. Nitric oxide regulates wound healing. *J Surg Res.*, 63(1): 237-240.
- Schaffer, M., Tantry, U., van Wesep, R., & Barbul, A. 1997. Nitric oxide metabolism in wounds. *J Surg Res.*, 71(1): 25-31.

- Schaffer, M., Tantry, U., Efron, P., Ahrendt, G., Thomson, F., & Barbul, A. 1997. Diabetes-impaired healing and reduced wound nitric oxide synthesis: a possible pathophysiologic correlation. *Surgery*, 121(5): 513-19.
- Schlessinger, J. 2000. Cell Signaling by Receptor Tyrosine Kinases. *Cell*, 103(2): 211-225.
- Schmidt, H. & Kelm, M. 1996. Determination of nitrite and nitrate by the Griess reaction. In M. Feelisch & J. Stamler (Eds.), *Methods in nitric oxide research*: 491-497. John Wiley & Sons Ltd.
- Schönfelder U, Abel M, Wiegand C, Klemm D, Elsner P, and Hipler UC. 2005. Influence of selected wound dressings on PMN elastase in chronic wound fluid and their antioxidative potential in vitro. *Biomaterials*, 26(33): 6664-6673.
- Schraufstatter IU, Hinshaw DB, Hyslop PA, Spragg RG, Cochrane CG. 1986. Oxidant injury of cells. DNA strand-breaks activate polyadenosine diphosphate-ribose polymerase and lead to depletion of nicotinamide adenine dinucleotide. *J Clin Invest.*, 77(4): 1312-1320.
- Schraufstatter, I., Hyslop, P., Jackson, J., & Cochrane, C. 1988. Oxidant-induced DNA damage of target cells. *J Clin Invest.*, 82(3): 1040-1050.
- Sen, CK, Khanna, S., Gordillo, G., Bagchi, D., Bagchi, M., and Roy, S. Oxygen, oxidants, and antioxidants in wound healing. An emerging paradigm. *Annals of New York Academy of Sciences* 957, 239-249. 2002.
- Sen, C., Khanna, S., Babior, B., Hunt, T., Ellison, E., & Roy, S. 2002. Oxidative-induced vascular endothelial growth factor expression in human keratinocytes and cutaneous wound healing. *The Journal of Biological Chemistry*, 277(36)(September 6): 33284-33290.
- Senger, D., Galli, S., Dvorak, A., Perruzzi, C., Harvey, V., & Dvorak, H. 1983. Tumor cells secrete a vascular permeability factor that promotes accumulation of ascites fluid. *Science*, 219: 983-985.
- Shah, A. M. and Channon, K. M. Free radicals and redox signalling in cardiovascular disease. *Heart* 90[5], 486-487. 1-5-2004.
- Sharma, R, Gupta, S, Ahmad, H, Ansari, GA, and Awasthi, YC. Stimulation of a human erythrocyte membrane ATPase by glutathione conjugates. *Toxicol Appl Pharmacol.* 104(3): 421-428. 1990.
- Sharma, R., Gupta, S., Singh, S. V., Medh, R. D., Ahmad, H., LaBelle, E. F., & Awasthi, Y. C. 1990. Purification and characterization of dinitrophenylglutathione ATPase of human erythrocytes and its expression in other tissues. *Biochemical and Biophysical Research Communications*, 171(1): 155-161.
- Sheffield, P. 1988. Tissue oxygen measurements. In J. Davis & T. Hunt (Eds.), *Problem wounds: the role of oxygen*: 17-55. New York: Elsevier.
- Sheffield, P. 1998. Measuring tissue oxygen tension: a review. *Undersea Hyperb Med*, 25(3): 179-188.
- Sheffield, PJ, Dietz, D, Posey, KI, Ziemba, TA, and Bakken, B. Use of transcutaneous oxygen tension measurement and laser Doppler with local heat provocation to assess patients with problem wounds. *The 1st Congress of Alps-Adria Working Community on Maritime, Undersea, and hyperb Med.* 341-344. 2001. Split, Croatia, Undersea and Hyperb Med Soc of Croatian Med Assoc.
- Sheikh, A., Gibson, J., Rollins, M., Hopf, H., Hussain, Z., & Hunt, T. 2000. Effect of hyperoxia on vascular endothelial growth factor levels in a wound model. *Arch Surg*, 135: 1293-1297.
- Sheikh, A., Rollins, M., Hopf, H., & Hunt, T. 2005. Hyperoxia improves microvascular perfusion in a murine wound model. *Wound Repair Regen.*, 13(3): 303-308.
- Shen, L. & Sevanian, A. 2001. OxLDL induces macrophage (gamma)-GCS-HS protein expression: a role for oxLDL-associated lipid hydroperoxide in GSH synthesis. *Journal of Lipid Research*, 42(5): 813-823.
- Shieh, R. C., Goldhaber, J. I., Stuart, J. S., & Weiss, J. N. 1994. Lactate transport in mammalian ventricle. General properties and relation to K<sup>+</sup> fluxes. *Circulation Research*, 74(5): 829-838.
- Shu, Z., Jung, M., Beger, H. G., Marzinzig, M., Han, F., Butzer, U., Bruckner, U. B., & Nussler, A. K. 1997. pH-dependent changes of nitric oxide, peroxynitrite, and reactive oxygen species in hepatocellular damage. *AJP - Gastrointestinal and Liver Physiology*, 273(5): G1118-G1126.
- Shweiki, D., Itin, A., Soffer, D., & Keshet, E. 1992. Vascular endothelial growth factor induced by hypoxia may mediate hypoxia-initiated angiogenesis. *Nature.*, 359(6398)(843): 845.
- Siddiqui, A., Galiano, R., Gonnors, D., Gruskin, E., Wu, L., Mustoe, T. 1996. Differential effects of oxygen on human dermal fibroblasts: acute versus chronic hypoxia. *Wound Repair and Regeneration*, 4: 211-218.
- Sies, H. 1991. *Oxidative Stress: Oxidants and Antioxidants*. Academic Press, New York.
- Singer, AJ and Clark, RAF. 1999. Cutaneous wound healing. *The New England Journal of Medicine* 341(10), 738-746.
- Singh, NP, McCoy, MT, Tice, RR, and Schneider, EL. A simple technique for quantitation of low levels of DNA damage in individual cells. *Exp Cell Res.* 175(1), 184-191. 1988.

- Singh, NP, Tice, RR, Stephens, RE, and Schneider, EL. 1991. A microgel electrophoresis technique for the direct quantitation of DNA damage and repair in individual fibroblasts cultured on microscope slides. *Mutat Res.* 252(3): 289-296.
- Snyder, R. 2005. Treatment of nonhealing ulcers with allografts. *Clinics in Dermatology*, 23(4): 388-395.
- Speit, G., Dennog, C., & Lampl, L. 1998. Biological significance of DNA damage induced by hyperbaric oxygen. *Mutagenesis.*, 13(1): 85-87.
- Speit, G., Dennog, C., Eichhorn, U., Rothfuss, A., & Kaina, B. 2000. Induction of heme oxygenase-1 and adaptive protection against the induction of DNA damage after hyperbaric oxygen treatment. *Carcinogenesis*, 21(10): 1795-1799.
- Speit, G, Dennog, C, Radermacher, P, and Rothfuss, A. Genotoxicity of hyperbaric oxygen. *Mutation Research* 521, 111-119. 2002.
- Sreekumar, P. G., Kannan, R., de Silva, A. T., Burton, R., Ryan, S. J., & Hinton, D. R. 2006. Thiol regulation of vascular endothelial growth factor-A and its receptors in human retinal pigment epithelial cells. *Biochemical and Biophysical Research Communications*, 346(4): 1200-1206.
- Staiano-Coico, L., Higgins, P., Schwartz, S., Zimm, A., & Goncalves, J. 2000. Wound fluids: a reflection of the state of healing. *Ostomy Wound Manage*, 46(1A Supplement): 85S-93S.
- Stamler, J., Singel, D., & Loscalzo, J. 1992. Biochemistry of nitric oxide and its redox-activated forms.. *Science.*, 258(5090): 1898-1902.
- Staniek, K. & Nohl, H. 1999. H<sub>2</sub>O<sub>2</sub> detection from intact mitochondria as a measure for one-electron reduction of diocynen requires a non-invasive assay system. *Biochimica Et Biophysica Acta*, 1413: 70-80.
- Steele, D., McAinsh, A., & Smith, G. 1996. Comparative effects of inorganic phosphate and oxalate on uptake and release of Ca<sup>2+</sup> by the sarcoplasmic reticulum in saponin skinned rat cardiac trabeculae. *J Physiol*, 490 ( Pt 3): 565-576.
- Steiling, H., Munz, B., Werner, S., & Brauchle, M. 1999. Different types of ROS-scavenging enzymes are expressed during cutaneous wound repair. *Exp Cell Res.*, 247(2): 484-494.
- Stein, I., Neeman, M., Shweiki, D., Itin, A., & Keshet, E. 1995. Stabilization of vascular endothelial growth factor mRNA by hypoxia and hypoglycemia and coregulation with other ischemia-induced genes. *Mol Cell Biol.*, 15(10): 5363-5368.
- Stein, I., Itin, A., Einat, P., Skaliter, R., Grossman, Z., & Keshet, E. 1998. Translation of vascular endothelial growth factor mRNA by internal ribosome entry: implications for translation under hypoxia. *Mol Biol Cell.*, 18(6): 3112-3119.
- Steinbrech, D., Longaker, M., Mehrara, B., Saadch, P., Chin, G., Gerrets, R., Chau, D., Rowe, N., & Gittes, G. 1999. Fibroblast response to hypoxia: the relationship between angiogenesis and matrix regulation. *Journal of Surgical Research*, 84: 127-133.
- Stephens, F. & Hunt, T. 1971. Effect of changes in inspired oxygen and carbon dioxide tensions on wound tensile strength: an experimental study. *Ann Surg*, 173: 515-519.
- Stevens, A. 2000. Tissue repair and wound healing. *Pathophysiology*: 43-332.
- Stone, J. & Cianci, P. 1997. The Adjunctive Role of Hyperbaric Oxygen Therapy in the Treatment of Lower Extremity Wounds in Patients With Diabetes. *Diabetes Spectrum*, 10(2): 118-123.
- Stone, J. & Cianci, P. 2003. The adjunctive role of hyperbaric oxygen therapy in the treatment of lower extremity wounds in patients with diabetes. *Diabetes Spectrum*, 10(2): 118-123.
- Storz, G. & Imlay, J. 1999. Oxidative stress. *Curr Opin Microbiol.*, 2(2): 188-194.
- Sudip, D., Tapat, C., Malay, M., Amritlal, M., & Sajal, C. 2002. Role of membrane-associated CA<sup>2+</sup>-dependent matrix metalloprotease-2 in the oxidant activation of Ca<sup>2+</sup>-ATPase by tertiary butylhydroperoxide. *Molecular and Cellular Biochemistry*, V237(1): 85-93.
- Sunakawa M, Yusa T. The effect of hyperbaric oxygenation on nitrite and nitrate production in rats treated with endotoxin. *Masui* 46(11): 1447-53. 1997.
- Suri, C., Jones, P., Patan, S., Bartunkova, S., M. P., Davis, S., Sato, T., & Yancopoulos, G. 1996. Requisite role of angiopoietin-1, a ligand for the TIE-2 receptor, during embryonic angiogenesis. *Cell*, 87: 1171-1180.
- Suzuki, Y. J., Cleemann, L., Abernethy, D. R., & Morad, M. 1998. Glutathione is a Cofactor for H<sub>2</sub>O<sub>2</sub>-Mediated Stimulation of C<sup>2+</sup>-Induced C<sup>2+</sup> Release in Cardiac Myocytes. *Free Radical Biology and Medicine*, 24(2): 318-325.
- Suzuki, Y. J. & Ford, G. D. 1999. Redox Regulation of Signal Transduction in Cardiac and Smooth Muscle. *Journal of Molecular and Cellular Cardiology*, 31(2): 345-353.

**[T]**

- Takamiya, M., Saigusa, K., & Aoki, Y. 2002. Immunohistochemical study of basic fibroblast growth factor and vascular endothelial growth factor expression for age determination of cutaneous wounds. *Am J Forensic Med Pathol.*, 23(3): 264-267.
- Taylor JE, Laity PR, Hicks J, Wong SS, Norris K, Khunkamchoo P, Johnson AF, and Cameron RE. 2005. Extent of iron pick-up in deferoxamine-coupled polyurethane materials for therapy of chronic wounds. *Biomaterials*, 26(30): 6024-6033.
- Teramoto, S., Tomita, T., Matsui, H., Ohga, E., Matsuse, T., & Ouchi, Y. 1999. Hydrogen peroxide-induced apoptosis and necrosis in human lung fibroblasts: protective roles of glutathione. *Jpn J Pharmacol*, 79: 33-40.
- Thom, S. 1996. Hyperbaric oxygen therapy. *J Int Care Med*, 4: 58-74.
- Thom, S. R., Fisher, D., Zhang, J., Bhopale, V. M., Ohnishi, S. T., Kotake, Y., Ohnishi, T., & Buerk, D. G. 2003. Stimulation of perivascular nitric oxide synthesis by oxygen. *AJP - Heart and Circulatory Physiology*, 284(4): H1230-H1239.
- Tice, RR, Agurell, E, Anderson, D, Burlinson, B, Hartmann, A, Kobayashi, H, Miyamae, Y, Ryu, JC, and Sasaki, YF. Single cell gel/comet assay: guidelines for in vitro and in vivo genetic toxicology testing. *Environ Mol Mutagen.* 35(3): 206-221. 2000.
- Tirosh, R; Resnik ER, Herron J; Sukovich DJ; Hong Z; Weir EK; Cornfield DN. 2006. Acute normoxia increases fetal pulmonary artery endothelial cell cytosolic Ca<sup>2+</sup> via Ca<sup>2+</sup>-induced Ca<sup>2+</sup> release. *Pediatr Res.* 60(3): 258-63.
- Tjörnström, J., Holmdahl, L., Falk, P., Falkenberg, M., Arnell, P., & Risberg, B. 2001. Effects of hyperbaric oxygen on expression of fibrinolytic factors of human endothelium in a simulated ischaemia/reperfusion situation. *Scandinavian Journal of Clinical and Laboratory Investigation*, 61: 539-545.
- Tjörnström, J., Holmdahl, L., Arnell, P., Falkenberg, M., & Risberg, B. 1999. Treatment with hyperbaric oxygen affects endothelial cell fibrinolysis. *Eur J Surg*, 165: 834-838.
- Tolentino, M., Miller, J., Gragoudas, E., Chatzistefanou, K., Ferrara, N., & Adamis, A. 1996. VEGF is sufficient to produce iris neovascularization and neovascular glaucoma in a non-human primate. *Arch Ophthalmol*, 114: 964-970.
- Tompach, P., Lew, D., & Stoll, J. 1997. Cell response to hyperbaric oxygen treatment. *Int.J.Oral Maxillofac.Surg*, 26(1997): 82-86.
- Torok J, Koprđova R; Cebova M; Kunes J; Kristek F. Functional and structural pattern of arterial responses in hereditary hypertriglyceridemic and spontaneously hypertensive rats in early stage of experimental hypertension. *Physiol Res.* 55 Suppl 1:[S65-71.]. 2006.
- Trabold, O., Wagner, S., Wicke, C., Scheuenstuhl, H., Hussain, M., Rosen, N., Seremetiev, A., Becker, H., & Hunt, T. 2003. Lactate and oxygen constitute a fundamental regulatory mechanism in wound healing. *Wound Repair Regen*, 11(6): 504-509.
- Tran, Q. K., Ohashi, K., & Watanabe, H. 2000. Calcium signalling in endothelial cells. *Cardiovascular Research*, 48(1): 13-22.
- Trump, B., Berezsky, I., Sato, T., Laiho, K., Phelps, P., & DeClaris, N. 1984. Cell calcium, cell injury and cell death. *Environ Health Perspect.*, 57: 281-287.
- Trump, B. & Berezsky, I. 1996. The role of altered [Ca<sup>2+</sup>]<sub>i</sub> regulation in apoptosis, oncosis, and necrosis. *Biochim Biophys Acta*, 1313(3): 173-178.
- Tschudi, M. R., Mesaros, S., Luscher, T. F., & Malinski, T. 1996. Direct In Situ Measurement of Nitric Oxide in Mesenteric Resistance Arteries : Increased Decomposition by Superoxide in Hypertension. *Hypertension*, 27(1): 32-35.
- Tschudi, M. R., Barton, M., Bersinger, N. A., Moreau, P., Cosentino, F., Noll, G., Malinski, T., & Luscher, T. F. 1996. Effect of Age on Kinetics of Nitric Oxide Release in Rat Aorta and Pulmonary Artery. *Journal of Clinical Investigation*, 98(4): 899-905.
- Tsien, RY, Rink, TJ, and Poenie, M. Measurement of cytosolic free Ca<sup>2+</sup> in individual small cells using fluorescence microscopy with dual excitation wavelengths. *Cell Calcium*. 6(1-2), 145-157. 1985.
- Tsikas, D. 2006. Analysis of nitrite and nitrate in biological fluids by assays based on the Griess reaction: Appraisal of the Griess reaction in the l-arginine/nitric oxide area of research. *Journal of Chromatography B*. In Press, Corrected Proof.
- Tsuchida, S, Hiraoka, M, Sudo, M, and Muramatsu, I. Hyporesponsiveness to nitrovasodilators in rat aorta incubated with endotoxin and L-arginine. *European Journal of Pharmacology* 281, 251-254. 1995.

**[U]**

UHMS Indications for Hyperbaric Oxygen Therapy.

Unemori, E., Ferrara, N., Bauer, E., & Amento, E. 1992. Vascular endothelial growth factor induces interstitial collagenase expression in human endothelial cells. *J Cell Physiol.*, 153(3): 557-562.

Uria, J., Balbin, M., Lopez, J., Alvarez, J., Vizoso, F., Takigawa, M., & Lopez-Otin, C. 1998. Collagenase-3 (MMP-13) expression in chondrosarcoma cells and its regulation by basic fibroblast growth factor. *Am J Pathol.*, 153(1)(91): 101.

**[V]**

Vaca, L., Kunze, D. L. (1995) IP<sub>3</sub>-activated Ca<sup>2+</sup> channels in the plasma membrane of cultured vascular endothelial cells. *Am. J. Physiol.* **269**,C733-C738

van der Zee, R., Murohara, T., Luo, Z., Zollmann, F., Passeri, J., Lckutat, C., & Isner, J. M. 1997. Vascular Endothelial Growth Factor/Vascular Permeability Factor Augments Nitric Oxide Release From Quiescent Rabbit and Human Vascular Endothelium. *Circulation*, 95(4): 1030-1037.

van Hinsbergh, V. 1988. Regulation of the synthesis and secretion of plasminogen activators by endothelial cells. *Haemostasis.*, 18(4-6): 307-327.

van Hinsbergh, V., van den Berg EA, Fiers, W., & Dooijewaard, G. 1990. Tumor necrosis factor induces the production of urokinase-type plasminogen activator by human endothelial cells. *Blood.*, 75(10)(1991): 1998.

van Klaveren, R. J., Demedts, M., & Nemery, B. 1997. Cellular glutathione turnover in vitro, with emphasis on type II pneumocytes. *European Respiratory Journal*, 10(6): 1392-1400.

Vandeputte, C and Guizon I, Genestie-Denis I Vannier B Lorenzon G. A microtiter plate assay for total glutathione and glutathione disulfide contents in cultured/isolated cells: performance study of a new miniaturized protocol. *Cell Biol Toxicol.* 10(5-6): 415-421. 1994.

Vandeputte, C., Guizon, I., Genestie-Denis, I., Vannier, B., & Lorenzon, G. 1994. A microtiter plate assay for total glutathione and glutathione disulfide contents in cultured/isolated cells: performance study of a new miniaturized protocol. *Cell Biology and Toxicology*, V10(5): 415-421.

Vangala, R., Kritzler, K., Schoch, G., & Topp, H. 1998. Induction of single-strand breaks in lymphocyte DNA of rats exposed to hyperoxia. *Arch Toxicol.*, 72(4): 247-248.

Vincenti, V., Cassano, C., Rocchi, M., & Persico, G. 1996. Assignment of the vascular endothelial growth factor gene to human chromosome 6p21.3. *Circulation.*, 93(8): 1493-1495.

**[W]**

Waltenberger, J., Claesson-Welsh, L., Siegbahn, A., Shibuya, M., & Heldin, C. 1994. Different signal transduction properties of KDR and Flt1, two receptors for vascular endothelial growth factor. *J Biol Chem.*, 269(43) (26988): 26995.

Wang WJ, Ho XP, Yan YL, Yan TH, Li CL. 1998. Intrasyntosomal free calcium and nitric oxide metabolism in central nervous system oxygen toxicity. *Aviat Space Environ Med.*, 69(6): 551-555.

Wang, G., Jiang, B., Rue, E., & Semenza, G. 1995. Hypoxia-inducible factor 1 is a basic-helix-loop-helix-PAS heterodimer regulated by cellular O<sub>2</sub> tension. *Proc.Natl.Acad.Sci.*, 92(June): 5510-5514.

Wang, R., Ghahary, A., Shen, Y., Scott, P., & Tredget, E. 1997. Nitric oxide synthase expression and nitric oxide production are reduced in hypertrophic scar tissue and fibroblasts. *J Invest Dermatol.*, 108(4): 438-444.

Watanabe, S., Wang, X., Hirose, M., Osada, T., Tanaka, H., & Sato, N. 1998. Rebamipide prevented delay of wound repair induced by hydrogen peroxide and suppressed apoptosis of gastric epithelial cells in vitro. *Dig Dis Sci.*, 43(9 Suppl): 107S-112S.

Watson JD, B. T. B. S. G. A. L. M. L. R. 2004. *Molecular Biology of the Gene*, ch. 9 and 10. Peason Benjamin Cummings; CSHL Press. 5th ed.

Wattel, F., Mathicu, D., Fossati, P., & et al 1991. Hyperbaric oxygen in treatment of diabetic foot lesions: search for healing predictive factors. *J Hyperbar Med*, 6: 263-267.

Wenger, R. & Gassmann, M. 1997. Oxygen(es) and the hypoxia-inducible factor-1. *Biol.Chem.* 378: 609-16.

Wennmalm, A., Benthin, G., & Petersson, A. S. 1992. Dependence of the metabolism of nitric oxide (NO) in healthy human whole blood on the oxygenation of its red cell haemoglobin. *British Journal Of Pharmacology*, 106(3): 507-508.

Wennmalm, A., Benthin, G., Edlund, A., Jungersten, L., Kieler-Jensen, N., Lundin, S., Westfelt, U. N., Petersson, A. S., & Waagstein, F. 1993. Metabolism and excretion of nitric oxide in humans. An experimental and clinical study. *Circulation Research*, 73(6): 1121-1127.

- Werner, S. 1998. Keratinocyte growth factor: a unique player in epithelial repair processes. *Cytokine Growth Factor Rev.*, 9(2): 153-165.
- Wickham, NW, Vercellotti, GM, Moldow, CF, Visser, MR, and Jacob, HS. 1988. Measurement of intracellular calcium concentration in intact monolayers of human endothelial cells. *J Lab Clin Med.* 112(2): 157-167.
- Wilson III, D. M. & Bohr, V. A. The mechanics of base excision repair, and its relationship to aging and disease. *DNA Repair*, In Press, Corrected Proof.
- Wood, P. G. & Gillespie, J. I. 1998. Evidence for Mitochondrial Ca<sup>2+</sup>-Induced Ca<sup>2+</sup>Release in Permeabilised Endothelial Cells. *Biochemical and Biophysical Research Communications*, 246(2): 543-548.
- Woodmansee, A. & Imlay, J. 2002. Reduced Flavins Promote Oxidative DNA Damage in Non-respiring *Escherichia coli* by Delivering Electrons to Intracellular Free Iron. *Journal of Biological Chemistry*, 277(37): 34055-34066.
- Wright, J. Hyperbaric oxygen therapy for wound healing.  
(<http://www.worldwidewounds.com/2001/april/Wright/HyperbaricOxygen.html>)
- Wu, L., Pierce, G., Ladin, D., Zhao, L., Rogers, D., & Mustoe, T. 1995. Effects of oxygen on wound responses to growth factors: Kaposi's FGF, but not basic FGF stimulates repair in ischemic wounds. *Growth Factors.*, 12(1): 29.-35.
- Wyss, C., Harrington, R., Burgess, E., & Matsen, F. 3. 1988. Transcutaneous oxygen tension as a predictor of success after an amputation. *J Bone Joint Surg Am.*, 70(2): 203-207.

**[X]**

- Xi, Q., Cheranov, S. Y., & Jaggar, J. H. 2005. Mitochondria-Derived Reactive Oxygen Species Dilate Cerebral Arteries by Activating Ca<sup>2+</sup> Sparks. *Circulation Research*, 97(4): 354-362.
- Xiong, M., Elson, G., Learda, D., & Leibovich, S. 1998. Production of vascular endothelial growth factor by murine macrophages-Regulation by hypoxia, lactate, and inducible nitric oxide synthase pathway. *American Journal of Pathology*, 153(2): 587-598.

**[Y]**

- Yang, Z. & Steele, D. S. 2000. Effects of cytosolic ATP on spontaneous and triggered Ca<sup>2+</sup>-induced Ca<sup>2+</sup> release in permeabilised rat ventricular myocytes. *The Journal of Physiology Online*, 523(1): 29-44.
- Yao, X. & Huang, Y. 2003. From nitric oxide to endothelial cytosolic Ca<sup>2+</sup>: a negative feedback control. *Trends in Pharmacological Sciences*, 24(6): 263-266.
- Yasuda, M., Ohzeki, Y., Shimizu, S., Naito, S., Ohtsuru, A., Yamamoto, T., & Kuroiwa, Y. 1999. Stimulation of in vitro angiogenesis by hydrogen peroxide and the relation with ETS-1 in endothelial cells. *Life Sci.* 1999; 64(4): 249-258.
- Ying, W., Alano, C., Garnier, P., & Swanson, R. 2005. NAD<sup>+</sup> as a metabolic link between DNA damage and cell death. *J Neurosci Res.*, 79(1-2): 216-223.
- Yogarathnam, JZ, Laden, G, Madden, LA, Seymour, AM, Guvendik, L, Cowen, M, Greenman, J, Cale, A, and Griffin, S. Hyperbaric oxygen: a new drug in myocardial revascularization and protection? *Cardiovasc Revasc Med.* 7(3): 146-154. 2006.
- Yuan LJ, Ueng SW Lin SS Yeh WL Yang CY Lin PY. Attenuation of apoptosis and enhancement of proteoglycan synthesis in rabbit cartilage defects by hyperbaric oxygen treatment are related to the suppression of nitric oxide production. *J Orthop Res* 22(5):1126-34. 2004.

**[Z]**

- Zabel DD, Feng JJ, Scheuenstuhl H, Hunt TK, Hussain MZ. 1996. Lactate stimulation of macrophage-derived angiogenic activity is associated with inhibition of Poly(ADP-ribose) synthesis. *Lab Invest.* 1996 Mar; 74(3):644-9.
- Zachary, I. & Glick, G. 2001. Signaling transduction mechanism mediating biological actions of the vascular endothelial growth factor family. *Cardiovascular Research*, 49: 568-581.
- Zamboni, W., Browder, L., & Martinez, J. 2003. Hyperbaric oxygen and wound healing. *Clinics in Plastic Surgery*, 30: 67-75.
- Zhang, C., Li, H., Zhou, S., & Yang, J. 2001. Study of the changes and effect of VEGF and bFGF in early stage of maxillofacial blast injury in rabbits. *Hua Xi Kou Qiang Yi Xue Za Zhi.*, 19(2): 77-79-82.
- Zhang, J, Sam, AD, Klitzman, B, and Piantadosi, CA. Inhibition of nitric oxide synthase on brain oxygenation in anesthetized rats exposed to hyperbaric oxygen. *Undersea Hyperb Med* 22(4), 377-382. 1995.

- Zhang, Q. & Huang, X. 2003. Induction of interleukin-6 by coal containing bioavailable iron is through both hydroxyl radical and ferryl species. *J Biosci.*, 28(1): 95-100.
- Zhiliaev Slu, Moskvina AN Platonova TF Gutsaeva DR Churilina IV Demchenko IT. Hyperoxic vasoconstriction in the brain is realized by inactivation of nitric oxide by superoxide anions. *Russ Fiziol Zh Im I M Sechenova.* 88(5): 553-9. 2002.
- Ziche, M. & Morbidelli, L. 2000. Nitric oxide and angiogenesis. *Journal of Neuro-Oncology*, 50: 139-148.
- Ziegler, DM. 1985. Role of reversible oxidation-reduction of enzyme thiols-disulfides in metabolic regulation. *Annu Rev Biochem.*, 54: 305-329.